Application of Functional Renormalization Group Approach

to spin systems and long range models

Nicolò Defenu

Department of Theory and Numerical simulation of Condensed Matter

International School for Advanced Studies (SISSA, Trieste).

Advisor: **A. Trombettoni**.
External Advisor: **A. Codello**.
Internal Advisor: **S. Ruffo**.

January 2017

I would like to dedicate this thesis to my sister, whose ability to read and speak russian will always be source of my greatest envy....

Declaration

I hereby declare that except where specific reference is made to the work of others, the contents of this dissertation are original and have not been submitted in whole or in part for consideration for any other degree or qualification in this, or any other University. This dissertation is the result of my own work and includes nothing which is the outcome of work done in collaboration, except where specifically indicated in the text.

Nicolò Defenu
January 2017

Acknowledgements

The four years I spent at the International School for Advanced Studies (SISSA) in Trieste have been studded of wonderful experience on the personal and scientific side. Give a precise account of all the persons I should be grateful for filling my personal life in the last four years would be extremely hard and long. Here I will then restrict myself to acknowledge only them who contributed to the development of my scientific profile. First of all I shall thank Andrea Trombettoni for always encouraging me to face new problems as well as teaching me the hidden secrets of scientific though. I am also grateful to Alessandro Codello for showing me the beauty of Renormalization Group techniques, which, even if not producing exact numerical quantities, guide ourselves to qualitative understanding of natural phenomena.

Stefano Ruffo only entered my scientific career in the last two years but his brilliant mind and his endless experience were an inspiration to continue my career in the world of research. The collaboration with Istvan Nandori has been crucial for my scientific development and I should acknowledge him for always believing in my competence. Together with him I want to thank all the MTA Atomki group in Debrecen for all the great experiences I lived there.

The infinite knowledge and physical insight of Giacomo Gori will never stop surprising me. A special acknowledgement goes to Tilman Enss for hosting me in Heidelberg sharing with me its knowledge on Fermionic systems and FRG techniques. The collaborations born in the last two years are countless and I do not pretend to precisely, but I shall thank Giovanna Morigi, Paola-Gori Giorgi, Jose Lorenzana for giving me the opportunity to share my ideas with them.

On the edges between the personal and scientific side I shall acknowledge the other fourth year PhD students of the Condensed Matter sector at SISSA, Lorenzo Del Re, Tommaso Gorni, Francesco Peronaci, Francesco Petocchi. They, together with Federico Bianchini, Marco Micciarelli and Loris Ercole, made the environment at SISSA the most fruitful for sharing ideas.

Finally I would like to thank all the secretaries and administrative staff of SISSA and in particular Riccardo Iancer for making my bureaucratic duties the lightest possible.

Table of contents

Summary

During the last two decades, functional renormalization group (FRG) emerged as a versatile class of methodologies which can be used in a variety of cases, ranging from statistical mechanics models and interacting field theories to condensed matter strongly interacting systems. The development of FRG techniques from one hand had a methodological side – aimed at testing different ways to handle with approximations of the functional equations – and from the other concurred to define FRG as a method to be seriously considered to face new and poorly/not yet understood problems. Both directions, i.e. improve and test known techniques and proposed refinements against well known problems and concretely deal with non-testbed problems, have motivated the work done during the PhD.

This thesis aims at present, provide details and put in perspective results obtained during my PhD in the last three years. Many of such results have been published, in a more synthetic way, in peer review journals, others are going to appear online soon. Some others will probably remain only in this thesis, but together with the published material will be instrumental to delineate a path leading to a deeper understanding and a (hopefully) clearer presentation of potentialities and issues of the FRG method.

Chapter 1 is divided into two parts. In Section 1.1 the basic concepts of multivariate calculus are summarized; indeed while field theoretical formalism generally involves functional analysis calculation, it is found that in most of the cases no complications are introduced by simply considering the continuous field spatial variable as the discrete index of an infinite component vector. Even if from the mathematical point of view some of the properties that can be demonstrated for multivariate calculus are not strictly valid in functional analysis most of the actual theoretical physics computation are pursued in this optics and they often yield the correct result. Section 1.2 contains the explicit derivation of the core FRG equation, often called the Wetterich equation. This derivation is pursued in full details and, while it will probably be boring for the expert reader, can be useful for people not familiar with basic functional calculus and to present the notation used in the rest of the Thesis. Finally in Section 1.3 it is reported a brief overview of the methods commonly used to treat the Wetterich equation.

In Chapter 2 the application of the derivative expansion to the derivation of the phase diagram for $O(N)$ field theories is reported. The $O(N)$ field theory can be easily mapped into lattice system of N components interacting spins and vice versa, as it is demonstrated in Appendix B.1. In Section 2.1 we show the derivation of the flow equation for the effective potential in the so-called Local Potential Approximation (LPA) for the $O(N)$ symmetric models. Successively, Section 2.2, we introduce Taylor expansions for the effective potential potential, deriving the β-functions for the couplings of vector φ^4 theories as it is done in traditional Renormalization group approaches. It is then demonstrated that truncation techniques are not consistent with the exact results of the Mermin-Wagner theorem, while, when full functional form for the effective potential is retained, LPA approach can produce the correct picture for the phase diagram of the $O(N)$ models. In Section 2.3 we use shooting technique to investigate the fixed point structure of LPA equations, showing explicitly how the Mermin-Wagner theorem is recovered from the behavior of critical exponents. In that section we also report numerical results for the critical exponents as a function of N and d and for various universality classes, showing how, even at the simple LPA$'$ level, numerical accuracy is never worse than 20%. Finally, in Section 2.4 $N = 1$ scalar field theories are considered increasing the approximation level to $O(\partial^2)$ in derivative expansion. It is demonstrated that shooting technique can be employed also in this case leading to a full and unbiased scenario for scalar field theories in 2 and 3 dimensions. The computational cost remains small and the results are in very good agreement with numerical simulations in $d = 3$ and exact Conformal Field Theory (CFT) result in $d = 2$.

In Chapter 3 the FRG approach is applied to the 2-dimensional sine-Gordon (SG) model. This model can be exactly mapped to the Coulomb gas and it is believed to be in the same universality class of XY model, providing a prototypical example of topological phase transition. In the SG model the effective potential has both $\mathbb{Z}_2$ and periodic symmetry in the scalar field. The FRG approach proved very useful in the case of periodic symmetries due to the possibility to project the Wetterich equation in Fourier space. Section 3.3 is devoted to the introduction of the c-function calculation in the FRG framework. In Section 3.4 the phase diagram of the SG model using FRG approach is retrieved, first in the simple case of constant frequency β and then in the scale dependent frequency case. Even at approximated level an FRG approach maintaining the periodicity of the model yields non perturbative results with almost constant accuracy in the whole u-β plane. In the following Section the results for the calculation of the c-function of the SG model for all values of β are shown, and the correct result is found in the low temperature region where numerical quantities are in agreement with the exact $\Delta c = 1$ CFT result in the small β case.

Chapter 4 is devoted to the investigation of long range interactions in spin systems. Indeed, while universal quantities are generally not influenced by the shape of the lattice or by modifications of microscopic interactions when they are short range, LR interactions radically modify the low energy behavior of the systems excitations introducing a non analytic p^σ momentum term alongside with the standard p^2 term of SR interactions. This non trivial effect in the scaling behavior of the system yields important effects on its phase diagram. As a function of the parameter σ three regions exist, as shown in Section 4.1, where the system undergoes SSB with radically different universal behaviors. In the following Sections spatial anisotropy is introduced together with LR interactions and its influence to the critical behavior of LR systems is investigated. The results demonstrate how LR interactions in one spatial direction can modify the critical behavior of SR interactions in the others and they can be used to study the physics of quantum LR rotor models.

Finally we discuss in the Conclusions possible future work and perspectives motivated by the results presented in this PhD thesis.

Introduction

The goal of this Introduction is to provide an historical introudction to the steps leading to the development of renormalization group (RG) concepts and to the introduction of modern RG techniques. I finally present a synthetic summary of the results presented in the next Chapters.

It was as early as 1920 when Wilhelm Lenz proposed to his student, Ernst Ising, a toy model to describe ferromagnetism. The model is made up of spin variables $S_i = \pm 1$ on a lattice. The spin variables are interacting via some exchange interaction J and are in presence of a magnetic field B. The Hamiltonian reads,

$$H = \sum_i B_i S_i + \frac{1}{2} \sum_{i,j} J(i,j) S_i S_j. \tag{1}$$

We have written the Ising Hamiltonian in the most general form, with an exchange coupling depending on the distance between the interacting sites. In most of the cases one assumes that the coupling depends just on the distance between the sites: $J(i,j) = J(|i-j|)$. The simplest case is obtained for a square lattice with N sites in d dimensions, in which only the nearest neighbors are interacting.

In magnetic systems where the spins tend to spontaneously align in the same direction it is natural to choose $J < 0$, the case $J > 0$ being used to characterize antiferromagnetic materials. In this thesis however we shall specially deal with the ferromagnetic case, which is the one originally proposed by Lenz.

In 1925 Ernst Ising bound forever his name to this model publishing the solution of the one dimensional case in his PhD Thesis [1]. The exact solution of the model showed no phase transition at finite temperature, in contrast with the mean field approximation, and Ising himself, extending this result to a general dimension d, concluded that this simple model was not sufficient to describe the transition behavior of magnetic systems.

After more than ten years Rudolf Peierls reconsidered the Ising's conclusion and demonstrated that this model does exhibit phase transition at finite temperature as long as $d \geq 2$ [2]. However thirty years more were necessary to recognize the universality phenomenon and to

obtain the clue that this simple model not only develops a finite temperature phase transition but contains, despite its simplicity, the needed ingredients to quantitatively reproduce the critical properties of a class of physical systems [3].

The importance of the Ising model, and more in general of its generalizations including the $O(N)$ models, in the physics of second order phase transition is justified by its simplicity and by the possibility to obtain a wide range of different behaviors as a function of the dimension. For a ferromagnetic nearest neighbor Ising model we have the following results: in $d = 1$ the system has only a paramagnetic phase and no phase transition occurs, in $d = 2$ the system is exactly solvable [4] for vanishing magnetic field $B = 0$, with an exactly determined finite temperature phase transition. In $d = 3$ the system can be shown to possess a finite critical temperature, but both the critical and non critical properties shall be obtained using approximated or numerical techniques [5–8]. For every $d \geq 4$ the system still displays two phases but its critical properties are the same of the Gaussian model and are obtained by mean field approximation.

Guided by the theoretical investigation on the Ising model and on a large number of experimental results, in which the critical behavior of different system showed the same power law scaling, the physics community introduced the concept of universality, i.e. the property of microscopically different physical systems to have the same power law behavior for the thermodynamic quantities close to a second order phase transition.

The simplest examples of universality are provided, in fact, by the central limit theorem, which deals with the average of independent random variables with the same probability distribution, or by the asymptotic behaviour of Markovian random walk at large times. Both problems concern the identification of collective properties for an infinite number of random variables. Under certain generic conditions the asymptotic distribution for the variables is always Gaussian, independently from the distribution of the single random variable or from the random walk transition amplitudes. In many physical examples however the calculation cannot be pursued explicitly, as in the previous cases, and the properties of the asymptotic distribution remain unaccessible.

In 1937 Landau's theory of critical phenomena was introduced to investigate continuous phase transitions in macroscopic systems. Such theory is based on Gaussian distribution function and non Gaussian effects can only be introduced using perturbative techniques. However, for SR interacting systems, in space dimensions two and three, quasi-Gaussian models do not correctly reproduce universal quantities.

The failure of Landau's theory and of mean field approach in general in describing the universal behavior of correlated systems lead Kenneth Wilson to introduce the notion of *Renormalization Group* (RG) [9]. In the Wilson's approach the system is described by a

microscopic Hamiltonian, which defines the energy of the system at a given configuration of the microscopic variable, and by an energy scale Λ. The RG method is based on the recursive integration of short distance degrees of freedom of the system to generate a sequence of effective low energy Hamiltonians H_k corresponding to increasing scales k^{-1} [10]. The family of Hamiltonians H_k defines a RG transformation $k \in [0, \Lambda]$ describing the evolution from the microscopic configurational Hamiltonian H_Λ to an effective low energy Hamiltonian $H_{k=0}$. If the RG transformation has attractive fixed points, then universality of the large distance properties can be understood since the effective Hamiltonians eventually converge as $k \to 0$ toward a fixed-point Hamiltonian. The basin of attraction of a given fixed point in the space of Hamiltonians is called a universality class. It can be verified that the Gaussian theory provides the simplest example of a fixed point, thus called Gaussian fixed point.

In the last 40 years numerous different both numerical and analytical approach have been developed based on Wilson's idea [8, 11–16]. In recent years RG concepts have been generalized and enlarged leading to the development of a very general framework to investigate the critical and non critical quantities of many body and complex systems in the thermodynamic limit [17–19]. This general framework is referred as Exact Renormalization Group (ERG), Non Perturbative Renormalization Group (NPRG) or Functional Renormalization Group (FRG). These names all underline different features of such method, *it is exact* since it is based on an in principle exact equation which describe the RG transformation for a general effective average action or Gibbs free energy [20] and it allows to reconstruct all the thermodynamic quantities and the correlation functions of the system. However such exact equation is presently impossible to solve and it is needed to resort to approximations. The method is *non perturbative* in the sense that it is possible to develop approximation techniques which do not broke down as a function of any internal parameter. It is *functional* since it allows to write the RG transformation as a set of functional differential equations rather than sets of non linear coupled differential equations in a finite parameter space.

This thesis deals with basic applications of FRG to spin systems and long range (LR) models aiming not only at the investigation of critical properties and phase diagrams but showing how modern RG approaches are able to retrieve and enlarge, in straightforward way, most of the numerical and traditional results already found in literature with diverse and costly approaches. Moreover it will be shown how basic approximations of the FRG equation are able to capture all the qualitative universal features for the models considered, allowing to discover new universality classes and to describe most of the traditional results with the help of simple differential equations, whose properties are closely related with the low energy behavior of lattice spin systems. Many conjectures and unproven relations regarding LR models are derived using this approach and their validity is shown not to always hold exactly.

In Chapter 1 we introduce the FRG approach, explicitly showing the derivation of the flow equation for the effective action after giving a brief introduction on the functional formalism which shall be used in the next chapters.

Chapter 2 is dedicated to the application of the FRG to the $O(N)$ vector field theories. After deriving the flow equations for these models in the Local Potential Approximation (LPA) it is shown that functional equations are able to recover the qualitative picture for the phase diagram of these models satisfying the Mermin-Wagner theorem, these results being recently published [21]. A step further, in Section 2.3, the results for the critical exponents of $O(N)$ spin systems are given as a function of d and N, demonstrating that LPA$'$ approach is reliable for every value of the parameters with accuracy never lower than 20%, these results together with the ones reported in [22] complete the numerical derivation of the Mermin-Wagner theorem [23]. The last Section is dedicated to the application of the shooting technique introduced in [24] to $O(\partial^2)$ derivative expansion in scalar field theories. The generalization of this procedure allow us to draw the phase diagram of φ^4 scalar field theories as a landscape in the σ-η plane, where η is the anomalous dimension associated to each universality and σ the square renormalized mass.

Chapter 3 contains the application of FRG equation to the sine-Gordon model showing how it is possible to recover the phase diagram for the topological phase transition and introducing the c-function calculation in the FRG framework [25]. This chapter also reports the numerical results obtained for the c-function in the SG model, recently published in [26].

In Chapter 4 LR interactions are introduced and the phase diagram for $O(N)$ models in this case is discussed. Due to the infinite range of the coupling matrix $J(i, j)$, LR interactions radically modify the universal behavior of $O(N)$ models. The existence of an effective dimension relating the universal quantities of short range and LR interacting systems is discussed. The obtained critical exponents have been reported in [23]. Successively the effects of anisotropy in LR systems are introduced leading to various considerations regarding the effect of different decay law for the interactions in different systems subspaces, these results are already available online [27] and they are relevant for the description of quantum LR rotor models.

Finally in Chapter 5 a conclusive discussion for all the presented results is reported and an overview of the most relevant future perspectives is given.

Chapter 1

Introduction to Functional Renormalization Group

1.1 Field Theoretical formalism

Condensed matter and statistical physics problems are often formulated in terms of lattice spin variables whose configuration is given by a certain Hamiltonian H. This traditional approach is generally not followed, apart for some exceptions [28, 29], in FRG applications. Indeed this technique has been firstly formulated in field theoretical formalism and it is still mostly employed using effective field theory approach.

This thesis will follow the traditional field theoretical approach, then thin chapter will serve as a bridge between the lattice Hamiltonian approach [20] and field theoretical approach. For a more complete review of this concepts we remind the reader to [30] which contains a fairly complete introduction to statistical field theory.

While the equivalence between lattice and field theoretical formalism can be often proved exactly, as it is shown in the following or in appendix B.1, it is worth noting that field theoretical approach for lattice formalism was already introduced by Lev Landau using phenomenological arguments.

1.1.1 Multivariate random variables

Let us consider an ensemble of real random variables $\{\phi_i\}$. We will firstly deal with a finite number of random variables $i \in \mathbb{N}$ and successively we will assume that the results obtained in this chapter are also valid in the case of continuous function $\phi(x)$. However, in most of the cases, this procedure has no mathematical rigor since the transformation from discrete to continuous variables, the so-called *continuous limit*, is not mathematically well defined.

Nevertheless, from the physicist point of view, this has low impact since practical application of functional technique has proven able to give consistent results in the study of theoretical models. Then in the following we will pursue most of the demonstration in finite dimensional multivariable space and then assume the mathematical results to be valid even for continuous field theories.

The probability distribution (pdf) for the variables ensemble $\{\phi_i\}$ to be in a particular configuration $(\phi_1,\cdots,\phi_n)$ is given by $P(\phi_1,\cdots,\phi_n)\equiv P[\phi]$, these variables are said to be *interacting* if the probability distribution does not decouple into the product of single probability distributions. Every pdf should satisfy,

$$\int \Pi_i d\phi_i P[\phi] = \int \mathscr{D}\phi P[\phi] = 1, \tag{1.1}$$

the single component pdf can be defined as the marginal probability,

$$\int \Pi_{i\neq n} d\phi_i P[\phi] = P(\phi_n). \tag{1.2}$$

The exact behavior of the system can be described by means of correlation functions

$$\langle \phi_{i_1}\cdots\phi_{i_r}\rangle = \int \mathscr{D}\phi P[\phi]\phi_{i_1}\cdots\phi_{i_r}. \tag{1.3}$$

The partition function for the system is defined as the generator of all possible correlation functions

$$Z[J] = \int \mathscr{D}\phi P[\phi] e^{\sum_i J_i\phi_i}, \tag{1.4}$$

where $Z[J]\equiv Z(J_1,\cdots,J_n)$. Any correlation function can be obtained as,

$$\frac{\partial^r Z[J]}{\partial J_{i_1}\cdots\partial J_{i_r}}\Big|_{\{J_i\}=0} = \langle \phi_{i_1}\cdots\phi_{i_r}\rangle, \tag{1.5}$$

where J_{i_n} can be any $J\in\{J_i\}$. In particular we have that the microscopic variable expectation is

$$\langle\phi_i\rangle = \phi_i = \frac{\partial Z[J]}{\partial J_i}\Big|_{\{J_i\}=0}. \tag{1.6}$$

The generator for the connected correlation functions is readily obtained as,

$$W[J] = \log\left(Z[J]\right). \tag{1.7}$$

We can get the expression for all possible connected correlation functions from the generating functon $W[J]$,

$$\frac{\partial^r W[J]}{\partial J_{i_1}\cdots\partial J_{i_r}}\Big|_{\{J_i\}=0} = \langle \phi_{i_1}\cdots\phi_{i_r}\rangle_c, \tag{1.8}$$

If $W[J]$ is a convex function of all the variables $\{J_i\}\equiv J$ then its first derivative with respect of any of them is a one valued function of J,

$$\frac{\partial W[J]}{\partial J_i}\Big|_J = \varphi_i[J], \tag{1.9}$$

where obviously $\varphi_i[0]=\varphi_i=\langle\phi_i\rangle$. Since all $\{\varphi_i[J]\}$ are one valued function they can be inverted in such a way to get the new set of functions $\{J_i[\varphi]\}$, thus we can perform the Legendre transform of $W[J]$ to obtain the so called *effective action*,

$$\Gamma[\varphi] = \sum_i J_i[\varphi]\varphi_i - W[J[\varphi]]. \tag{1.10}$$

It should be noted that now φ does not indicate the ensemble of average values of the variables ϕ over the initial pdf but indicates just the variable dependence of the effective action, from here to now the average values over the initial pdf will be denoted by $\varphi^*\equiv\{\varphi_i^*\}$ while φ will only indicate the variable dependence of the effective action. Taking the first derivative of the effective action $\Gamma[\varphi]$ we get

$$\begin{aligned}\frac{\partial\Gamma[\varphi]}{\partial\varphi_i} &= \sum_k \frac{\partial J_k[\varphi]}{\partial\varphi_i}\varphi_k + \sum_k J_k[\varphi]\delta_{k,i} - \sum_k \frac{\partial W[J[\varphi]]}{\partial J_k[\varphi]}\frac{\partial J_k[\varphi]}{\partial\varphi_i} \\ &= J_i[\varphi],\end{aligned} \tag{1.11}$$

where to get last equivalence we used the fact that

$$\frac{\partial W[J]}{\partial J_k}\Big|_{J_k=J_k[\varphi]} = \varphi_k, \tag{1.12}$$

as it must be. Since the average values of the variables $\{\phi\}$ over the initial pdf was given by equation (1.6) setting all the J variables to zero ($\{J_i\}=0$), then correct average values for the variables $\{\phi_i\}$ satisfy equation (1.12) with $\{J_i\}=0$,

$$\frac{\partial\Gamma[\varphi]}{\partial\varphi_i}\Big|_{\varphi=\varphi^*} = 0 \;\forall\; i. \tag{1.13}$$

Thus the effective action is stationary at the correct values for the variables' averages.

Let us now introduce the formalism which will turn extremely useful in the following calculations, rewriting the initial probability distribution function as,

$$P[\phi] = e^{-S[\phi]}, \tag{1.14}$$

which is the definition of *bare action* $S[\phi]$. It is evident that the *bare action* $S[\phi]$ plays the same role of the Hamiltonian in lattice systems, in such a way that

$$S[\varphi] \equiv -\beta H[\varphi], \tag{1.15}$$

latter relation between *bare action* and microscopic Hamiltonian is valid for classical systems at equilibrium, since the Hamiltonian does not depend on the conjugate momenta of the microscopic variables. However in the following the interaction between the microscopic variables will be conveniently represented by spatial derivatives. Taking the exponential of the effective action we obtain

$$e^{-\Gamma[\varphi]} = e^{-(\sum_i J_i[\varphi]\varphi_i - W[J[\varphi]])} = e^{-\sum_i J_i[\varphi]\varphi_i} Z[J], \tag{1.16}$$

where we have used equations (1.10) and (1.7). Now we use the definition of generating function (1.4)

$$e^{-\sum_i J_i[\varphi]\varphi_i} Z[J] = \int \mathscr{D}\varphi P[\varphi] e^{\sum_i J_i[\varphi](\phi_i - \varphi_i)}, \tag{1.17}$$

at last we use equation (1.4) and the bare action definition (1.14) to get

$$e^{-\Gamma[\varphi]} = \int d\varphi e^{-S[\phi] + \sum_i \Gamma_i[\varphi](\phi_i - \varphi_i)}, \tag{1.18}$$

where $\Gamma_i[\varphi]$ is a short hand notation for $\frac{\partial \Gamma[\varphi]}{\partial \varphi_i}$. The last thing we are left to do is a shifting of the integration variables $\{\phi_i\} \to \{\chi_i\}$ with $\chi_i = (\phi_i - \varphi_i)$. The new random variables χ are such that $\langle \chi_i \rangle = 0 \, \forall \, i$. Finally the connection between the effective action and the bare action is,

$$\begin{aligned} e^{-\Gamma[\varphi]} &= \int \mathscr{D}\chi e^{-S[\varphi+\chi] + \sum_i \Gamma_i[\varphi]\chi_i}, \\ \Gamma_i[\varphi] &= \frac{\partial \Gamma[\varphi]}{\partial \varphi_i}. \end{aligned} \tag{1.19}$$

Let us now consider the correct field configuration φ^*, defined by (1.13), which represents the exact average of all the field components in absence of the currents $\{J\}$, latter equation

becomes

$$e^{-\Gamma[\varphi^*]} = \int \mathscr{D}\chi e^{-S[\varphi_* + \chi]} = Z[0], \tag{1.20}$$

thus we get a straightforward relation between the stationary effective action and the zero current $J = 0$ partition function,

$$\Gamma[\varphi^*] = -\log(Z[0]). \tag{1.21}$$

Thus the exact equilibrium free energy of the system is obtained from the *effective action* when evaluated in the stationary field configuration. All the connected correlation functions can be obtained from the effective action derivatives,

$$\sum_k G_{ik}\Gamma_{kl} = \delta_{il} \rightarrow G_{ik} = \Gamma^{-1}_{ik}. \tag{1.22}$$

Thus the second derivative of the effective action with respect to the field is noting but the propagator of the theory. We can construct all the connected correlations functions of the theory as sum of diagrams where the line represents the propagator and the vertexes are given by the n-th order derivatives of the effective action

$$\frac{\partial^n \Gamma}{\partial\varphi_{i_1}\cdots\partial\varphi_{i_n}} = \Gamma_{i_1\cdots i_n}. \tag{1.23}$$

For the three points connected correlation function we have

$$\langle\varphi_i\varphi_j\varphi_k\rangle_c = -\sum_{lmn} G_{il}G_{jm}G_{kn}\Gamma_{lmn}. \tag{1.24}$$

1.1.2 Saddle point approximation

It is in general not possible to exactly pursue the integral in equation (1.4) apart for few cases. Thus we rely on approximations, usually the convenience of field theoretical formalism, apart its generality, is the possibility to develop various consistent approximation tools. The most simple and popular one is the *saddle point approximation*, this technique is often not very precise and cannot give precise accounts of a variety of phenomena descending from the highly correlated distribution functions of most many body systems. However the simplicity and versatility of this tool make it the first choice to investigate physical systems.

Saddle point approximation consists in approximating the value of the integral in equation (1.4) with the maximum of its integrand. Then using definition (1.7) together with equation

(1.14) we obtain the saddle point free energy

$$W_0[J] = S[\varphi^*] - \sum_i J_i \varphi_i^* \tag{1.25}$$

where the value φ^* is defined by

$$\frac{\partial S[\varphi]}{\partial \varphi_i}\Big|_{\varphi^*} = J_i \; \forall \, i \tag{1.26}$$

with the obvious addition

$$\frac{\partial^2 S[\varphi]}{\partial \varphi_i \partial \varphi_j}\Big|_{\varphi^*} \geq 0 \; \forall \, i, j. \tag{1.27}$$

The effective action is readily obtained using Legendre transformation, if we redefine $\varphi \equiv \varphi_*$ the saddle point effective action becomes

$$\Gamma_0[\varphi] = S[\varphi], \tag{1.28}$$

the same result could be obtained starting from equation (1.19) using saddle point approximation.

1.1.3 Loop expansion

Saddle point approximation can be also obtained as the lowest order of *perturbative expansion*, or *loop expansion*. The main assumption of perturbative expansion is that field configurations ϕ different from the field expectation φ give only small contribution to the functional integral. This is equivalent to require that the fluctuation field is small compared to the expectation value φ

$$\frac{\chi}{\varphi} \sim \lambda^{\frac{1}{2}}, \tag{1.29}$$

with $\lambda \ll 1$. We can rescale the fluctuation field $\chi \to \sqrt{\lambda}\chi$, in such a way that $\chi \approx O(1)$ and any dependence of the actions on the fluctuation field will contain an appropriate power of the small parameter λ. Both the effective action and the bare action can be developed in a power series of the λ parameter,

$$\begin{aligned} S[\varphi + \sqrt{\lambda}\chi] = S[\varphi] + \sqrt{\lambda} S^{(1)}[\varphi]\chi + \frac{1}{2}\lambda S^{(2)}[\varphi]\chi^2 \\ + \frac{1}{6}\sqrt{\lambda}^3 S^{(3)}[\varphi]\chi^3 + \frac{1}{24}\lambda^2 S^{(4)}[\varphi]\chi^4 + O(\lambda^{\frac{5}{2}}). \end{aligned} \tag{1.30a}$$

$$\Gamma[\varphi] = S[\varphi] + \lambda\Gamma_1[\varphi] + \lambda^2\Gamma_2[\varphi] + O(\lambda^3). \tag{1.30b}$$

Let us compare the latter two equation term by term in order to clarify their meaning; the expansion for the bare action seem rather natural since it is nothing but Taylor expansion and $S^{(n)}[\varphi]\chi^3$ is a short hand notation for all the possible three order derivatives of the bare action in its variables multiplied by the appropriate power of the fields. On the other hand the expansion for the effective action can be easily justified considering the true meaning of statement (1.12), the careful reader has probably been little disappointed by it, since the χ are integration variable running over all possible real values, however the actual sense of that statement is rather simple, we assume that the integral in equation (1.9) gets contribution only from regions where (1.12) is valid due from a particular form of the integrand. Then in the $\lambda \to 0$ limit assumption (1.30b) can be satisfied only if $S[\varphi+\chi]$ has a sharp peak in $\chi = 0$, in such a way that the integral over the χ variables can be eliminated and saddle point approximation, equation (1.28), becomes exact.

The remaining part of the expansion contains only integer power of the λ parameter since the integration over the χ is over a symmetric set, then only even powers of an expansion of the integrand in (1.9) can give contribution to the effective action.

Inserting expansions (1.30a) and (1.30b) into equation (1.9) one gets

$$\begin{aligned}
&e^{-S[\varphi]-\lambda\Gamma_1[\varphi]-\lambda^2\Gamma_2[\varphi]+\cdots} \\
=&\int d\chi e^{-S[\varphi]-\sqrt{\lambda}S^{(1)}[\varphi]\chi-\frac{1}{2}\lambda S^{(2)}[\varphi]\chi^2-\frac{1}{6}\sqrt{\lambda}^3 S^{(3)}[\varphi]\chi^3-\frac{1}{24}\lambda^2 S^{(4)}[\varphi]\chi^4+\sqrt{\lambda}S^{(1)}[\varphi]\chi+\lambda^{3/2}\Gamma_1^{(1)}[\varphi]\chi+\cdots} \\
&e^{-\lambda\Gamma_1[\varphi]-\lambda^2\Gamma_2[\varphi]+\cdots} \\
=&e^{-\lambda\Gamma_1[\varphi]-\lambda^2\Gamma_2[\varphi]+\cdots} = \int d\chi e^{-\frac{1}{2}\lambda S^{(2)}[\varphi]\chi^2-\frac{1}{6}\lambda^{3/2}S^{(3)}[\varphi]\chi^3-\frac{1}{24}\lambda^2 S^{(4)}[\varphi]\chi^4+\lambda^{3/2}\Gamma_1^{(1)}[\varphi]\chi+\cdots}
\end{aligned} \tag{1.31}$$

Re-absorbing λ into the field χ and in the effective action, it is possible to develop the exponential on the r.h.s. of equation (1.31) into Taylor series. Only the quadratic term, $-\frac{1}{2}S^{(2)}[\varphi]\chi^2$, is left in the exponential since it allows for exact integration,

$$\begin{aligned}
e^{-\Gamma_1[\varphi]-\lambda\Gamma_2[\varphi]+\cdots} = \int d\chi e^{-\frac{1}{2}S^{(2)}[\varphi]\chi\chi}\Big[1 &- \frac{1}{6}\lambda^{1/2}S^{(3)}[\varphi]\chi\chi\chi + \lambda^{1/2}\Gamma_1^{(1)}[\varphi]\chi \\
&- \frac{1}{24}\lambda S^{(4)}[\varphi]\chi\chi\chi\chi + \lambda\Big(\frac{1}{6}S^{(3)}[\varphi]\chi\chi\chi + \Gamma_1^{(1)}[\varphi]\chi\Big)^2 + \cdots\Big].
\end{aligned} \tag{1.32}$$

Finally reminding that odd terms in the field χ would not contribute since the integral is on infinite set, we obtain the exponential of the effective action as a series in the λ parameter

where the coefficient are Gaussian correlation function of the fluctuation fields χ,

$$e^{-\Gamma_1[\varphi]-\lambda\Gamma_2[\varphi]+\cdots} = \int d\chi e^{-\frac{1}{2}S^{(2)}[\varphi]\chi\chi}\Big[1-\frac{1}{24}\lambda S^{(4)}[\varphi]\chi\chi\chi\chi+\lambda\Big(\frac{1}{6}S^{(3)}[\varphi]\chi\chi\chi+\Gamma_1^{(1)}[\varphi]\chi\Big)^2+O(\lambda^2)\Big]. \tag{1.33}$$

From latter expression in the $\lambda \to 0$ limit the *one loop* effective action is obtained

$$e^{-\Gamma_1[\varphi]} = \int d\chi e^{-\frac{1}{2}S^{(2)}[\varphi]\chi\chi}, \tag{1.34}$$

The last integral is a Gaussian integral and can be performed analytically, before this we only remind that we are using a short and notation of the type,

$$S^{(2)}[\varphi]\chi\chi \equiv \sum_{ij}\frac{\partial^2 S(\varphi_1,\cdots,\varphi_n)}{\partial\varphi_i\partial\varphi_j}\chi_i\chi_j. \tag{1.35}$$

Thus the $S^{(2)}[\varphi]$ is a n by n matrix and the result of the integral yield,

$$e^{-\Gamma_1[\varphi]} = \int d\chi e^{-\frac{1}{2}S^{(2)}[\varphi]\chi\chi} = \sqrt{\det S^{(2)}[\varphi]}^{-1}, \tag{1.36}$$

taking the logarithm on both sides and using the well known identity $\log\det M = Tr\log M$ we get

$$\Gamma_1[\varphi] = \frac{1}{2}Tr\log S^{(2)}[\varphi], \tag{1.37}$$

this equation is going to have a crucial role in all our subsequent discussion then we will often return on it.

For the moment let us notice that if we take the first order derivative with respect to any of the fields φ of both sides equation (1.15) we obtain,

$$\begin{aligned}
-\frac{\partial\Gamma_1[\varphi]}{\partial\varphi}e^{-\Gamma_1[\varphi]} &= -\frac{1}{2}\int d\chi S^{(3)}[\varphi]\chi\chi e^{-\frac{1}{2}S^{(2)}[\varphi]\chi\chi},\\
\frac{\partial\Gamma_1[\varphi]}{\partial\varphi} &= \frac{\frac{1}{2}\int d\chi S^{(3)}[\varphi]\chi\chi e^{-\frac{1}{2}S^{(2)}[\varphi]\chi\chi}}{e^{-\Gamma_1[\varphi]}}\\
\Gamma_1^{(1)}[\varphi] &= \frac{\frac{1}{2}\int d\chi S^{(3)}[\varphi]\chi\chi e^{-\frac{1}{2}S^{(2)}[\varphi]\chi\chi}}{\int d\chi e^{-\frac{1}{2}S^{(2)}[\varphi]\chi\chi}},\\
\Gamma_1^{(1)}[\varphi] &= S^{(3)}[\varphi]\langle\chi\chi\rangle,
\end{aligned} \tag{1.38}$$

which rewritten in explicit notation reads

$$\frac{\partial \Gamma_1[\varphi]}{\partial \varphi_k} = \sum_{ij} \frac{\partial^3 S[\varphi]}{\partial \varphi_i \partial \varphi_j \partial \varphi_k} \langle \chi_i \chi_j \rangle = \sum_{ij} \frac{\partial^3 S[\varphi]}{\partial \varphi_i \partial \varphi_j \partial \varphi_k} G_{ij}[\varphi]. \tag{1.39}$$

A more convenient notation is $\frac{\partial \Gamma_1[\varphi]}{\partial \varphi_k} = \Gamma^{(1)}_{1,k}[\varphi]$ and $\frac{\partial^3 S[\varphi]}{\partial \varphi_i \partial \varphi_j \partial \varphi_k} = S^{(3)}_{ijk}[\varphi]$ resulting in

$$\Gamma^{(1)}_{1,k}[\varphi] = \sum_{ij} S^{(3)}_{ijk}[\varphi] G_{ij}[\varphi]. \tag{1.40}$$

The latter equation has a straightforward expression using Feynman diagrams: the $S^{(3)}_{ijk}[\varphi]$ represent a three lines vertex, while the $G_{ij}[\varphi]$ represent a close line going from the open line i of the vertex to the open line j and one line remains open since the expression must still depend from the explicit index k. This pictorial representation is valid for every term on the r.h.s. of equation (1.36), since all the n field correlation functions of the fluctuation field χ are taken over a Gaussian distribution and can be obtained from all possible combination of two point functions $G_{ij}[\varphi]$, as it is stated by Wick's theorem. Thus at the n loop order we will have $n+2$ lines vertices which are nothing but the derivatives of the bare action with respect to the fields φ.

It can be also shown that only one particle irreducible Feynman diagrams contribute to the effective action, where for *one particle irreducible* diagrams we intend all those diagrams that cannot be reduced to disconnected one particles diagram cutting any internal line.

1.1.4 Ising model and φ^4 theory

Let us now show how can we apply the formalism depicted above on the case of spin systems on lattice. In order to use the above formalism we need continuous variables, then we use an Hubbard Stratonovic transformation to rewrite the partition function for the Ising model as an integral over continuous fields. The partition function for the Ising Hamiltonian reads [30]

$$\begin{aligned} Z &= \sum_{\{\sigma_i\}} e^{\sum_{ij} \frac{\beta}{2} J_{ij} \sigma_i \sigma_j + \sum_i \beta B_i \sigma_i}, \\ \sigma_i &\in \{-1, 1\}. \end{aligned} \tag{1.41}$$

where $\beta = T^{-1}$ is the inverse temperature and B is some external magnetic field.

The *Hubbard-Stratonovich transformation* reads

$$e^{\sum_{ij}\frac{J_{ij}}{2}\sigma_i\sigma_j} = \left((2\pi)^{n/2}\sqrt{\det K}\right)^{-1}\int \mathscr{D}\varphi e^{-\sum_{ij}\varphi_i\frac{J^{-1}_{ij}}{2}\varphi_j-\sum_i\sigma_i\varphi_i} \tag{1.42}$$

where n is the number of lattice sites and we assume the matrix J to be positively defined. Latter transformation is an obvious consequence of gaussian integrals. It is then possible to transform expression (1.41) and perform explicitly the sum over the spin variables $\{\sigma_i\}$

$$\begin{aligned}
Z &= \left(\frac{(2\pi)^{-n/2}}{\sqrt{\det J}}\right)\sum_{\{\sigma_i\}}\int d\varphi^{-\frac{1}{2\beta}\sum_{ij}\varphi_iJ^{-1}_{ij}\varphi_j+\sum_i(\varphi_i+\beta B_i)\sigma_i} \\
&= \left(\frac{(2\pi)^{-n/2}}{\sqrt{\det J}}\right)^{-1}\int d\varphi^{-\frac{1}{2\beta}\sum_{ij}\varphi_iJ^{-1}_{ij}\varphi_j}\sum_{\{\sigma_i\}}\Pi_i e^{(\varphi_i+\beta B_i)\sigma_i} \\
&= \left(\frac{(2\pi)^{-n/2}}{\sqrt{\det J}}\right)^{-1}\int d\varphi^{-\frac{1}{2\beta}\sum_{ij}\varphi_iJ^{-1}_{ij}\varphi_j}\Pi_i\cosh(\varphi_i+\beta B_i) \\
&= \left(\frac{(2\pi)^{-n/2}}{\sqrt{\det J}}\right)^{-1}\int d\varphi^{-\frac{1}{2\beta}\sum_{ij}\varphi_iJ^{-1}_{ij}\varphi_j+\sum_i\log\cosh(\varphi_i+\beta B_i)}.
\end{aligned} \tag{1.43}$$

This is noting but an explicit variable change which maps the Ising model into a lattice field theory

$$Z = \int d\varphi e^{-\frac{1}{2\beta}\sum_{ij}\varphi_iJ^{-1}_{ij}\varphi_j+\sum_i\log\cosh(\varphi_i+\beta B_i))}, \tag{1.44}$$

where we omitted the constant in front of the integral since it is not physically relevant. The action of the lattice field theory corresponding to an Ising model reads

$$S[\varphi] = \frac{1}{2\beta}\sum_{ij}\varphi_iJ^{-1}_{ij}\varphi_j + \sum_i\log\cosh(\varphi_i+\beta B_i), \tag{1.45}$$

let us now try to use the zero loop approximation, the so called tree level. We identify bare action (1.45) with zero order loop effective action $\Gamma_0[\varphi] = S[\varphi]$. Now according to our previous discussion we have that the average value of the field makes the effective action stationary,

$$\frac{\partial\Gamma_0[\varphi]}{\partial\varphi_i}\Big|_{\varphi^*} = \frac{\partial S[\varphi]}{\partial\varphi_i}\Big|_{\varphi^*} = \frac{1}{\beta}\sum_j J^{-1}_{ij}\varphi^*_j - \tanh(\varphi^*_i+\beta B_i) = 0. \tag{1.46}$$

The tree level approximation of the effective action method corresponds to the mean field solution of the Ising model [30]. At this approximation level we can also identify

$$\langle \sigma_i \rangle = m_i = \varphi^*. \tag{1.47}$$

It is always possible to go beyond mean field theory using the loop expansion technique outlined in previous subsection.

Perturbative expansion are however not useful in presence of a phase transition. Indeed it can be demonstrated that at the critical point of a second order phase transition assumption (1.29) does not hold and actually all the possible field configurations contribute to the functional integral (1.20). Perturbative techniques becomes useless in this condition and need to be revised and regularized by means of *renormalization group* (RG) [30] which will be introduced in the next section.

At this stage let us only note that we can do some clever manipulations to simplify (1.45). Introducing the fluctuation field χ and considering the $B = 0$ casewe get

$$\begin{aligned} Z &= \int d\chi e^{-\frac{1}{2}\sum_{ij}(\varphi_i^*+\chi_i)J_{ij}^{-1}(\varphi_j^*+\chi_j)+\sum_i \log\cosh(\varphi_i^*+\chi_i)} \\ &\propto \int d\chi e^{-\frac{1}{2}\sum_{ij}\chi_i J_{ij}^{-1}\chi_j+\sum_i \frac{\partial^2 \log\cosh(\varphi)}{\partial\varphi^2}\Big|_{\varphi=\varphi^*}\chi_i^2+\sum_i \frac{\partial^4 \log\cosh(\varphi)}{\partial\varphi^4}\Big|_{\varphi=\varphi^*}\chi_i^4} \\ &= \int d\chi e^{-\frac{1}{2}\sum_{ij}\chi_i J_{ij}^{-1}\chi_j-\sum_i \mu_i'\chi_i^2-\sum_i \frac{g'}{24}\chi_i^4}, \end{aligned} \tag{1.48}$$

where Taylor expansion of the $\log(\cosh(\phi))$ term has been employed. Now we assume that the matrix J_{ij}^{-1} only connects nearest neighbors. This is not generally true, even in the case of short range J_{ij}, but can be considered a first approximation level in the interaction strength. We are now ready to pass from lattice to continuous field theory.

$$\begin{aligned} J_{ij} &= -J\delta_{\langle ij\rangle}, \\ \{\chi_i\} &\to \chi(x), \\ a^d\sum_i &\to \int dx, \\ \chi_{i+1}-\chi_i &\to a\frac{d\chi(x)}{dx}. \end{aligned} \tag{1.49}$$

where a is the lattice spacing and $\langle ij \rangle$ are nearest neighbors. Using above substitutions and rescaling a factor $\frac{\beta J}{a^2}$ into the field definition we obtain

$$Z = \int \chi e^{-S[\chi]},$$

where

$$S[\chi] = \int dx \left\{ \frac{1}{2} \partial_\alpha \chi(x) \partial_\alpha \chi(x) + \frac{\mu}{2} \chi(x)^2 + \frac{g}{24} \chi(x)^4 \right\} \tag{1.50}$$

is the action of the Ginzburg Landau model [30]. In latter formula α is a spatial index and the summation over repeated indexes is intended.

The action (1.49) has been obtained from the exact lattice field theory of the Ising model (1.45) taking lowest order Taylor expansion in the fluctuation field χ and discarding non local interaction terms. These approximations have been demonstrated not to spoil the nature of the second order phase transition and the continuous field theory model defined by action (1.50) can be shown to be in the same universality class of the lattice Ising model. It is called *scalar φ^4 theory*.

1.2 Functional Renormalization Group

This section is aimed to introduce *functional renormalization group* (FRG) concepts to the reader, for a more complete description of the method one shall look at [19, 31, 32]. The FRG approach, which is known also as *non perturbative renormalization group* (NPRG) or *exact renormalization group* (ERG), is formally exact and that an exact solution of its core equation would lead to the complete partition function of the addressed system. However it is important to remark that there is, till now, no way to get an exact solution of the FRG equation. However the existence of an exact equation for the RG transformation allows for various systematic approximation technique, which, as shown in the following chapter, lead to a complete picture of second order phase transition in a unified and even simple formalism.

1.2.1 Effective action flow

Let us start with a few remarks, in previous chapter we make a large use of field theory formalism, however now we want explain how all the formal passage above can be translated into statistical physics. The partition function in (1.45) is, apart for obvious notation the same partition function of statistical field theory, thus the bare action $S[\phi]$ in the same equation (1.45) corresponds to the microscopic system Hamiltonian $H[\phi]$, on the same foot $W[J]$ in equation (1.7) is nothing but the free energy of the system, that of course will depend only on

the external fields J, which has been referred as the currents. Finally the effective action $\Gamma[\varphi]$ is the Legendre transform of the free energy $W[J]$ (1.10), thus it will depend on the internal system variables ϕ and has all the properties of an Helmholtz free energy.

For the Ising model of the first chapter the bare action will be the microscopic Hamiltonian appearing in (1.41) the field variables are the spin variables $\{\sigma_i\}$ and the currents are the value of the magnetic field at all lattice position $\{B_i\}$, while the field variable of the effective action will be the magnetization $\{m_i\}$ which is nothing but the spin average.

We will now build a family of running effective actions Γ_k which depend on a parameter k. The parameter k will represent an inverse scale $k \propto l^{-1}$ and the effective action Γ_k will play the role of an effective Hamiltonian at the scale k, i.e. will give the configuration energy of some effective variables build up to explicitly include all the fluctuations of the real microscopic variables at a scale $l' < l$.

The scale dependent effective action Γ_k shall satisfy

$$\begin{aligned} \Gamma_{k=\Lambda}[\varphi] &= S[\varphi], \\ \Gamma_{k=0} &= \Gamma[\varphi], \end{aligned} \tag{1.51}$$

the first statement requires that the first element of our effective action flow, which we will regard as the effective action at the microscopic scale $k = \Lambda \propto a^{-1}$, is equal to the bare action, while for $k = 0$ the flow will end in the exact effective action. These requirements lead to two important consequences:

- The first step of the effective action flow is noting but the tree level approximation for the effective action, i.e. the mean field. Thus our flow can be seen as an evolution of the effective action from its most crude approximation $k = \Lambda$ to the exact expression $\Gamma[\varphi]$ (notice that in the case of statistical field theory $\Lambda \propto a^{-1}$ is the inverse lattice spacing while for quantum field theories $\Lambda = \infty$).

- k labels the energy scale of the effective action $\Gamma_k[\varphi]$. When the scale is equal to the ultraviolet cutoff then the action $\Gamma_k[\varphi]$ is the bare action of the model, then lowering k means including in the action high energy modes, i.e. rapid modes $p > k$, leaving slow modes $p < k$ frozen; in the limit $k \to 0$ all the modes are integrated and $\Gamma_k[\varphi]$ becomes equal to the exact effective action.

Now we must explicitly generate this effective action flow. The basic idea of the FRG is that we will obtain the effective action at scale k not sharply cutting the integration in equation (1.20) or in (1.4) but slightly modifying the bare action $S[\phi] \to S[\phi] + \Delta S_k[\phi]$ in such a way that the new bare action will avoid the propagation of slow modes $p < k$.

Modifying the bare action means changing the physics of the system. Indeed any bare action allows for a particular set of field excitation ϕ_p which are characterized by a particular momentum p and by a mass m. In statistical field theory the mass represents the inverse correlation length $m \propto \xi^{-1}$ of the field excitations and parametrize the thermal fluctuation of a system. For large correlation length thermal field fluctuations are relevant, since long wavelength excitations will propagate coherently all over the system. In particular at criticality we have that the correlation length of the excitations goes to infinity (the mass goes to zero) then the low energy excitations, i.e. the slow modes $p \sim 0$, are excited by the presence of energy fluctuations and the distribution function of the system becomes highly correlated eventually leading to spontaneous symmetry breaking.

Thus adding an extra term $\Delta S_k[\varphi]$, which suppress the propagation of slow modes, to the bare action is equivalent to move in the theory space from a system which is close to criticality to a system with finite correlation length. The best way to avoid propagation of slow mode is adding to the bare action a mass term which depends on the excitations momentum, which should be large for low momenta $p < k$ and vanishes for high ones $p > k$.

This mass term is obviously quadratic in the field

$$\Delta S_k[\phi] = \frac{1}{2}\int d^d x \phi(x) R_k(\Delta)\phi(x) \tag{1.52}$$

where $R_k(\Delta)$ is a function of the Laplacian. The Laplacian expression can be changed in such a way to satisfy the covariant invariance of the model we are dealing with, for example we can choose,

$$\begin{aligned} &\Delta = -\partial^2, \\ &\Delta = -(\partial_\mu - eA_\mu)(\partial^\mu - eA^\mu), \end{aligned} \tag{1.53}$$

where the first choice is the common Laplacian operator while the second is the gauge invariant operator in presence of a electromagnetic field.

Equation (1.52) can be rewritten in Fourier space,

$$\Delta S_k[\phi] = \frac{1}{2}\int d^d p \phi_p R_k(p)\phi_p \tag{1.54}$$

where $\phi_p = \int d^d x e^{ipx}\phi(x)$ is the Fourier transform of the field. The choice (1.52) has been rather natural. The correlation function of the modified model with the cutoff action will have small ranges for values of p where $R_k(p)$ is large.

The regulator function $R(\Delta)$ in Fourier space is a function of the square momentum $z = p^2$ and it must satisfy some crucial rquirements,

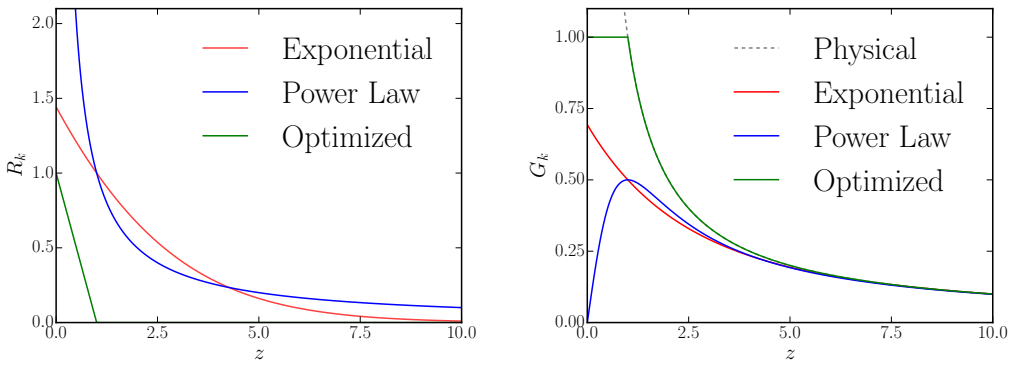

(a) Common regulator forms

(b) Regularized propagators

Fig. 1.1 In panel (a) we show the traditionally employed regulator shapes as a function of $z = q^2$ the power law regulator $R_k(z) = z^{-1}$, blue solid line, allows for analytical computation but is diverging in $q = 0$ and influences substantially the quality of the results. The exponential regulator $R_k(z) = z(e^{\log(2)z} - 1)^{-1}$, red solid line, does not allow analytic computation for the β-functions but produces nicely convergent numerical integrals. The optimized (Litim) regulator $R_k(z) = (1-z)\theta(1-z)$ produces nice analytical expression at simple approximation levels and has very good convergence properties since it modifies the propagator only on a small window of length k. In panel (b) the regularized propagators are shown for vanishing mass, the physical bare propagator is shown as a gray dashed line.

1. For $k = 0$ we must have $R_{k=0}(z) = 0 \forall z \in \mathbb{R}$ this ensures that in the zero k limit the effective action becomes the exact one for the original model.

2. For $k = \Lambda$ we shall remove all fluctuations and we must be at tree level $\Gamma_{k=\Lambda}[\varphi] = S[\varphi]$ thus the regulator function should diverge for all z values $R_{k=\Lambda}(z) = \infty \, \forall \, z \in \mathbb{R}$. However it is practically easier to choose $R_{k=\Lambda}(z) \sim \Lambda^2 \forall z \in \mathscr{R}$ which ensures only the condition $\Gamma_{k=\Lambda}[\varphi] \simeq S[\varphi]$.

3. For $0 < k < \Lambda$ the regulator function must be such that the rapid modes $z \gg k^2$ are almost unaltered, $R_k(z) \simeq 0$ if $z \gg k^2$ while the slow modes $z \ll k^2$ must have heavy masses, $R_k(z) \gg 1$ if $z \ll k^2$.

Many different choices exist for the regulator function and the results will crucially depend on this choice. One possible criterium is for selecting R_k is making the computation as easy as possibles . Some possible alternatives for R_k are shown in figure 1.1a for $k = 1$. All the functions are such that their value for $z = 0$ is proportional to k^2 while the typical width is of order k^2 this choice satisfies all the above requirements.

The running effective action is defined introducing the cutoff action (1.52) into the definition of effective action (1.20)

$$e^{-\Gamma_k[\varphi]} = \int d\chi e^{-S[\varphi+\chi]-\Delta S_k[\chi]+\int d^dx\Gamma_k[\varphi]\chi}.$$

One can think this is equivalent to take simply,

$$S[\varphi] \to S[\varphi] + \Delta S_k[\varphi]$$

this is however not the case. Indeed if we do the above substitution without any other care we would get by equation (4.3),

$$\Gamma_k[\varphi] = \int d^dxJ(x)\varphi(x) - W_k[J],$$

the latter equation is well behaved in the $k \to 0$ limit since it leads to the desired property $\Gamma_{k=0}[\varphi] = \Gamma[\varphi]$, but do not satisfy our second requirement

$$\lim_{k\to\Lambda} \Gamma_k[\varphi] = S[\varphi] + \Delta S_k[\varphi] \neq S[\varphi].$$

This is a consequence of not vanishing R_k in the $k \to \Lambda$ limit. Then it is not sufficient to include the regulator term (1.52) into the bare equation, but we shall also modify effective action definition. This can be achieved transforming equation (1.10) into

$$\Gamma_k[\varphi] + W_k[\varphi] = \int d^dx\varphi(x)J(x) - \frac{1}{2}\int d^dx\varphi(x)R_k(\Delta)\varphi(x), \tag{1.55}$$

if we use the latter equation instead of (1.10) to compute the current $J(x)$ we obtain,

$$J(x) = \frac{\delta\Gamma_k[\varphi]}{\delta\varphi(x)} + \int d^dxR_k(\Delta)\varphi(x). \tag{1.56}$$

Using latter equation rather than (1.11) and following the same derivation used for equation (1.20) we get to equation

$$e^{-\Gamma_k[\varphi]} = \int d\chi e^{-S[\varphi+\chi]-\Delta S_k[\chi]+\int d^dx\Gamma_k[\varphi]\chi(x)}, \tag{1.57}$$

which is exactly the relation we were looking for. The effective action flow obtained by latter equation fills both conditions (1.58).

1.2.2 Exact RG equation

It is now necessary to define an RG time $t = -\log(\frac{k}{k_0})$, where k_0 is the initial point of the flow and can be any value of the momentum, in general we consider the case $k_0 = \Lambda$ in such a way that the flow starts at $t = 0$ in $k = \Lambda$ and end in $t = \infty$ at $k = 0$.

From equation (1.57) we derive with respect to the RG time, $\frac{d}{dt} = \partial_t$

$$\begin{aligned}
\partial_t e^{-\Gamma_t[\varphi]} &= \int d\chi \partial_t \Big(-\Delta S_k[\chi] + \int d^d x \Gamma_k[\varphi]\chi(x)\Big) e^{-S[\varphi+\chi]+\Delta S_k[\chi]+\int d^d x \Gamma_k[\varphi]\chi(x)} \\
-\partial_t \Gamma_t[\varphi] &= \frac{1}{e^{-\Gamma_t[\varphi]}} \int d\chi \partial_t \Big(\Delta S_k[\chi]\Big) e^{-S[\varphi+\chi]+\Delta S_k[\chi]+\int d^d x \Gamma_k[\varphi]\chi(x)} \\
-\partial_t \Gamma_t[\varphi] &= -\frac{1}{2}\frac{1}{e^{-\Gamma_t[\varphi]}} \int d\chi \partial_t \Big(\int d^d x \chi(x) R_t(\Delta)\chi(x)\Big) e^{-S[\varphi+\chi]+\Delta S_k[\chi]+\int d^d x \Gamma_k[\varphi]\chi(x)} \\
\partial_t \Gamma_t[\varphi] &= \frac{1}{2}\frac{1}{e^{-\Gamma_t[\varphi]}} \int d\chi \int d^d x \chi(x) \partial_t R_t(\Delta)\chi(x) e^{-S[\varphi+\chi]+\Delta S_k[\chi]+\int d^d x \Gamma_k[\varphi]\chi(x)} \\
\partial_t \Gamma_t[\varphi] &= \frac{1}{2} \int d^d x \partial_t R_t(\Delta) \langle \chi(x)\chi(x)\rangle. \qquad (1.58)
\end{aligned}$$

First line is obtained by standard derivation, the second one is obtained by imposing that the term proportional to $\chi(x)$ vanish, since it is integrated on a symmetric domain. The third line descends from equation (1.52) and the derivative shall act only on the regulator function which depends explicitly on t. However we must remind that the cutoff function depends on the Laplacian of the field, thus when we write $\partial_t R_t(\Delta)$ we remark that it is an operator that acts on the two field over which the average is taken.

The derivative of the effective action with respect to the renormalization time is proportional to the two point function of the fluctuation field $\langle \chi(x)\chi(x)\rangle$. As demonstrated in A.2 this is the inverse second derivative of the effective action with respect to the fields,

$$\langle \chi(x)\chi(y)\rangle = G(x,y) = \frac{\delta^2 \Gamma_k[\varphi]}{\delta\varphi(x)\delta\varphi(y)}^{-1} \qquad (1.59)$$

where the minus one has to be intended in matrix space and the second derivative must be evaluated at the field value which makes the effective action stationary.

Applying latter equation to last calculation but keeping in mind that we are now using definition (1.55) rather than (1.10) for the effective action we finally get to functional renormalization group core equation, i.e. *the Wetterich equation*

$$\partial_t \Gamma_k[\varphi] = \frac{1}{2} \mathrm{Tr} \left(\frac{\partial_t R_t(\Delta)}{\frac{\partial^2 \Gamma_t[\varphi]}{\delta\varphi\delta\varphi} + R_t(\Delta)} \right), \qquad (1.60)$$

where we replaced the integral over the field index x with the trace symbol and we substitute the derivative in some field component $\delta\varphi(x)$ with the symbol of functional derivative $\delta\varphi$ since we can interpret the second derivative of the effective action as a matrix in the two field index, x and y in our case. The r.h.s. of equation (1.60) represents the trace of an operator over the space spanned by the field indexes.

Latter equation becomes more explicit in Fourier space. Indeed spatial coordinates is only one possible index for the field, while the equation is obviously valid whatever representation is employed.

$$\begin{aligned}
\partial_t\Gamma_t[\varphi] &= \frac{1}{2}\int d^dx\,\partial_t R_t(\Delta)\langle\chi(x)\chi(x)\rangle \\
&= \frac{1}{2}\int d^dx\,\partial_t R_t(\Delta)\langle\int\frac{d^dq}{(2\pi)^d}e^{-iqx}\chi_q\int\frac{d^dq'}{(2\pi)^d}e^{-iq'x}\chi_{q'}\rangle \\
&= \frac{1}{2}\int d^dx\int\frac{d^dq}{(2\pi)^d}\int\frac{d^dq'}{(2\pi)^d}e^{-iqx}\partial_t R_t(\Delta)e^{-iq'x}\langle\chi_q\chi_{q'}\rangle \\
&= \frac{1}{2}\int d^dx\int\frac{d^dq}{(2\pi)^d}\int\frac{d^dq'}{(2\pi)^d}e^{-i(q+q')x}\partial_t R_t(q'^2)\langle\chi_q\chi_{q'}\rangle \\
&= \frac{1}{2}\int d^dq\int\frac{d^dq'}{(2\pi)^d}\delta(q+q')\partial_t R_t(q'^2)\langle\chi_q\chi_{q'}\rangle \\
&= \frac{1}{2}\int\frac{d^dq'}{(2\pi)^d}\partial_t R_t(q'^2)\langle\chi_{-q'}\chi_{q'}\rangle
\end{aligned}$$

and equation (1.58) has been rewritten in momentum space,

$$\partial_t\Gamma_t[\varphi] = \frac{1}{2}\int\frac{d^dq}{(2\pi)^d}\partial_t R_t(q^2)\langle\chi_{-q}\chi_q\rangle. \tag{1.61}$$

It is instructive to reproduce the calculation which lead to equation (1.60) from latter equation. However to avoid excessive length we perform it for effective action definition (1.10) and only in the final result we re-introduce modified definition (1.55).

First of all we derive a useful relation between functional derivatives,

$$\begin{aligned}
\frac{\delta}{\delta\varphi_q} &= \int d^dx\frac{\delta\varphi(x)}{\delta\varphi_q}\frac{\delta}{\delta\varphi(x)}, \\
\frac{\delta\varphi(x)}{\delta\varphi_q} &= (2\pi)^{-d}\frac{\delta}{\delta\varphi_q}\int d^dq'e^{-iq'x}\varphi_{q'} = (2\pi)^{-d}e^{-iqx},
\end{aligned}$$

and thus we get

$$\frac{\delta}{\delta\varphi_q} = (2\pi)^{-d}\int d^d x e^{-iqx}\frac{\delta}{\delta\varphi(x)}, \tag{1.62}$$

Let us now restart from equation (1.22) which we rewrite in the case of continuous fields,

$$\int d^d y \Gamma^{(2)}(x,y)\, G(y,z) = \delta(x-z), \tag{1.63}$$

where $\Gamma^{(2)}(x,y) = \frac{\delta^2\Gamma[\varphi]}{\delta\varphi(x)\delta\varphi(y)}$. From this equation we can find a relation between the Fourier transforms,

$$\int d^d y \Gamma^{(2)}(x,y)G(y,z) = \delta(x-z)$$
$$\int \frac{d^d p}{(2\pi)^d}\int \frac{d^d p'}{(2\pi)^d}\int \frac{d^d q}{(2\pi)^d}\int \frac{d^d q'}{(2\pi)^d}\int d^d x e^{iqx}e^{iq'y}\Gamma^{(2)}(q,q')e^{ip'y}e^{ipz}G(p',p) = \delta(x-z)$$
$$\int \frac{d^d p}{(2\pi)^d}\int \frac{d^d p'}{(2\pi)^d}\int \frac{d^d q}{(2\pi)^d}\int \frac{d^d q'}{(2\pi)^d}\int d^d x e^{iqx}\Gamma^{(2)}(q,q')e^{i(p'+q')y}e^{ipz}G(p',p) = \delta(x-z)$$
$$(2\pi)^d\int \frac{d^d p}{(2\pi)^d}\int \frac{d^d p'}{(2\pi)^d}\int \frac{d^d q}{(2\pi)^d}\int \frac{d^d q'}{(2\pi)^d}e^{iqx}\Gamma^{(2)}(q,q')\delta(p'+q')e^{ipz}G(p',p) = \delta(x-z)$$
$$\int \frac{d^d p}{(2\pi)^d}\int \frac{d^d q}{(2\pi)^d}\int \frac{d^d q'}{(2\pi)^d}e^{iqx}\Gamma^{(2)}(q,q')G(-q',p)e^{ipz} = (2\pi)^d\int \frac{d^d p}{(2\pi)^d}\int \frac{d^d q}{(2\pi)^d}e^{iqx}e^{ipz}\delta(q+p)$$
$$\int \frac{d^d q'}{(2\pi)^d}\Gamma^{(2)}(q,q')G(-q',p) = (2\pi)^d\delta(q+p),$$

leading to

$$\Gamma^{(2)}(q,q')^{-1} = (2\pi)^{-2d}G(q,q') \tag{1.64}$$

which apart from a constant factor $(2\pi)^{-d}$ is the real space relation, even in this case the inverse is intended in matrix notation. The correlation function $G(q,q')$ is the two point function of the fields in Fourier space

$$\begin{aligned} G(q,q') &= \int d^d x \int d^d y e^{iqx}G(x,y)e^{iq'y} \\ &= \int d^d x \int d^d y e^{iqx}\langle\chi(x)\chi(y)\rangle e^{iq'y} \\ &= \langle\chi_q\chi_{q'}\rangle, \end{aligned}$$

while for the $\Gamma^{(2)}(q,q')$ we have

$$\begin{aligned}\Gamma^{(2)}(q,q') &= \int d^dx \int d^dy e^{iqx}\Gamma^{(2)}(x,y)e^{iq'y} \\ &= \int d^dx \int d^dy e^{iqx}\frac{\delta^2\Gamma[\varphi]}{\delta\varphi(x)\delta\varphi(y)}e^{iq'y} \\ &= (2\pi)^{2d}\frac{\delta^2\Gamma[\varphi]}{\delta\varphi_{-q}\delta\varphi_{-q'}}\end{aligned}$$

where the last equivalence comes from equation (1.62).

The desired relation is finally obtained

$$\left(\frac{\delta^2\Gamma[\varphi]}{\delta\varphi_{-q}\delta\varphi_{-q?}}\right)^{-1} = G(q,q') = \langle\chi_q\chi_{q'}\rangle, \tag{1.65}$$

as it happens in real space. From latter equation together with (1.61) we can rewrite equation (1.60) in Fourier space,

$$\partial_t\Gamma_t[\varphi] = \frac{1}{2}\int\frac{d^dq}{(2\pi)^d}\partial_t R_t(q^2)\left(\frac{\delta^2\Gamma[\varphi]}{\delta\varphi_q\delta\varphi_{-q}} + R_t(q^2)\right)^{-1}, \tag{1.66}$$

which has the same form as (1.60).

The Wetterich equation (1.60) is far from being a simple equation. Indeed it is a functional equation for $\Gamma_t[\varphi]$ which depends in a non linear way from the Hessian of the functional itself. The presence of the cutoff function in the non linear part guarantees that the equation is well behaved in the ultra violet (UV) limit $q \to \infty$ while the linear dependence in the regulator derivative protects from infra red (IR) divergences $q \simeq 0$. Therefore for $k \to 0$, due to the structure of $R_k(z)$ shown in figure 1.1, only the modes with $q \simeq k$ contributes to the integral on the r.h.s. of equation (1.66) and no IR divergences appear.

Let us describe equation (1.60) in details,

1. If our microscopic Hamiltonian $S[\phi]$ is invariant under some transformation S then our system is symmetric under the transformation $\mathscr{S}$. However it is necessary to ensure that the FRG procedure, and thus the flow equation, is also invariant under this transformation S. If we can find a mass term $\Delta S_k[\varphi]$ which is invariant under the transformation $\mathscr{S}$ then the effective action will be symmetric at all steps of the flow. It is not always possible to find such a symmetric regulator term, as it happens for gauge invariance where it is in general not possible to preserve the symmetry at each flow step.

2. We can rewrite equation (1.60) in another convenient way

$$\partial_t \Gamma_t[\varphi] = \frac{1}{2}\tilde{\partial}_t \,\mathrm{Tr}\log\left(\frac{\delta^2\Gamma_t[\varphi]}{\delta\varphi\delta\varphi} + R_t(\Delta)\right), \tag{1.67}$$

where the symbol $\tilde{\partial}_t = \partial_t R_t(\Delta)\frac{\partial}{\partial R_t[\Delta]}$ means that we derive only in the t dependence of the cutoff function and not on that of the effective action. We can integrate latter equation on t' from zero to a generic value t we get

$$\begin{aligned}
\int_0^t dt'\partial_{t'}\Gamma_{t'}[\varphi] &= \frac{1}{2}\int_0^t \tilde{dt}'\tilde{\partial}_{t'}\,\mathrm{Tr}\log\left(\frac{\delta^2\Gamma_{t'}[\varphi]}{\delta\varphi\delta\varphi} + R_{t'}(\Delta)\right)\\
\Gamma_t[\varphi] - S[\varphi] &= \frac{1}{2}\mathrm{Tr}\log\left(\frac{\delta^2\Gamma_t[\varphi]}{\delta\varphi\delta\varphi} + R_t(\Delta)\right) + \frac{1}{2}\mathrm{Tr}\log\left(\frac{\partial^2 S[\varphi]}{\delta\varphi\delta\varphi} + R_0(\Delta)\right)\\
\Gamma_t[\varphi] &= S[\varphi] + \frac{1}{2}\mathrm{Tr}\log\left(\frac{\delta^2\Gamma_t[\varphi]}{\delta\varphi\delta\varphi} + R_t(\Delta)\right),
\end{aligned}$$

last line is obtained since for $t = 0$ the $k = k_0 = \Lambda$ the effective action is equal to the microscopic Hamiltonian and the regulator should diverge at all q values, or at least should be very big. Then the last term on the right hand side of second line becomes a field independent (even if infinite) constant and can be omitted. Equation

$$\Gamma_t[\varphi] = H[\varphi] + \frac{1}{2}Tr\log\Big(\frac{\delta^2\Gamma_t[\varphi]}{\delta\varphi\delta\varphi} + R_t(\Delta)\Big), \tag{1.68}$$

is a one loop equation, indeed the term $\left(\frac{\delta^2\Gamma_t[\varphi]}{\delta\varphi\delta\varphi} + R_t(\Delta)\right)^{-1}$ is the full propagator G_t of the model and the equation is equivalent to (1.33) which is the effective action at one loop in perturbation theory. This shows that, in spite of its apparently complex form, equation (1.60) is much more simple than perturbation theory. Indeed at n-th order in perturbation theory it is necessary to compute n integrals, while from equation (1.68) we need just one integral to get to an exact result.

3. As we pointed out above due to the presence of the term $\partial_t R_t(\Delta)$ equation (1.60) is well behaved both in the ultra violet and in the infra red limit, then we can compute directly the flow of the couplings without worrying about possible divergences and thus avoiding regularization which is necessary in traditional RG procedures [30].

4. One very convenient feature of the effective action flow Γ_k is that R_k is an IR regulator. Then the system behaves as a finite volume system, which has no phase transition and has a continuous effective action, i.e. Gibbs free energy. This allows us to expand the

action in powers, without worrying about possible non analyticity of the free energy itself. At every finite k we have that the singularities of the effective action are lowered by the presence of the regulator and the order parameter of a phase transition builds up smoothly from a finite value of k down to $k = 0$.

1.3 Approximation methods

Since equation (1.60) cannot be solved exactly it is necessary to develop approximation procedures. FRG allows to recover within the same framework most of the approximations traditionally employed in field theory and critical phenomena, but it also admits standard technique to solve partial differential equations. The most common approximation methods are:

1. **Iterative solution**: it is possible to solve the equation iteratively, starting from a guess effective action $\Gamma_t^{(0)}[\varphi]$ substituting it in right hand side of equation (1.60) find the new effective action $\Gamma_t^{(1)}[\varphi]$ and the proceeding self consistently to the right solution. This approach even if, in principle, possible still lacks of practical implementations.

2. **Vertex expansion**: it consists in expanding the effective action in powers of the field in a similar way as done in standard pertrbative expansions.

3. **Derivative expansion**: it consist in expanding the effective action in powers of the spatial derivative of the field, i.e. the momentum. Such expansions shall contain all possible field terms which preserve the model symmetries.

1.3.1 Vertex expansion

Let us recall the definition of n points vertex,

$$\Gamma^{(n)}_{k,p_1,\cdots,p_n} = \frac{\partial^n \Gamma_k[\varphi]}{\partial \varphi^n}\Big|_{\varphi_1 \cdots \varphi_n} = \frac{\partial^n \Gamma_k[\varphi]}{\partial \varphi_{p_1} \cdots \partial \varphi_{p_n}}, \tag{1.69}$$

where for simplicity we are using the components of the field in Fourier space. We can obtain an infinite set of coupled equation for the vertexes defined above and from them reconstruct the effective action. Let us consider a particular field configuration φ^*, usually uniform, the effective action shall be rewritten as,

$$\Gamma_k[\varphi] = \sum_{n=0}^{\infty} \frac{1}{n!} \int \Pi_{i=1}^n dp_i \Gamma^{(n)}_{k,p_1,\cdots,p_n}\Big|_{\varphi^*} (\varphi_{p_1} - \varphi^*_{p_1}) \cdots (\varphi_{p_n} - \varphi^*_{p_n}). \tag{1.70}$$

An equation for any vertex in latter expression is obtained by deriving equation (1.60). One shall start from the full propagator definition,

$$G_k[\varphi] = \left(\frac{\partial^2 \Gamma_t[\varphi]}{\delta\varphi\delta\varphi} + R_t(\Delta) \right)^{-1}. \tag{1.71}$$

It is better to take this calculation completely since the functional nature of equation (1.60) can lead to misunderstandings. The term $\left(\frac{\partial^2 \Gamma_t[\varphi]}{\delta\varphi\delta\varphi} + R_t(\Delta) \right)^{-1}$ is an operator and it depends on two field configurations φ_A and φ_B, these are the directions at which we evaluate the second derivative. The trace symbol $\mathrm{Tr}(\cdots)$ means that we have to trace the operator over a complete basis. Now if we take the first derivative with respect to some field state φ_C of right hand side of equation (1.60) we must first derive the operator and then evaluate the trace of the derivative operator this is easily done,

$$\begin{aligned}
\frac{\partial}{\partial\varphi_p}\partial_t\Gamma_t[\varphi] &= \frac{1}{2}\frac{\partial}{\partial\varphi_p}\,\mathrm{Tr}\left[\left(\frac{\partial^2 \Gamma_t[\varphi]}{\delta\varphi\delta\varphi} + R_t(\Delta) \right)^{-1} \partial_t R_t(\Delta) \right] \\
\partial_t\Gamma^{(1)}_{t,p} &= -\frac{1}{2}\,\mathrm{Tr}\left[\left(\frac{\partial^2 \Gamma_t[\varphi]}{\delta\varphi\delta\varphi} + R_t(\Delta) \right)^{-1} \Gamma^{(3)}[\varphi] \left(\frac{\partial^2 \Gamma_t[\varphi]}{\delta\varphi\delta\varphi} + R_t(\Delta) \right)^{-1} \partial_t R_t(\Delta) \right] \\
\partial_t\Gamma^{(1)}_{t,p} &= -\frac{1}{2}\,\mathrm{Tr}\left[\sum_{q_1,q_2} \left(\frac{\partial^2 \Gamma_t[\varphi]}{\delta\varphi\delta\varphi} + R_t(\Delta) \right)^{-1} |q_1\rangle\langle q_1|\Gamma^{(3)}[\varphi]|q_2\rangle\langle q_2| \left(\frac{\partial^2 \Gamma_t[\varphi]}{\delta\varphi\delta\varphi} + R_t(\Delta) \right)^{-1} \partial_t R_t(\Delta) \right] \\
\partial_t\Gamma^{(1)}_{t,p} &= -\frac{1}{2}\int dq_1 dq_2 dq\, G_t(q,-q_1)\Gamma^{(3)}(q_1,-q_2,p)G_t(q_2,-q)\partial_t R_t(q)
\end{aligned}$$

where the $\sum_i |q_i\rangle\langle q_i|$ is the complete basis of all direction with respect of which the second derivative of the action can be evaluated.

The first vertex equation reads

$$\partial_t\Gamma^{(1)}_{t,p} = -\frac{1}{2}\int dq_1 dq_2 dq\, G_t(q,-q_1)\Gamma^{(3)}(q_1,-q_2,p)G_t(q_2,-q)\partial_t R_t(q) \tag{1.72}$$

this equation has very nice pictorial form. Since $G_t(q,-q_1)$ is the full propagator it can be represented as a thick line which carries momenta q and $-q_1$ this line ends on the q side in an insertion $\partial_t R_t(q)$ and on the other side in a three point vertex $\Gamma^{(3)}(q_1,-q_2,p)$; this vertex has three lines coming from it, one is occupied by the line propagator $G_t(q,-q_1)$ another is joined with the propagator $G_t(q_2,-q)$, thick line, which ends on the other side in the insertion $\partial_t R_t(q)$. The third line of the vertex is left open and carries a momentum p the result is obviously a one loop equation with an open line, as we can see in figure 1.2. Using diagrammatic representation it is easy to calculate the equation for any vertex.

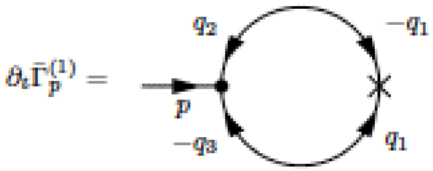

Fig. 1.2 Diagrammatic representation of the first vertex equation, as it is clear it is a one loop equation.

The equation for the n points vertex will depend on the the $n+1$ and $n+2$ points vertexes, thus we get an infinite tower of coupled equations. One solution strategy is eliminating some vertexes using physical consideration or approximation schemes. In this way one can get a closed set of equations. In $\mathbb{Z}_2$ symmetric filed theory we can set all the odd vertexes to zero. Then we can decide to neglect the 6 point vertex $\Gamma_k^{(6)}$ obtaining closed equations for $\Gamma_k^{(4)}$ and $\Gamma_k^{(2)}$, or we can make an ansatz rewriting $\Gamma_k^{(6)}$ as a function of $\Gamma_k^{(4)}$ and $\Gamma_k^{(2)}$. In both cases the scope is obtain a closed set of equations for the vertex functions. This kind of approximation is equivalent to neglect some high order dependence of the effective action on the fields, while retaining all the momentum dependence.

1.3.2 Derivative expansion

In statistical field theory we are mostly interested in the long range physics of a system $k \simeq 0$, since these modes are those driving the phase transition. Then the best approximation strategy is to drop high order momentum terms in the action, i.e. its dependence on the field derivative, focusing on full field dependence. This is obtained in derivative expansion by assuming the ansatz,

$$\Gamma_k[\varphi] = \int d^d x \left\{ U_k[\varphi] + \frac{1}{2} Z_k[\varphi] \partial_\mu \varphi \partial_\mu \varphi + O\left[\left(\partial_\mu \phi \right)^4 \right] \right\}, \tag{1.73}$$

where we again assumed that thanks to $\mathbb{Z}_2$ invariance the effective action depends only on even powers of the gradient.

One important property of derivative expansions is that we can systematically improve the by adding further derivative terms in the ansatz. Another crucial fact is that we can combine this approximation with the vertex approximation given in the previous paragraph.

If we expand both equations $U_k[\varphi]$ and $Z_k[\varphi]$ in powers of the field we get,

$$U_k[\varphi] = \sum_{n=0} \frac{1}{n!} g_k^{(2n)} \varphi(x)^{2n} \tag{1.74}$$

$$Z_k[\varphi] = \sum_{n=0} \frac{1}{n!} k_k^{(2n)} \varphi(x)^{2n}, \tag{1.75}$$

where obviously

$$g_k^{(2n)} = \frac{\partial^n U_k[\varphi]}{\partial \varphi^{2n}}\Big|_{\varphi^*}$$
$$k_k^{(2n)} = \frac{\partial^n Z_k[\varphi]}{\partial \varphi^{2n}}\Big|_{\varphi^*}.$$

It is quite remarkable that most of the qualitative properties of the Ising model phase transition and in general of the RG flow can be inferred even retaining just second and fourth order in the potential $U_k[\varphi]$ and only the zero order of the function $Z_k[\varphi]$. Latter procedure lead to constrain the RG flow to effective action of the form of φ^4 theories.

$$\Gamma_k[\varphi] = \int d^d x \left(\frac{1}{2} g_k^{(2)} \varphi(x)^2 + \frac{g_k^{(4)}}{24} \varphi(x)^4 + \frac{1}{2} \partial_\mu \varphi \partial_\mu \varphi \right), \tag{1.76}$$

Previous ansatz combined with equation (1.60) yields the running of the couplings in the Ginzburg Landau model as it is shown in the following chapter.

Chapter 2

Application to Spin Systems

In this chapter we will consider interacting spin systems, they can be obtained as straightforward generalization of the Ising model introduced in the previous chapter. These models describe a lattice of interacting N components spins of unit length.

$$H = \sum_{ij} \frac{J_{ij}}{2} S_i S_j \tag{2.1}$$

where the S_i variables are N components vectors which satisfy the condition $S_i^2 = 1$. In our treatment we will not consider directly Hamiltonian (2.1), but we will rather consider the equivalent $O(N)$ field theories.

The $O(N)$ models are probably the most celebrated field theoretical models, they have been subject to intense investigations all along the last 50 years and are currently an important testbed for theoretical and numerical methods. In the present chapter we will show how basic approximations of functional renormalization are able to reproduce the full phase diagram for $O(N)$ field theories irrespective of the numbers of field components N and of the dimension d at which they are studied. Also we will furnish numerical results for the critical exponents which are found to be in good agreement with more expensive numerical techniques.

The importance of these field theoretical models in condensed matter is out of doubt, indeed the partition function of $O(N)$ symmetric spin systems exactly maps over $O(N)$ field theories. As it is shown in appendix B.1 the partition function computed from Hamiltonian (2.1) is equivalent to the generator obtained from the action,

$$S[\varphi] = \sum_{ij} \frac{K_{ij}^{-1}}{2} \varphi_i \varphi_j + \sum_i U(\rho_i) \tag{2.2}$$

where φ_i is an N component vector and $\rho_i = \frac{1}{2}\varphi_i(x)^2$ is the $O(N)$ invariant. The action (2.2) is invariant under $O(N)$ rotation of the components of the φ_i vectors and it is thus an $O(N)$ invariant theory. The inverse in (2.2) is intended in the matrix sense and the interaction matrix $K_{ij} = \beta J_{ij} + \mu\,\delta_{ij}$ is positively defined, see appendix B.1.

The matrix K^{-1} can be expanded into tailor series

$$K^{-1} = \frac{\mathbb{1}}{\mu} + \sum_{k=0}^{\infty} (-1)^k \frac{J^k}{\mu^{k+1}} \tag{2.3}$$

as long as the eigenvalues of the matrix J are smaller than μ as it is ensured by the positiveness of the matrix K. The inverse temperature coefficient has been absorbed in the J definition.

Let us now turn on short range ferromagnetic interactions $J_{ij} = -J\delta_{\langle ij\rangle}$, where $J > 0$ and the Dirac's δ-function is such that the matrix J only connects first neighboring sites. Expression (2.3) contains all possible powers J^k, which thus connect each site with its k-th neighbor, then using mapping in appendix B.1 we cast a SR spin system into a non local discrete field theory. On the other hand, thanks to the universality phenomenon, we can discard the non locality of expression (2.2) and retain only the first order term of expansion (2.3) obtaining

$$S[\phi] = -J \sum_{\langle ij\rangle} \varphi_i \varphi_j + \sum_i U(\rho_i). \tag{2.4}$$

Latter expression describe a discrete field model with only first neighbors interactions and has the same universal behavior of the spin system in (2.1). Indeed universal quantities do not depend on the microscopic properties of the models such has the precise interaction form or on the lattice shape, but only on some macroscopic features like the dimension of the system and the symmetries of the action.

Finally thanks to the continuous limit introduced in (1.49) we obtain the continuous field theory

$$S[\phi] = \int d^d x \left\{ \frac{1}{2} \partial_\mu \varphi_i(x) \partial_\mu \varphi_i(x) + U(\rho) \right\} \tag{2.5}$$

where the old spatial index i has been substituted with the continuous variable x and the index i now runs over the internal field components $i \in 1, \cdots, N$. Summation over repeated indexes is intended.

2.1 Local Potential Approximation

In this section we will consider the Local Potential approximation (LPA) which will turn useful to get qualitative understanding of the phase diagram of $O(N)$ field theories. The simplicity of this approach and the reliability of its results make it a very good alternative to mean field approximation.

The LPA procedure works as follows: we choose a peculiar functional space parametrized by a finite numbers of parameters or functions, this functional space will be described by an *ansatz* for the effective action. Such theory space should contain both the mean field approximation for our model and the expected final form of the effective action, in such a way that, projecting equation (1.60) over this ansatz we find a finite set of solvable differential equations which represents the RG flow for the theory under consideration. We choose a simple form for the ansatz

$$\Gamma_k[\varphi] = \int d^d x \left\{ \frac{1}{2}\partial_\mu \varphi_i(x)\partial_\mu \varphi_i(x) + U_k(\rho) \right\}, \tag{2.6}$$

where summation over repeated indexes is intended. The ansatz has the same form of action (2.5) and describes the functional space of all actions with local field content $U(\rho) \equiv U(\rho(x))$. It corresponds to take only the lowest order approximation in the derivative expansion $Z_k[\varphi] = 1$ and only the second derivative of the field are present, this is due to $O(N)$ invariance.

In equation (1.60) it appears the trace of the inverse second derivative of the exact effective action, this quantity can be explicitly computed for actions of the form of ansatz (2.6). Thanks to translational invariance this computation is more easily done in Fourier space,

$$\partial_t \Gamma_k[\varphi] = \frac{1}{2}\frac{V}{(2\pi)^d}\,\mathrm{Tr}\int \frac{d^d q}{(2\pi)^d}\partial_t R_k(q)\left(\Gamma^{(2)}_{ij}(q,-q) + R_k(q)\right)^{-1}, \tag{2.7}$$

where the trace operator in equation (1.60) has been resolved into momentum integration and trace over internal field indexes.

$$\Gamma^{(2)}_{ij}(q,-q) = \left.\frac{\delta^2\Gamma_k[\varphi]}{\delta\varphi_i(q)\delta\varphi_j(-q)}\right|_{\varphi(x)=\varphi^*} \tag{2.8}$$

is the second derivative of the effective action with respect to the field, which, due to translational invariance, is evaluated at the homogeneous equilibrium configuration φ^*. Now we shall project equation (2.7) on the finite functional space described by ansatz (2.6). If we are in the constant field configuration $\varphi(x) = \varphi^* \ \forall\ x$ where φ^* is a constant, then the derivative will vanish and the space integration yields just a constant volume factor V, thus

the action becomes,

$$\Gamma_k[\varphi^*] = VU_k(\rho^*). \tag{2.9}$$

Using latter equation as a definition for $U_k(\rho)$ it is possible to write a flow equation for the local potential

$$\partial_t U_k(\rho^*) = \frac{1}{V}\partial_t \Gamma_k[\varphi^*] = \frac{1}{2}\,\mathrm{Tr}\int \frac{d^dq}{(2\pi)^d}\partial_t R_t(q)\left(\Gamma^{(2)}_{ij}(q,-q)+R_t(q)\right)^{-1}, \tag{2.10}$$

from here on we can forget the finite volume term. We shall now compute the theory propagator, i.e. the effective action second derivative,

$$\frac{\delta}{\delta\varphi_q} = \int \frac{d^dx}{(2\pi)^d}\, e^{-iqx}\frac{\delta}{\delta\varphi(x)}. \tag{2.11}$$

Using latter equation we get the relation

$$\Gamma^{(2)}_{ij}(q,-q) = \int \frac{d^dx}{(2\pi)^d} e^{-iqx}\int \frac{d^dx'}{(2\pi)^d} e^{-iq'x'}\Gamma^{(2)}_{ij}(x,x') \tag{2.12}$$

which has to be applied to ansatz (2.7).

The second derivative with respect to the field of effective action (2.7) is,

$$\frac{\delta\Gamma_t[\varphi]}{\delta\varphi_i(x)\delta\varphi_j(x')} = \frac{\delta}{\delta\varphi_j(x')}\left(\Delta\varphi_i(x)+U'_k(\rho)\right) = \left(-\Delta\delta_{ij}+U''_k(\rho)\right)\delta(x-x'), \tag{2.13}$$

where

$$U''_k(\rho) = \frac{\delta^2 U_k(\rho)]}{\delta\varphi_i(x)\delta\varphi_j(x)} = U^{(1)}(\rho)\delta_{ij}+\varphi_i\varphi_j U^{(2)}(\rho) \tag{2.14}$$

and the symbol Δ is the Laplacian operator. The presence of the term $\delta(x-x')$ in equation (2.13) comes from the assumption (2.6) which is local in the field. We shall now perform the Fourier transform in equation (2.12)

$$\begin{aligned}
\Gamma^{(2)}_{ij}(q,q') &= (2\pi)^{-2d}\int d^dx e^{-iqx}\int d^dx' e^{-iq'x'}\Gamma^{(2)}_{ij}(x,x') \\
&= (2\pi)^{-2d}\int d^dx e^{-iqx}\int d^dx' e^{-iq'x'}\left(-\Delta+U''_k(\rho)\right)\delta(x-x')\Big|_{\varphi(x)=\varphi^*} \\
&= (2\pi)^{-2d}\int d^dx e^{-i(q+q')x}\left(q'^2+U''_k(\rho)\right)\Big|_{\varphi(x)=\varphi^*} \\
&= (2\pi)^{-d}\delta(q+q')\left(q'^2+U''_k(\rho)\right)\Big|_{\varphi(x)=\varphi^*}
\end{aligned} \tag{2.15}$$

where we used the fact that the second derivative of the potential evaluated at constant field is independent from the coordinate x. From latter equation together with relation (2.14) we obtain the Hessian of the effective action

$$\Gamma^{(2)}_{ij}(q,-q) = \left[\left(q^2 + U^{(1)}(\rho)\right)\delta_{ij} + \varphi_i\varphi_j U^{(2)}(\rho)\right]\Big|_{\varphi(x)=\varphi^*} \tag{2.16}$$

In order to insert latter equation into (2.10) we shall specify the stationary state φ^*. Due to rotational invariance this state can be written as

$$\begin{aligned}\varphi_1 &= \sqrt{2\rho^*}\\ \varphi_i &= 0 \;\forall\; i \neq 1,\end{aligned} \tag{2.17}$$

indeed for $\rho^* = 0$ latter vector describes a state with zero magnetization, while $\rho^* = \frac{m^2}{2} \neq 0$ describe a state with finite average magnetization parallel to the 1 direction. The physical configurations with finite magnetization in other directions can be always rewritten using state (2.17). The flow equation for the potential reads

$$\partial_t U_k(\rho^*) = \frac{1}{2}\int \frac{d^dq}{(2\pi)^d}\partial_t R_k(q)\left(\frac{1}{q^2 + R_k(q) + U_k^{(1)}(\rho^*) + 2\rho^* U_k^{(2)}(\rho^*)} + \frac{(N-1)}{q^2 + R_k(q) + U_k^{(1)}(\rho^*)}\right). \tag{2.18}$$

Due to rotational invariance in real space of action (2.6) all the terms in the integrand of latter equation depend just on the square modulus of the momentum q, then we can perform the angular integral explicitly and write the integral in the variable $y = q^2$,

$$\partial_t U_k(\rho) = s_d \int \partial_t R_k(y)\left(\frac{1}{y + R_t(y) + m_g^2} + \frac{N-1}{y + R_t(y) + m_m^2}\right) y^{d/2-1}dy \tag{2.19}$$

where

$$s_d = \frac{2(\pi)^{d/2}\Gamma(d/2)^{-1}}{(2\pi)^d}, \tag{2.20}$$

$$m_m^2 = U^{(1)}(\rho), \tag{2.21}$$

$$m_g^2 = U^{(1)}(\rho) + 2\rho U^{(2)}(\rho), \tag{2.22}$$

and the * superscript has been omitted for convenience. We can rescale a geometrical factor into the definition of effective action and field, thanks to the transformation

$$\begin{aligned} \Gamma_k[\varphi] &\to \zeta\,\Gamma_k[\varphi], \\ \varphi &\to \sqrt{\zeta}\,\varphi, \end{aligned} \tag{2.23}$$

where imposing $\zeta = s_d$ we obtain

$$\partial_t U_k(\rho) = \int \partial_t R_k(y) \left(\frac{1}{y + R_t(y) + m_g^2} + \frac{N-1}{y + R_t(y) + m_m^2} \right) y^{d/2-1} dy. \tag{2.24}$$

We shall now choose an explicit form for the cutoff function, the most typically adopted are

$$R_k(y) = \begin{cases} \frac{y}{e^{\frac{y}{k^2}-1}} & \text{exponential regulator,} \\ \frac{k^{2b+2}}{y^b} & \text{power law regulator,} \\ (k^2-y)^b \theta(k^2-y) & \text{optimized regulator,} \end{cases} \tag{2.25}$$

where b is a free integer parameter useful when higher spatial derivatives are included in ansatz (2.6), while, in our simple LPA case, it is sufficient to choose $b = 1$. It is interesting to show the shape of the integrand in equation (2.24) in the various regulator cases listed above (2.24), see Fig. 2.1. Fig. 2.1 shows how the presence of a typical cutoff function leads to the decoupling of slow modes from the effective action.

The optimized (or Litim regulator) is known to yield the best possible results at lowest order in derivative expansion and it also allow for analytic derivation of the flow equations. We thus choose

$$R_k(z) = (k^2 - y)\theta(k^2 - y), \tag{2.26}$$

we can now perform the integral in equation (2.23) explicitly,

$$\begin{aligned} &\int y^{d/2-1} dy \frac{\partial_t R_k(y)}{y + R_k(z) + m^2} \\ &\int y^{d/2-1} dy \frac{2k\theta(k^2-y)}{y + (k^2-z)\theta(k^2-z) + m^2} \\ &\int_0^{k^2} y^{d/2-1} dy \frac{2k}{y + (k^2-z) + m^2} \\ &\int_0^{k^2} y^{d/2-1} dy \frac{2k}{k^2 + m^2} \end{aligned} \tag{2.27}$$

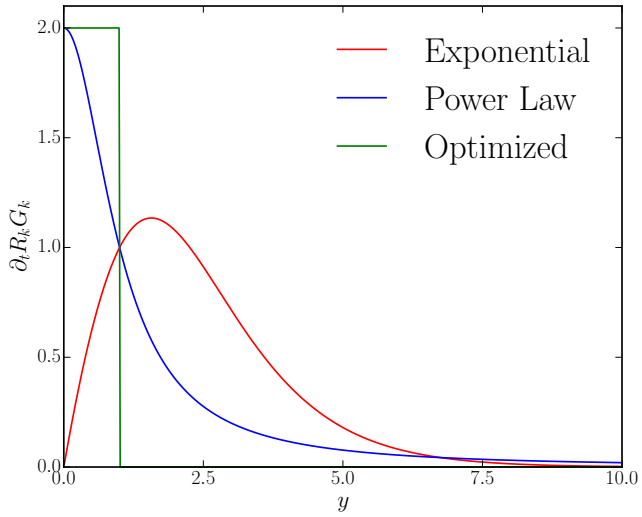

Fig. 2.1 Typical integrand in equation (2.24) , as it easy to see only a window of momenta around k contributes to the flow of the potential. The constants are $k = 1$ and $m_g^2 = m_m^2 = 0$.

and we get to the very simple expression,

$$\partial_t U_k(\rho) = -\frac{k^{d+2}}{k^2 + U_k^{(1)}(\rho) + 2\rho\, U_k^{(2)}(\rho)} - \frac{(N-1)k^{d+2}}{k^2 + U_k^{(1)}(\rho)}, \tag{2.28}$$

where an overall factor as been rescaled using again transformation (2.22).

Equation (2.19) describes the flow of the effective local potential under RG transformation. In order to obtain the critical properties of the system we shall impose scale invariance of the effective action. Indeed at the critical point the correlation length diverges and we expect the free energy of the system to become invariant under RG transformation. We shall then require

$$[\Gamma_k[\varphi]] = [k]^0, \tag{2.29}$$

where the external square brackets stand for the scaling dimension of the object inside. Assuming scale invariance of the kinetic terms in equation (2.6) one gets

$$\begin{aligned} [\rho] &= [k]^{\frac{d-2}{2}} \\ [U_k] &= [k]^d \end{aligned} \tag{2.30}$$

thus we define all the rescaled, or dimensionless, variables,

$$\begin{aligned}
&\tilde{y} = \tilde{q}^2 = \frac{q^2}{k^2} = e^{2t} q^2. \\
&\tilde{R}_k(y) = k^{-2} R_k(y) = e^{2t} R_k(y) = \tilde{y} r(\tilde{y}). \\
&\tilde{\rho} = k^{2-d} \rho = e^{(d-2)t} \rho. \\
&\tilde{U}_k = k^{-d} U_k = e^{dt} U_k.
\end{aligned} \tag{2.31}$$

In order to rewrite equation (2.23) in terms of dimensionless variables is necessary to rewrite the derivatives as follows

$$\frac{\partial}{\partial t}\Big|_{\rho} = \frac{\partial}{\partial t}\Big|_{\tilde{\rho}} + (d-2)\tilde{\rho}\frac{\partial}{\partial \tilde{\rho}}, \tag{2.32}$$

$$\frac{\partial}{\partial t}\Big|_{y} = \frac{\partial}{\partial t}\Big|_{\tilde{y}} + 2\tilde{y}\frac{\partial}{\partial \tilde{y}}. \tag{2.33}$$

Using these relations into equation (2.26) we obtain

$$\begin{aligned}
&\partial_t e^{dt} \tilde{U}_t(\tilde{\rho}) + (2-d)\tilde{\rho} U_t^{(1)}(\tilde{\rho}) = \int y^{d/2-1} dy \frac{\left(\partial_t e^{-2t} \tilde{R}_k(\tilde{y}) + 2e^{-2t}\tilde{y}\frac{\partial \tilde{R}_t(\tilde{y})}{\partial \tilde{y}}\right)}{\tilde{y} + R_t(y) + m_m^2} \\
&e^{dt}\left(\partial_t \tilde{U}_t(\tilde{\rho}) - d\tilde{U}_t(\tilde{\rho}) - (2-d)\tilde{\rho}\tilde{U}_t^{(1)}(\tilde{\rho})\right) = \int y^{d/2-1} dy \frac{\left(\partial_t e^{-2t}\tilde{y} r(\tilde{y}) + 2e^{-2t}\tilde{y}\frac{\partial \tilde{y} r(\tilde{y})}{\partial \tilde{y}}\right)}{\tilde{y} + R_t(y) + m_m^2} \\
&e^{dt}\left(\partial_t \tilde{U}_t(\tilde{\rho}) - d\tilde{U}_t(\tilde{\rho}) - (2-d)\tilde{\rho}\tilde{U}_t^{(1)}(\tilde{\rho})\right) = \int y^{d/2-1} dy \frac{e^{-2t}\left(2\tilde{y} r(\tilde{y}) - 2\tilde{y} r(\tilde{y}) - 2\tilde{y}^2\frac{\partial r(\tilde{y})}{\partial \tilde{y}}\right)}{\tilde{y} + R_t(y) + m_m^2} \\
&e^{dt}\left(\partial_t \tilde{U}_t(\tilde{\rho}) - d\tilde{U}_t(\tilde{\rho}) - (2-d)\tilde{\rho}\tilde{U}_t^{(1)}(\tilde{\rho})\right) = \int y^{d/2-1} dy \frac{-2\tilde{y}^2\frac{\partial r(\tilde{y})}{\partial \tilde{y}}}{\tilde{y} + \tilde{R}_t(\tilde{y}) + m_m^2} \\
&\partial_t \tilde{U}_t(\tilde{\rho}) = d\tilde{U}_t(\tilde{\rho}) - \frac{d-2}{2}\tilde{\rho}\tilde{U}_t^{(1)}(\tilde{\rho}) - \int \tilde{y}^{d/2-1} d\tilde{y} \frac{\tilde{y}^2\frac{\partial r(\tilde{y})}{\partial \tilde{y}}}{\tilde{y} + \tilde{R}_t(\tilde{y}) + m_m^2} \\
&\partial_t \tilde{U}_t(\tilde{\rho}) = d\tilde{U}_t(\tilde{\rho}) - (2-d)\tilde{\rho}\tilde{U}_t^{(1)}(\tilde{\rho}) - \int \tilde{y}^{d/2+1} d\tilde{y} \frac{\frac{\partial r(\tilde{y})}{\partial \tilde{y}}}{\tilde{y} + \tilde{R}_t(\tilde{y}) + m_m^2}.
\end{aligned} \tag{2.34}$$

where for simplicity the above calculation has been carried out with $N = 1$. The FRG equation for the dimensionless potential reads

$$\partial_t \tilde{U}_t(\tilde{\rho}) = d\tilde{U}_t(\tilde{\rho}) - (d-2)\tilde{\rho}\tilde{U}_t^{(1)}(\tilde{\rho}) - \int \tilde{y}^{d/2+1} d\tilde{y} \left(\frac{r'(\tilde{y})}{\tilde{y} + \tilde{R}_t(\tilde{y}) + \tilde{m}_m^2} + \frac{(N-1)r'(\tilde{y})}{\tilde{y} + \tilde{R}_t(\tilde{y}) + \tilde{m}_g^2}\right), \tag{2.35}$$

while the expression in the Litim regulator case is,

$$\partial_t \tilde{U}_k(\tilde{\rho}) = d\tilde{U}_t(\tilde{\rho}) - (d-2)\tilde{\rho}\tilde{U}_k^{(1)}(\tilde{\rho}) + \frac{1}{1+\tilde{U}_k^{(1)}(\tilde{\rho})+2\tilde{\rho}\tilde{U}_k^{(2)}(\tilde{\rho})} + \frac{N-1}{1+\tilde{U}_k^{(1)}(\tilde{\rho})}. \quad (2.36)$$

2.2 Truncation schemes and Mermin Wagner theorem

The state introduced in (2.17) is well suited to describe phase transitions where spontaneous symmetry breaking occurs (SSB). Indeed for $\rho = 0$ the state is symmetric under $O(N)$ rotations of the field components, while for $\rho \neq 0$ the state is polarized along the first direction, even if the action of the system (2.6) is rotational invariant. SSB is a cornerstone concept in a variety of systems, from field theory and particle physics to statistical mechanics and interacting lattice models. The study of the occurrence of SSB play a crucial role in the theory of phase transitions and in the characterization of ordered phases and it highlights the interplay between SSB and the dimensionality of the system: this interplay is customarily expressed by defining a lower critical dimension d_L for which SSB cannot occur [20].

A celebrated exact result connecting SSB and dimensionality is provided by the Mermin-Wagner theorem [33–35]. According to the Mermin-Wagner theorem a continuous symmetry cannot be spontaneously broken in two dimensions: $d_L = 2$. This theorem has been formulated for classical systems [33] and then extended to quantum systems [34, 35]. For magnetic systems with continuous symmetry it rules out the possibility of having a non vanishing magnetization at finite temperature in two dimensions, and for $2d$ interacting Bose gases predicts that no Bose-Einstein condensation occurs at finite temperature [34]. As well known, even though the Mermin-Wagner theorem rules out SSB and the existence of a local order parameter in two dimensions, nonetheless the Berezinskii-Kosterlitz-Thouless transition may yet occur for the $U(1)$ symmetry and it signaled by the algebraic behaviour of correlation functions in the low temperature phase [36].

The Mermin-Wagner theorem for the $O(N)$-symmetric scalar field theory states that for $N \geq 2$ in two dimensions no SSB occurs. Although originally formulated in integer dimensions, this result was later extended to graphs with fractional dimensions [37]: in this way one can explicitly show that for $N \geq 2$ there is no SSB for $d \leq 2$, with d being real, while SSB occurs for $d > 2$ [38]. In [24] the study of how $O(N)$ universality classes depend continuously on the dimension d (and as well on N), in particular for $2 < d < 3$ was recently presented. The Ising model, i.e. the $N = 1$ case, is different from $O(N)$ models with continuous symmetry ($N \geq 2$) because the symmetry is discrete: in two dimensions it notoriously has a finite temperature phase transition [7] and it can be shown that this happens

for $d \geq 2$ with d real [39]. The large N-limit of $O(N)$ models is also interesting because for $N \to \infty$ it is equivalent to the spherical model [40], which is exactly solvable [41].

In the FRG framework one has to solve an integro-differential equation valid for functionals which is usually handled resorting to approximations. It is in general of great importance to know "how good" are the used approximations and to test them against exact results. An approximation commonly used is the Local Potential Approximation (LPA), in which the wave-function renormalization and higher derivative terms in the effective action are discarded, resulting in a vanishing anomalous dimension [19, 31, 42–45]. Furthermore, one often treats LPA introducing further approximations via the introduction of a finite number of couplings, defined as the Taylor coefficient of an expansion of the potential around the zero (or the minimum) of the field, and studying their renormalization group (RG) flow.

In this section our goal is two-fold: *i)* from one side we aim at discussing what level of approximation is needed to reproduce the Mermin-Wagner theorem and to show that no SSB occurs for $d \leq 2$ with d real and $N \geq 2$, *ii)* from the other we intend to investigate how truncation affects the occurrence or non occurrence of SSB comparing/contrasting the obtained findings with the exact prediction of the Mermin-Wagner theorem. Our findings for systems with continuous symmetry can be summarized as follows:

- *i)* LPA, when treated exactly, is enough to reproduce the Mermin-Wagner theorem;
- *ii)* defining the couplings as the coefficients of a Taylor expansion of the effective potential centered in the zero, we have that, for any finite number of couplings in LPA, SSB appears also when it should not (i.e., for $d \leq 2$), and the corresponding (spurious) Wilson-Fisher fixed points lie on the line defined by vanishing mass beta functions. On the other hand using a Taylor expansion of the potential around the minimum we can recover Mermin-Wagner theorem even for finite number of couplings.

For the Ising model ($N = 1$) the SSB occurs for $d > 2$, again in agreement with exact results. We will also discuss in detail the limit $N \to \infty$ (the spherical model), where LPA provides exact results for the critical exponents, due to vanishing anomalous dimension (the question of exactness of large N LPA equation was raised in [46] and then fully understood in [47]).

The solution of the RG equation (2.36) sometimes requires further approximations: e.g., in case of the $O(N)$ symmetric scalar field theory the potential can be expanded in powers of the field variable around zero (with a truncation at the power $N_{\rm CUT}$).

The Taylor expansion of the dimensionless effective potential around zero reads as

$$\tilde{U}_k(\tilde{\rho}) = \sum_{n=1}^{N_{\rm CUT}} \frac{1}{n!} g_n(k)\, \tilde{\rho}^n. \tag{2.37}$$

2.2.1 The truncated $O(N)$ model ($N < \infty$, $N_{\rm CUT} < \infty$)

Truncation around the zero field

Let us first demonstrate the existence of SSB in the expanded O(N) model with finite $N_{\rm CUT}$ and finite N.

Let consider to start with the simplest case: two couplings ($N_{\rm CUT} = 2$) for the Ising case ($N = 1$) in $d = 1$. The RG flow equations for the couplings can be derived from (2.37) and read in this case

$$\partial_t g_1 = -2g_1 - \frac{1}{\pi}\frac{g_2}{(1+g_1)^2} \tag{2.38}$$

$$\partial_t g_2 = -3g_2 + \frac{6}{\pi}\frac{g_2^2}{(1+g_1)^3} \tag{2.39}$$

which is obtained by using the Litim regulator. Similar equations are obtained for general N, d and $N_{\rm CUT}$ (not reported here). In 2.2 the RG flow diagram obtained from equations (2.38) and (2.39) for the $1d$ $O(N = 1)$ model with two couplings ($N_{\rm CUT} = 2$) for $d = 1$. The model does not have any phase transition at finite temperature [7], however a Wilson-Fisher (WF) fixed point is clearly visible in 2.2.

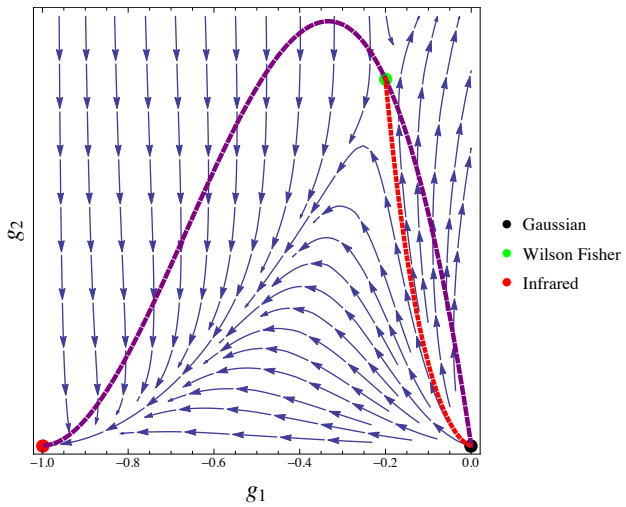

Fig. 2.2 Phase diagram of the $O(N = 1)$ model for $d = 1$ dimensions obtained by the numerical solution of the RG equations for two dimensionless couplings ($N_{\rm CUT} = 2$) using the Litim regulator. Arrows indicate the direction of the flow. The red (dotted) line shows the separatrix and the purple (dashed) line stands for the vanishing mass beta function curve. The Gaussian (black), the Wilson-Fisher (green) and the IR convexity (red) fixed points are also shown.

The important point we want to stress is that flow diagrams similar to the one depicted in 2.2 can be obtained for any finite N and any finite $N_{\rm CUT}$ for dimensions $1 \leq d < 4$ (by using any regulator functions). In $d = 4$, the WF fixed point (green dot in 2.2) merges to the Gaussian one (black). The IR fixed point (red) appears in any dimensions and is related to the convexity of the potential [48–52].

Although one finds similar flows for $d \leq 2$ and $d > 2$, there is of course an important difference between the two cases. For $d \leq 2$the appearance of SSB is not allowed by the Mermin-Wagner theorem, but 2.2 clearly signals the presence of SSB: the red curve from the Gaussian to the WF fixed points separates the phases and the RG trajectories run to the IR fixed point corresponds to the symmetry broken phase. (More comments on the $N = 1$ will be given in the following.)

The WF fixed point is situated on the dashed purple line in 2.2 which is determined by the vanishing mass beta function (to which we will refer as the VMB curve). Indeed, from equations (2.38) and (2.39) one finds

$$g_2 = -2\pi g_1 (1 + g_1)^2 \tag{2.40}$$

which depends on g_1 and does not depend on higher order couplings even if $N_{\rm CUT}$ is increased. As a consequence, the VMB curve on the g_1, g_2 plane remains unchanged for *any* finite value of $N_{\rm CUT}$. Another important observation is that any fixed point should be situated on the VMB curve (by definition). The role of the VMB curve at LPA level was recently discussed in [25] in connection to the FRG determination of the central charge in $d = 2$.

The position of the WF fixed point on the VMB curve depends on $N_{\rm CUT}$. Similar VMB curves can be drawn for any regulator function with the same properties, as shown in 2.3 by projecting on the (g_1, g_2)-plane and applying the so called Litim-like regulator class. Using the notation of Appendix B.2, this regulator class corresponds to various values of the parameter h but with $b = 1$ ($h = 1$, $b = 1$ is just the Litim regulator):

$$r = \left(\frac{1}{y} - h \right) \Theta(1 - hy), \tag{2.41}$$

the regulator (2.39) is obtained by taking the $c \to 0$ limit in (B.22).

We observe that the position of the Gaussian fixed point is scheme-independent and thus the VMB curves always start form zero and go through the scheme-dependent IR fixed point.

We found and verified that plots qualitatively similar to 2.3 are obtained for general N and $1 \leq d \leq 2$ (with d real): in these cases the WF fixed points corresponding to the different regulators for increasing $N_{\rm CUT}$ tend to the (respective) IR fixed points. This has to be contrasted with the situation in $d = 3$ (or more generally for real $d \geq 2$), as it is shown

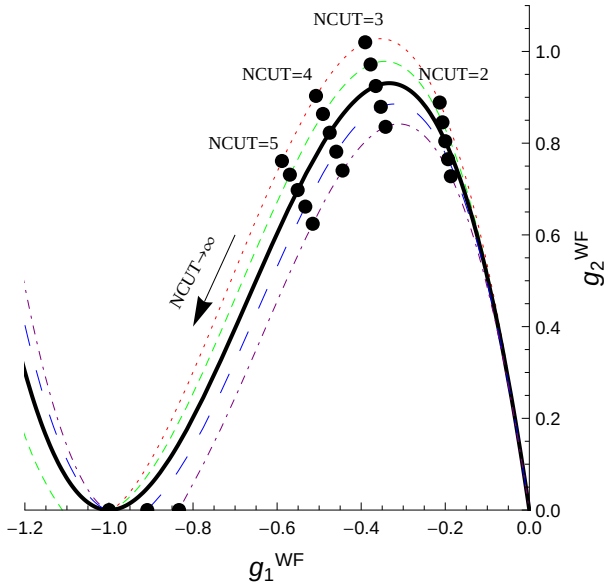

Fig. 2.3 Position of the WF fixed point on the VMB curves for the $O(N=1)$ model in $d=1$ for various values of N_{CUT}. Different lines correspond to different regulators, i.e. $0.8 < h < 1.2$ is chosen in (2.41). The solid line corresponds to $h=1$, i.e. to the Litim regulator. The IR fixed point remains unchanged if $h \leq 1$.

in 2.4: namely, for increasing values of N_{CUT} the WF fixed points does not tend to the IR ones as for $d=1$, but tend to constant (non trivial) WF fixed points for $d=3$, as indicated in 2.21. These non trivial WF fixed points can be computed for $N_{\mathrm{CUT}} \to \infty$, i.e. treating exactly LPA, using the spike plot method [18, 24]. Clearly, the position of these non trivial WF fixed points depend on the choice of the regulator.

Again, the scenario presented in 2.4 is the same to what happens for general N and $2 < d < 4$. In order to illustrate this we plot the dependence of g_1 (2.5) and g_2 (2.6) on the truncation parameter N_{CUT} for $d=1$ and $d=3$ for three different values of N.

Let us come back to our truncation (2.37) every coupling can be defined as

$$\frac{d^n \tilde{U}_k(\tilde{\rho})}{d\tilde{\rho}^n}\Big|_{\tilde{\rho}=0}, \tag{2.42}$$

using the same method we used above to derive the flow of the mass and of the interaction we can find the flow equation for every coupling in the field expansion of the potential which is nothing but an equation for the β functions,

$$\beta_n = \frac{\partial^n \partial_t \bar{U}_k(\tilde{\rho})}{\partial \tilde{\rho}^n}\Big|_{\tilde{\rho}=0}. \tag{2.43}$$

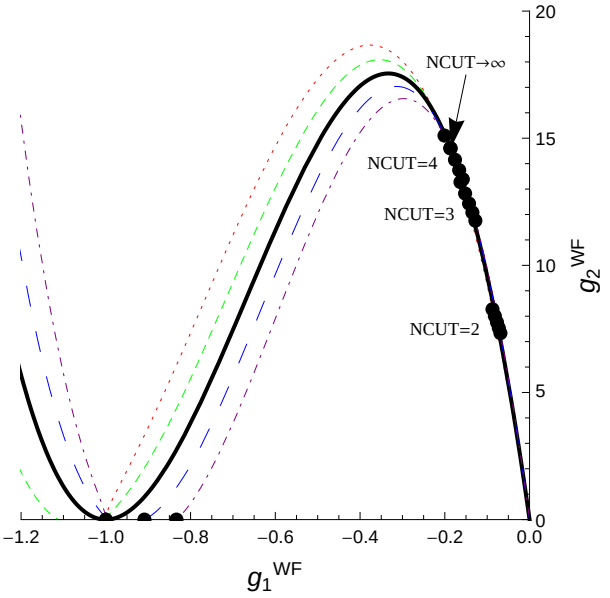

Fig. 2.4 Position of the WF fixed point on the VMB curves for the $O(N=1)$ model in $d=3$ for various values of N_{CUT}. Different lines correspond to different regulators, i.e. $0.8 < h < 1.2$ is chosen in (2.41) as in 2.3. The $N_{\mathrm{CUT}} \to \infty$ WF fixed point (shown for the Litim regulator) is computed using the spike plot method [18, 24].

Using latter equation together with equation (2.36) we can compute an infinite set of tied equation, which describe the flow of all possible couplings for a $O(N)$ invariant theory. This set is obviously not closed and once again different approximations rely in different way of truncating the equations in order to get a complete set. Once this has been done it is possible to solve the equations and obtain the fixed points$\{\lambda_n^*\}$ and then linearize the previous system around those fixed points. Latter procedure defines the stability matrix

$$M_{mn} = \frac{\partial \beta_n}{\partial \lambda_m}\bigg|_{\{\lambda_n^*\}}. \tag{2.44}$$

The correlation length is given by the inverse largest eigenvalue of latter matrix

$$\nu = \lambda_{max}^{-1}. \tag{2.45}$$

When we truncate the equations set obtained from equation (2.43) we obtain some spurious effect. The most relevant is that we can have more fixed points than those that must be in our theory, this problem is common to every polynomial truncation, where the number of zeroes is equal to the polynomial grade and it is not that of the approximated function. Thus we need a method to enumerate all possible fixed point in our theory space, this can be done rather simple in FRG using the arguments of [53].

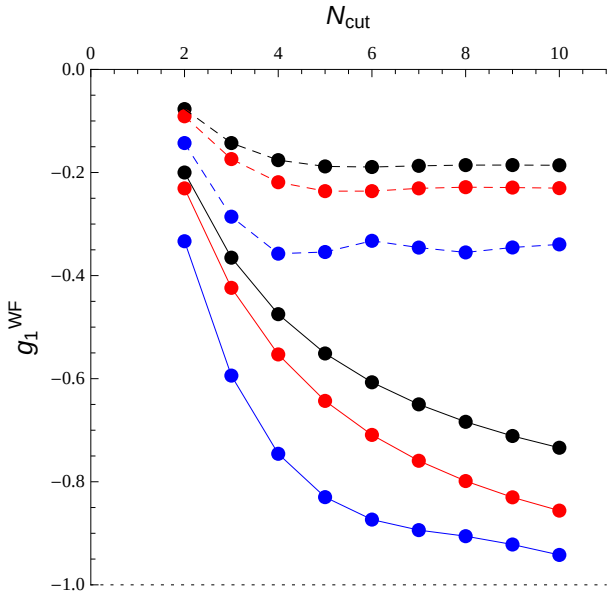

Fig. 2.5 The g_1 coordinate of the WF fixed point of the $O(N)$ model is shown as a function of $N_{\rm CUT}$ for $N = 1$ (black), $N = 2$ (red) and $N = 10$ (blue) from top to bottom for $d = 1$ (solid lines) and for $d = 3$ (dashed lines).

In summary, the results obtained for the $O(N)$ model with finite N and finite $N_{\rm CUT}$ show the existence of SSB and a WF fixed point (distinct from the Gaussian one) for $1 \leq d < 4$ (with d real), but indicated that for $N_{\rm CUT} \to \infty$ the symmetry broken phase disappears (persists) for $d \leq 2$ ($d > 2$).

It is interesting to show the results for the critical exponents ν in LPA as a function of the truncation index $N_{\rm CUT}$. In figure 2.7 the curves are shown for different values of the dimension $d = 3, 2.5, 2, 1$ for the $N = 1, 2$ cases, panel (a) and (b) respectively. At this approximation level anomalous dimension effects are not included $\eta = 0$ and the results for $N = 1, 2$ does not show any qualitative difference in $d = 2$.

Truncation around the minimum

Now we will consider a Taylor expansion of the effective potential around the minimum,

$$\tilde{U}_k(\tilde{\rho}) = \sum_{i=2}^{N_{\rm CUT,m}} \frac{\lambda_{k,i}}{i!}(\tilde{\rho} - \rho_0)^i, \tag{2.46}$$

where $N_{\rm CUT,m}$ is the truncation number around the minimum. In this case the results are drastically different. First of all we will consider this truncation at the minimum level $N_{\rm CUT,m} = 2$. Obviously it is possible to relate the values of the coupling defined around the

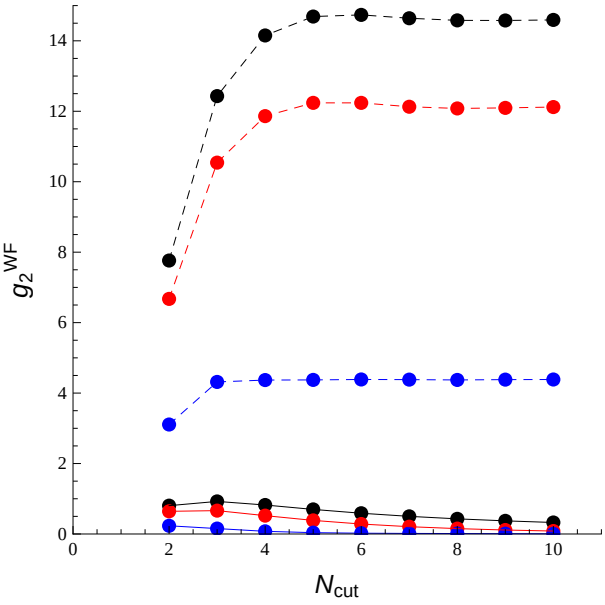

Fig. 2.6 The g_2 coordinate of the WF fixed point of the $O(N)$ model as a function of N_{CUT}: as in 2.5 from top to bottom it is $N = 1$ (black), $N = 2$ (red) and $N = 10$ (blue) for $d = 1$ (solid lines) and for $d = 3$ (dashed lines).

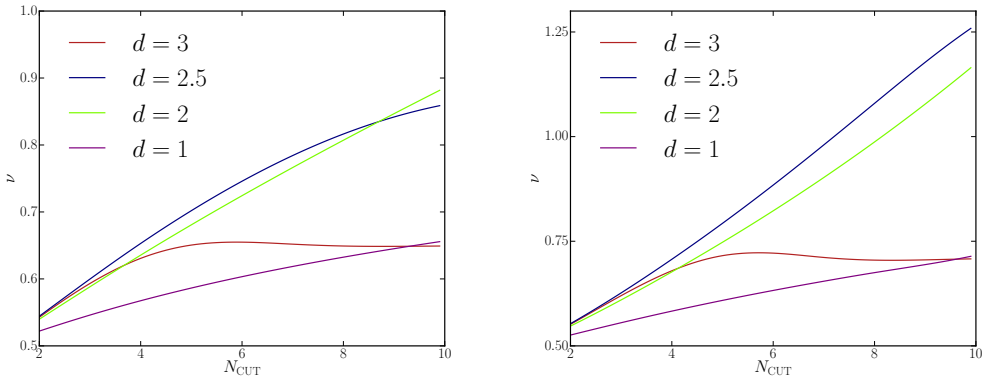

(a) N=1 (b) N=2

Fig. 2.7 In the figure we show the correlation length critical exponent ν as a function of the truncation number N_{CUT} for $N = 1, 2$, panel (a) and (b) respectively.

zero g_1 and g_2 with the values of the coupling λ and the running minimum ρ_0. However these relations, which give the correct result for the WF fixed point, are not working for the Gaussian fixed point, which is $g_1 = g_2 = 0$, but no solution of the fixed point equations for ρ_0 and λ has a vanishing ρ_0.

The truncation around the minimum includes just one running coupling $\lambda_{k,2} \equiv \lambda$ and the running minimum value ρ_0. From equation (2.39) we can obtain flow equations for these

two quantities [31], we report them for general real dimension d and N,

$$\partial_t \rho_0 = (d-2)\rho_0 - \frac{3N}{(1+2\rho_0\lambda)^2} \tag{2.47}$$

$$\partial_t \lambda = \lambda\left(4-d-\frac{18N\lambda}{(1+2\rho_0\lambda)^3}\right). \tag{2.48}$$

One can look for the fixed point solutions for ρ_0 and λ. In the particular case of the Ising model ($N=1$) one gets, for example, the Wilson-Fisher fixed point given by

$$\rho_0 = \frac{4(2d-5)^2}{3(d-2)^3}, \tag{2.49}$$

$$\lambda = \frac{3(4-d)(d-2)^3}{16(2d-5)^3}. \tag{2.50}$$

The corresponding expression for $N>1$ are very lengthy and are not reported here.
From the solution (2.49)–(2.50) one sees that the value of the minimum ρ_0 is well defined (positive) for every value of d as long as $d>2$: a similar result is valid for every N.
For $d>4$ the solution for λ is negative, and, again, this is true for every N. Also it should be noted that the coupling λ, for $N=1$, is diverging at $d=2.5$ and turns out to be negative for $d<2.5$, thus giving an unphysical solution for $d<2.5$: we know that this is not true, since in $d=2$ for $N=1$ there is SSB. This is not valid in the general N case where the coupling λ has only a maximum and is not diverging at $d=2.5$ and no sign change is present at any value of $d>2$.

In 2.8 is reported the minimum value ρ_0 as a function of the dimension at the WF fixed point for various N values, the minimum diverges for $d=2$ for every N in agreement with the Mermin-Wagner theorem. In the inset the values for the coupling λ are shown. The coupling stays finite and positive for $d>2$ and $N>1$, but for $N=1$ it is diverging at $d=2.5$ and turning negative at $d<2.5$, then this truncation is not giving a reliable lower critical dimension for the Ising model.

We expect larger values of $N_{\mathrm{CUT,m}}$ do not to change the main qualitative results just presented. This truncation, while giving the correct behavior for the SSB, cannot catch the non interacting (Gaussian) fixed point and thus gives only a partial description of the theory phase space. In the next sections we will show how it is possible to reproduce some of the correct result retrieved here and to go beyond them with a simple analysis of the exact flow equation for the effective potential (2.39).

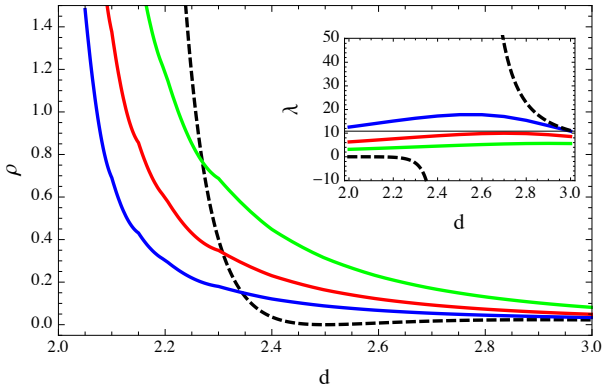

Fig. 2.8 Running minimum (main plot) and coupling (inset) values for the WF fixed point in the truncation around the minimum at $N_{\mathrm{CUT,m}} = 2$ as a function of the dimension d, for the Ising model ($N = 1$ black dashed curves), the XY model ($N = 2$, blue solid curves), the Heisenberg model ($N = 3$, red solid curves) and the $N = 5$ model (green solid curves). The Ising coupling λ is the only one which is diverging and then turning negative at $d = 2.5$ this is in contrast both with the well known exact solution of the Ising model in $d = 2$ and with the following argument on exact solutions of equation (2.39).

2.2.2 The spherical model without truncations ($N = \infty$, $N_{\mathrm{CUT}} = \infty$)

In this section we consider the $O(N)$ model in the large N limit: thus we can neglect the terms in (2.39) which are in the order of $1/N$. To see this we are going to rescale (2.39)by the parameter N, using again transformation (2.23), one finds

$$\partial_t \tilde{U}_k = (d-2)\tilde{\rho}\tilde{U}_k^{(1)} - d\tilde{U}_k + \frac{1}{1+\tilde{U}_k^{(1)}} - \frac{1}{N}\frac{1}{1+\tilde{U}_k^{(1)}} + \frac{1}{N}\frac{1}{1+\tilde{U}_k^{(1)}+2\tilde{\rho}\tilde{U}_k^{(2)}}. \tag{2.51}$$

By taking the limit $N \to \infty$ the following terms remain:

$$\partial_t \tilde{U}_k = (d-2)\tilde{\rho}\tilde{U}_k^{(1)} - d\tilde{U}_k + \frac{1}{1+\tilde{U}_k^{(1)}}. \tag{2.52}$$

This simplified expression represents the RG equation for the effective potential of the large N O(N) model in arbitrary dimension. From the equation (2.52) we can extract some useful information. First we should differentiate it by ρ in order to get an equation for the derivative of the potential. It reads then

$$\partial_t \tilde{U}_k^{(1)} = (d-2)\tilde{U}_k^{(1)} + (d-2)\tilde{\rho}\tilde{U}_k^{(2)} - d\tilde{U}_k^{(1)} - \frac{\tilde{U}_k^{(2)}}{(1+\tilde{U}_k^{(1)})^2}. \tag{2.53}$$

Since in a physically reasonable theory the potential is bounded from below, we can assume that this potential has a global minimum at some $\rho = \rho_0$. For ρ_0 we have the following value for the derivatives of the potential at the fixed point: $\tilde{U}_k^{(1)}(\rho_0) = 0$, $\tilde{U}_k^{(2)}(\rho_0) \equiv \lambda$. Assuming that the quartic coupling λ is finite, we have then the following equation:

$$0 = (d-2)\rho_0\lambda - \lambda \tag{2.54}$$

with the solution

$$\rho_0 = \frac{1}{d-2} \tag{2.55}$$

which determines the cases where the minimum of the potential can be found or not in the large N case. There is SSB if the potential has the minimum at some finite $\rho_0 > 0$: in the case of (2.55) we can satisfy this condition for $d > 2$. For $d < 2$ we find $\rho_0 < 0$, hence there will be no SSB. The $d = 2$ case seems to be undefined, since $\rho_0 \to \infty$ in this limit. However, if the minimum of the potential is sent to infinity one cannot define a proper minimum. The absence of a finite minimum indicates the absence of the spontaneous symmetry breaking for $d = 2$ dimensions. This can be also seen by solving equation (2.53) using the method of characteristics. The large N limit is a frequently used technique [19] where the results obtained can be considered as exact ones since the LPA approximation becomes exact when $N \to \infty$ [54].

2.2.3 Lower critical dimension

In this section we finally consider the problem of determining the lower critical dimension for the $O(N)$ model for a finite N but keeping the potential non truncated in LPA.

Let us first consider the $N = 1$ case by trying the following strategy: numerically calculate the WF fixed point position for finite N_{CUT} and approximate the limit $N_{\mathrm{CUT}} \to \infty$. Notice that, without knowing the exact WF fixed point positions, it is difficult for dimensions around $d = 2$ to unambiguously extract from the limit of increasing N_{CUT} the value of the non truncated model. For this reason we determine the WF fixed point for $N_{\mathrm{CUT}} = \infty$ by using the spike plot method [18, 24] in LPA.

The (finite N_{CUT}) results are plotted in 2.9 where we show that the N_{CUT} dependence of the WF fixed points on the VMB curves (obtained for Litim regulator) depends on the value of the dimension d: several d between $d = 1$ and $d = 3$ (including $d = 2$) are plotted for $N = 1$. Similar plots are obtained for general value of N. The positions of the exact WF fixed points, computed by the spike plot method, are also indicated for each case (by the symbol X).

2.9 clearly shows that for $N_{\rm CUT} \to \infty$ the g_2 coordinate of the WF fixed point tends to a finite value for $d > 2$ and runs to zero for $d \leq 2$: since this property is found to be valid in LPA for general values of N, when applied to $N \geq 2$ this result implies that the LPA is enough to reproduce the content of the Mermin-Wagner theorem. For $d = 2$ (sixth line from top in 2.9) one finds from the spike plot analysis that (for all N) no WF fixed point occurs: this result is correct for $N \geq 2$, but not for the Ising model ($N = 1$). As we will later comment, for the Ising model in $d = 2$ one needs to apply LPA$'$ approximation.

Given the clear numerical evidence that Mermin-Wagner is well obtained in the limit of increasing $N_{\rm CUT}$ and the excellent agreement with the spike plot method findings for the WF fixed points, we investigated and present in the following two analytical arguments valid for the non truncated (exactly treated) LPA confirming these results.

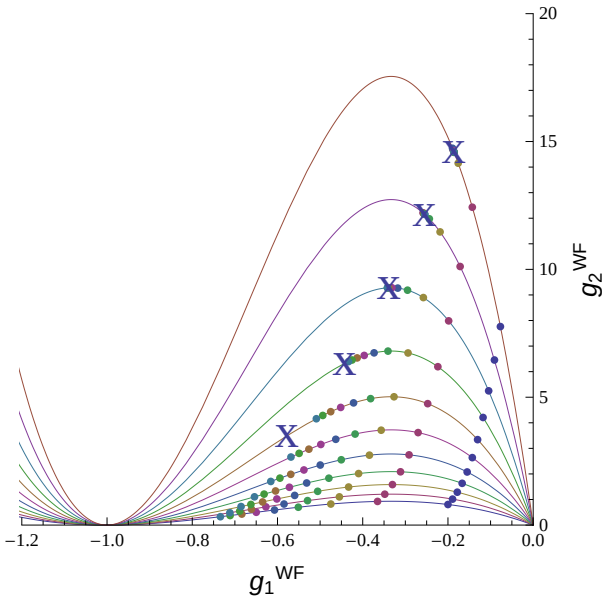

Fig. 2.9 The figure shows the positions of the WF fixed points and the corresponding VMB curves of the $O(N = 1)$ model for various values of $N_{\rm CUT}$ for 11 different values of the dimension $1 \leq d \leq 3$ having the values $d = 3, 2.8, 2.6, 2.4, 2.2, 2, 1.8, 1.6, 1.4, 1.2, 1$. The VMB curves obtained for these dimensions are plotted from the top to the bottom in decreasing order. For each value of d, from right one has $N_{\rm CUT} = 2, \cdots, 10$. The exact WF points are indicated by the symbol X and are obtained by the spike plot method [18, 24].

In order to consider the appearance of SSB for the $O(N)$ model for finite N but keeping the potential unexpanded ($N_{\rm CUT} = \infty$), let us start with the fixed point equation of (2.39): putting $\partial_t u = 0$ one has

$$d\tilde{U}_k - (d-2)\tilde{\rho}\tilde{U}_k^{(1)} = \frac{(1-\frac{1}{N})}{1+\tilde{U}_k^{(1)}} + \frac{1}{1+\tilde{U}_k^{(1)}+2\tilde{\rho}\tilde{U}_k^{(2)}}. \tag{2.56}$$

The l.h.s of the RG equation (2.56) is linear in the effective potential. The r.h.s. depends on the effective potential and its derivatives non linearly, thus we introduce the notation

$$LP \equiv d\tilde{U}_k - (d-2)\tilde{\rho}\tilde{U}_k^{(1)}, \tag{2.57}$$

$$NLP \equiv \frac{(N-1)}{1+\tilde{U}_k^{(1)}} + \frac{1}{1+\tilde{U}_k^{(1)}+2\rho\tilde{U}_k^{(2)}}. \tag{2.58}$$

where *LP* (*NLP*) stands for the linear (non linear) part. Let us consider the large field limit ($\rho \gg 1$) of equation (2.56). First of all we assume analyticity of the effective potential [47] at any finite value of the field, then the potential at infinity can only either be a constant or divergent. In the first case *NLP* is constant at infinity and the potential will be just a constant at any ρ. In the second case *NLP* in principle may vanish or tend to a constant (eventually zero) at infinity, thus the fixed point potential $\tilde{U}_k(\tilde{\rho})$ must satisfy for large field the condition

$$LP = C, \tag{2.59}$$

where C is a finite (or zero) constant to be consistently determined. Then one finds the solution for $\rho \gg 1$

$$\tilde{U}_k(\tilde{\rho}) = \frac{C}{d} + a\tilde{\rho}^{\frac{d}{d-2}}, \tag{2.60}$$

where a is a proportionality constant. Now let us differentiate the previous expression of $\tilde{U}_k(\rho)$: this yields $\tilde{U}_k^{(1)}(\tilde{\rho}) = a\frac{d}{d-2}\tilde{\rho}^{\frac{2}{d-2}}$, which for large $\tilde{\rho}$ gives a diverging quantity for $d > 2$ and a zero for $d < 2$. In the former case we are violating the assumption that u' is bounded for large $\tilde{\rho}$, while in the latter the constant C is zero. In both cases we find

$$\tilde{U}_k(\tilde{\rho}) = a\tilde{\rho}^{\frac{d}{d-2}} \tag{2.61}$$

for $\tilde{\rho} \to \infty$,

The general solution of equation (2.56), which is not a constant, can be then divided into two parts,

$$\tilde{U}_k(\tilde{\rho}) = f(\tilde{\rho}) + a\tilde{\rho}^{\frac{d}{d-2}}, \tag{2.62}$$

where the function $f(\rho)$ is subjected to the condition

$$\lim_{\tilde{\rho}\to\infty} f(\tilde{\rho}) = 0. \tag{2.63}$$

The physical Gibbs free energy $F(m)$ can be computed from the effective potential $\tilde{U}_k(\tilde{\rho})$ passing from dimensionless variables to the dimensional ones [17]: one finds

$$F(m) = k^d u(k^{2-d}m^2) = k^d f(k^{2-d}m^2) + am^{\frac{2d}{d-2}}, \tag{2.64}$$

where m is the dimensional field of our model, which in the case of a spin system is the average magnetic moment. The free energy of the system is obtained then in the $k \to 0$ limit of equation (2.64), where we should distinguish between three cases.

$d > 2$

When $d > 2$ the factor k^{2-d} in the argument of the function $f(\tilde{\rho})$, in equation (2.64) is diverging. However we know from the analysis of the general solution that the function $f(\tilde{\rho})$ tends to a constant in the infinite limit of its argument, hence the Gibbs free energy for an $O(N)$ model in LPA for $d > 2$ reads

$$am^{\frac{2d}{d-2}}, \tag{2.65}$$

where a is positive and can be fixed following the procedure described in [55].

$d < 2$

In the case $d < 2$ the situation drastically changes. Indeed, the factor k^{2-d} in the argument of $f(\tilde{\rho})$ in equation (2.64) is now vanishing. The behavior of the $f(\tilde{\rho})$ function for vanishing argument can be obtained from equation (2.62).

Since we know that such expression should be defined for any finite value of field $\tilde{\rho}$ [55], then $f(\tilde{\rho})$ is diverging in zero, in order to compensate the divergence of $\tilde{\rho}^{\frac{d}{d-2}}$, which has a negative exponent in $d < 2$. Thus the behaviour of $f(\tilde{\rho})$ in the limit of vanishing arguments is

$$\lim_{x\to 0} f(x) = w(x) - ax^{\frac{d}{d-2}}, \tag{2.66}$$

where $w(x)$ is finite in zero. Substituting the last expression into equation (2.64) one obtains

$$k^d w(k^{2-d}m^2), \tag{2.67}$$

which is zero in the $k \to 0$ limit.

In summary, we obtained that for $d > 2$ the critical free energy of a $O(N)$ model can have the form (2.65) or can be zero, thus the phase transition is present [18]. For $d < 2$ the fixed point free energy can only be zero and no spontaneous symmetry breaking is allowed.

$d = 2$

The previous argument cannot be directly used for $d = 2$. The numerical study of the equation (2.56), i.e. $LP = NLP$, reveals in this case that for $N \geq 2$ the LPA gives the Mermin-Wagner result: indeed the solution for large field of $\tilde{U}_k(\tilde{\rho})$ turns out to be oscillatory, therefore correctly implying the absence of SSB and the Mermin-Wagner theorem. However, such oscillatory solutions persist for $N = 1$, predicting the absence of SSB, which is clearly wrong.

To have a complete picture of the $d = 2$ case one should go beyond LPA: as discussed in [24], in LPA' the limit of the anomalous dimension η for $d \to 2$ is vanishing provided that $N \geq 2$, and non vanishing for $N = 1$. This gives a clear explanation in the FRG framework of the presence or the lack of SSB in $O(N)$ models in $d = 2$. Of course, the fact that there is no SSB for $N = 2$ does not imply the absence of the Berezinskii Kosterlitz-Thouless transition [49, 56], as can be seen also in FRG treatments [22, 57, 58].

2.3 Functional solutions and anomalous dimension effects

As outlined in the previous section it is necessary to go beyond Taylor truncated solutions in order to recover the correct phase diagram for $O(N)$ models in $d < 2$ where there is no SSB for $N \geq 2$. In the present section we will show how functional solutions of (2.36) are able to correctly reproduce all the qualitative features of the $O(N)$ phase diagram, including the possibility of SSB in $d = 2$ for discrete symmetries $N < 2$.

The critical points of our theory correspond to the scaling solutions of equation (2.36) this leads to the condition,

$$\partial_t \tilde{U}_t(\tilde{\rho}) = 0, \tag{2.68}$$

from this equation it is easy to find all possible universality class of a scalar theory. In LPA the anomalous dimension η is set to zero, however, as we will see, this is not a problem for the research of critical points.

The scaling solutions for our local potential satisfy equation,

$$d\tilde{U}(\tilde{\rho}) - (d-2)\tilde{\rho}\tilde{U}^{(1)}(\tilde{\rho}) + \frac{1}{1+\tilde{U}^{(1)}(\tilde{\rho}) + 2\tilde{\rho}\tilde{U}^{(2)}(\tilde{\rho})} + \frac{N-1}{1+\tilde{U}^{(1)}(\tilde{\rho})} = 0 \tag{2.69}$$

This is a non linear second order differential equation which need two initial conditions to be solved. We call $\sigma = \tilde{U}^{(1)}(0)$ the convexity of the potential in the origin and than we have that the value of the potential in the origin must be $\tilde{U}^{(1)}(0) = \frac{N/d}{1+\sigma}$, thus we get an infinite set of solutions labelled by the σ parameter and depending on the dimension of our model $\tilde{U}_\sigma(\tilde{\rho})$. This can seem strange, since we expected to have just one potential which describes our

theory at criticality, while we are left with an entire set labelled by a real index σ. However most of the solutions for our potential blow up for a finite value of the field, those represent solutions which are not physical since are not defined for any value of the field [18, 59]. Let us now define a function $\tilde{\rho}_\infty(d,\sigma)$ which represents the value of the field at which the potential $\tilde{U}_\sigma(\tilde{\rho})$ blows up in dimension d.

The function $\tilde{\rho}_\infty(d,\sigma)$ is a well defined one value function. Since at any fixed point we shall have a potential $\tilde{U}(\tilde{\rho})$ finite for every real value of the field. Then the function $\tilde{\rho}_\infty(d,\sigma)$ will have a divergence at the value σ which represents the correct condition for the fixed point potential. Therefore the number of divergences, or spikes, of the function $\tilde{\rho}_\infty(d,\sigma)$ is the number of universality classes for the model in d dimensions [18, 22, 23, 60].

The function $\tilde{\rho}_\infty(d,\sigma)$ gives an effective representation of the phase diagram of $O(N)$ field theories. For $d=4$ only the Gaussian fixed point is found, then, as the dimension is lowered, at $d=3$ the function develops a new spike for a negative value of σ which represent the Wilson Fisher universality, as shown in figure 2.10. Then lowering again the dimension we found an increasing number of universality classes which accumulate to two dimensions, this can be retrieved with a very simple argument which allows us to compute the upper critical dimension for any fixed point.

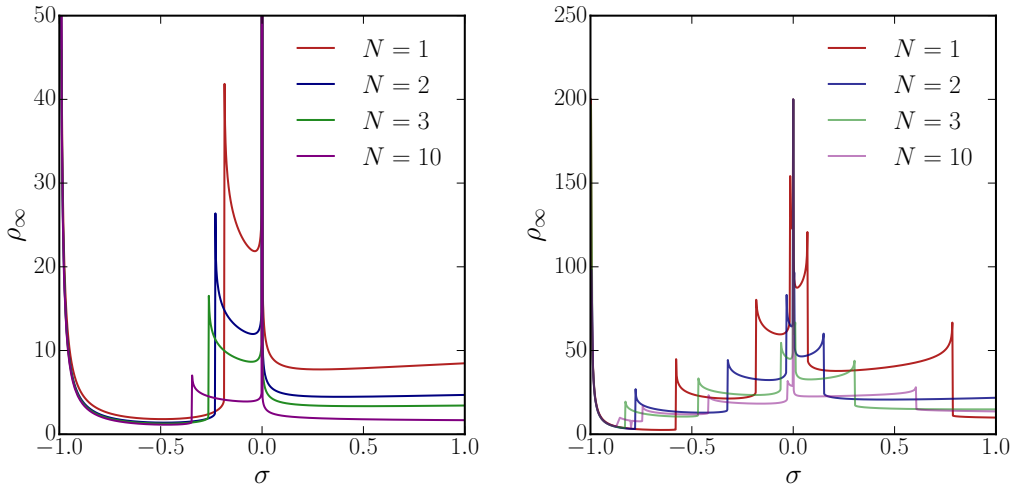

(a) $d=3$ (b) $d=2.2$

Fig. 2.10 The function $\tilde{\rho}_\infty(d,\sigma)$ in $d=3$, panel (a), and $d=2.2$ panel (b).

The Taylor expansion for the potential of $O(N)$ symmetric models is given in equation (2.37). Every dimensional coupling g_i is multiplied by the power of the field ρ^i, then it must have a dimension equal to $D_{g_i} = d - i(d-2)$ as it must be if the effective action has to be dimensionless and the kinetic term has no coupling in front. Any dimensional coupling will

then scale as $k^{D_{g_i}}$. For $D_{g_i} > 0$ the coupling will be lowered by the renormalization procedure, $k \to 0$, an it will be *irrelevant* in the thermodynamic limit. On the other hand for negative exponents $D_{g_i} < 0$ the dimensional coupling will blow up during the flow and it will be a *relevant coupling* [10]. The simple condition is obtained

$$\begin{aligned} d - i(d-2) &= 0 \\ d &= \frac{2i}{i-1}, \end{aligned} \tag{2.70}$$

which gives the upper dimension at which the coupling g_i becomes relevant, i.e. the *upper critical dimension* for the ith multicritical universality class [61]. We find that for natural n we have a sequence of dimensions $d_{c,i}$ starting from $d_{c,1} = \infty$, which is the upper critical dimension of the Gaussian fixed point, and accumulating at $d_{c,\infty} = 2$. In fact the $n \to \infty$ limit of the sequence is exactly $d = 2$, where there is an infinite number of universality classes as it can be seen from the behavior of the function $\tilde{\rho}_\infty(d, \sigma)$ [24], figure 2.10b.

In $d = 2$ correlation effects are large, since all the couplings are relevant, thus the simple LPA ansatz (2.6) cannot correctly reproduce the transition behavior. Indeed the function $\tilde{\rho}_\infty(d, \sigma)$ will show an infinite number of spikes. We will thus have an infinite number of physical solutions of equation (2.36), leading to the impossibility to correctly identify the Wilson Fisher universality, which describes traditional $\mathbb{Z}_2$ symmetry breaking in $d = 2$. It is then convenient to introduce a new ansatz for the effective action

$$\Gamma_k[\varphi] = \int d^d x \left\{ \frac{Z_k}{2} \partial_\mu \varphi_i(x) \partial_\mu \varphi_i(x) + U_k[\rho] \right\}, \tag{2.71}$$

where the running coefficient Z_k is called *wavefunction renormalization*.

The functional space described by ansatz (2.71) is larger than the one introduced by ansatz (2.6), since the kinetic term in the action is now allowed to renormalize with the RG flow. This defines the LPA$'$ approach. It is worth noting that the coefficient Z_k could be scaled away using transformation (2.23). Then we do not expect the bare value Z_Λ of the coupling to modify the phase diagram obtained by previous arguments. On the other hand the introduction of a running wavefunction Z_k introduce a crucial effect in the description of the critical points.

The derivation of the flow equation for Z_k is given in the appendix B.3, the result in scaled variables reads

$$\partial_t Z_k = \frac{4 Z_k^2 \rho_0 \tilde{U}^{(2)}(\rho_0)^2}{(Z_k + \mu_m)^2 (Z_k + \mu_g)^2} \tag{2.72a}$$

$$\partial_t Z_k = \frac{4\rho_0 Z_k^2 \left(2\rho_0 \tilde{U}^{(3)}(\rho_0) + 3\tilde{U}^{(2)}(\rho_0)\right)^2}{(Z_k + \mu_m)^4} \tag{2.72b}$$

where the two results depend on wether we define the anomalous dimension as the running of the coefficient of the momentum term in the Goldstone or massive propagator respectively [19]. Latter equations have been obtained from (B.50a) and (B.50b) transforming to scaled variables, as defined in (2.31) and evaluating the right hand side at ρ_0, i.e. the potential minimum defined by

$$\tilde{U}^{(1)}(\tilde{\rho})\Big|_{\rho_0} = 0. \tag{2.73}$$

The wavefunction Z_k cannot attain any finite value at the fixed point, since $\rho_0 \neq 0$ and $Z_k \neq 0$ at criticality and then the r.h.s. of flow equations (2.72) do not vanish. The wavefunction term in (2.71) is increasing during the RG flow with a power law behavior of the scale k, it is thus necessary to absorb its divergence into the definition of scaled field. We redefine the dimensionless field according to

$$\begin{aligned} &\tilde{\rho} = Z_k k^{2-d} \rho = Z_k e^{(d-2)t} \rho. \\ &\frac{\partial_t Z_k}{Z_k} = \eta_k, \end{aligned} \tag{2.74}$$

where we also defined the scale dependent exponent η_k. Applying latter definition to the flow equations (B.50a) and (B.50b) obtained in the appendix, we get

$$\eta_k = \frac{4, \rho_0 \tilde{U}^{(2)}(\rho_0)^2}{(1 + 2\rho_0 \tilde{U}_k(\rho_0))^2}, \tag{2.75a}$$

$$\eta_k = \frac{4\rho_0 \left(2\rho_0 \tilde{U}^{(3)}(\rho_0) + 3\tilde{U}^{(2)}(\rho_0)\right)^2}{(1 + 2\rho_0 \tilde{U}_k(\rho_0))^4}, \tag{2.75b}$$

where the minimum value ρ_0 has been redefined according to (2.74). At the critical point the flow for the effective potential attains its fixed point and the $\eta_k \equiv \eta$ quantity is fixed [31]. The actual scaling dimension of the field will be not $d-2$ has expected from mean field arguments but rather $d-2+\eta$. For this reason the exponent η is often called *anomalous dimension*.

At exact level only one anomalous dimension exist and the two results in equations (2.75) should be equal [19]. However the truncation defined by (2.71) introduce an inconsistency in

the definition of anomalous dimension and then we have two possible results for this quantity. The consequence of such inconsistency will be discussed in the following.

At LPA$'$ level the flow equation for the effective potential reads

$$d\tilde{U}(\tilde{\rho}) - (d-2+\eta)\tilde{\rho}\tilde{U}^{(1)}(\tilde{\rho}) + \frac{1+\frac{\eta}{d+2}}{1+\tilde{U}^{(1)}(\tilde{\rho})+2\tilde{\rho}\tilde{U}^{(2)}(\tilde{\rho})} + (N-1)\frac{1+\frac{\eta}{d+2}}{1+\tilde{U}^{(1)}(\tilde{\rho})} = 0 \tag{2.76}$$

The anomalous dimension η fixes the scaling properties of the field at any particular fixed point. In the following we will derive such quantity using equation (2.75a), leaving the discussion of the definition (2.75b) to the next subsection.

Every solution of equation (2.76), together with its domain of attraction, represents a different $O(N)$ universality class [24]. For every d and N one finds a discrete set of solutions corresponding to multi-critical potentials of increasing order, i.e. with i minima, which describe multi-critical phase transitions (in which one needs to tune multiple parameters to reach the critical point). For each of these it is possible to obtain the anomalous dimension $\eta_i(d,N)$ (we define $\eta \equiv \eta_2$) as a function of d and N, by means of which we can follow the evolution through theory space of the fixed point representing the i–th multi-critical potential [24].

The analysis presented in [22] revealed that for $d > 4$ and for any N, in accordance with the Ginzburg criterion, one finds only the Gaussian fixed point ($i = 1$). (See [62] for a discussion on the possible existence of non trivial universality classes in $d \geq 4$ raised by [63]). Starting at $d = 4$, the upper critical dimension for $O(N)$ models, the Wilson–Fisher (WF) fixed points ($i = 2$) branch away from the Gaussian fixed point. When $d = 3$ these fixed points describe the known universality classes of the Ising, XY, Heisenberg and other models.

Approaching $d = 2$ one clearly observes that only the $N = 1$ anomalous dimension continues to grow: for all other values of $N \geq 2$ the anomalous dimension bends downward to become zero exactly when $d = 2$, as shown in 2.10. As explained in [24], this non trivial fact, not evident from the structure of equation (2.76) alone, is a manifestation of the Mermin-Wagner theorem. We now complement this analysis with the results for the correlation length critical exponents $\nu_i(d,N)$ as a function of d and N. We obtained results for the first several multi-critical universality classes $i = 2,3,4,5,....$ Here we will only report in detail the analysis for the WF and tri-critical cases ($i = 2,3$), and briefly comment on the other multi-critical cases. See Fig. 2.14 for results on $\nu = \nu_2$ as a function of d for various values of N.

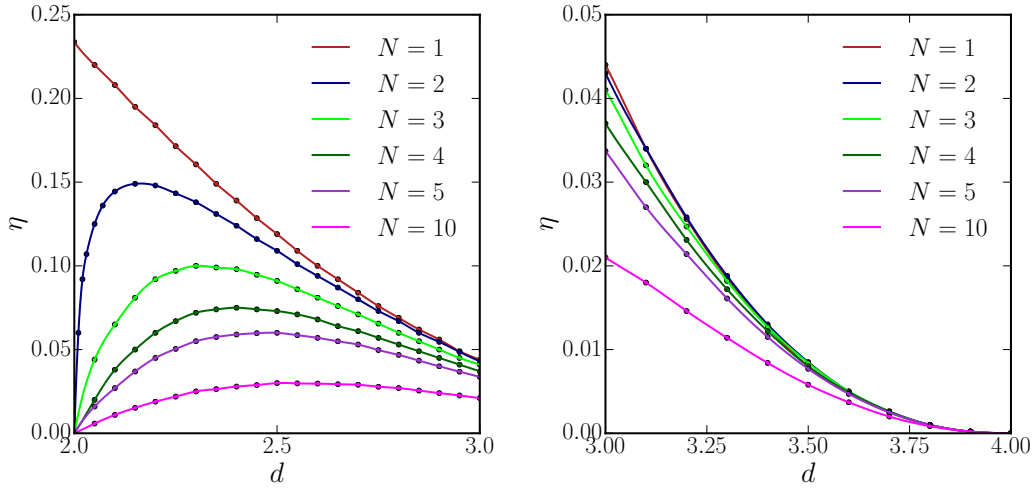

(a) $d \in [2,3]$ (b) $d \in [3,4]$

Fig. 2.11 The values of the anomalous dimension $\eta(d,N)$ as a function of the dimension.

2.3.1 Eigen–perturbations and Correlation length exponent

The correlation length exponent ν can be computed using coupling expansion and stability matrix method depicted in previous section. Thanks to the presence of finite anomalous dimension in the LPA$'$ the correlation length exponent in the Ising case should not diverge as in the LPA case, shown in figure 2.7a. The results for the correlation length exponent as a function of the dimension for various truncation index N_{CUT} it is shown in figure 2.12. Thanks to anomalous dimension effects the effective dimension of the field in the LPA$'$ case is greater than in LPA, then truncation techniques show better convergence at lower dimension. Indeed in figure 2.13 the result for $d = 2.5$ is already converged for $N_{CUT} = 7$, while in figure 2.7a we were unable to get convergence even for $N_{CUT} = 10$. However it is evident from figure 2.12 that truncation procedure in $d \geq 2$ do not achieve convergence ever for large couplings number $N_{CUT} > 10$, it is then convenient to introduce an alternative functional method to compute the ν exponent in the LPA and LPA$'$ schemes.

The correlation length exponent ν_i is related to the larges negative (infrared repulsive) eigenvalue $y_{1,i}$ of the linearized RG transformation by $\nu_i = 1/y_{1,i}$ (we define $\nu \equiv \nu_2$). In order to calculate it, we will use the eigen–perturbation method described in [64]. As a starting point, we expand the dimensionless effective potential as follows:

$$\tilde{U}_k = \tilde{U}_*(\tilde{\rho}) + \varepsilon\, \tilde{u}_k(\tilde{\rho})\, e^{yt}\,, \tag{2.77}$$

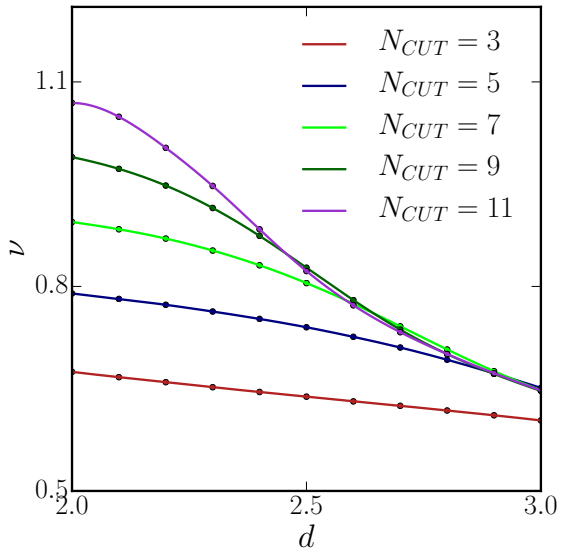

Fig. 2.12 Correlation length exponent ν as a function of the dimension for various N_{CUT}. The curves are really close for $d < 2.5$ showing that truncation techniques are able to recover consistent values for ν even when only few couplings are included. However for $d \simeq 2$ the convergence seems out of reach for any treatable number of coupling.

where $\tilde{U}^*(\tilde{\rho})$ is a solution of the fixed point equation (2.76) and $\tilde{u}_k(\tilde{\rho})$ is a perturbation around the solution whose eigenvalue is y. Substituting this expression into the flow equation, and considering only terms of first order in ε, we obtain an equation for the perturbation:

$$(d+y)\tilde{u}_k(\tilde{\rho}) - (d-2+\eta)\tilde{\rho}\,\tilde{u}_k^{(1)}(\tilde{\rho}) = -(N-1)\left(1-\frac{\eta}{d+2}\right)\frac{\tilde{u}_k^{(1)}(\tilde{\rho})}{(1+\tilde{U}_*^{(1)}(\tilde{\rho}))^2} - \left(1-\frac{\eta}{d+2}\right)\frac{\tilde{u}_k^{(1)}(\tilde{\rho})+2\tilde{\rho}\,\tilde{u}_k^{(2)}(\tilde{\rho})}{(1+\tilde{U}_*^{(1)}(\tilde{\rho})+2\tilde{\rho}\,\tilde{U}_*^{(2)}(\tilde{\rho}))^2}\,. \tag{2.78}$$

In order to solve this equation we need two initial conditions. The first is obtained by noting that the perturbation equation (2.78) is linear, so we can require the normalization condition $\tilde{u}_k(0) = 1$, while the second one is imposed on $\tilde{u}_k^{(1)}(0)$ from continuity at zero field:

$$(y+d)\tilde{u}_k(0) = -\frac{\left(1-\frac{\eta}{d+2}\right)N}{(1+\tilde{U}_*^{(1)}(0))^2}\tilde{u}_k^{(1)}(0)\,. \tag{2.79}$$

It should be noted that in the special case $N = 0$ the continuity at zero field is given by $\tilde{u}_k(0) = 0$ and then the normalization condition should be imposed on the first derivative of the perturbation $\tilde{u}'_k(0) = 1$.

Now we can identify a single solution for any value of y, but we know that just a discrete set of y values will be the ensemble of the physical eigenvalues of equation (2.76). The supplementary condition to identify this discrete set is given on the shape of the solutions. A generic solution of equation (2.78) in the $\rho \to \infty$ limit behaves at leading order as:

$$\tilde{u}_k(\tilde{\rho}) = a(y)\rho^{\frac{(d-y)}{(d-2+\eta)}} + b(y)e^{C\rho^{\frac{2d}{d-2+\eta}-1}}, \tag{2.80}$$

where $a(y)$, $b(y)$ are two functions of the eigenvalue y and C is a constant depending on d and η. This shows that in the infinite field limit, the solution is a linear combination of power-law and exponential diverging parts [64]. In order to find the discrete set of eigenvalues that we need, we have to require the solution to grow no faster than a power-law, so the condition is just $b(y) = 0$. Using this condition we found just one infrared (IR) repulsive eigenvalue for the WF fixed point, two for the tri-critical fixed point, three for the tetra-critical fixed point and so on, see Fig. 2.13a. In this way we were able to construct the curves shown in Figs. 2.13a, 2.13b, 2.14a, 2.14b, 2.17 and 2.18.

The proliferation of eigenvalues is due to the fact that the i–th universality class has $i-1$ IR repulsive directions in theory space, and thus we have $i-1$ solutions with negative eigenvalue in the perturbation equation (2.78). In the following we will denote as $y_{j,i}$ the j–th eigenvalue of the i–th universality class.

As was already observed in [24], the vanishing of the anomalous dimension, when combined with the behaviour of the ν_i exponents, implies that there are no continuous phase transitions for $N > 2$ in $d = 2$. The case $N = 2$ is peculiar due to the presence of the Kosterlitz–Thouless phase transition [65]; our method is not able to recover this result because of its topological nature. Note that this will apply also to the following, and the case $N = 2$ is to be understood in light of the previous remark. Consistently with this argument, here we find that only the $N = 1$ model has finite correlation length exponent in two dimensions; in all other cases, $N \geq 2$, ν diverges as $d \to 2$. This allows us to distinguish the spherical model, related to the $N \to \infty$ limit [66], from the Gaussian model, both having $\eta = 0$. In the $N \to \infty$ limit instead we recover the known exact relation $\nu(d,\infty) = \frac{1}{d-2}$ [64]. Fig. 2.14 shows η and $y_{1,2} = \nu^{-1}$ as function of $N \in [-2, 2.5]$, for the two cases $d = 2$ and $d = 3$. The critical exponents are continuous in the whole range and in particular around $N = 0$; this is an indication that the $N \to 0$ limit, relevant to the problem of self avoiding random walks (SAW) [67], is well defined.

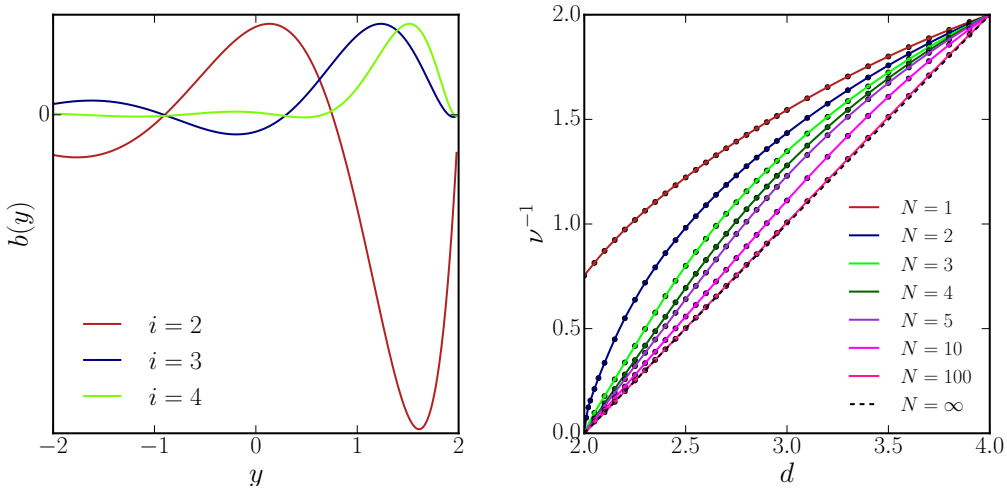

(a) Coefficient $b(y)$. (b) ν_1 for $d \in [2,4]$.

Fig. 2.13 Panel (a) estimation of the $b(y)$ coefficient in $d = 2$ for $N = 1$ and $i = 2,4,6$. The zeros of this function reproduce the discrete spectrum of the eigenvalues of the linear perturbation of equation (2.76). Panel (b) the correlation length exponent is obtained as $\nu = y_{\max}$. Correlation length critical exponent ν, for the WF universality class, as a function of d between two and three for $N = 1,2,3,4,5,10,100$, from bottom to top.

These curves strictly follow the prescription of the Mermin-Wagner theorem: for $N \geq 2$ both $\eta(2,N)$ and $y_{1,2}(2,N)$ vanish, while in $d = 3$ they have finite values; thus $O(N)$ models with continuous symmetries cannot have a spontaneous symmetry breaking in two dimensions. We remark that both exponents are necessary to distinguish between the case of no phase transition, where we have seen both exponents vanish, and the $N = \infty$ case where, for example $\eta(3,\infty)$ vanishes but $y_{1,2}(3,\infty)$ attains a finite nonmean field value. Our computation of $\nu(d,N)$ thus completes the RG derivation of the Mermin-Wagner theorem started in [24] with the analysis of $\eta(d,N)$. In the limit $N \to -2$ both exponents attain their mean field values (namely $\eta = 0$ and $\nu = 1/2$), where indeed the model is know to have Gaussian critical exponents in both dimensions [68].

The functions $\eta(d,1)$ and $\nu(d,1)$ can be compared with results from the bootstrap (BS) approach [69, 70]. The anomalous dimension compares fairly well considering that our computation is based on the solution of a single ODE, while the correlation length critical exponent is slightly overestimated for d in the proximity of two, see Fig. 2.15. It will be interesting to have BS results for the $N > 1$ cases in dimension other than three [71] and in particular to see the emergence of the Mermin-Wagner theorem in this approach. It is worth noting that the functions that are both universal and in principle experimentally accessible.

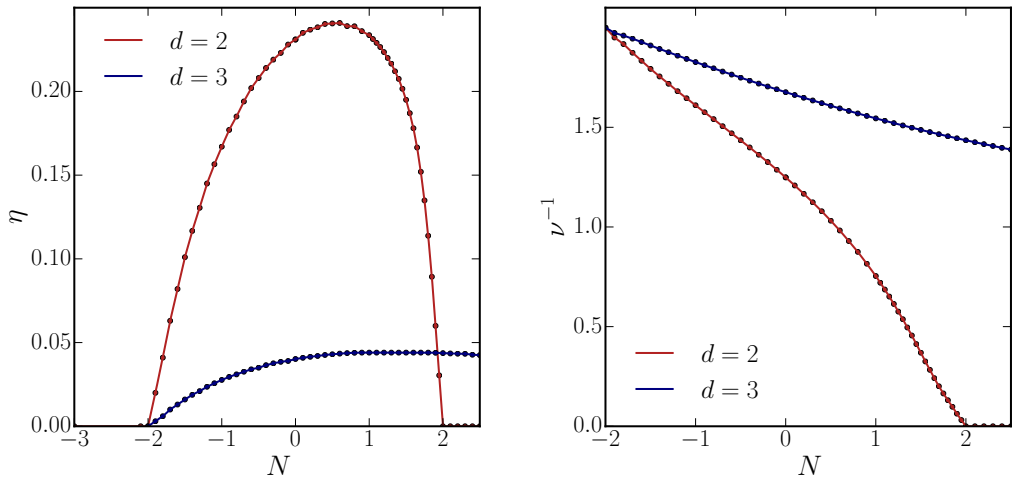

(a) Anomalous dimension η. (b) Inverse correlation length exponent ν.

Fig. 2.14 Critical exponents η and $y_{1,2} = 1/\nu$ as a function of N in two and three dimensions for the WF universality class. The fact that the two dimensional curves are zero for $N \geq 2$ is a manifestation of the Mermin-Wagner theorem.

2.3.2 Alternative definition for η

In latter section we computed the universal functions $\eta(d,N)$ and $\nu(d,N)$, see Figs. 2.12 and 2.13b, these results have been obtained using only the fixed point equation (2.76) and the associated stability equation (2.78). The value of the anomalous dimension η has been computed using definition (2.74) in self consistent procedure. It should be underlined that we employed definition (2.74) and not (2.75) even in the $N = 1$ case, where definition (2.74) is not strictly valid. Indeed the first definition has been derived using the flow of the Goldstone excitations propagator, which are not present for discrete $\mathbb{Z}_2$.

For the sake of explanation we will now show the reason of choosing (2.72a) rather then (2.72b). In figure 2.15 we plot the anomalous dimension and correlation length exponent in the $N = 1$ case computed using the two alternative definitions for the anomalous dimension (2.72a) and (2.72b), the results for the two exponents are compared with the numerically exact quantities obtained with bootstrap technique [69]. It is evident that definition (2.72a) performs better in the anomalous dimension case, while definition (2.72b) is more accurate in reproducing the correlation length exponent.

In figure 2.15 we also report results obtained by truncation technique at LPA$'$ level and functional LPA results for the ν exponents. In the LPA case the ν exponent is diverging in the $d \to 2$ limits while it is finite in the LPA$'$ case.

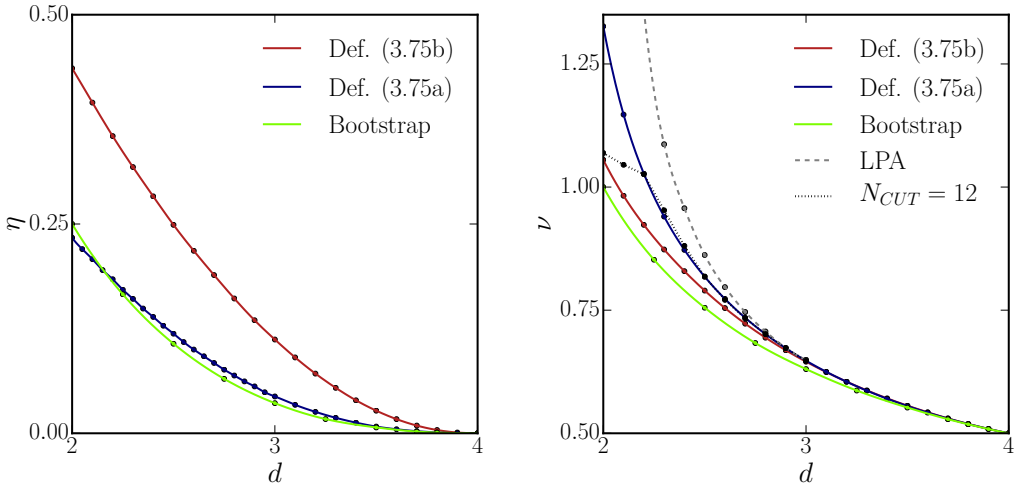

(a) Anomalous dimension η. (b) Correlation length exponent ν.

Fig. 2.15 Critical exponents η and ν in the $N = 1$ case. The results have been obtained using the two alternative definitions given in equations (2.74) and (2.75), the results are compared with numerically exact bootstrap quantities.

2.3.3 Scaling relations and $\alpha, \beta, \gamma, \delta$

Having obtained ν and η as a function of d and N, we can now use the standard scaling relations to obtain the other critical exponents:

$$\begin{aligned} \alpha &= 2 - \nu d \qquad & \beta &= \nu \frac{d-2+\eta}{2} \\ \gamma &= \nu(2-\eta) \qquad & \delta &= \frac{d+2-\eta}{d-2+\eta}. \end{aligned} \tag{2.81}$$

Our results are shown in Fig. 2.16 for $2 \leq d \leq 4$ and for $N = 1, 2, 3, 4, 5, 10, 100$. The first thing we notice is that in the large–N limit we smoothly recover the critical exponents of the spherical model [41] $\alpha = 0$, $\beta = \frac{1}{2}$, $\gamma = \frac{2}{d-2}$ and $\delta = \frac{d+2}{d-2}$. Our results indicate that the $N = 100$ case is perfectly approximated by the spherical model, while already at $N = 10$ deviations from this limit are appreciable. This shows that, for that as regards critical exponents (or related) quantities, the leading large–N estimates are quantitatively good only for N of order 10^2 or larger [72].

For $N = 1$ and $d = 2$ our results can be compared with the known exact Ising critical exponents found by Onsager and others [4, 73], the comparison can be found in table 2.1. Quantitative agreement is not excellent, as expected by the simplicity of our approach, based entirely on the solution of a single ODE (2.76) and the relative eigenvalue problem (2.78). Also it should be noted that the errors of our method are found to be most relevant in this

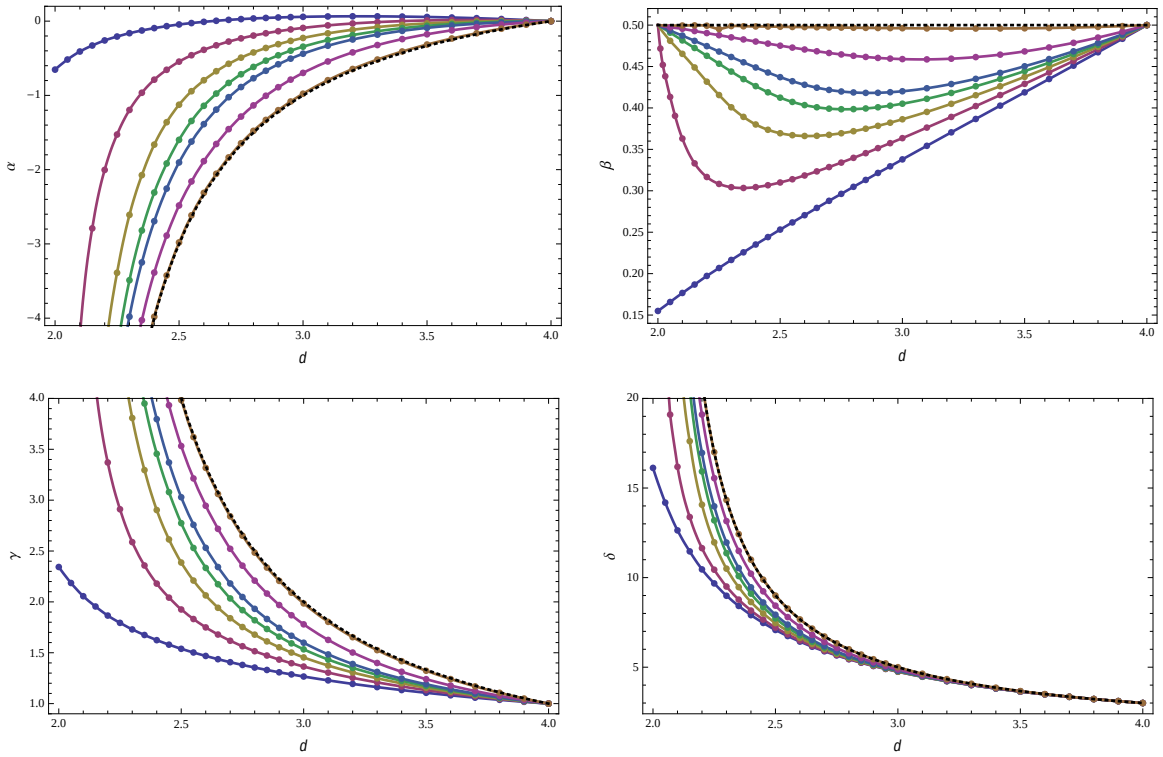

Fig. 2.16 Critical exponents of $O(N)$ field theories.

Table 2.1 Ising results

Exp.	3d(BS[5])	3d([23])	2d(exact [7])	2d([23])
η	0.036	0.044	$1/4$	0.23
ν	0.63	0.65	1	1.33
α	0.11	0.050	0	-0.65
β	0.33	0.34	0.125	0.15
γ	1.24	1.27	1.75	2.34
δ	4.79	4.75	15	16.12

case, as it will be clear in the following. This is due to the fact that the error we commit is of the same order of the anomalous dimension of the model considered [19, 46]. However no other method, at present, has a similar versatility. In any case, once qualitative understanding has been achieved, one can obtain arbitrarily good quantitative estimates by resorting to higher orders of derivative expansion [74, 75], of which equation (2.76) represents just the first order.

It is possible to find a better ν value in the $N = 1$ case using the definition (2.72b) for the anomalous dimension rather than the (2.72a) one. This definition gives a worse value for $\eta(\simeq 0.4)$, but a much better result for $\nu(= 1.01)$, as shown in figure 2.15. In table 2.1 we

also show the results obtained for the three dimensional Ising model, as expected, in this case the agreement is much better. This is again due to the fact that the derivative expansion can be considered as an expansion in terms of the anomalous dimension: the error we commit will then be of the order of the anomalous dimension, which is smaller in $d = 3$ than in $d = 2$.

In fact the LPA$'$ ansatz for the effective action neglects the dependence of the wave function renormalization on momentum and field; this dependence is essentially governed by the anomalous dimension of the model and it is small when the anomalous dimension itself is small. Thus the LPA$'$ approximation turns out to be quite effective in these cases [19, 46]. As a confirmation of this fact one should consider the good results obtained in the three–dimensional case (again table 2.1) and the fact that the results become exact in the $N \to \infty$ limit, where in fact the anomalous dimension vanishes. As N grows our quantitative estimates become better; we made comparisons in the cases $N = 2, 3, 4$ and higher and we found good agreement with best known values [8]. Also our predictions are found to be better in the case of multi critical universality classes, where the results for the anomalous dimension are smaller than the standard WF case.

2.3.4 Tricritical universality class

In this case we have two IR repulsive eigenvalues of the linearized flow, both shown in Fig. 2.17 for $2 \leq d \leq 3$, and $N = 1, 2, 3, 4$. The exponent $y_{1,3} = 1/\nu_3$ is the inverse correlation length exponent; indeed at the upper tri-critical dimension, $d_{c,3} = 3$, it reaches its mean field value $y_{1,3} = 2$. When $N = 1$ the exponent does not depart so much from the mean field result as in the standard WF case. The $d = 2$ value we obtain is $y_{1,3} = 1.90$ to be compared with the exact result [41] $y^{ex}_{1,3} = 1.80$, both rather close to the mean field value. In the case of continuous symmetries ($N \geq 2$) the tri-critical universality class disappears in $d = 2$, and the $y_{1,3}$ exponents correctly return to their mean field values for every N. The $y_{2,3}$ exponent, instead, describes the divergence of the correlation length as a function of an additional critical parameter. At the upper tri-critical dimension the mean field result is $y_{2,3} = 1$. When $N = 1$ we find in two dimensions $y_{2,3} \simeq 0.4$ which should be compared with the exact value [41] $y^{ex}_{2,3} = 0.8$. In this case the agreement is rather low, but this is not surprising since we know that the LPA$'$ approximation is rather inefficient in $d = 2$. However it should be noted that even if not quantitatively correct, these results can be used to evaluate the crossover exponent $\phi = \frac{y_{2,3}}{y_{1,3}}$. In $d = 2$ this gives $\phi \simeq 0.2$ which, despite the quantitative error, gives a much better estimation than the ε–expansion, which provides a negative value for this exponent at order ε^2 [76]. For continuous symmetries, $N \geq 2$, $y_{2,3}$ vanishes in $d = 2$, in the same way as the exponent $y_{1,2}$ does in the WF case.

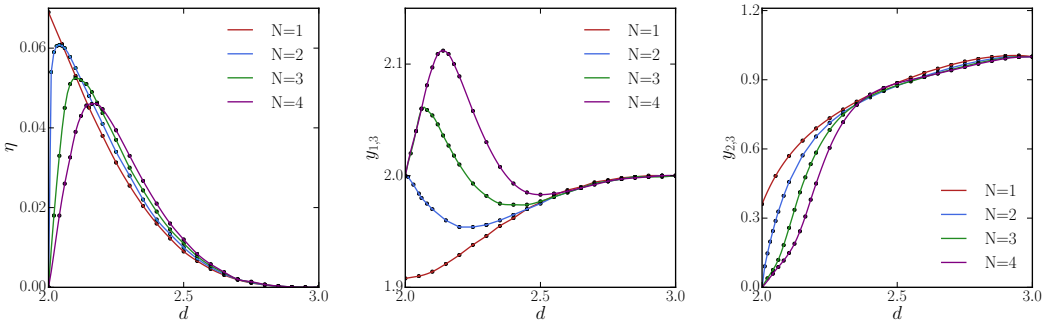

(a) Anomalous dimension η. (b) Eigenvalue y_1. (c) Eigenvalue y_2.

Fig. 2.17 Critical exponents $\eta_3, y_{1,3}, y_{2,3}$ of the tri-critical fixed points as a function of d for $N = 1,2,3,4$. These exponents describe the divergence of the correlation length as a function of the two critical parameters of the tri-critical universality class.

2.3.5 Higher multi-critical universality classes

The behaviour of the tri-critical case can be generalized to the other multi-critical universality classes. For these classes with $i > 3$, we have that at the upper critical dimension, $d_{c,i} = 2 + \frac{2}{i-1}$ [24], all the $i-1$ IR repulsive eigenvalues attain their mean field values. The largest one will always be $y_{1,i} = 2$, as in the standard WF case, with all the others having a mean field value smaller than 2. For $N \geq 2$ all the exponents, but the lowest one, will have different values as a function of $d < d_{c,i}$, all remaining pretty close to the mean field value, which is eventually recovered in $d = 2$. Conversely the lowest eigenvalue will decrease monotonically until it vanishes in $d = 2$. For $N = 1$ instead, all the multi-critical universality classes will still exist in $d = 2$ and thus all the exponents will reach a finite non mean field value, which will be given by the relative Conformal Field Theory (CFT) result [7].

2.3.6 The $N = 0$ case

Multi-critical scaling solutions are also found for $N = 0$, which survive in infinite number when $d \to 2$ [24]. A plot of η_i and ν_i for the first four universality classes $i = 2,3,4,5$ is shown in Fig. 2.18; these are numerically very similar to those of the $N = 1$ cases (see [24] and Fig. 2.14 for the WF class). This was indeed expected, judging from Fig. 2.14. In table 2.2 we compare the $d = 2$ exact and the $d = 3$ Monte Carlo (MC) results for (WF) self-avoiding walks (SAW) [77], which correspond to the $N = 0$ limit of $O(N)$ models [67], with the results obtained from our analysis and using scaling relations: From these comparisons we see that the $N = 0$ estimates are better than the $N = 1$ estimates, since also the $N \geq 2$

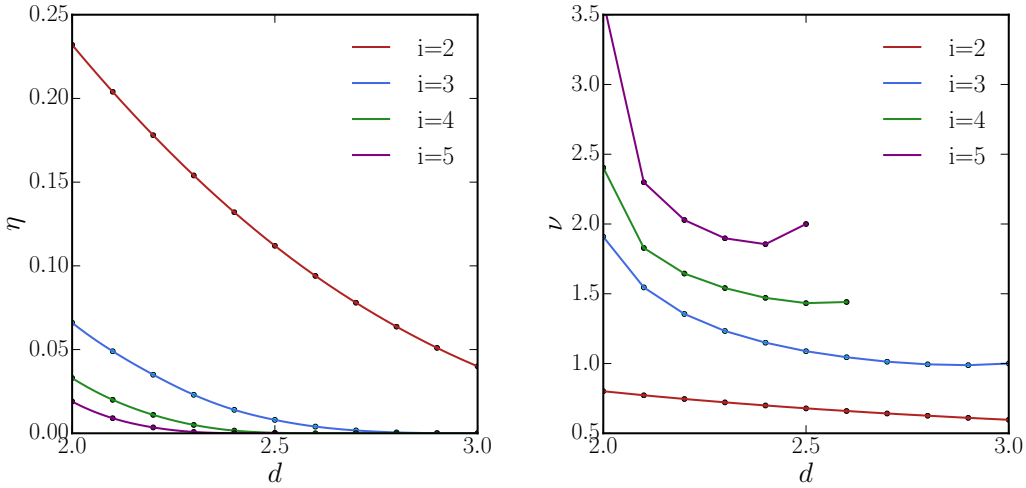

(a) Anomalous dimension η.

(b) Eigenvalue y_1.

Fig. 2.18 Critical exponents in the $N = 0$ case. In the main plot are shown the values of ν_i in the range $2 \leq d \leq 3$ for the (from the bottom) WF, tri-critical, tetra-critical and penta-critical universality classes, corresponding respectively to $i = 2,3,4,5$. In the inset the corresponding values of η_i are reported (in inverted order, from top to bottom).

Table 2.2 SAW results

Exp.	3d(MC[78])	3d(this work)	2d(exact[77])	2d(this work)
η	0.028	0.04	$5/24 \simeq 0.208$	0.232
ν	0.587	0.597	$3/4 = 0.75$	0.801
α	0.239	0.210	$1/2 = 0.5$	0.398
β	0.302	0.310	$5/64 \simeq 0.078$	0.093
γ	1.157	1.169	$43/32 \simeq 1.344$	1.416
δ	4.837	4.769	$91/5 = 18.2$	16.24

estimates are so, this indicates that the (WF) Wilson–Fisher universality class is the one for which our estimates are poorer.

In this section we reported the computation of critical exponents of $O(N)$ universality classes as a function of the dimension and of the number of field components. The correlation length critical exponent ν was computed by studying the eigenvalue problem obtained linearizing the RG flow of the running effective potential around the scaling solutions found in [24], representing the $O(N)$ multi-critical fixed point theories. From this and the previous knowledge of the anomalous dimensions, all the remaining exponents α, β, γ, δ were found using scaling relations. In particular we displayed the critical exponents for the Wilson–Fisher and tri-critical phase transitions for general d and N.

The critical exponents for the multi-critical classes in the $N \to 0$ limit were firstly investigated with LPA$'$ approximation. These, via the De Gennes correspondence [67], are universal, observable quantities which can be associated to possible new phases of polymeric systems.However this physics is yet to be observed.

We conclude this section by stressing that here we explored just the simplest realization of our method and this alone allowed a complete qualitative understanding of $O(N)$ universality classes.

2.4 Landscape of scalar field theories

The aim of this section is twofold, on one side we aim at demonstrating how it is possible to improve quantitative understanding of critical properties by enlarging the truncation considered for the effective action ansatz. On the other side it will be shown that the solution technique employed in latter section can be extended, with some modifications, to more complex truncation schemes. In this section we consider a one component scalar field field theory with a $\mathbb{Z}_2$ symmetry, the derivative expansion for the effective action to order ∂^2 reads [74]:

$$\Gamma_k[\varphi] = \int d^d x \left\{ \frac{1}{2} Z_k(\varphi)(\partial\varphi)^2 + V_k(\varphi) \right\}. \tag{2.82}$$

The effective potential $V_k(\varphi)$, the wave-function renormalization function $Z_k(\varphi)$ are now written in the field φ notation rather than in the invariant $\rho = \frac{\varphi^2}{2}$ since we are considering only scalar field theories.

We derive now the flow equations for the effective potential $V_k(\varphi)$ and for the wave-function renormalization function $Z_k(\varphi)$, dropping the fourth order functions. The definitions to derive the flow equations can be obtained projecting properly the Wetterich equation (1.60),

$$V_k(\varphi) = \Gamma_k[\varphi]\Big|_{\varphi=\tilde{\varphi}} \tag{2.83}$$

$$Z_k(\varphi) = \lim_{p\to 0} \frac{1}{2}\frac{d^2}{dp^2}\Gamma_k^{(2)}[\varphi]\Big|_{\varphi=\tilde{\varphi}} \tag{2.84}$$

The flow equation for the effective potential is given by:

$$\partial_t V_k(\varphi) + d\,V(\varphi) - \frac{(d-2+\eta)}{2}\varphi V^{(1)}(\varphi) = Q_{\frac{d}{2}}\left[\left(\dot{R}_k - \eta R_k\right) G_k(\varphi)\right], \tag{2.85}$$

where $\dot{R} = \partial_t R_k$ is the scale derivative of the cutoff function and the ˜ symbol over the φ field has been omitted for convenience. The cutoff function can be expressed as,

$$R_k(q) = q^2 r(q^2/k^2) \tag{2.86}$$

which ensures the correct dimension for the cutoff term in the action. Then in equation (2.85) the regularized propagator at the constant field configuration φ is defined as:

$$G_k(x,\varphi) = \frac{1}{Z_k(\varphi)\,x + V_k''(\varphi) + x\,r(x/k^2)}\,. \tag{2.87}$$

In equation (2.85) we wrote the r.h.s. as a "Q-functional" as defined in equation (B.83) of Appendix B.3. In this section we will always write the beta functions, before a particular cutoff shape function as been chosen, in terms of Q-functionals. In this sense a Q-functional is a functional that maps a cutoff shape function to the explicit form of the beta function. The anomalous dimension of the scalar field in (2.85) is defined by $\eta = -\partial_t \log Z_k(0)$.

This definition of the anomalous dimension is valid both in the symmetric and in the broken phase [19]. It is a little more involved to derive the flow equation for the wave-function renormalization function. Taking the second functional derivative of (1.60) with respect to the fields we can readily write down the flow equation for the two-point function of the effective action in momentum space. We have:

$$\begin{aligned}\partial_t \Gamma^{(2)}_{p,-p}(\varphi) = \\ \int_q G_q(\varphi)\Gamma^{(3)}_{q,p,-q-p}(\varphi)G_{q+p}(\varphi)\Gamma^{(3)}_{q+p,-p,-q}(\varphi)G_q(\varphi)\partial_t R_q + \\ -\frac{1}{2}\int_q G_q(\varphi)\Gamma^{(4)}_{q,p,-p,-q}(\varphi)G_q(\varphi)\partial_t R_q\,.\end{aligned} \tag{2.88}$$

Introducing on the r.h.s. of equation (2.86) the vertices of the effective action at order ∂^2 and extracting the p^2 terms gives, after some algebra, the following flow equation for the wave-function renormalization function is found

$$\begin{aligned}\partial_t Z_k(\varphi) = &-Z^{(2)}(\varphi)\frac{d}{2}Q_{\frac{d}{2}}\left[G^2\left(\dot{R}_k - \eta R_k\right)\right] + Z^{(1)}(\varphi)^2 2dQ_{\frac{d}{2}+1}\left[G^3\left(\dot{R}_k - \eta R_k\right)\right] \\ &+ Z^{(1)}(\varphi)^2 dQ_{\frac{d}{2}+2}\left[G^2 G_x\left(\dot{R}_k - \eta R_k\right)\right] + Z^{(1)}(\varphi)^2 2Q_{\frac{d}{2}+3}\left[G^2 G_{xx}\left(\dot{R}_k - \eta R_k\right)\right] \\ &+ Z^{(1)}(\varphi)V^{(3)}(\varphi)dQ_{\frac{d}{2}}\left[G^3\left(\dot{R}_k - \eta R_k\right)\right] + Z^{(1)}(\varphi)V^{(3)}(\varphi)2dQ_{\frac{d}{2}+1}\left[G^2 G_x\left(\dot{R}_k - \eta R_k\right)\right] \\ &+ V^{(3)}(\varphi)^2 dQ_{\frac{d}{2}}\left[G^2 G_x\left(\dot{R}_k - \eta R_k\right)\right] + V^{(3)}(\varphi)^2 2Q_{\frac{d}{2}+1}\left[G^2 G_{xx}\left(\dot{R}_k - \eta R_k\right)\right] \\ &+ Z^{(1)}(\varphi)V^{(3)}(\varphi)4Q_{\frac{d}{2}+2}\left[G^2 G_{xx}\left(\dot{R}_k - \eta R_k\right)\right].\end{aligned} \tag{2.89}$$

Equations (2.85) and (2.89) represent the flow equations for $V_k(\varphi)$ and $Z_k(\varphi)$ for general cutoff shape function at order ∂^2 of the derivative expansion.

Once an appropriate cutoff shape function has been chosen, the integrals in (2.85) and (2.87) can be pursued, sometimes analytically. In this way we obtain a system of partial differential equations for $V_k(\varphi)$ and $Z_k(\varphi)$ in the variables k and φ. After re-writing the flow equations (2.87) and (2.87) in terms of the dimensionless field $\tilde{\varphi} = k^{\frac{d}{2}-1} Z_k^{-1}(\varphi_0)\varphi$ and of the dimensionless functions $\tilde{V}_k(\tilde{\varphi})$ and $\tilde{Z}_k(\tilde{\varphi})$, we can study the system

$$\partial_t \tilde{V}_k(\tilde{\varphi}) = 0 \qquad\qquad \partial_t \tilde{Z}_k(\tilde{\varphi}) = 0\,,$$

to find the fixed point effective potential and fixed point wave-function renormalization function, as we did in previous sections. It is possible, for example, to show that in $d = 3$ there is only one scaling solution to the latter system.

The investigation of $\mathbb{Z}_2$ symmetry breaking in $d = 3$ is not a crucial test for the derivative expansion technique. Indeed in the context of RG approaches very good results for the critical exponents of φ^4 theory can be obtained using ε-expansion techniques [54]. It is in $d = 2$, where every perturbative approach fails to describe correctly the various universality classes, first constructed exactly using conformal field theory (CFT) methods [7], that the system (2.89) reveals its non perturbative potentialities. It was shown in [79] that the system (2.90), in $d = 2$, has several scaling solutions, each of which corresponds to one of the universality classes know from CFT. It was also found in [59] that the derivative expansion (2.82) breaks down as the anomalous dimension of the scalar field grows, making the contributions of the neglected higher derivative terms, increasingly more important.

2.4.1 Scaling solutions

In order to solve equations (2.85) and (2.89) we shall specify the form of the cutoff function. In this section we will again consider the optimized cutoff case

$$R_k(q) = (k^2 - q^2)\theta(k^2 - q^2)$$

which is believed to always produce better results, rather than the power law cutoff employed in [18]. We shall then solve equations for the optimized cutoff at the fixed point and then compare our results with the ones obtained with the equations obtained in the power law cases, which were already solved in [18, 59].

The main focus of this section is to show how it is possible to obtain reliable results for the universality class of the model considered using the spikeplot method to solve the flow

equations. As shown in previous sections this method has diverse advantages. First of all it does not require to solve the flow for equations in function of the renormalization "time" t. Also we solve the fixed point equations (expressions (2.85) and (2.89) with the l.h.s. equal to zero) in their full functional form, without relying on truncations as it was done in [74]. Moreover our solution method does not need any external input as in [18, 59], where the relaxation method was used starting from the exact spherical model solution. This approach even if very effective is rather involved even at this order in derivative expansion and one needs to carefully study the flow equations before the actual computation, in order to have a qualitative pictures of the expected phase diagram.

Conversely our technique consists in solving the fixed point equations with the spikeplot method introduced in [24]. As shown in previous section this method proves useful in the LPA$'$ approximation, allowing to depict a full qualitative and in many case quantitative phase diagram of $O(N)$ models [22, 25].

For parity reasons we expect the following boundary conditions for the local potential and the wave-function renormalization evaluated for vanishing fields,

$$V^{(1)}(0) = 0, \tag{2.90}$$
$$V^{(2)}(0) = \sigma, \tag{2.91}$$
$$Z(0) = 1, \tag{2.92}$$
$$Z^{(1)}(0) = 0. \tag{2.93}$$

Conditions (2.90) and (2.93) are a direct consequence of the $\mathbb{Z}_2$ symmetry. The condition (2.92) is obtained using field scale invariance to absorb a term $Z(0)$ into the field definition. Thus we are left with only an unspecified condition over the $V^{(2)}(0)$ value. In equation (2.91) σ is some real values to be computed using the shooting method as it happens in the simpler LPA$'$ case of section 2.3 [24].

At LPA$'$ the value of the anomalous dimension can be uniquely defined from the fixed point potential, see (2.75). On the other hand in the present case the anomalous dimension η is a free parameter to be chosen using the shooting method.

Let us describe the procedure in more details, we solve equations (2.85) and (2.87) in a specified cutoff scheme for different values of σ and η. For any arbitrary point in the (η, σ) plane the solution will blow up at a finite value of the field, we call this finite value $\tilde{\varphi}_\infty(\sigma, \eta)$, in analogy with $\tilde{\rho}_\infty(d, \sigma)$ of previous section. As already explained there are some points in which $\tilde{\varphi}_\infty$ diverges, indicating a fixed point effective action well defined at any field value. Thus the physical fixed points in the (η, σ) plane is indicated by a singularity of $\tilde{\varphi}_\infty$. At this

points the solutions of the fixed point equations represent the effective action of scalar field theories at criticality.

2.4.2 The three dimensional case

First of all we consider the case $d = 3$, which is the less involved since the anomalous dimension is small. Moreover in $d = 3$ we have just one universality class, apart form the non interacting gaussian fixed point. This is the standard Wilson Fisher fixed point, which represents the critical behavior of interacting φ^4 theories. The equations in the optimized cutoff case (B.107) and (B.108), given in the appendix, are solved using the spikeplot method. We shall specify four initial conditions in order to solve these two second order differential equations, we already showed that the only independent initial condition left after an accurate analysis of the differential system is the bare value of the dimensionless mass $\tilde{V}^{(2)}(0) = \sigma$ we obtain a three dimensional plot of $\tilde{\varphi}_\infty$ as a function of σ and η. The theory space of the three dimensional Ising model emerges from the phase space of the solutions of equations (2.85) and (2.87). In figure 2.19 the value at which the numerical solver interrupts integration $\tilde{\phi}_\infty$ is represented by colors in the plane of the initial conditions (σ, η). Apart for the maximum in the origin, which represents the free theory, we see a family of maxima arising along a curve which separates the dark blue region of the severely ill defined solutions from the light green region of intermediate solutions. The WF universality is located at the end of the line of maxima as it is clearly seen in panel (a). It is remarkable that modifying the cutoff function we obtain similar results for the critical exponent but different ranges for the physical values of the coupling. In particular the equations in the optimized cutoff case develop a divergence for $\sigma = -1$ often called spinodal instability. It is not clear wether this divergence which is IR attractive in all directions is the physical IR fixed point or rather an artifact of the cutoff scheme. However it has been demonstrated that it is possible to recover information over the universal quantities studying the scaling of the solutions close to this instability [52].

Moreover we find that only the small η portion of the plane is a non trivial support for the φ_∞ function, which is identically zero for all $\eta > 0.05$. Thus the identification of the Wilson Fisher universality class is unique and does not need and special analysis such as large field expansions or relaxation methods. The results of 2.19 have been obtained solving numerically the fixed point with a fourth order Runge-Kutta approach.

In Fig. 2.19 panel (a) it is evident that apart for the red sharp spike in $\sigma = \eta = 0$ another less sharp peak occur at some finite value of the initial conditions. However this sharper spike is part of a family of peaks branching from the Gaussian universality. It is not easy to decide at which precise value of the (σ, η) plane the spike actually occurs due to the errors introduced by the finite grid. Also the three dimensional shape of the spike is rather complex

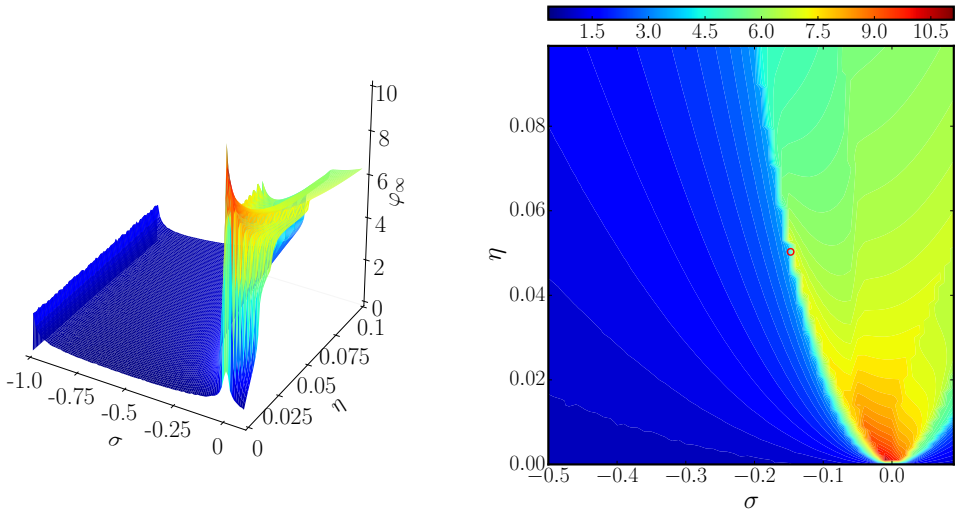

(a) 3 dimensional plot of $\phi_\infty(\sigma,\eta)$ in $d=3$.

(b) Contour plot of $\phi_\infty(\sigma,\eta)$ in $d=3$.

Fig. 2.19 Spike plot in three dimension for the optimized cutoff case in panel (a). The value of φ_∞ in the (σ,η) planes has two divergences: the one located at $(0,0)$ is the Guassian theory. The other divergence represents the Wilson Fisher universality class, which occurs at a finite positive value of the anomalous dimension and for a negative dimensionless mass. Contour plot of $\phi_\infty(\sigma,\eta)$ in panel (b).

and it is difficult to extrapolate the correct maximum value from the results on the discrete grid.

The red circle in the contour plot of Fig. 2.19 panel (b) represents the location of the Wilson-Fisher universality class obtained after a careful analysis described in the following. As it is easily seen the point is not located on one of the maxima of the function $\varphi_\infty(\sigma,\eta)$ due to the finiteness of the two dimensional grid used to compute the landscapes of Fig. 2.19.

2.4.3 The two dimensional case

The $d=2$ case is more involved, due to the infinite number of universality classes of a two dimensional scalar theory. These universality classes correspond with the minimal models of CFT and then the critical exponents are known exactly.

It is however important to reproduce such results even at approximate level with an independent method. Indeed to obtain our flow equations we did not impose any further condition rather than $\mathbb{Z}_2$ symmetry. Even in this oversimplified computation scheme and without any imposition on the symmetries of the model or the shape of the solutions we found a complete picture of the phase landscape of scalar field theories. The result for the

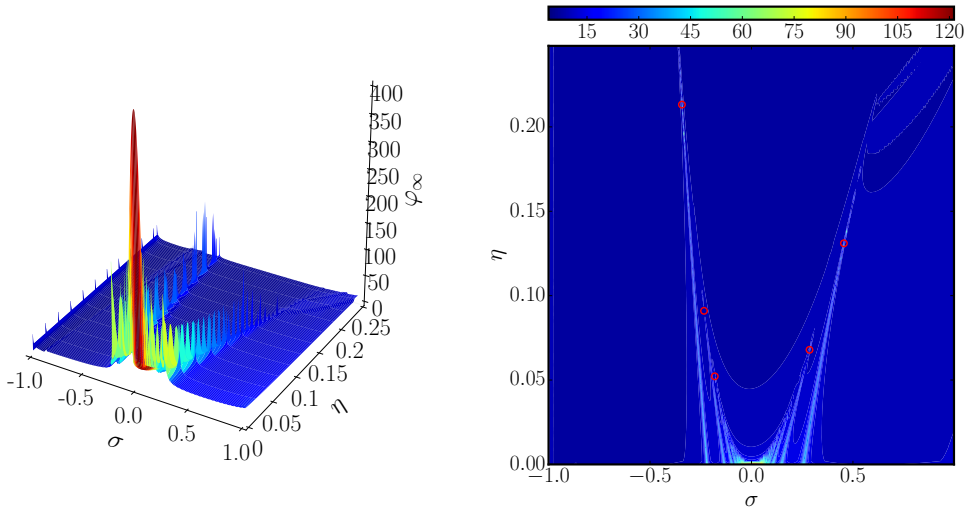

(a) 3 dimensional plot of $\varphi_\infty(\sigma,\eta)$ in $d=2$. (b) Contour plot of $\varphi_\infty(\sigma,\eta)$ in $d=2$.

Fig. 2.20 Spike plot in two dimensions for the optimized regulator case. The landscape of scalar quantum field theories at this approximation level is quite complicated. The maxima of φ_∞ form mountain chains located on some special curves in the (σ,η) plane.

landscape of interacting fixed points in two dimensional scalar field theories is reported in figure 2.20, in the optimized cutoff scheme. It si difficult to correctly identify the exact value of the anomalous dimension for any universality class. Indeed the maxima of $\tilde{\varphi}_\infty$ are disposed on special lines of the (σ,η) plane, forming spike chains.

The minimal models universality classes should be located at the tallest peak of every chain. However it is not easy to identify the desired solution due to the infinite number of solutions accumulating at the origins. The simplest cases are the one with largest values of the anomalous dimension which are the furthest from the accumulation points.

In panel (a) of Fig. 2.20 the Gaussian universality appears as a infinitely tall spike located at $\sigma=\eta=0$. The two peaks chain at the extrema of the origin are the longest in the η direction and they represent the Wilson-Fisher and tricritical universalities which have the largest anomalous dimension values. In both these peak chains, going from $\eta=0$ to $\eta=\infty$, have a maxima at a finite value of the anomalous dimension which roughly corresponds to the expected value.

The results are more clear as seen in Fig. 2.20 panel (b), we have infinitely many peak chains starting at $\eta=0$ and drawing sharp cuts in the (σ,η) plane. These chains accumulate in the origin, becoming shorter and shorter, as expected since the represent high order universalities. Every chain is almost a straight line and posses one or few maxima (the bright

spots in Fig. 2.20 panel (b)) at a finite value of the anomalous dimension, which roughly corresponds with the expected value of the corresponding universality.

The presence of more then one maxima in most of the spike chains of Fig. 2.20 make the determination of the correct maximum rather complex. Indeed we shall expect only one singularity to emerge for any chain. However this is not the case due to the extremely complex three dimensional structure of every chain which makes difficult to correctly represent it using the results of the shooting technique over a finite square grid.

Moreover increasing the precision of the grid will need an exponential growing computation time due to the necessity to increase accordingly the precision of the numerical solution of the differential equations. In the following section we outline a general procedure which allow to compute the correct value of the anomalous dimension maintaining low computational cost.

2.4.4 The anomalous dimension

The best approach to compute the anomalous dimension of every universality class is to reduce the problem of finding the maxima of the two dimensional surface $\varphi_\infty(\sigma,\eta)$ to the simpler one to find the maximum of a single one dimensional chain. This is possible using the results of Figs. 2.19 and 2.20 as a guide. First of all we fit the locations of the maxima of a single chain in the (σ,η) plane with a simple function, a straight line was sufficient in most of the cases. This procedure give us an explicit expression for the maxima chain as a function $\sigma(\eta)$ along which we can pursue a standard one dimensional shooting technique. Obviously the coefficients of the fit will contain errors due to the finiteness of the grid in the landscape of Figs. 2.19 and 2.20.

The best value for the fit is obtained varying the coefficient in order to maximize the height of the spike as it is shown in Fig. 2.21 panel (a) for the tricritical universality.

During the optimization procedure of the fit parameters it occurs that two minima are found in the line, this is due to the complex three dimensional structure of the peaks in the (σ,η) plane. However as it appears from Fig. 2.20 panel (a) the highest divergence is obtained in the case of a single peak, showing that the two peaks structure occurs only when the fit line does not cross the singularity at the center. The optimization procedure is straightforward since we should allow only for very small variation of the fit coefficients and the one dimensional shooting computation is extremely fast.

Optimizing the fit coefficients to maximize the height of the peak in every chain we obtain a one dimensional spike plot for every universality class from the standard Wilson-Fisher case $i = 2$ to the esacritical universality $i = 6$ as it is shown in Fig. 2.19. The values, at which

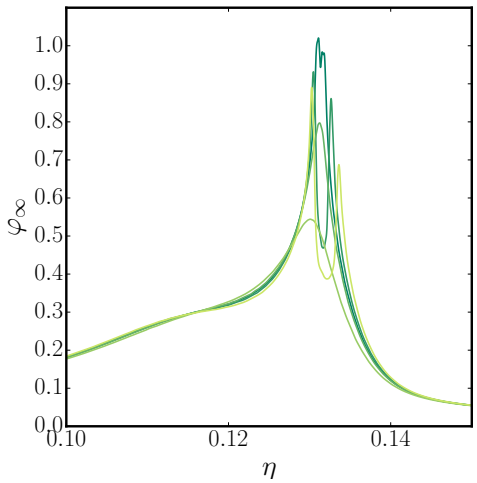

(a) Convergence procedure for the tricritrical universality in $d = 2$.

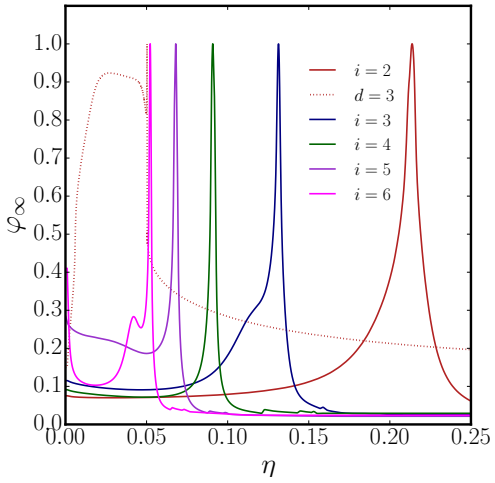

(b) Shooting technique along the chains.

Fig. 2.21 In panel (a) we show different results for the one dimensional shooting technique along the WF universality peak chain in two dimension, the different curves represent different values for the chain curve fit parameters. In panel (b) the 1 dimensional spike plots along the chains lines, with optimized fit parameters, are shown for the first six universality classes in $d = 2$ (solid lines) and for the WF universality in $d = 3$ (dotted line).

the singularities of $\tilde{\varphi}_\infty$ occur, are in agreement with the expected values for the anomalous dimensions.

In Fig. 2.22, panel (a), we show the results obtained for the anomalous dimensions obtained using the shooting technique described above to solve the fixed point equations. The results of this work (green line) are compared to the ones found in [59] and to the exact results of CFT solutions (red line). The curve obtained here is more precise than the results found in the power law cutoff scheme of [59], which confirms the expected better performance of the optimized cutoff scheme. It should be also noted that, as expected, the precision of FRG truncation scheme increases lowering the anomalous dimension values, with the esacritical value for the η exponent reproduced up to 99% even in this rather simple approximation.

In panel (b) of Fig. 2.22 we show the potential $V(\varphi)$ and the field dependent wavefunction renormalization $Z(\varphi)$ for the first six universality classes in $d = 2$. The solutions are shown only for positive values of the field $\tilde{\varphi}$, since the other branch can be simply obtained using reflection symmetry. Each potential shows a number of minima i, as indicated by its criticality order, and the corresponding wavefunction renormalization has a relative maximum in correspondence of each minimum position.

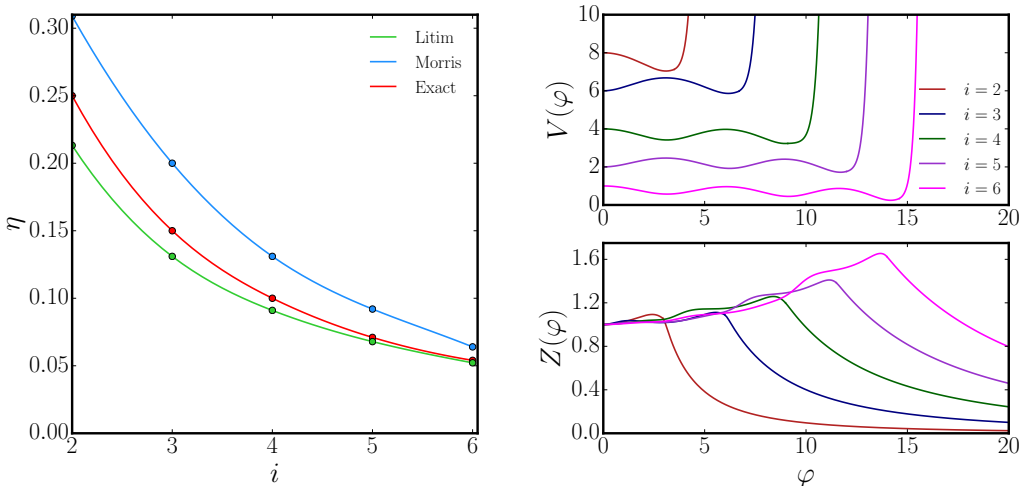

(a) Anomalous dimensions of the first six multicritical universalities in $d = 2$.

(b) Fixed point solutions for the function $V(\varphi)$ and $Z(\varphi)$ in $d = 2$.

Fig. 2.22 n panel (a) we show the anomalous dimensions as a function of the critical index i for the optimized (green line) and power law (blue line) cutoff case, compared to the exact CFT results (red line). In panel (b) the solutions for the functions $Z(\varphi)$ and $V(\varphi)$ are shown for the first six multicritical universalities.

The solutions shown in figure 2.22 panel (b) have been obtained solving equations (2.85) and (2.87) with the values of η and $V''(0)$ found using the shooting technique described in Fig. 2.21. These solutions however break down at some finite value $\tilde{\varphi}_\infty$ which occurs soon after the last minima of the fixed point potential. The asymptotic behaviors shown in Fig. 2.22 have been computed using large field expansion of equations (2.85) and (2.87).

2.4.5 Regulator dependence

As it should be understood from above investigations. The efficiency of our shooting technique crucially depends on the structure of the 3 dimensional surface $\varphi_\infty(\sigma, \eta)$, which has non trivial shape only on a finite number of quasi-2 dimensional manifolds, i. e. the lines in Fig. 2.20. It is then necessary to test wether this simplified structure is just an artifact of our particular regulator or if it is a general result valid for equations (2.85) and (2.87) independently from the particular form assumed by the Q-functionals.

In order to check the stability of our approach we consider another regulator form to explicitly compute the Q-functional. The most effective choice in this perspective is the

power law regulator already adopted in [59]

$$R_k(q) = \frac{k^4}{q^2}. \tag{2.94}$$

Indeed such regulator, even if not optimal to compute numerical quantities, produces simple results for the flow equations. Moreover the power law has a rather peculiar shape very different from the Litim one, indeed while the last one is compact with extremely localized derivatives the first has infinite support and it has finite derivatives at all orders.

The derivation of the flow equations in the power law cutoff case (2.94) is reported in the appendix. We apply the same procedure already considered for the flow equations in the Litim regulator case. Both in $d = 2$ and $d = 3$ we retrieve the expected phase structure, with only one correlated fixed point in the first case and infinitely many solutions in $d = 2$, as in Fig. 2.23. It is worth noting that in the power law regulator case the height of the peaks in the

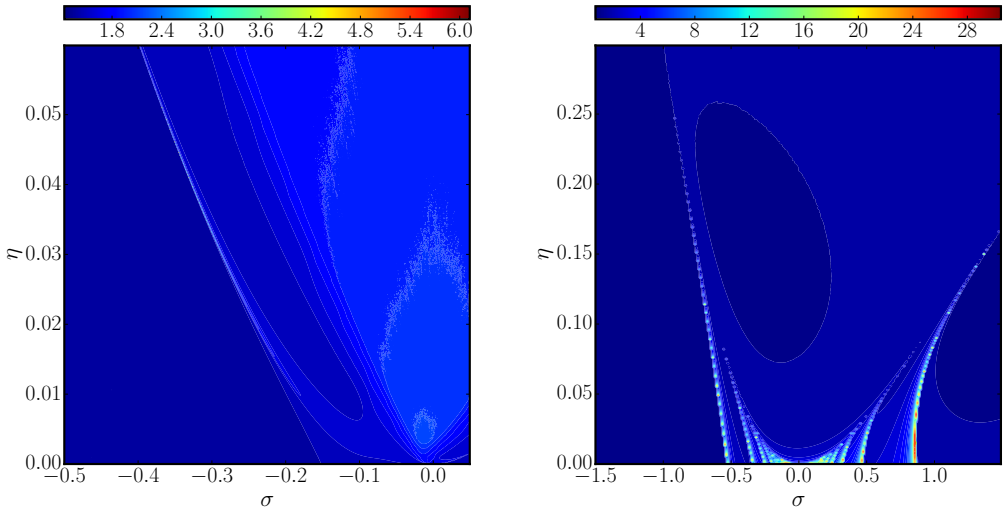

(a) $d = 3$ (b) $d = 2$

Fig. 2.23 Spike plot in two dimensions for the power law cutoff case. The landscape of scalar quantum field theories at this approximation level is quite complicated. The maxima of φ_∞ form mountain chains located on some special curves in the (σ, η) plane.

contour plot is much smaller than in the previous case. However both in 2, Fig. 2.23 panel (a), and 3 dimensions, panel (b), the peak chains are evident, thus demonstrating that the structure of the $\tilde{\varphi}_\infty(\sigma, \eta)$ function, even if influenced by the regulator form, maintain a very small non trivial support. In both the regulator cases every universality class of the theory appears has a chain of peaks in the σ η plane.

2.5 Conclusion

When one starts writing a thesis the first problem is choosing a suitable title. Since the beginning of the project this thesis was aimed at exploring the possible application of the FRG approach to Condensed Matter and Statistical Physics problems. Then the methodological focus of the Thesis should have been clearly stated in the title of the thesis. However different communities employ different names to indicate the same RG approach. All these names are devised to underline a different characteristic of the approach, which in the mind of the users is the most relevant in actual computations.

The name *Exact Renormalization Group* is the most traditional one and drives attention on the Wetterich equation (1.60) which is in principle exact. The exactness of the FRG core equation has played a crucial role in the success of the approach, indeed, even if not exactly exploited, it is responsible for the possibility to develop tower of convergent approximation schemes [19, 31, 32].

On the other hand the name *Non-Perturbative Renormalization Group* is employed to highlight the possibility to produce non perturbative results in the FRG framework. This is probably the most relevant property of FRG. Nevertheless it is hard to define what non perturbative really means. An *a posteriori* definition consist to call non perturbative the results which cannot be obtained using perturbative approaches. An *a priori* definition can be devised as follow *non perturbative techniques allow to produce numerical quantities whose accuracy does not lowers exponentially with any of the model parameters.* This latter definition seems more compelling; indeed it has been shown in Chapter 2 that LPA$'$ truncation, when treated at full potential level [80], is able to reconstruct all the qualitative picture and to furnish semi-quantitative results for the universal quantities as a function of N and d. Thanks to the spikeplot technique outlined in [22] and fully developed in [23, 25] we are able to draw the full picture for the phase diagram in any dimension and even in some special limits such as the $N = -2, -1, 0$ limits, recovering all the expected features provided by exact computations. These results are the best evidences of the non perturbative characteristic of derivative expansions of FRG.

While the absence of any perturbative approximations is probably the most relevant feature of FRG, it is obtained only when derivative expansions are employed. Nevertheless FRG approach is also used to pursue perturbative computations in Fermionic systems [32, 81]. FRG formalism profoundly simplifies the regularization of perturbative series and brought new insight into perturbative investigations of Fermionic field theories. Then the name *Non-Perturbative Renormalization Group* while emphasizes the potentialities of derivative expansion reduces the importance of other approximation techniques, such as vertex expansions, which however prove useful in many different context.

In the title of this thesis it was chosen the definition *Functional Renormalization Group*, since, in the opinion of the author, it is the most suitable to describe the characteristics of the method. Indeed FRG is based on a functional RG equation (1.60) and, thanks to derivative expansions, allows to explore functional flow equations. Only when full functional form of the flow equations is retained it is possible to obtain qualitatively correct results, see Section 2.2.

For systems with continuous symmetry ($N \geq 2$) LPA gives no SSB for $d \leq 2$ and SSB for $d > 2$ in agreement with the Mermin-Wagner theorem and its extension to systems with fractional dimension; in particular, simple analytical expressions are found in the large N limit, correctly retrieving the expected results for the spherical model. We observe that the presented results rule out any type of SSB, not only the standard (bicritical) Wilson-Fisher (WF) fixed point, but also all the other possible multicritical fixed points.

As a tool to assess the validity of different truncation schemes, for general N we studied the solutions of the LPA renormalization group equations using a finite number of terms (and different regulators), showing that SSB always occurs even where it should not (i.e. for $d \leq 2$ for $N \geq 2$). The SSB is signaled by WF fixed points which for any possible truncation are shown to stay on the line defined by vanishing mass beta functions. Increasing the number of couplings these WF fixed points tend to the infrared convexity fixed point for $d \leq 2$ and to the pertinent exact LPA WF point for $d > 2$. Moreover we studied the case of Taylor expansion of the effective potential around the minimum ρ_0. Even when this expansion is truncated at lowest order $N_{\mathrm{CUT,m}} = 2$, it is possible to retrieve the correct behavior for the Mermin-Wagner theorem, since ρ_0 is diverging when $d \to 2$. However at this order the truncation around the minimum cannot provide the expected behavior for the $N = 1$ case, in fact the coupling λ diverges at $d = 2.5$ and becomes negative below this threshold, even if it is well known that in the Ising model the SSB occurs even at $d = 2$.

For the Ising model ($N = 1$) the SSB is shown to occur for $d > 2$ (as it should be), but not for $d = 2$ (as it should not be). At variance, finding the correct results for $d = 2$ and $N = 1$, as well as for the Ising model in $1 < d < 2$, requires to go beyond LPA since the anomalous dimension cannot be neglected: in $d = 2$ the LPA without truncations is sufficient to explain the absence of SSB for $N \geq 2$, but not to predict the presence of SSB for the Ising model. To have qualitatively correct results in $d = 2$ valid for all N anomalous dimension effects as introduced in LPA$'$ have to be considered. This has been recently shown in [22], which shows how LPA$'$ is able to reproduce numerically the behaviour predicted by the Mermin-Wagner theorem for $d \to 2$ and $N \geq 2$ (with the anomalous dimension $\eta \to 0$ and the correlation length exponent $\nu \to \infty$ [25]), and correctly predicting at the same time SSB and a finite anomalous dimension exponent for the Ising model. We extended these results showing that

when the anomalous dimension vanishes then no SSB transition is possible in $d \leq 2$ (as it happens for the $O(N \geq 2)$ models).

In Section 2.3 we reported the computation of critical exponents of $O(N)$ universality classes as a function of the dimension and of the number of field components. The correlation length critical exponent ν was computed by studying the eigenvalue problem obtained linearizing the RG flow of the running effective potential around the scaling solutions found in [24], representing the $O(N)$ multi-critical fixed point theories. From this and the previous knowledge of the anomalous dimensions, all the remaining exponents α, β, γ, δ were found using scaling relations.

In particular we displayed the critical exponents for the Wilson–Fisher and tri-critical phase transitions for general d and N. Another result which is new to our knowledge are the critical exponents for the multi-critical classes in the $N \to 0$ limit. These, via the De Gennes correspondence [67], are universal, observable quantities which can be associated to possible new phases of polymeric systems. To the best of our knowledge, this physics is yet to be observed.

One interesting feature which is worth mentioning is that there is a correspondence between critical exponents of models with short range interactions in fractional dimension and models with long range interactions in integer dimension [80]. This means that our curves $\eta(d,N)$ and $\nu(d,N)$ have direct physical interpretation, not only for systems in fractional dimensions, but as describing the critical behaviour of models with long range interactions in two or three dimensions. In this case our universal results could be indirectly tested in the near future, both by numerical simulations and laboratory experiments. Further details on this correspondence can be found in [80], see Chapter 4. By computing the function $\nu(d,N)$ we provided the information necessary to complete the non perturbative RG scenario of $O(N)$ models universality classes as put forward in our previous work [24]. This constitutes a first important example of how one can use RG equations to give precise statements on how universality classes depend on dimension and symmetry group parameters, a general and fundamental problem whose solution has important applications in physical model building in both condensed matter and high energy physics.

It is worth noting that the approach here presented makes a bridge between all the known features of the critical behavior of $O(N)$ models. In fact, perturbative ε–expansion techniques while providing good numerical results close to four dimensions are unable to reproduce even the qualitative features of the models in $d \simeq 2$ [8]. In $d = 2$ it is necessary to use ad hoc methods as CFT to obtain exact quantities. These exact results are however difficult to connect with the $d > 2$ approximate results. Also other expansions based on the exact solution of the spherical model are difficult to calculate at high orders [72] and they fail both

in quantitative and qualitative agreement for small N values. In particular multi-critical results are not available in $1/N$ expansions and are also qualitatively incorrect in ε–expansions [41], while the approach described here gives all the qualitatively correct results even for these models. The correctness of these findings is granted by the functional description of the theory space of $O(N)$ models which is developed here to full extent.

In the last section of this Chapter 2.4 we demonstrated the flexibility of the spikeplot technique, employed for the LPA$'$ case in section 2.3, applying it to the $O(\partial^2)$ ansatz of the derivative expansion for scalar field theories. Without any external input the method can recover the full phase diagram of the 2 dimensional scalar field theory. Every universality class is obtained as a family of peaks of the function $\varphi_\infty(\sigma, \eta)$ in the (σ, η) plane, see figure 2.20. Later on the height of the tallest maximum for every peak chain in the plane is used to locate the correct values of the anomalous dimension of each universality class. The obtained results are shown in figure 2.22a.

The method described and tested in the last section of this chapter will be particularly useful to analyze the phase diagram of exotic field theories where no a priori information is available, since it does not need any external input and allows to immediately visualize the qualitative structure of the theory phase space.

Chapter 3

FRG Studies of Sine-Gordon Models

The FRG is a powerful technique to study SSB and $O(N)$ models as discussed in Chapter 2, but it gives indirect informations, at least in derivative expansions [82, 83], on the occurrence of topological BKT transition in the $N = 2$ $d = 2$ case. To investigate topological transitions, where SSB is not present, it turns convenient to apply FRG to sine-Gordon (SG) models as it is done in the present chapter.

In the last section of Chap. 2 we compared our results for the anomalous dimension with the exact quantities obtained by CFT. This discussion showed how FRG techniques can reproduce, at least qualitative, the exact values found with conformal methods in a more general framework.

Another bridge between conformal field theory (CFT) techniques and the RG description of field theories is provided in two dimensions by the c-theorem. Far from fixed points, Zamolodchikov's c-theorem [84] can be used to get information on the scale-dependence of the model. In particular the theorem states that it is always possible to construct a function of the couplings, the so-called c-function, which monotonically decreases when evaluated along the trajectory of the RG flow. Furthermore, at the fixed points this function assumes the same value as the central charge of the corresponding CFT [7].

Although the c-theorem is by now a classical result, the determination of the c-function is not straightforward and its computation far from fixed points is non-trivial even for very well known models, so that methods as form factor perturbation theory, truncated conformal space approach and conformal perturbation theory has been developed [85]. In $d = 2$ an expression of the c-function has been obtained in the framework of form factor perturbation theory [86] for theories away from criticality and it has been applied to the sinh-Gordon model [85]. The sinh-Gordon model is a massive integrable scalar theory, with no phase transitions. In [85] one finds $\Delta c = 1$ for the sinh-Gordon theory. In a recent result [87], the analytical continuation of the sinh-Gordon S-matrix produces a roaming phenomenon

exhibiting $\Delta c = 1$ and multiple plateaus of the c-function. The analytic continuation $\beta \to i\beta$ of the sinh-Gordon model leads to the well-known sine-Gordon (SG) model with a periodic self interaction of the form $\cos(\beta\varphi)$.

The SG model presents the unique feature to have a whole line of interacting fixed points with coupling (temperature) dependent critical exponents. It is in the same universality of the 2-dimensional Coulomb gas [88] and of the 2-dimensional XY [36], thus being one of the most relevant and studied 2-dimensional model, with applications ranging from the study of the Kosterlitz-Thouless transition [36] to quantum integrability [89] and bosonization [90]. In particular, for the SG model an ubiquitous issue is how to deal with the issue of the periodicity of the field [91], which unveils and plays a crucial role for $\beta \neq 0$. Given the importance of the SG as a paradigmatic 2-dimensional model, the determination of the c-function from the non-perturbative RG flow is a challenging goal, in particular to clarify the role played by the periodicity of the field for $\beta \neq 0$.

From the RG point of view, the determination of the behavior of the c-function is a challenging task requiring a general non-perturbative knowledge of the RG flow. Recently [25], an expression for the Zamolodchikov's c-function has been derived for 2-dimensional models in the Functional RG (FRG) framework [19, 31, 43]: resorting to an approximation well established and studied in the FRG, the Local Potential Approximation (LPA), an approximated and concretely computable RG flow equation for the c-function was also written down [25]. By using this expression known results were recovered for scalar models on some special trajectories of the Ising and SG models. For the SG model, having a Lagrangian proportional to $\cos(\beta\varphi)$, the determination and the integration of the c-function was carried out for $\beta = 0$ as a massive deformation of the Gaussian fixed point [25]. Motivated by these results, both for the Ising and SG models and for general 2-dimensional models, it would be highly desirable to have a complete description of the c-function on general RG trajectories.

In the present chapter we present the first numerical calculation of the c-function on the whole RG flow phase diagram of the SG model. The goal is to determine the behavior of the c-function, and the presence of known results (namely, $\Delta c = 1$) helps to assess the validity of our approach along the different flows. We also complete the description initiated in [25] moving to more complex trajectories and showing that these cases are not a straightforward generalization of the known results. We finally discuss the dependence of these results on the approximation scheme used to compute FRG equations.

3.1 Introduction to the Sine-Gordon model

Sine-Gordon type models considered in this chapter are reviewed in this section putting emphasis on their symmetries and their phase diagrams. Symmetry considerations are important since together with the dimensionality, they can be used to determine the phase structure. The effective action of the sine-Gordon (SG) model contains a scalar field with periodic self-interaction

$$S_{\rm sg}[\varphi] = \int d^d x \left[\frac{1}{2} (\partial_\mu \varphi)^2 + u \cos(\beta \varphi) \right]. \tag{3.1}$$

where u is the Fourier amplitude and β is the frequency. In addition to the reflection ($\mathbb{Z}_2$) symmetry, the action of the SG model (3.1) under the transformation

$$\varphi(x) \to \varphi(x) + \frac{2\pi}{\beta} \tag{3.2}$$

remains unchanged, thus, it has another discrete symmetry: is periodic in the field variable. Due to this additional symmetry one expects changes in the phase structure compared to the Ising model. Indeed, the SG model has two phases in $d = 2$ dimensions and it is known to undergo an infinity order (topological) phase transition. The phase transition is controlled by the frequency, i.e., its critical value $\beta^2 = 8\pi$ separates the two phases. Let us note, both the periodicity and the reflection symmetry have been broken spontaneously in one of the phases of the model but this is in agreement to the Mermin-Wagner theorem since they are discrete symmetries. Furthermore, the SG model (3.1) can be mapped onto the scalar model with $O(N = 2)$ symmetry in $d = 2$ dimensions, thus, the signature of the infinite order phase transitions of the SG theory has been observed by the critical slowing of the running of the coupling in the two-dimensional $O(2)$ model [83, 92, 93].

In the next section we review some traditional results on the possible mappings between the SG and various type of 2 dimensional and layered condensed matter systems.

3.2 Gas of Topological Defects, Spin models, Superconductivity

Various types of mappings of sine-Gordon type models exist, in the following we introduce the ones which are most tightly connected to condensed matter physics. In this section we follow the lines of the presentation given in [94].

3.2.1 Ginzburg-Landau theory of superconductivity

In order to describe the phenomena of superconductivity one can use three different strategies. The most fundamental one is the microscopic description; in case of conventional superconductors this is the celebrated BCS theory. The second opportunity is the Ginzburg–Landau (GL) model which can be derived from the microscopic theory. The third scenario is the electrodynamical description which is nothing but the equations of motion derived from the corresponding GL model. These three stages work for high transition temperature superconductors as well (e.g. the corresponding GL theory is the so-called Lawrence-Doniach model), however, no well-accepted (single) microscopic model is available in the literature for high-T_c materials.

Here, we focus on the GL theory which has been developed by applying a variational method to an assumed expansion of the free energy in powers of $|\psi|^2$ and $|\partial_\mu \psi|^2$ where ψ is a complex order parameter

$$\psi(r) = |\psi(r)|e^{i\theta(r)} \equiv \psi_0(r)\, e^{i\theta(r)} \tag{3.3}$$

(the inhomogeneous condensate of the superconducting electron pairs) and $|\psi|^2$ represents the local density of superconducting electron pairs (charged superfluid density). The total free energy has the form of a field theory

$$F = \int \mathrm{d}^3 r \left(\alpha|\psi|^2 + \frac{\beta}{2}|\psi|^4 + \frac{\hbar^2}{2m_\star}| \left(\partial_\mu - \frac{i e_\star}{\hbar c} A \right) \psi|^2 + \frac{|B|^2}{8\pi} \right) \tag{3.4}$$

where α, β and $e_\star, m_\star$ are parameters, A is the electromagnetic vector potential and the last term stands for the magnetic field energy which does not depend on the material ($B = \nabla \times A$). In the absence of electromagnatic fields ($A \equiv 0$), the total free energy becomes

$$F = \int \mathrm{d}^3 r \left(\alpha \psi_0^2 + \frac{\beta}{2}\psi_0^4 + \frac{\hbar^2}{2m_\star} \left[(\partial_\mu \psi_0)^2 + \psi_0^2 (\partial_\mu \theta)^2 \right] \right) \tag{3.5}$$

where the functional form of the order parameter has been substituted.

Layered GL theory – Josephson coupling

Let us first discuss the free energy functional in the absence of electromagnetic fields (uncharged superfluid). Since a strong spatial anisotropy is a typical property of high T_c materials the free energy functional should be discretised in one of the spatial direction which results in a layered stucture. Another important assumption is the so-called London-limit

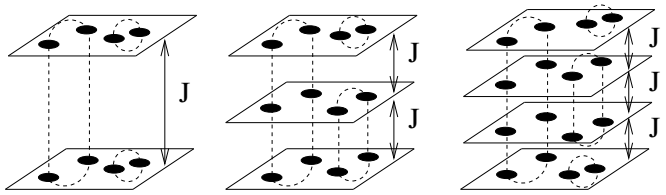

Fig. 3.1 Schematic representation of the Lawrence-Doniach model with $N = 2,3,4$ layers which can describe the vortex properties of layered superconductors. The planes are coupled by the Josephson coupling $J \sim 1/m_c$. The solid discs represent the topological excitations of the model, the vortex-antivortex pairs. Two such pairs belonging to neighbouring layers can form vortex loops and rings due to weak Josephson coupling. The critical behaviour of the vortices is found to depend on the number of layers and is again different in the limit of an infinite number of layers.

which requires that the superconducting state is homogenous in every layer, i.e., $\psi_0(r) \equiv \psi_0$ is constant (does not depend on the coordinate). Let us first use the London limit, then equation (3.5) reads as (in natural units: $\hbar = c = \varepsilon_0 = 1$)

$$F = \frac{\psi_0^2}{2m_\star} \int \mathrm{d}^3 r (\partial_\mu \theta)^2 \tag{3.6}$$

and then apply the discertization of the z-coordinate which results in

$$F = s\psi_0^2 \int \mathrm{d}^2 r \left(\sum_{n=1}^{N} \frac{1}{2m_{ab}} (\partial_\mu \theta_n)^2 + \sum_{n=1}^{N-1} \frac{1}{2m_c} \frac{(\theta_{n+1} - \theta_n)^2}{s^2} \right). \tag{3.7}$$

Here, m_{ab} and m_c represent the intralayer and interlayer effective masses, s is the interlayer distance, and N stands for the total number of layers. The gradient operator is two-dimensional, i.e., $\partial_\mu \equiv \partial_\mu$ where μ covers the spatial coordinates $\mu = x, y$.

The layered structure has important consequences on the phase structure. The elementary excitations are conducting electrons in the 3d bulk model but vortex-antivortex pairs (supercurrent rings with normal core) in the layered system, see 3.1. Furthermore, the phase structure and the vortex dynamics depend on the number of layers. For a single layer $N = 1$, (3.7) reduces to

$$F = \frac{\psi_0^2}{2m_\star} \int \mathrm{d}^2 r (\partial_\mu \theta)^2 \tag{3.8}$$

which is known to undergo a KTB type phase transition (strictly speaking if no spin-wave fluctuations are taken into account). In the molecular phase the vortices-antivortices form

closely bound pairs, in the ionised phase they dissociate into a neutral plasma. Let us note, that this situation is related to an uncharged superfluid. For realistic description of vortex dynamics in a single superconducting layer requires the incorporation of electromagnetic field (charged superfluid) which will be discussed later. For a finite number of layers $1 < N < \infty$ the Josephson coupling modifies the phase structure and for infinite number of layers $N = \infty$ one expects that equation (3.7) recovers the phase structure of the bulk model.

It constructive is to show that equation (3.7) can also be obtained by the discretised version of (3.4) (in the absence of external fields) which is the Lawrence–Doniach model,

$$F = s \int \mathrm{d}^2 r \left(\sum_{n=1}^{N} \left(\alpha |\psi_n|^2 + \frac{\beta}{2} |\psi_n|^4 + \frac{|\partial_\mu \psi_n|^2}{2 m_{ab}} \right) + \sum_{n=1}^{N-1} \frac{|\psi_{n+1} - \psi_n|^2}{2 m_c s^2} \right) . \tag{3.9}$$

and then taking it in the London-limit by introducing a complex layer-dependent order parameter as $\psi_n(r) = \psi_{0,n}(r) \exp[\mathrm{i}\theta_n(r)]$ with real $\psi_{0,n}(r)$, where the $\theta_n \in [0, 2\pi)$ are compact variables,

$$\begin{aligned} F = & s \int \mathrm{d}^2 r \left(\sum_{n=1}^{N} \alpha \psi_{0,n}^2 + \frac{\beta}{2} \psi_{0,n}^4 + \frac{1}{2 m_{a,b}} \left[(\partial_\mu \psi_{0,n})^2 + \psi_{0,n}^2 (\partial_\mu \theta_n)^2 \right] \right. \\ & \left. + \sum_{n=1}^{N-1} \frac{1}{s^2 2 m_c} (\psi_{0,n+1}^2 + \psi_{0,n}^2) - \frac{1}{s^2 m_c} \psi_{0,n+1} \psi_{0,n} \cos(\theta_{n+1} - \theta_n) \right) \end{aligned} \tag{3.10}$$

and in the London approximation the moduli $\psi_{0,n}$ are assumed to be constant and identical in every layer (i.e. $\psi_{0,n}(r) = \psi_0$) which results in

$$F = s \psi_0^2 \int \mathrm{d}^2 r \left(\sum_{n=1}^{N} \frac{1}{2 m_{ab}} (\partial_\mu \theta_n)^2 + \sum_{n=1}^{N-1} \frac{1}{s^2 m_c} \left[1 - \cos(\theta_{n+1} - \theta_n) \right] \right) \tag{3.11}$$

and recovers equation (3.7) after expanding the cosine in Taylor series and keeping the quadratic terms only. This is the London-type form of the Lawrence-Doniach model where the interaction between the compact fields θ_n of various layers is represented by the so-called Josephson coupling.

Layered GL theory – Magnetic coupling

Let us now turn to the analysis of the GL free energy in the presence of electromagnetic fields. The London-type approximation of (3.5) in case of a non-vanishing vector potential A

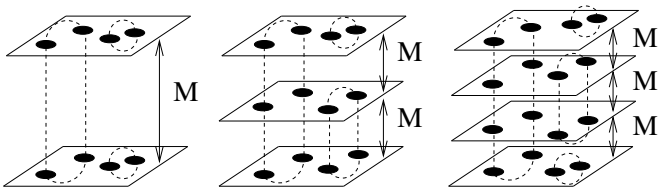

Fig. 3.2 Schematic representation of the vortex properties of layered superconductors where the Josephson coupling vanishes $J \sim 1/m_c = 0$ and the vortices (antivortices) of each layers are coupled by magnetic-type coupling (3.14).

reads as,

$$F = \frac{\psi_0^2}{2m_\star} \int \mathrm{d}^3 r (\partial_\mu \theta - e_\star A)^2 \tag{3.12}$$

with a compact field θ. Strong anisotropy can be taken into account by discretising (3.12) in one spatial dimension,

$$F = s\psi_0^2 \int \mathrm{d}^2 r \left(\sum_{n=1}^{N} \frac{1}{2m_{ab}} (\partial_\mu \theta_n - e_\star A)^2 + \sum_{n=1}^{N-1} \frac{1}{2m_c} \frac{(\theta_{n+1} - \theta_n)^2}{s^2} \right). \tag{3.13}$$

In the limit of infinite anisotropy, i.e., for vanishing Josephson coupling $m_c = \infty$, the total free energy becomes

$$F = s\psi_0^2 \int \mathrm{d}^2 r \left(\sum_{n=1}^{N} \frac{1}{2m_{ab}} (\partial_\mu \theta_n - e_\star A)^2 \right) \tag{3.14}$$

where the coupling between the layers is mediated by the vector potential A which represents a magnetic-type coupling between the vortices (antivortices) of each layers, see 3.5. The vortex dynamics of the magnetically coupled model (3.14) depends on the number of layers (similarly to the Josephson coupled case). For $N = 1$ equation (3.14) reads as

$$F = \frac{\psi_0^2}{2m_\star} \int \mathrm{d}^2 r (\partial_\mu \theta - e_\star A)^2 \tag{3.15}$$

which is known to describe a real two-dimensional superconductor, i.e., charged superfluid. Due to the presence of the electromagnetic field, no KTB type phase transition is observed. For finite number of layers $1 < N < \infty$, the screening effect of A is partial and a model undergoes a KTB phase transition where the transition temperature depends on the number of layers. For $N = \infty$ the effect of the electromagnetic field can be neglected, thus (3.14) recovers (3.8).

In order to show how the layered GL theory with Josephson and magnetic couplings is related to various sine-Gordon type scalar field theories one has to determine the so-called gases of topological excitations which is our goal in the upcoming subsections.

3.2.2 Models in $d = 2$ dimensions

Uncharged superfluid

Our starting point is the partition function of the 2d–SG model which reads as ($\hbar = 1$)

$$\mathscr{Z}_{\mathrm{2d-SG}} = \mathscr{N} \int \mathscr{D}[\varphi] \exp\left[- \int \mathrm{d}^2 r \left(\frac{1}{2} (\partial_\mu \varphi)^2 + u \cos(\beta\, \varphi) \right) \right] \tag{3.16}$$

where $\varphi \in [-\infty, \infty]$ is a one-component scalar field, u is a fundamental Fourier amplitude, and β is a dimensionless frequency. The partition function (3.16) can be identically rewritten as the partition function of the equivalent gas of topological excitations using the following steps. One expands the periodic piece of the partition function (3.16) in a Taylor series, and one introduces the integer-valued charges $\sigma_\alpha = \pm 1$ of the topological defects which are subject to the neutrality condition $\sum_{\alpha=1}^{2\nu} \sigma_\alpha = 0$,

$$\exp\left[\int \mathrm{d}^2 r\, u \cos(\beta\varphi) \right] = \sum_{\nu=0}^{\infty} \frac{(u/2)^{2\nu}}{(2\nu)!} \sum_{\sigma_1,\ldots,\sigma_\nu = \pm 1} \prod_{j=1}^{2\nu} \int \mathrm{d}^2 r_j \exp\left(i\beta\sigma_j \varphi \right). \tag{3.17}$$

This leads to the intermediate result,

$$\mathscr{Z} = \mathscr{N} \sum_{\nu=0}^{\infty} \frac{(u/2)^{2\nu}}{(2\nu)!} \left(\prod_{i=1}^{2\nu} \int \mathrm{d}^2 r_i \right) \sum_{\sigma_1,\ldots,\sigma_\nu = \pm 1} \int \mathscr{D}[\varphi] \exp\left[- \int \mathrm{d}^2 r \frac{1}{2} \varphi\, (-\partial^2) \varphi + \mathrm{i}\, \beta\, \rho\, \varphi \right], \tag{3.18}$$

where $\partial^2 \equiv \partial_\mu \partial_\mu$ and $\rho(r) = \sum_{\alpha=1}^{2\nu} \sigma_\alpha \delta(r - r_\alpha)$. We have thus placed the 2ν vortices, labeled by the index i, onto a two-dimensional plane (single layer). The Gaussian integration in equation (3.18) can now be performed easily, and the inversion of $-\partial^2$ can be accomplished by going to momentum space. Via a subsequent back-transformation to coordinate space, we finally arrive at the result

$$\mathscr{Z}_{\mathrm{2d-SG}} = \sum_{\nu=0}^{\infty} \frac{(u/2)^{2\nu}}{(2\nu)!} \left(\prod_{i=1}^{2\nu} \int \mathrm{d}^2 r_i \right) \sum_{\sigma_1,\ldots,\sigma_\nu} \exp\left[- \frac{\beta^2}{2(2\pi)} \sum_{\alpha,\gamma=1}^{2\nu} \sigma_\alpha \sigma_\gamma \ln\left(\frac{r_{\alpha\gamma}}{a} \right) \right],$$

which is equivalent to the two-dimensional Coulomb gas (2d-CG)

$$\mathscr{Z}_{\mathrm{2d-CG}} = \sum_{\nu=0}^{\infty} \frac{(z)^{2\nu}}{(\nu!)^2} \int \mathrm{d}^2 r_1 \ldots \int \mathrm{d}^2 r_{2\nu} \sum_{\sigma_1,\ldots,\sigma_\nu} \exp\left[-\frac{1}{2k_{\mathrm{B}}T} \sum_{\alpha,\gamma}^{2\nu} \sigma_\alpha \sigma_\gamma \ln\left(\frac{r_{\alpha\gamma}}{a}\right)\right] \quad (3.19)$$

where $\sigma_\alpha = \pm 1$ is the charge of the αth particle, z is the dimensionful fugacity, k_{B} is the Boltzmann constant, T is the temperature and a stands for the lattice spacing which serves as short-distance cutoff. The interaction potential between two charges depends on their relative distance ($r_{\alpha\beta} = |\vec{r}_\alpha - \vec{r}_\gamma|$). The frequency parameter β^2 of the 2d–SG model can be identified as the inverse of the temperature of the equivalent Coulomb gas, $\beta^2 \equiv 2\pi/(k_{\mathrm{B}}T)$ and the Fourier amplitude plays the role of the fugacity, $u \sim z$.

It is generally assumed that the 2d–SG model belongs to the universality class of the two-dimensional classical XY spin-model (if no spin wave fluctuations are taken into account) which is given by the partition function

$$\mathscr{Z}_{\mathrm{2d-XY}} = \int \mathscr{D}[\vec{S}]\, \delta(\vec{S}^{\,2} - 1) \exp\left[-\frac{1}{k_{\mathrm{B}}T} \sum_{<x,y>} (-J)\, \vec{S}_x \cdot \vec{S}_y \right], \quad (3.20)$$

where the classical spin $\vec{S}$ is a unit-vector in the two-dimensional internal space; $\sum_{<x,y>}$ stands for the sum over pairs of nearest neighbor lattice sites. Representing the classical unit spin vector by an angle $\vec{S}_x \equiv (\cos(\theta_x), \sin(\theta_x))$ the partition function of the 2D–XY model can be written as

$$\mathscr{Z}_{\mathrm{2d-XY}} = \int \mathscr{D}[\theta] \exp\left[\frac{J}{k_{\mathrm{B}}T} \sum_{<x,y>} \cos(\theta_x - \theta_y) \right] \approx \mathscr{N} \int \mathscr{D}[\theta] \exp\left[-\int \mathrm{d}^2 r \left(\frac{J}{2k_{\mathrm{B}}T} (\partial_\mu \theta)^2 \right) \right], \quad (3.21)$$

where the cosine is Taylor-expanded and the quadratic term generates $\partial_\mu \theta$ in the continuum limit. The higher order derivatives are neglected and the field-independent term has been built in the normalization constant $\mathscr{N}$.

The structure of equation (3.21) is similar to equation (3.16) however there is an important difference, namely $\theta \in [0, 2\pi]$ is a compact variable. In case of the 2d–XY model, the compact nature of the field generates the topological excitations of the theory, which are the point-like vortices. In case of the 2d–SG model, the periodic self-interaction is responsible for the existence of the topological defects which are solitons.

Let us note, the partition function (3.21) is equivalent to the GL model (3.8) which describes a 2d superconducting film in the absence of electromagnetic fields taken in the London-type approximation (with $J \equiv \psi_0^2/m_{\mathrm{ab}}$). It is used to describe the vortex dynamics of an uncharged superfluid. Moreover, the 2d–XY model can also be mapped onto the 2d–CG.

To show this the field variable is rewritten

$$\theta(r) = \theta_v(r) + \theta_{\rm sw}(r) \tag{3.22}$$

in terms of vortex (θ_v) and spin-wave ($\theta_{\rm sw}$) terms with the following properties

$$\int_V \partial_\mu \partial^\mu \theta_v = \int_{\partial V} \partial_\mu \theta_v = 2\pi \sum_i q_i, \qquad \int_V \partial_\mu \partial^\mu \theta_{\rm sw} = \int_{\partial V} \partial_\mu \theta_{\rm sw} = 0, \tag{3.23}$$

where the integrals are independent of the two-dimensional volume (V) and its surface (∂V) which is a closed contour in $d = 2$. The integer valued variable q_i is the so-called vortex charge (vorticity or winding number). Based on the analogy to electrostatic (where θ_v plays the role of the scalar electric potential in $d = 2$) it is easy to show that

$$\partial_\mu \partial^\mu \theta_v(r) = 2\pi\rho, \qquad \rho = \sum_i q_i \delta(r - r_i) \quad \rightarrow \quad \theta_v(r) = \sum_i q_i \ln\left(\frac{r - r_i}{a}\right). \tag{3.24}$$

The action for the continuous XY model can be rewritten in three terms

$$S = -\frac{J}{2k_{\rm B}T}\left[\int {\rm d}^2 r (\partial_\mu \theta_v)^2 + \int {\rm d}^2 r (\partial_\mu \theta_{\rm sw})^2 + 2\int {\rm d}^2 r (\partial_\mu \theta_v)(\partial_\mu \theta_{\rm sw})\right] \tag{3.25}$$

in which the last term is zero. If one neglect the second term (i.e. the spin-wave fluctuation) than the partition function of the model form a Coulomb gas.

Therefore, the continuous version of the 2d–XY (without spin-wave fluctuation) and the 2d–SG model are dual to each other. Indeed, the two models can be mapped onto each other by a suitable duality relation based on the Gaussian integration which inverts the coupling of the derivative term ($\beta^2 \sim J/T$).

3.2.3 Models in $d = 3$ dimensions

The partition function of the three-dimensional sine–Gordon (3d–SG) model is

$$\mathscr{Z}_{\rm 3d-SG} = \mathscr{N} \int \mathscr{D}[\varphi] \exp\left[-\int {\rm d}^3 r \left(\frac{1}{2}(\partial_\mu \varphi)^2 + u\cos(\beta\,\varphi)\right)\right] \tag{3.26}$$

where $\varphi \in [-\infty, \infty]$ is a one-component scalar field, $(\partial_\mu \varphi)^2 \equiv \sum_{\mu=1}^{3} (\partial_\mu \varphi)^2$. The partition function of the equivalent gas of topological excitations reads as

$$\mathscr{Z}_{\mathrm{3d-SG}} = \sum_{\nu=0}^{\infty} \frac{(u/2)^{2\nu}}{(2\nu)!} \left(\prod_{i=1}^{2\nu} \int \mathrm{d}^3 r_i \right) \sum_{\sigma_1,\ldots,\sigma_\nu = \pm 1} \exp\left[\frac{\beta^2}{2(\Omega_3)} \sum_{\alpha,\gamma}^{2\nu} \sigma(r_\alpha) \, \frac{1}{r_{\alpha\gamma}} \, \sigma(r_\gamma) \right],$$

where Ω_3 is the three-dimensional solid angle. Since the equivalence of the sine–Gordon field theory and the Coulomb gas holds in arbitrary dimensions, the partition function (3.27) is equivalent to the partition function of the 3d-CG

$$\begin{aligned} \mathscr{Z}_{\mathrm{3d-CG}} = \sum_{\nu=0}^{\infty} \frac{(z)^{2\nu}}{(\nu!)^2} \int \mathrm{d}^3 r_1 \ldots \int \mathrm{d}^3 r_{2\nu} \\ \sum_{\sigma_1,\ldots,\sigma_\nu = \pm 1} \exp\left[\frac{1}{2 k_{\mathrm{B}} T} \sum_{\alpha,\gamma}^{2\nu} \sigma(r_\alpha) \, \frac{1}{r_{\alpha\gamma}} \, \sigma(r_\gamma) \right] \end{aligned} \tag{3.27}$$

where $\sigma_\alpha = \pm 1$ is the charge of the αth particle, z is the dimensionful fugacity, T is the dimensionful temperature and the interaction potential between two point-like charges depends on their relative distance ($r_{\alpha\beta} = |\vec{r}_\alpha - \vec{r}_\gamma|$). The dimensionful frequency parameter β^2 of the 3d–SG model can be identified as the inverse of the dimensionful temperature of the equivalent 3d–CG, $b^2 \equiv \Omega_3/(k_{\mathrm{B}} T)$ and again the Fourier amplitude plays the role of the fugacity, $u \sim z$.

The 2d–SG and the 2d–XY model belong to the same universality class, however, this is not necessary true for the 3d counterparts since the topological defects of the XY model are point-like objects in $d = 2$ but $d - 1$ surfaces in higher dimensions, e.g. vortex lines (or loops) in three dimensions. The partition function of the 3d–XY model taken in the continuum limit reads as

$$\mathscr{Z}_{\mathrm{3d-XY}} = \int \mathscr{D}[\theta] \exp\left[\frac{J}{k_{\mathrm{B}} T} \sum_{<x,y>} \cos(\theta_x - \theta_y) \right] \approx \mathscr{N} \int \mathscr{D}[\theta] \exp\left[- \int \mathrm{d}^3 r \left(\frac{J}{2 k_{\mathrm{B}} T} (\partial_\mu \theta)^2 \right) \right], \tag{3.28}$$

where $\theta \in [0, 2\pi]$. Let us note, equation (3.28) is equivalent to the 3d GL theory of superconductivity taken in the London-type approximation in the absence of electromagnetic fields (3.6). The partition function of the corresponding gas of topological excitations (vortex-loop gas) is

$$\begin{aligned} \mathscr{Z}_{\mathrm{3d-VLG}} = \quad & \textstyle\sum_{\nu=0}^{\infty} \frac{1}{(\nu!)} \left(\prod_{L=1}^{\nu} \int d^3 r_L \, z^{(L)} \right) \\ & \textstyle\sum_{j_\mu^{(L)}} \exp\left[\frac{J\pi}{2 k_{\mathrm{B}} T} \sum_{L,L'} \sum_{\alpha,\gamma} j_\mu^{(L)}(r_\alpha) \; U(r_{\alpha\gamma}) \; j_\mu^{(L')}(r_\gamma) \right] \end{aligned} \tag{3.29}$$

where the interaction potential is $U(r_{\alpha\gamma}) \approx 1/r_{\alpha\gamma}$ asymptotically. Here the topological excitations are vortex lines (currents) and equation (3.29) can be considered as a Biot-Savart law for these "topological currents" $j_\mu(r)$. Although the asymptotic form of the interaction potentials are the same for the 3d–CG and for the 3d–VLG models, the topological defects are different, consequently, the 3d–SG and 3d–XY models belong to different universality classes.

It has been argued that the field theory equivalent to the 3d–XY model is a QED-type Abelian model which has the following partition function (see equation (3.11) of [Savit])

$$\mathscr{Z} = \mathscr{N} \sum_{j_\mu} \int \mathscr{D}[A_{\mu,l}] \exp\left[\sum_{\mu,\nu,l} -\frac{1}{2} \frac{k_B T}{J} F_{\mu\nu,l} F_{\mu\nu,l} + i2\pi j_{\mu,l} A_{\mu,l} \right]. \tag{3.30}$$

with integer-valued currents j_μ and $F_{\mu\nu,l} = \partial_\mu A_{\nu,l} - \partial_\nu A_{\mu,l}$. The above QED-type quantum field theory is not a sine–Gordon type scalar model. Therefore, one should conclude that the 3d–SG and the 3d–XY are not the dual theory of each other.

3.3 The c-function in the Framework of Functional Renormalization Group

An expression for the c-function in FRG was recently developed in [25]. In this section we are going to give the guidelines of this derivation, reviewing the main results used in the next sections.

Let us start considering an effective action $\Gamma[\varphi, g]$ for a single field φ in curved space, with metric $g_{\mu\nu}$. We can study the behavior of this effective action under transformation of the field and the metric:

$$\varphi \to e^{d_\varphi \tau} \varphi \tag{3.31}$$

$$g_{\mu\nu} \to e^{2\tau} g_{\mu\nu} \tag{3.32}$$

where d_φ is the conformal weight of the field ($d_\varphi = -\frac{d-2+\eta}{2}$ for a scalar field) while the background metric $g_{\mu\nu}$ has always conformal weight 2. From the requirement that the effective action must be invariant under the Weyl transformation (3.31)-(3.32), we obtain the following expression for a conformal field theory (CFT) in curved space [25],

$$\Gamma[\varphi, g] = S_{CFT}[\varphi, g] + c S_P[g]. \tag{3.33}$$

$S_{CFT}[\varphi, g]$ is the curved space generalization of the standard CFT action, which is recovered in the flat space case $g_{\mu\nu} = \delta_{\mu\nu}$, c is the central charge of our theory and $S_P[g]$ is the Polyakov action term which is necessary to maintain the Weyl invariance of the effective average action in curved space.

To obtain FRG equations one has to add an infra-red (IR) cutoff term $\Delta S_k[\varphi, g]$ to the ultra-violet (UV) action of the theory. This is a mass term which depends both on the momentum of the excitations and on a cutoff scale k.

$$\Delta S_k[\varphi, g] = \frac{1}{2}\int d^2x\sqrt{g}\varphi(x)R_k(\Delta)\varphi(x), \tag{3.34}$$

where Δ is the spatial Laplacian operator. The effect is to freeze the excitation of momentum $q \ll k$, but leaving the excitation at $q > k$ almost untouched. The result of this modification of the UV action is to generate, after integrating over the field variable, a scale-dependent effective action $\Gamma_k[\varphi, g]$ which describes our theory at scale k. When the scale k is sent to zero the cutoff term in the UV action vanishes and the $\Gamma_k[\varphi, g]$ is the exact effective average action of the theory.

The generalization of (3.33) in presence of the cutoff terms is

$$\Gamma_k[\varphi, g] = S_k[\varphi, g] + c_k S_P[g] + \cdots, \tag{3.35}$$

where c_k is now the scale-dependent c-function and the dots stands from some geometrical terms which do not depend on the field. We should now consider the case of a flat metric with a dilaton background $g_{\mu\nu} = e^{2\tau}\delta_{\mu\nu}$. Using the standard path integral formalism for the effective action we can write

$$\begin{aligned} e^{-\Gamma_k[\varphi, e^{2\tau}\delta]} &= e^{-S_k[\varphi, e^{2\tau}\delta] - c_k S_P[e^{2\tau}\delta]} = \\ &\int \mathscr{D}\chi_{d.b.} e^{-S_{UV}[\varphi+\chi, e^{2\tau}\delta] - c_{UV} S_P[e^{2\tau}\delta] - \Delta S_k[\chi, e^{2\tau}\delta]} \end{aligned} \tag{3.36}$$

where $S_{UV}[\varphi, g]$ is some UV action, c_{UV} is the value of the c-function in the UV (which can be equal to the central charge of some CFT if we are starting the flow from a conformal invariant theory) and χ is the fluctuation field. The notation $\mathscr{D}\chi_{d.b.}$ stands for an integration over the fluctuation field χ in the curved space of the dilaton background [25]. We can further manipulate latter expression moving c_{UV} on the l.h.s

$$\begin{aligned} e^{-S_k[\varphi, e^{2\tau}\delta] + (c_{UV} - c_k) S_P[e^{2\tau}\delta]} &= \\ \int \mathscr{D}\chi_{d.b.} e^{-S_{UV}[\varphi+\chi, e^{2\tau}\delta] - \Delta S_k[\chi, e^{2\tau}\delta]}&. \end{aligned} \tag{3.37}$$

The Polyakov action in the dilaton background case assumes the form

$$S_P[g] = -\frac{1}{24}\int \tau\Delta\tau, \tag{3.38}$$

where τ is the dilaton field, Δ is the laplacian operator and the integral is over an implicit spatial variable. Substituting latter expression into (3.37) we obtain

$$\begin{aligned} &e^{-S_k[\varphi,e^{2\tau}\delta]-\frac{(c_{UV}-c_k)}{24}\int\tau\Delta\tau} = \\ &\int \mathscr{D}\chi_{d.b.} e^{-S_{UV}[\varphi+\chi,e^{2\tau}\delta]-\Delta S_k[\chi,e^{2\tau}\delta]}. \end{aligned} \tag{3.39}$$

In order to recover the usual flat metric integration we have to pursue a Weyl transformation (3.31) for the fields φ and χ

$$\begin{aligned} &e^{-S_k[e^{d_\varphi\tau}\varphi,e^{2\tau}\delta]-\frac{(c_{UV}-c_k)}{24}\int\tau\Delta\tau} = \\ &\int \mathscr{D}\chi e^{-S_{UV}[e^{d_\varphi\tau}(\varphi+\chi),e^{2\tau}\delta]-\Delta S_k[e^{d_\varphi\tau}\chi,e^{2\tau}\delta]}, \end{aligned} \tag{3.40}$$

and now the integration measure is in flat space.

Finally deriving previous expression with respect to the logarithm of the FRG scale we obtain that the flow of the c-function $\partial_t c_k$ can be extracted from the flow of the cutoff action (3.34) by taking the coefficient of the $\int\tau\Delta\tau$ term,

$$k\partial_k c_k = 24\pi\langle k\tilde{\partial}_k \Delta S_k[e^{d_\varphi\tau}\chi, e^{2\tau}\delta]\rangle\Big|_{\int\tau\Delta\tau}, \tag{3.41}$$

which after some manipulation becomes [25]

$$k\partial_k c_k = -12\pi k\tilde{\partial}_k G_k[\tau]\Big|_{\int\tau\Delta\tau}. \tag{3.42}$$

Equation (3.42) shows that the c-function flow is proportional to the coefficient of the $\int\tau\Delta\tau$ term in the expansion of the propagator flow $k\tilde{\partial}_k G_k[\tau]$, also this flow has to be computed taking into account only the k dependence of the regulator function, i.e.

$$k\tilde{\partial}_k = k\partial_k R_k \frac{\partial}{\partial R_k}. \tag{3.43}$$

This equation describes the exact flow of the c-function into the FRG framework.

Since it is not in general possible to solve exactly equation (1.60) and also equation (3.42) needs to be projected into a simplified theory space to be computed numerically. In Ref. [25]

an explicit expression for the flow equation of the c-function in the LPA scheme has been derived with the mass cutoff

$$k\partial_k c_k = \frac{[k\partial_k \tilde{V}_k''(\varphi_{0,k})]^2}{[1+\tilde{V}_k''(\varphi_{0,k})]^3}, \tag{3.44}$$

with the dimensionless blocked potential $\tilde{V}_k(\varphi)$ which is evaluated at its running minimum $\varphi = \varphi_{0,k}$ (i.e. the solution of $\tilde{V}_k'(\varphi) = 0$). We observe that an explicit expression for the c-function beyond LPA is not available in literature.

It should be noticed that, while (3.42) is valid for any regulator (cutoff) function, the expression for the c-function (3.44) has been obtained by using the mass cutoff, i.e. (B.23b) with $b = 1$. Other cutoff choices proved to be apparently very difficult to investigate. In the following, we will argue that while the expression (3.44) is sufficient to obtain a qualitative (and almost quantitative) picture of the c-function phase diagram the usage of other regulator functions is necessary to achieve full consistency. Where it is possible we will check the cutoff dependence of our numerical results.

3.4 RG study of the sine-Gordon model

In LPA higher derivative terms are neglected and the wave-function renormalization is set equal to constant, i.e. $Z_k \equiv 1$. In this case (1.60) reduces to the partial differential equation for the dimensionless blocked potential ($\tilde{V}_k = k^{-2}V_k$) which has the following form in 2 dimensions

$$(2+k\partial_k)\tilde{V}_k(\varphi) = -\frac{1}{4\pi}\int_0^\infty dy \frac{y^2 \frac{dr}{dy}}{(1+r)y+\tilde{V}_k''(\varphi)}. \tag{3.45}$$

The SG scalar field theory is defined by the Euclidean action for $d = 2$

$$\Gamma_k[\varphi] = \int d^2x \left[\frac{1}{2}(\partial_\mu \varphi_x)^2 - u\cos(\beta\varphi_x)\right], \tag{3.46}$$

where β and u are the dimensional couplings. Since we are interested in the FRG study of the SG model which is periodic in the field variable, the symmetry of the action under the transformation [57]

$$\varphi(x) \to \varphi(x) + \mathscr{A} \tag{3.47}$$

is to be preserved by the blocking and the potential $\tilde{V}_k(\varphi)$ must be periodic with period length $\mathscr{A}$. It is actually obvious that the blocking, i.e. the transformation given by replacing the

derivative with respect to the scale k by a finite difference in (3.45) preserves the periodicity of the potential [57, 95].

3.4.1 The FRG equation for the SG model for scale-independent frequency.

In LPA one should look for the solution of (3.45) among the periodic function which requires the use of a Fourier expansion. When considering a single Fourier mode, the scale-dependent blocked potential reads

$$\tilde{V}_k(\varphi) = -\tilde{u}_k \cos(\beta\varphi), \tag{3.48}$$

where β is scale-independent.

In the mass cutoff case, i.e. the power law regulator (B.23b) with $b = 1$, one can derive [96] the flow equation for the Fourier amplitude of (3.48) from (3.45):

$$(2 + k\partial_k)\tilde{u}_k = \frac{1}{2\pi\beta^2\tilde{u}_k}\left[1 - \sqrt{1 - \beta^4\tilde{u}_k^2}\right] \tag{3.49}$$

(see equation (21) of [96] for vanishing mass). Similarly, using the optimized regulator (B.23c) gives

$$(2 + k\partial_k)\tilde{u}_k = \frac{1}{2\pi\beta^2\tilde{u}_k}\left[\frac{1}{\sqrt{1 - \beta^4\tilde{u}_k^2}} - 1\right]. \tag{3.50}$$

3.4.2 The FRG equation for the SG model for scale-dependent frequency.

A very simple, but still sensible, modification to ansatz (3.46) is the inclusion of a scale dependent frequency, which, in order to explicitly preserve periodicity, should be rather considered as a running wave-function renormalization. The ansatz then becomes

$$\Gamma_k = \int d^2x \left[\frac{1}{2} z_k (\partial_\mu \varphi_x)^2 + V_k(\varphi_x)\right], \tag{3.51}$$

where the local potential contains a single Fourier mode

$$V_k(\varphi) = -u_k \cos(\varphi), \tag{3.52}$$

and the following notation has been introduced

$$z_k \equiv 1/\beta_k^2 \tag{3.53}$$

via the rescaling of the field $\varphi \to \varphi/\beta_k$ in (3.46), where z_k plays the role of a field-independent wave-function renormalization. Then (1.60) leads to the evolution equations

$$k\partial_k V_k = \frac{1}{2}\int_p \mathscr{D}_k k\partial_k R_k, \tag{3.54}$$

$$k\partial_k z_k = \mathscr{P}_0 V_k'''^2 \int_p \mathscr{D}_k^2 k\partial_k R_k \left(\frac{\partial^2 \mathscr{D}_k}{\partial p^2 \partial p^2} p^2 + \frac{\partial \mathscr{D}_k}{\partial p^2}\right) \tag{3.55}$$

with $\mathscr{D}_k = 1/(z_k p^2 + R_k + V_k'')$ and $\mathscr{P}_0 = (2\pi)^{-1}\int_0^{2\pi} d\varphi$ is the projection onto the field-independent subspace. The scale k covers the momentum interval from the UV cutoff Λ to zero. It is important to stress that equations (3.54)-(3.55) are directly obtained using power-law cutoff functions. One may expect that these equations continue to be valid for a general cutoff provided that $R_k \to z_k R_k$ [19]. This substitution has been tested for $O(N)$ models, but its validity has been not yet discussed in the literature for the SG model.

Inserting the ansatz (3.52) into equations (3.54) and (3.55) the RG flow equations for the coupling constants can be written as [49]

$$k\partial_k u_k = \frac{1}{2\pi}\int_p \frac{k\partial_k R_k}{u_k}\left(\frac{P_k}{\sqrt{P_k^2 - u_k^2}} - 1\right), \tag{3.56}$$

$$k\partial_k z_k = \frac{1}{2\pi}\int_p k\partial_k R_k \left(\frac{u_k^2 p^2 (\partial_{p^2} P_k)^2 (4P_k^2 + u_k^2)}{4(P_k^2 - u_k^2)^{7/2}} - \frac{u_k^2 P_k (\partial_{p^2} P_k + p^2 \partial_{p^2}^2 P_k)}{2(P_k^2 - u_k^2)^{5/2}}\right) \tag{3.57}$$

with $P_k = z_k p^2 + R_k$. In general, the momentum integrals have to be performed numerically, however in some cases analytical results are available. Indeed, by using the power-law regulator (B.23b) with $b = 1$, the momentum integrals can be performed [96] and the RG flow equations read as

$$\begin{aligned}(2 + k\partial_k)\tilde{u}_k &= \frac{1}{2\pi z_k \tilde{u}_k}\left[1 - \sqrt{1 - \tilde{u}_k^2}\right] \\ k\partial_k z_k &= -\frac{1}{24\pi}\frac{\tilde{u}_k^2}{[1 - \tilde{u}_k^2]^{\frac{3}{2}}}\end{aligned} \tag{3.58}$$

with the dimensionless coupling $\tilde{u} = k^{-2}u$. By using the replacements

$$z_k \to 1/\beta_k^2, \tag{3.59a}$$

$$\tilde{u}_k \to \beta_k^2 \tilde{u}_k, \tag{3.59b}$$

and keeping the frequency scale-independent ($\partial_k z_k = 0$ i.e. $\partial_k \beta_k^2 = 0$) one recovers the corresponding LPA equation (3.49).

3.5 c-function of the sine-Gordon model for $\beta = 0$

In this section we discuss the case $\beta = 0$. We start by summarizing the results obtained for the c-function of the SG model in [25]. The ansatz considered in [25] is

$$\tilde{V}_k(\varphi) = -\frac{\tilde{m}_k^2}{\beta_k^2}\left(\cos(\beta_k\varphi) - 1\right), \tag{3.60}$$

where the frequency β_k is assumed to be scale-dependent. If one directly substitutes (3.60) into the RG equation (3.45), then the l.h.s. of (3.45) generates non-periodic terms due to the scale-dependence of β_k. Thus, the periodicity of the model is not preserved and one can use the Taylor expansion of the original periodic model

$$\tilde{V}_k(\varphi) \approx \frac{1}{2}\tilde{m}_k^2\varphi^2 - \frac{1}{4!}(\tilde{m}_k^2\beta_k^2)\varphi^4. \tag{3.61}$$

In this case, (3.60) is treated as a truncated Ising model and the RG equations for the coupling constants read as

$$k\partial_k \tilde{m}_k^2 = \frac{\tilde{m}_k^2[\beta_k^2 - 8\pi(1+\tilde{m}_k^2)]}{4\pi(1+\tilde{m}_k^2)} \tag{3.62}$$

$$k\partial_k \beta_k^2 = -\frac{1}{4\pi}\frac{(1+4\tilde{m}_k^2)\beta_k^4}{(1+\tilde{m}_k^2)^2}. \tag{3.63}$$

The disadvantage of the scale-dependent frequency is that the periodicity of the model is violated changing the known phase structure of the SG model. However, the authors of [25] were interested in the massive deformation of the Gaussian fixed point which is at $\beta = 0$ and $\tilde{u} = 0$, so one has to take the limit $\beta \to 0$ where the Taylor expansion represents a good approximation for the original SG model. Indeed, in the limit $\beta \to 0$, the RG equations

(3.62), (3.63) reduce to

$$k\partial_k \tilde{m}_k^2 \approx \frac{\tilde{m}_k^2[\beta_k^2 - 8\pi(1+\tilde{m}_k^2)]}{4\pi(1+\tilde{m}_k^2)} \approx -2\tilde{m}_k^2 \tag{3.64}$$

$$k\partial_k \beta_k^2 \approx 0. \tag{3.65}$$

Similar flow equations for the couplings $\tilde{m}_k^2$ and β_k were given in [25]. The solution for the c-function based on (3.60) is in agreement with the known exact result, i.e. at the Gaussian UV fixed point $c_{\mathrm{UV}} = 1$ and in the IR limit $c_{\mathrm{IR}} = 0$, thus the exact result in case of the massive deformation of the Gaussian fixed point is $\Delta c = 1$ ($\Delta c = c_{UV} - c_{IR}$). The numerical solution [25] gives $\Delta c = 0.998$ in almost perfect agreement with the exact result.

Although the numerical result obtained for the c-function in [25] is more than satisfactory, due to the Taylor expansion, the SG theory is considered as an Ising-type model. Thus, the RG study of the c-function starting from the Gaussian fixed point in the Taylor expanded SG model is essentially the same as that of the deformation of the Ising Gaussian fixed point. So, it does not represent an independent check of (3.44). Indeed, inserting (3.64) into (3.44) using the ansatz (3.60) one finds

$$k\partial_k c_k = \frac{4\tilde{m}_k^4}{[1+\tilde{m}_k^2]^3} \tag{3.66}$$

which is identical to equation (5.3) of [25] (with $a = 1$) obtained for the massive deformation of the Gaussian fixed point in the Ising model and it can be also derived from equation (5.19) of [25] in the limit of $\beta^2 \to 0$.

Therefore, it is a relevant question whether one can reproduce the numerical results obtained for the c-function (with the same accuracy) if the SG model is treated with scale-independent frequency (3.48), or beyond LPA, by the rescaling of the field (3.52). Also ref. [25] treats only massive deformations of non interacting UV fixed points, then on such trajectories only the mass coupling is running. Nevertheless the c-theorem should hold on all trajectories, even when more couplings are present. Our aim is to demonstrate that the derivation of [25] is valid even in these more general cases, but, due to truncation approach, the approximated FRG phase diagram does not fulfill the requirements of the c-theorem exactly and, therefore, only approximated results are possible.

3.6 c-function of the sine-Gordon model on the whole flow diagram

In this section we study the c-function of the SG model on the whole phase diagram, studying both the scale independent wave-function renormalization and the treatment with the running frequency.

3.6.1 Scale-independent frequency case

The definition for the SG model used in this work, i.e. (3.46), differs from (3.60) because the frequency parameter is assumed to be scale-independent in LPA. The running of β can only be achieved beyond LPA by incorporating a wave-function renormalization and using a rescaling of the field variable which gives $z_k = 1/\beta_k^2$.

Let us first discuss the results of LPA. Equations (3.49) and (3.50) have the same qualitative solution. In 3.1 we show the phase structure obtained by solving (3.50).

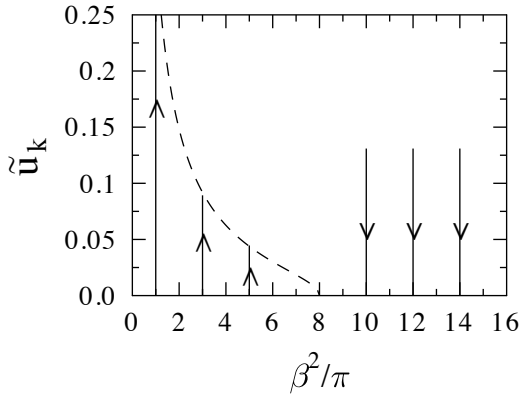

Fig. 3.3 The figure shows the phase structure of the SG model obtained by the FRG equation using Litim's regulator in the scale-independent frequency case. The two phases are separated by $\beta_c^2 = 8\pi$. The dashed line shows the line of IR fixed points of the broken phase.

The RG trajectories are straight lines because in LPA the frequency parameter of (3.46) is scale independent. Above (below) the critical frequency $\beta_c^2 = 8\pi$, the line of IR fixed points is at $\tilde{u}_{\rm IR} = 0$ ($\tilde{u}_{\rm IR} \neq 0$). For $\beta^2 < 8\pi$ the IR value for the Fourier amplitude depends on the particular value of β^2 thus, one finds different IR effective theories, i.e. the corresponding CFT depends on the frequency too.

The scaling for the c-function is the one expected from the c-theorem. It is a decreasing function of the scale k which is constant in the UV and IR limits, see 3.1. Due to the

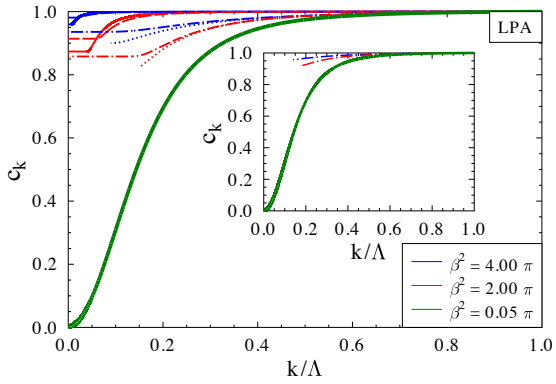

Fig. 3.4 Running of the c-function obtained in the scale-independent frequency case by solving (3.49) (dotted lines - mass cutoff) and (3.50) (dot-dashed lines - Litim cutoff) combined with (3.44) for the SG model is plotted for various values of the frequency β^2. From top to bottom it is $\beta^2/\pi = 4, 2, 0.005$. Due to the poor convergence properties of (3.49), where the mass cutoff was used, the RG flow stops at some finite momentum scale and the deep IR value of the c-function cannot be reached (dotted lines). The use of the Litim cutoff (3.50) (dot-dashed lines) can produce us the IR constant for the c-function. However, for very small value of β^2 the low-frequency approximation is the best choice, i.e. one has to solve (3.68) (green line): results from different cutoff functions are indistinguishable. The solid lines represent the results obtained with power law cutoff ($b = 2$), while the dashed lines are the results with the exponential cutoff. The inset shows the results for an enlarged theory space where higher harmonics are included in (3.52) (dot-dashed lines - Litim cutoff).

approximation of scale independent frequency β, here, the IR value of the c-function depends on the particular initial condition for β^2. Then when we start at the Gaussian fixed points line ($c = 1$), in the symmetric phase, the flow evolves towards an IR fixed point, but at this approximation level, we have different IR fixed points which are all at different $\tilde{u}$ values and consequently the Δc values differ from the exact one. The exact result $\Delta c \simeq 1$ is obtained only in the $\beta \to 0$ limit.

We notice that equation (3.49), where the mass cutoff was used, has very poor convergence properties and the flow, obtained from them, stops at some finite scale, thus the deep IR values of the c-function cannot be reached (dashed lines in Fig. 3.4).

The use of the Litim cutoff RG equation (3.50) improves the convergence of the RG flow but the IR results for the c-function are very far from the expected $\Delta c = 1$, which can be recovered only in the vanishing frequency limit. Also the inclusion of higher harmonics in (3.52) (inset in Fig. 3.4) does not improve this result.

It should be noted that equation (3.44) is strictly valid only in the mass cutoff case, however in Fig. 3.4 we used equation (3.44) even in the optimized cutoff case. This inconsistence

cannot be regarded as the cause for the unsatisfactory results obtained in the large β cases, indeed we expect very small dependence of the flow trajectories upon the cutoff choice.

This small dependence on the regulator is evident from the comparison of the mass and Litim regulator results of trajectories for the c-function in Fig. 3.4, which are very similar, at least in the region where no convergence problems are found. This similarity justifies the use of the mass cutoff result (3.44) with RG flow equations (3.50) obtained by the optimized (Litim) regulator.

We also computed the c-function flow for other cutoff functions, namely the power-law $b = 2$ (solid lines in Fig. 3.4) and the exponential one (dashed lines). Apart from the mass cutoff, all the others converge to the IR fixed point. The conclusion is that there is not a pronounced dependence of the findings on the cutoff schemes and that the constant frequency case in not sufficient to recover the correct behavior for the c-function.

We observe that the lack of convergence observed in mass cutoff case is not present in the small frequency limit analyzed in [25]. Indeed, expanding flow equations (3.49) and (3.50) we get

$$k\partial_k\tilde{u}_k \approx -2\tilde{u}_k + \frac{\tilde{u}_k\beta^2}{4\pi} \approx -2\tilde{u}_k, \tag{3.67}$$

which is valid for vanishing frequency and it is independent of the particular choice of the regulator function, i.e. it is the same for the mass and Litim cutoffs. Substituting (3.67) into (3.44) using (3.48) the following equation is obtained for the c-function of the SG model:

$$k\partial_k c_k = \frac{\left(k\partial_k\tilde{u}_k\beta^2\right)^2}{\left(1+\tilde{u}_k\beta^2\right)^3} \approx \frac{\left(-2\tilde{u}_k\beta^2\right)^2}{\left(1+\tilde{u}_k\beta^2\right)^3} \equiv \frac{4\tilde{m}_k^4}{[1+\tilde{m}_k^2]^3} \tag{3.68}$$

where the identification $\tilde{m}_k^2 = \tilde{u}_k\beta^2$ is used. The scale dependence of the c-function in that case is identical to the massive deformation of the Gaussian fixed point and the corresponding RG trajectory is indicated by the green line in 3.5.

It is important to note that for finite frequencies $\beta^2 \neq 0$ the Taylor expanded potential (3.61) cannot be used to determine the c-function since it violates the periodicity of the model. In this case only equations (3.49) or (3.50) can produce reliable results.

In order to improve the LPA result for the c-function of the SG model without violating the periodicity of the model one has to incorporate a scale-dependent frequency, i.e. a wave-function renormalization (we refer to this approximation as z+LPA), as it is discussed in the next subsection.

3.6.2 The scale-dependent wave function renormalization

The inclusion of the running wave-function renormalization changes the whole picture of the SG phase diagram, with all the $\tilde{u} \neq 0$ fixed points collapsing into a single $(\beta_k = 0, \tilde{u} = 1)$ fixed point, as it is expected from the exact CFT solution. The phase diagram obtained at

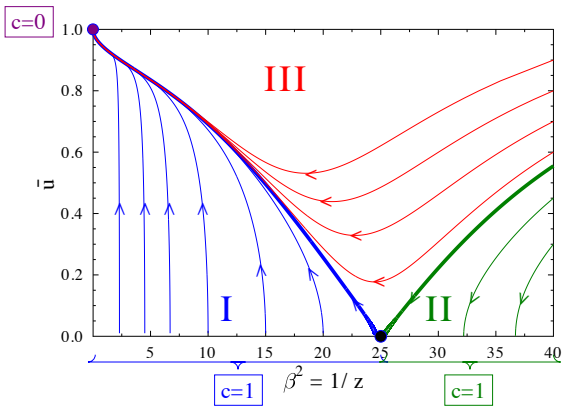

Fig. 3.5 The flow diagram of the SG model in the scale-dependent frequency approximation. The phase space is divided into three regions. In region I we have a line of UV repulsive Gaussian fixed points $(\bar{u} = 0, \beta^2 < 8\pi)$. Every trajectory starting in the vicinity of this line ends in an IR attractive fixed point (purple full circle, $\bar{u} = 1, \beta^2 = 0$). The Δc observed along the trajectories of this region should be equal to 1. Region II contains a line of IR attractive Gaussian fixed points $(\bar{u} = 0, \beta^2 > 8\pi,)$ which are the end points of trajectories starting at $\beta^2 \approx \infty$ below the thick green line, i.e. the separatrix. Region III contains those trajectories starting at $\beta^2 \approx \infty$ which end in the IR attractive fixed point (purple full circle).

this approximation level is sketched in Fig. 3.5, where we evidence three different regions. The Δc is strictly well defined only in region I, where we start from a Gaussian fixed point $c_{UV} = 1$ and we end up on a massive IR fixed point $c_{IR} = 0$. The massive IR fixed point related to the degeneracy of the blocked action is an important feature of the exact RG flow [48, 50, 52, 97] and it was considered in SG type models [49, 51, 98].

In region II the trajectories end in the Gaussian fixed points $c = 1$ but they are coming from infinity where actually no fixed point is present. This is due to the fact that we are not considering in our ansatz (3.51) any operator which can generate a fixed point at $c > 1$ and then the trajectories ending at $c = 1$ are forced to start at infinity. Thus, Δc is not defined in this region.

Region III contains those trajectories which start at $\beta = \infty$ but end in the IR massive fixed point at $c = 0$. Even in this case the Δc is not well defined.

In the following we are going to discuss in details the results of region *I* where all the trajectories should give $\Delta c = 1$. We shall ignore region *II* where the Δc is not defined, briefly discussing region *III*.

The presence of wave-function renormalization is necessary to obtain the qualitative correct flow diagram for the SG. Note that equation (3.44) has been derived only in the case of scale-independent kinetic term and the derivation of an equivalent expression in the case of running wave function renormalization appears far more demanding than the calculation sketched in Section 3.3. However, it is still possible to get a sensible result using the mapping between the running wave-function renormalization and the running frequency β_k cases (as shown in equations (3.59a) and (3.59b)), finally obtaining equation (3.71) In other words the equation (3.44) is valid only at LPA level, but it is still possible to apply it to the z+LPA scheme, since, thanks to the mapping described in equations (3.59a) and (3.59b) the z+LPA ansatz can be mapped into an LPA one.

We will then use directly the ansatz,

$$\tilde{V}_k = \tilde{u}_k \cos(\beta_k \varphi) \tag{3.69}$$

with no wave function renormalization present in the kinetic term. This ansatz is equivalent to ansatz (3.51) if we rescale the field and use the relations (3.59a) and (3.59b), with the running frequency playing the role of a wave-function renormalization.

Ansatz (3.69) is not suited to study the SG model when full periodicity has to be preserved, indeed when we substitute it into equation (3.54) symmetry breaking terms appear. The same happens when we substitute it into equation (3.44). However in the latter case symmetry breaking terms are not dangerous, since we have to evaluate the expression at the potential minimum where all the symmetry breaking terms vanish.

Proceeding in this way we obtain

$$k\partial_k c_k = \frac{(\beta_k^2 k\partial_k \tilde{u}_k + 2\tilde{u}_k \beta_k k\partial_k \beta_k)^2}{(1+\tilde{u}_k \beta_k^2)^3} \tag{3.70}$$

where no inconsistency is present.

We still cannot use expression (3.70), since we cannot write a flow for β_k due to the non-periodic terms. To avoid these difficulties we rewrite expression (3.70) using the inverse transformation of (3.59a) and (3.59b),

$$k\partial_k c_k = \frac{(k\partial_k \tilde{u}_k)^2}{(1+\tilde{u}_k)^3}. \tag{3.71}$$

The last expression is fully coherent and represents the flow of the c-function in presence of a running wave-function renormalization into the SG model; it is worth noting that the use of transformations (3.59a) and (3.59b) gave us the possibility to derive the expression (3.70) from equation (3.44), which was derived in [25] in the case of no-wave-function renormalization.

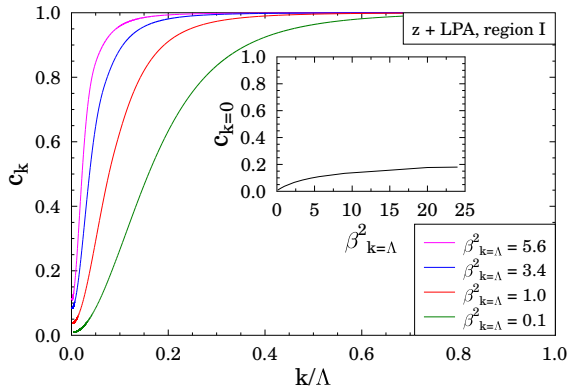

Fig. 3.6 Running of the c-function obtained in the case of scale-dependent wave-function renormalization for the single-frequency SG model, as expected the case of small frequency ($\beta_{k=\Lambda} < 0.1$) was already very well described by the scale-independent frequency case 3.1. The inset shows the results obtained for c_{IR} as a function of $\beta_{k=\Lambda}$, these results show lower accuracy in the large frequency limit, while they become practically exact in the limit $\beta_{k=\Lambda} \to 0$, accordingly with [25].

In the limit $\beta^2_{k=\Lambda} \to 0$, the IR result of the c-function (see the inset of 3.6) tends to zero. This implies that in the limit $\beta^2_{k=\Lambda} \to 0$ the difference $\Delta c \to 1$. The numerical result found in this case reaches the accuracy $1 \geq \Delta c \geq 0.99$ of the scale-independent frequency solution (3.60) but now the periodicity of the SG model is fully preserved (which was not the case in [25]). It should be also noted that the accurate results of Fig. 3.6 could not be obtained in the mass cutoff framework (B.23b) with $b = 1$, which does not allow the flow to converge, but our findings were obtained with the smoother $b = 2$ cutoff.

Fig 3.6 reports the running of the c-function for various values of the initial condition β_Λ. The final Δc value depends on the trajectory even if it should not be at exact level. This discrepancy shows that the flow obtained by approximated FRG procedure cannot satisfy the exact CFT requirements for the c-function.

The discrepancy between the exact $\Delta c = 1$ value and the actual results obtained by the FRG approach can be used to quantify the error committed by the truncation ansatz in the description of the exact RG trajectories.

We observe that the results of 3.6 main and inset are obtained by using power-law regulator with $b = 2$. The same computation appears to be considerably more difficult using general cutoff functions, including the exponential one.

Let us note that for vanishing frequency the RG flow equations become regulator-independent and that the c-function value tends to the exact result $\Delta c = 1$. This justifies the accuracy obtained in [25] even though the mass cutoff was used and the periodicity violated.

Finally we go on showing the results in region *III*. As discussed in the description of 3.5, trajectories in region *III* of the SG flow diagram should not have a well defined value for the c-function, due to the fact that those trajectories start at $\beta_{k=\Lambda} = \infty$ where no real fixed point is present.

However the numerical results obtained for those trajectories 3.7 are not so far from $\Delta c = 1$, due to the fact that they get most of the contribution in the region where they approach the "master trajectory" separatrix of region *I* i.e. the blue thick line in Fig. 3.5, which we know to have a value $\Delta c \approx 1$, while the portion of the trajectories close to region *II* get almost zero contribute. The results of region *III* are also in agreement with the findings of region *II*

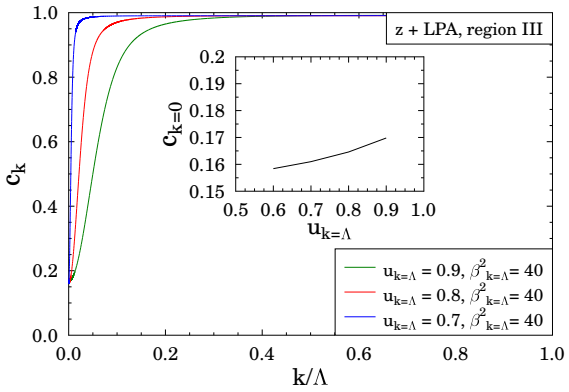

Fig. 3.7 The flow of the c-function in Region *III* of the SG flow diagram 3.5, the result is approximately $\Delta c = 1$ due to the fact that in region *III* most of the contribution to the c-function comes from the part of the trajectories very close to "master trajectory" separatrix of region *I* (the blue thick line in 3.5).

(not shown) where $\Delta c \approx 0$ for all the initial conditions.

3.7 Conclusions

In this chapter we introduced the reader to the Sine-Gordon (SG) model, showing how the substantial difference in the symmetry content of the bare action (3.1) leads to a finite

temperature phase transition even if in absence of spontaneous breaking of any continuous symmetry.

In section 3.2 the importance of the SG model in condensed matter is demonstrated giving a brief overview of some exact mappings and relations between the continuous effective field theory described by (3.1)

In this chapter we provided an estimation of the c-function over the RG trajectories of the sine-Gordon (SG) model in the whole parameter space. Using this result we showed that the numerical functional RG study of the SG model with scale-dependent frequency recovers for $\beta^2 < 8\pi$ (region I of 3.5) the exact result $\Delta c = 1$ with a good quantitative agreement while preserving the periodicity, which is the peculiar symmetry of the model. We also pointed out the dependence of this c-function calculation on the approximation level considered. For $\beta = 0$ one retrieves directly $\Delta c = 1$, also in the scale-independent frequency case, while for $\beta \neq 0$, again using scale independent frequency, we recover this result in the $\beta^2 \to 0$ limit, while increasing β^2 up to 8π in region I as a result of the used approximation the agreement becomes worst, remaining anyway reasonably good, as shown in 3.1.

Retrieving $\Delta c = 1$ is the SG counterpart of the computation of Δc for the sinh-Gordon model [85, 87]. This result can be understood by noticing that the analytical continuation $\beta \to i\beta$ [99] may be expected not to alter the Δc defined in the Zamolodchikov theorem, and that functional RG even in its crudest approximation does not spoil such correspondence for Δc, provided that the periodicity of the SG field is correctly taken into account.

We developed a fully coherent expression for the c-function in the case of running frequency, which gives better results in the whole region I (defined in 3.5). These results are compatible with the exact scenario up to an accuracy of 80% in the whole region I. Such accuracy grows to 99% in the small beta region in agreement with [25], as we discussed in 3.6.

We also noticed that for $\beta^2 > 0$ the use of the mass cutoff, as necessary to be consistent with expression (3.44), is not possible due to bad convergence properties, and the use of different b values or of different cutoff types is needed.

It should be noted that while the numerical results are quite accurate the exact property that all trajectories of region I should have the same value for Δc is not preserved by truncations schemes (3.51) (results in 3.1) nor (3.46) (results in 3.6). Actually the $\beta^2 \to 0$ limit always gives the correct result even when treated with the most rough truncation, this result being independent from the cutoff function. At variance one needs to go to the running frequency case to obtain reliable results for $\beta^2 >> 0$.

Even when full periodicity in the field is maintained, the $z+LPA$ truncation scheme is not sufficient to recover exact results for the c-function. Indeed the quantity computed using expression (3.44) satisfies two requirements of Zamalodchikov's c-theorem,

1. $\partial_t c_t \geq 0$ along the flow lines,

2. $\partial_t c_t = 0$ at the fixed points,

but it fails to reproduce the exact central charge of SG theory.

The final result of our calculation also depends on the chosen cutoff function and, as already mentioned, it was not possible to use the same cutoff scheme for both the couplings flow equations and the c-function flow (3.44). We do not expect these issues to be responsible for the error in the fixed point value of the c-function. Modifications of the cutoff scheme in LPA calculations have small influence on the results (around 5%) and we may expect this property to be maintained at z+LPA level, where calculations with different cutoff functions were not possible.

The main source of deviation from the exact result $\Delta c = 1$ is then probably due to z+LPA truncation in itself. We are not able to identify whether this deviation is only due to the approximation in the c-function flow or rather to the description of the fixed point given in z+LPA, which does not reproduce the exact central charge.

Certainly the c-function flow at z+LPA level not merely violates the exact fixed point value of the c-function, but it is also not able to produce trajectory independent results, as shown in 3.6. This scenario is not consistent with an unique central charge value at the SG fixed point and it is then impossible to dig out any information about this quantity from this approach. In this perspective it would be interesting to have an independent method to calculate the fixed point central charge at a given truncation level.

Obviously the reproduction of the Zamalodchikov's c-theorem should be better satisfied increasing the truncation level considered. However it has been shown that, at LPA level, the addition of further harmonics in the potential does not improve the results presented, while the introduction of running frequency is crucial to achieve consistency of the phase diagram.

This situation is peculiar of the LPA truncation level. Beyond z+LPA we expect the most relevant corrections from higher harmonics in the potential and only small variations are expected from the introduction of higher fields derivatives in (3.51)

Finally we remark that the trajectories of the other two regions do not have a definite Δc value, however while region II gives results $\Delta c \approx 0$, region III has the Δc values close to the ones obtained in region I 3.7, due to the fact that all the trajectories in this region merge with the "master trajectory" separatrix of region I in the $k \to 0$ limit.

Using the same techniques it is possible to study interpolating models between the SG model and the sinh-Gordon model. This investigation is currently under work.

Chapter 4

Application to Long Range Interactions

In the first chapter we introduced the reader to the concepts and methods of the FRG approach. In the second and third chapter we showed how FRG based techniques may be used reproduce and extend the current picture for the critical behavior of $O(N)$ symmetric models.

In the present chapter we are going to apply the concepts and tools of previous chapters to long range (LR) interactions, showing the capability of the FRG formalism to deal with model of crucial importance in the description of condensed matter physics, whose are still unknown and sometimes controversial

Among the interactions studied in the context of $O(N)$ models LR interactions play an important and paradigmatic role, having the form of power law decaying couplings. Apart from the motivation *per se*, internal to $O(N)$ models, another even more important reason for such studies is given by the long lasting interest in understanding the properties of systems with LR interactions motivated by their crucial presence in many systems ranging from plasma physics to astrophysics and cosmology [100]. For a general $O(N)$ model with the power law interactions the Hamiltonian reads

$$H = -\frac{J}{2}\sum_{i\neq j}\frac{\mathbf{S}_i\cdot\mathbf{S}_j}{|i-j|^{d+\sigma}}\,, \tag{4.1}$$

where $\mathbf{S}_i$ denote a unit vector with N components in the site i of a lattice in dimension d, J is a coupling energy and $d+\sigma$ is the exponent of the power law decay (we refer in the following to cubic lattices). When $\sigma \leq 0$ a diverging energy density is obtained and to well define the thermodynamic limit it is necessary to rescale the coupling constant J [101]. When $\sigma > 0$ the model may have a phase transition of the second order, in particular as a function of the parameter σ three different regimes occur [102, 103]: *(i)* for $\sigma \leq d/2$ the mean–field approximation is valid even at the critical point; *(ii)* for σ greater than a critical value, σ_*, the model has the same critical exponents of the short range (SR) model (formally, the SR

model is obtained in the limit $\sigma \to \infty$); *(iii)* for $d/2 < \sigma \leq \sigma_*$ the system exhibits peculiar LR critical exponents. For the Ising model in $d = 1$ [104–106] the value $\sigma_* = 1$ is found, and for $\sigma = \sigma_*$ a phase transition of the Berezinskii-Kosterlitz-Thouless universality class occur [107–109] (see more references in [110]); effects of disorder were studied in [111].

Many efforts have been devoted to the determination of σ_* and to the characterization of the universality classes in the region $d/2 < \sigma \leq \sigma_*$ for general N in dimension $d \geq 2$, which is the case we are going to consider in this chapter. In the classical paper [102] the expression $\eta = 2 - \sigma$ was found for the critical exponent η by an ε-expansion (at order ε^2) and conjectured to be exact. This implies a discontinuity of the anomalous dimension η as a function of the parameter σ, when σ reaches σ_*, with $\sigma_* = 2$ [102].
A way out was proposed by Sak [103], who found $\eta = 2 - \sigma$ for all $\sigma < \sigma_*$ and gave $\sigma_* = 2 - \eta_{SR}$ (where η_{SR} is the η exponent of the SR model). This η is a continuous function of σ and there is no correction to the canonical dimension of the field in the case of LR interactions. Subsequent Monte Carlo (MC) results, based on MC algorithms specific for LR interactions [112], confirmed this picture [113]. However the Sak scenario was recently challenged by new MC results [114], suggesting that the behavior of the anomalous dimension may be far more complicated than the one provided by Sak [103]. We should define the critical exponent η_{LR} of the $O(N)$ LR models in dimension d with power–law exponent $d + \sigma$ as

$$\eta_{LR}(d, \sigma) \equiv 2 - \sigma + \delta\eta \,, \tag{4.2}$$

where $2 - \sigma$ is the conventional result, obtained solving the LR Ising model at mean field level [102], while $\delta\eta$ is an eventual non mean field correction to the anomalous dimension. In [114] it was reported that there is a non–vanishing correction $\delta\eta$ to Sak's result $\eta = 2 - \sigma$ in the region $d/2 < \sigma < \sigma_*$ and that $\sigma_* = 2$, as in the earliest work of Fisher, Ma and Nickel [102]. In a subsequent work [114] the presence of a $\delta\eta \neq 0$ was discussed using an ε–expansion, and as a result the correction $\delta\eta$ should be less than the anomalous dimension of a SR system in dimension $D_{\rm eff}^{BPR} \equiv 4 + d - 2\sigma$ (we refer to such dimension as $D_{\rm eff}^{BPR}$ from the authors of [114]). In the following we are going to show that most of the critical properties of a LR model in dimension d with power law exponent $d + \sigma$ can be inferred from those of a SR model in the effective fractional dimension $D_{\rm eff} \neq D_{\rm eff}^{BPR}$, this result being exact in the $N \to \infty$ limit. We also observe that the MC results recently presented for a percolation model with LR probabilities [115] seem to agree with the findings of [114] and not with the Sak scenario. In a very recent work new MC results for the Ising model with LR interaction in $d = 2$ were presented [116]: these results evidence the presence of logarithmic corrections into the correlation function of this kind of systems when the value of σ is very close to

$\sigma = 2 - \eta_{SR}$, implying the numerical difficulty of extracting reliable results for the critical exponents with small error bars around $\sigma = 2 - \eta_{SR}$.

The controversy about the actual value of σ_* raised by recent MC results has not really a compelling quantitative *raison d'être*: after all, for the Ising model in $d = 2$ the value $\sigma_* = 7/4$ predicted by Sak should be contrasted with $\sigma_* = 2$ suggested in [114] (even though the value of η at $\sigma = 7/4$ obtained in [114] is $\eta = 0.332$ and it should be contrasted with $\eta = 1/4$ predicted by Sak). The issue raised by recent MC results is rather of principle, since it generally questions how the LR terms (p^σ) renormalize and especially how the SR term (p^2) in the propagator is dressed by the presence of LR interactions.

4.1 FRG Approach to Long Range Effective Action

In this section we aim to clarify such issues using a functional renormalization group approach [19, 31]. We are interested in universal quantities, and as usual we replace the spin variables $\{\mathbf{S}_i\}$ with an N–component vector field $\phi(x)$ in continuous space. We define a scale dependent effective action Γ_k depending on an infrared cutoff k and on the continuous field ϕ: when $k \to k_0$, where k_0 is some ultraviolet scale, the effective action is equal to the mean–field free energy of the system, while for $k \to 0$ it is equal to the exact free energy [19]. Our first ansatz for the effective action reads

$$\Gamma_k[\phi] = \int d^d x \left\{ Z_k \partial_\mu^{\frac{\sigma}{2}} \phi_i \partial_\mu^{\frac{\sigma}{2}} \phi_i + U_k(\rho) \right\}, \tag{4.3}$$

where the summation over repeated indexes is assumed, $\rho = \frac{1}{2}\phi_i\phi_i$, and ϕ_i is the i–th component of ϕ. The notation $\partial_\mu^{\frac{\sigma}{2}}$ is a compact way to intend that the inverse propagator of the effective action (4.3) in Fourier space depends on q^σ and not on q^2 as in the SR case. Z_k is the wave function renormalization of the model that at this level of approximation is field independent.

This ansatz is well justified if we analyze the bare propagator of the LR Ising model. It is well known that at mean field level the momentum dependence of the propagator for an Ising type system is obtained inverting the interaction matrix. In the LR case this inversion cannot be pursued analytically but it is possible to read out a series expansion in power of the momentum q for the propagator. This series expansion starts with a non-analytic term q^σ, which is then the most relevant at large scales. We expect the renormalization procedure not to generate more relevant terms and then the large scale behavior of the system should be completely dominated by the momentum term included in ansatz (4.3). Actually one could expect this ansatz to be incomplete in the $\sigma \simeq 2$ region where the non analytic term q^σ is

very similar to the successive analytic term q^2, this problematics is fixed later in the text introducing ansatz (4.9).

The effective potential $U_k(\rho)$ satisfies a renormalization group flow equation [17]; in order to obtain such flow equation in the FRG scheme it is necessary to define an infrared cutoff function $R_k(q)$, which plays the role of a momentum dependent mass of the excitations [17]. This artificial mass should be vanishing for excitations with momentum $q >> k$ while it should prevent the propagation of low momentum $q << k$ excitations.

Using an infrared cutoff suited for LR interactions, $R_k(q) = Z_k(k^\sigma - q^\sigma)\theta(k^\sigma - q^\sigma)$, we obtain the flow equation for the effective potential, when this is rewritten in terms of dimensionless variables (denoted by bars) one can find the fixed points, or scaling solutions, $\bar{U}_*(\bar{\rho})$ by solving it [24]. The form of this flow equation is

$$\begin{aligned}\partial_t \bar{U}_k &= -d\bar{U}_k(\bar{\rho}) + (d-\sigma+\delta\eta)\bar{\rho}\,\bar{U}_k'(\bar{\rho}) \\ &+ \frac{\sigma}{2} c_d (N-1)\frac{1-\frac{\delta\eta}{d+\sigma}}{1+\bar{U}_k'(\bar{\rho})} + \frac{\sigma}{2} c_d \frac{1-\frac{\delta\eta}{d+\sigma}}{1+\bar{U}_k'(\bar{\rho})+2\bar{\rho}\,\bar{U}_k''(\bar{\rho})}\,,\end{aligned} \tag{4.4}$$

where $c_d^{-1} = (4\pi)^{d/2}\Gamma(d/2+1)$ and $\delta\eta$ is an eventual anomalous dimension correction, related to the flow of the wave function renormalization by $\delta\eta = -\partial_t \log Z_k$, where $t = \log(k/k_0)$ is the RG time and k_0 is the ultraviolet scale.

4.1.1 Effective fractional dimension

We start our analysis considering the case $Z_k = 1$, which implies $\delta\eta = 0$. It is then possible to show that the flow equation (4.4) for the effective potential can be put in relation with the corresponding equation for a SR model [18, 24] in an effective fractional dimension

$$D_{\text{eff}} = \frac{2d}{\sigma} \tag{4.5}$$

(in the following we denote by capital D the dimension of the SR $O(N)$ model). Within this approximation it is also possible to establish a mapping between the LR correlation length exponent $\nu_{LR}(d,\sigma)$ and the LR susceptibility exponent $\gamma_{LR}(d,\sigma)$ and the equivalent SR ones $\nu_{SR}(D_{\text{eff}})$ and $\gamma_{SR}(D_{\text{eff}})$. The relation is found to be:

$$\nu_{LR}(d,\sigma) = \frac{2}{\sigma}\nu_{SR}(D_{\text{eff}});\quad \gamma_{LR}(d,\sigma) = \gamma_{SR}(D_{\text{eff}})\,. \tag{4.6}$$

As a check, we observe that the relations (4.50) and (4.6) are satisfied exactly by the spherical model [41]. In fact in the $N \to \infty$ limit our approximation provides exact critical exponents [46]. In conclusion, we can see that the LR and SR critical exponents in, respectively, dimension d and D_{eff} are obtained from each other: e.g., using as the two independent SR critical exponents ν_{SR} and γ_{SR} to derive the LR ones, using (4.6) and the usual scaling relations among critical exponents one gets all the other four LR exponents, including $\eta_{LR} = 2 - \sigma$. The equivalence between the fixed point structure of these two models can also be seen using the spike plot technique described in [18, 24] as shown in Fig. 4.1. From this

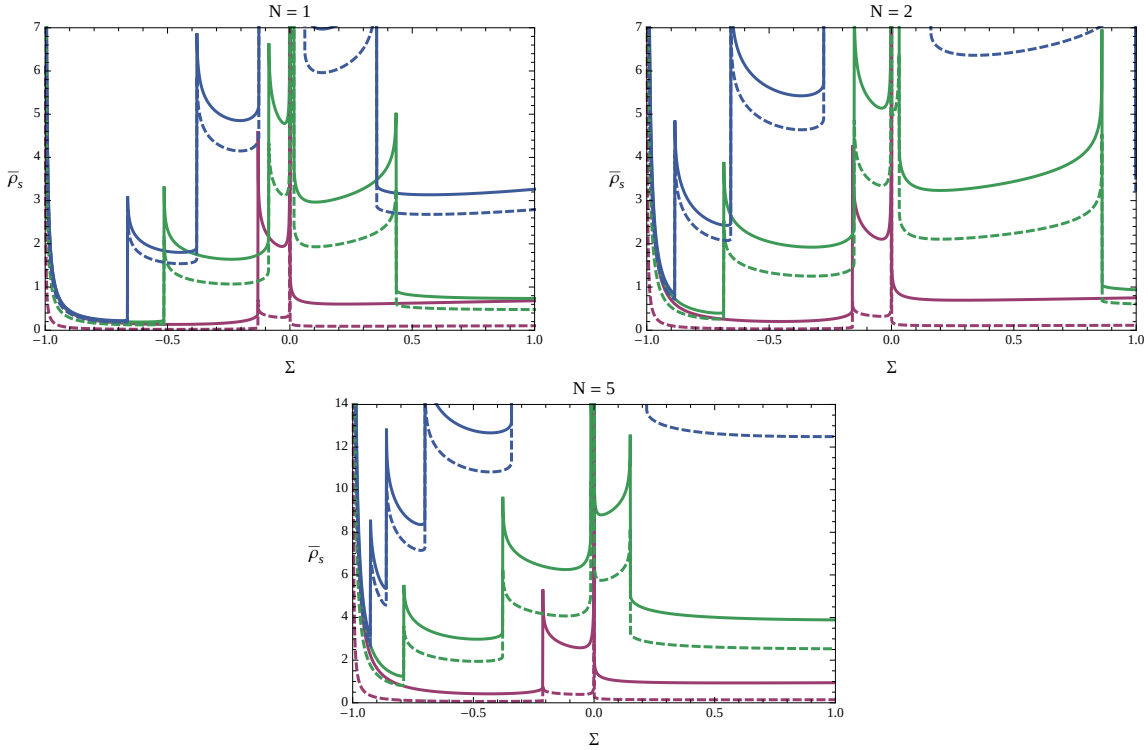

Fig. 4.1 Each value of $\Sigma \equiv \bar{U}'_*(0)$ for which we have a spike in the above figure is the derivative at the origin of a well defined fixed point effective potential: thus every spike is the signature of a different universality class. Solid lines represents spike plots of LR models in dimension d with power–law exponent σ, while dashed lines represent spike plots of SR models in dimension $D = D_{\text{eff}} = 2d/\sigma$. The plot is for the case $N = 1, 2, 5$ and $d = 2$ for the cases $\sigma = 1.25, 1.75, 1.9$.

analysis it follows that by varying σ at fixed d we go trough a sequence of $\sigma_{c,i}$ at which new multicritical LR universality classes appear, in a way analogous to the sequence of upper critical dimensions found in SR models as d is varied [24]. For the Ising universality class the lower critical decay exponent is $\sigma_{c,2} = d/2$ in agreement with known results [102]. In the case of a i–th multicritical model with LR interaction the lower critical decay exponent is

found to be $\sigma_{c,i} = \frac{d(i-1)}{i}$. Since the new fixed points branch from the Gaussian fixed point, their analysis based on the ansatz (4.3), first term of an expansion of the effective action in powers of the anomalous dimension, is consistent and the existence of multicritical LR $O(N)$ models can be extrapolated to be valid in the full theory.

To study anomalous dimension effects one has to study the equation for the effective potential U_k in the case $\delta\eta \neq 0$, i.e. when Z_k in (4.3) is non–constant. One obtains the scale derivative of the wave function renormalization from $\partial_t Z_k = \lim_{p\to 0} \frac{d}{dp^\sigma} \partial_t \Gamma_k^{(2)}(p,-p)$ and computes the anomalous dimension using $\delta\eta = -\partial_t \log Z_k$. Since the flow equation generates no non–analytic terms in p, from this definition we find $\delta\eta = 0$, in agreement with Sak's result [103], in which the anomalous dimension does not get any non mean–field contribution. However, an anomalous dimension is present, at this approximation level, in the SR system, thus we obtain a new dimensional equivalence:

$$D'_{\rm eff} = \frac{[2-\eta_{SR}(D'_{\rm eff})]d}{\sigma}\,, \tag{4.7}$$

which is in agreement with the results of the dimensional analysis performed for the Ising model in [116] and with the arguments presented for the LR and SR Ising spin glasses in [117]. equation (4.7) is valid for any N and it is an implicit equation, indeed one has to know the critical exponent η_{SR} in fractional dimension [22, 69, 118, 119] to calculate $D'_{\rm eff}$. In the case of a running, not field dependent, wave function renormalization we also obtain the following relation for the critical exponent ν_{LR}:

$$\nu_{LR}(d,\sigma) = \frac{2-\eta_{SR}(D'_{\rm eff})}{\sigma}\,\nu_{SR}(D'_{\rm eff})\,. \tag{4.8}$$

In Fig. 4.2 we compare the exact behavior for the $y_t = 1/\nu_{LR}$ LR exponent in the spherical $N\to\infty$ limit with the behavior obtained using the effective dimension D'_{eff} for various values of N. In the inset of Fig. 4.2 we plot MC results from [113] and [116] together with the results obtained by the effective dimension $D'_{\rm eff}$ both at our approximation level and with the use of high–precision estimates of the SR critical exponents in fractal dimensions from [69] in (4.7). We expect these results to be more reliable as N grows due to the relative decrease of anomalous dimensions effects in these cases. Relations (4.7) and (4.8) can be also used to extend this analysis to multicritical fixed points in LR systems.

In Fig. 4.3 we plot the exponent y_t for various N in three dimensions using (4.7): due to the better performances of our approximation in three dimensions, we expect these results to be quantitatively very reliable, when compared with future numerical simulations. The curves of Fig. 4.2 and Fig. 4.3 are genuine universal predictions of our analysis.

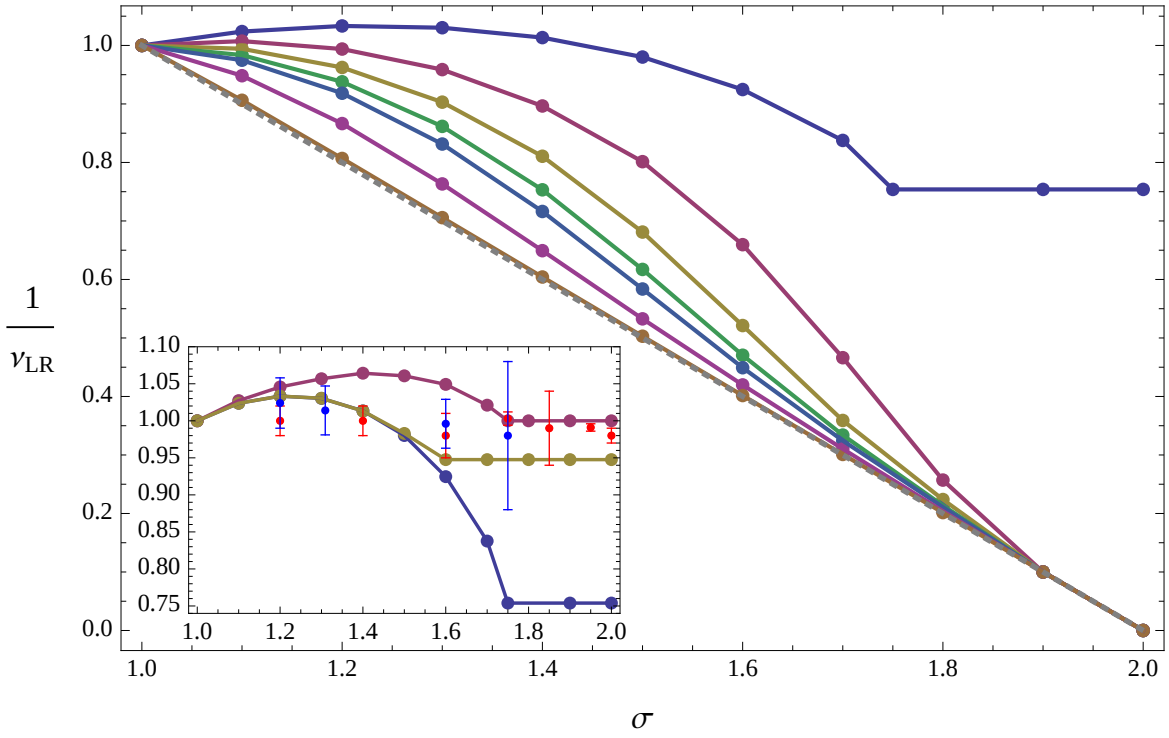

Fig. 4.2 $y_t = 1/\nu_{LR}$ exponent as a function of σ in $d = 2$ for some values of N (from top: $N = 1, 2, 3, 4, 5, 10, 100$). The dashed line is the analytical result obtained for the spherical model $N = \infty$. Inset: $y_t = 1/\nu_{LR}$ vs. σ for the $d = 2$ LR Ising model compared with MC data of [113] (red circles) and of [116] (blue circles). The three continuous lines represents the estimates made using (4.8) with the numerical values of $\nu_{SR}(D'_{\rm eff})$ and $\eta_{SR}(D'_{\rm eff})$ taken from recent high–precision estimates in fractional dimensions [69] (top red line), from [22, 25] where the $O(N)$ model definition for η_{SR} is used (blue bottom line) and from [24] where the Ising definition of η_{SR} is used instead (yellow middle line) [69].

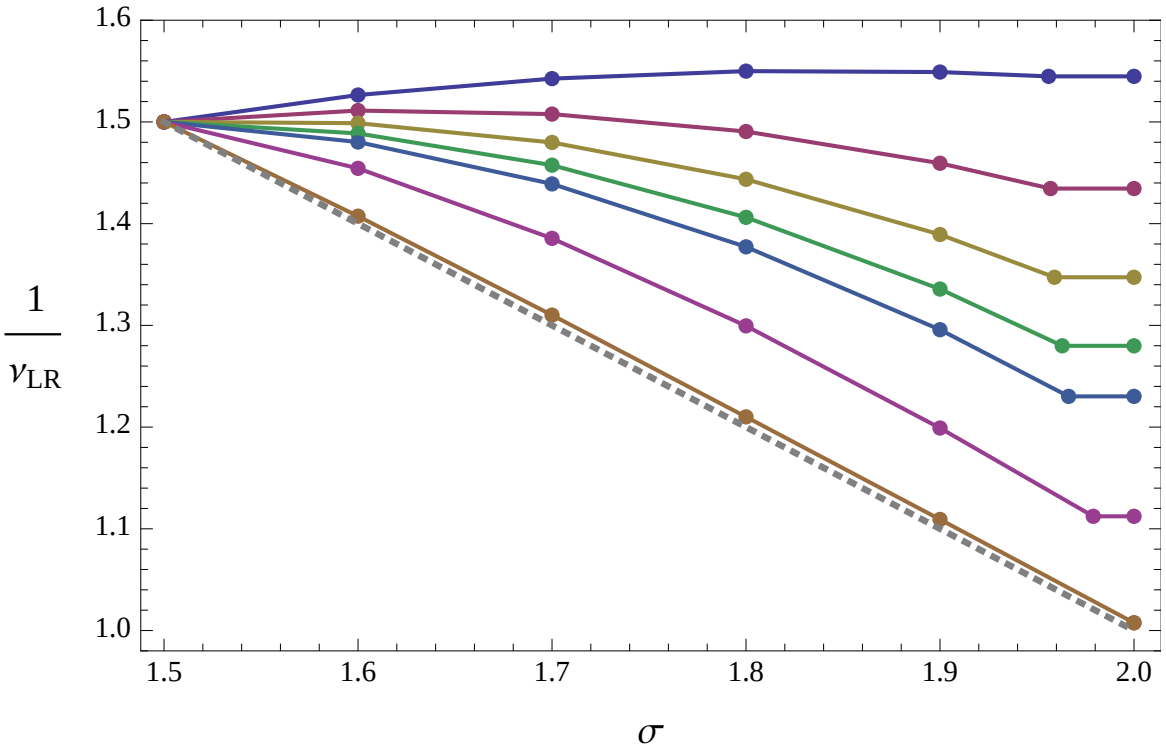

Fig. 4.3 $y_t = 1/\nu_{LR}$ exponent as a function of σ in $d = 3$ for some values of N (from top: $N = 1,2,3,4,5,10,100$). As in Fig. 4.2 the dashed line is the analytical result obtained for the spherical model.

4.1.2 Effects of the short range term

The present analysis suggests the validity of Sak's results for the value of σ_*. On the other hand, since the ansatz (4.3) does not contain any SR term, such approximation is not able to describe the case $\sigma > \sigma_*$, in which SR interactions could become dominant. In order to investigate these effects we enlarge our theory space and we propose the new ansatz:

$$\Gamma_k[\phi] = \int d^d x \left\{ Z_{\sigma,k} \partial_\mu^{\frac{\sigma}{2}} \phi_i \partial_\mu^{\frac{\sigma}{2}} \phi_i + Z_{2,k} \partial_\mu \phi_i \partial_\mu \phi_i + U_k(\rho) \right\} , \tag{4.9}$$

where we have both LR and SR terms in the propagator. Since a SR analytic term is already present in the series expansion of the lattice model propagator, ansatz (4.9) is the natural extension of the ansatz (4.3).

We need to choose a proper cutoff function for the propagator of the theory (4.9). Since we do not know *a priori* which will be the dominant term for $\sigma \simeq \sigma_*$ we take the following combination:

$$R_k(q) = Z_{\sigma,k}(k^\sigma - q^\sigma)\theta(k^\sigma - q^\sigma) + Z_{2,k}(k^2 - q^2)\theta(k^2 - q^2) . \tag{4.10}$$

The ansatz (4.9) and the cutoff choice (4.10) are consistent with the ones of the previous analysis when LR interactions are dominant, but they are still valid when SR become important and will allow us to study the whole σ range. This cutoff has the desired property to not choose any term as the relevant one, it acts on both terms, assuring us to be valid in the whole σ range. The choice (4.10) turns out to be the most simple, since it always influences the dominant term, while only adding an irrelevant modification to the other, yet it drastically simplifies the calculation.

We proceed deriving the flow equation for all the quantities in latter definition

$$\partial_t Z_2 = \frac{1}{2} \lim_{p \to 0} \frac{d^2}{dp^2} \partial_t \Gamma_k^{(2)}(p, -p) \tag{4.11}$$

$$\partial_t Z_\sigma = \lim_{p \to 0} \frac{d}{dp^\sigma} \partial_t \Gamma_k^{(2)}(p, -p) , \tag{4.12}$$

while the flow for the potential derives from the flow of the effective action evaluated at constant fields. These equations were obtained starting from the usual Wetterich equation [17], with the ansatz (4.9). The cutoff function is shown in equation (4.10). We derived the equations for dimensional quantities,

$$\partial_t Z_\sigma = 0 , \tag{4.13a}$$

$$\partial_t Z_2 = -\frac{\rho_0 U_k''(\rho_0)^2 (\sigma Z_\sigma k^\sigma + 2Z_2)^2 k^{d+2}}{(Z_\sigma k^\sigma + Z_2 k^2)^2 (Z_\sigma k^\sigma + Z_2 k^2 + 2\bar{\rho}_0 U_k''(\rho_0))^2}\,, \tag{4.13b}$$

$$\begin{aligned}\partial_t U_k(\rho) = &\frac{Z_2 k^2 - \frac{\partial_t Z_2}{d+2} + \frac{\sigma}{2} Z_\sigma}{Z_\sigma k^\sigma + Z_2 k^2 + U_k'(\rho) + 2\rho U_k''(\rho)} + \\ &(N-1)\frac{Z_2 k^2 - \frac{\partial_t Z_2}{d+2} + \frac{\sigma}{2} Z_\sigma}{Z_\sigma k^\sigma + Z_2 k^2 + U_k'(\rho)}\,.\end{aligned} \tag{4.13c}$$

To further proceed we need to choose the dimension of the field with the constraint that the effective action must be dimensionless. To properly define the dimensionless couplings, we have two natural choices: the first one is the one we did in previous section to make the Z_σ coupling dimensionless and absorb it into the field – we refer to this choice as to *LR-dimensions*. On the other hand in this case we could also follow the usual way for $O(N)$ models defining the field dimension to make Z_2 dimensionless and then absorbing it in the field. This will lead to the definition of a LR coupling $J_\sigma = \frac{Z_\sigma}{Z_2}$ (*SR-dimensions*).

The two possible choices are summarized in the following table:

Quantity	*SR–dimensions*	*LR–dimensions*
q	$k\bar{q}$	$k\bar{q}$
ρ	$k^{d-2} Z_2^{-1} \bar{\rho}$	$k^{d-\sigma} Z_\sigma^{-1} \bar{\rho}$
$U(\rho)$	$k^d \bar{U}(\bar{\rho})$	$k^d \bar{U}(\bar{\rho})$
Z_2	$\bar{Z}_2$	$k^{\sigma-2} \bar{Z}_2$
Z_σ	$k^{2-\sigma} \bar{Z}_\sigma$	$\bar{Z}_\sigma$

Physical results should be the same in both cases. If we choose SR-dimensions we find three equations: one for the potential, one for the LR coupling and one for the anomalous dimension. These three equations reproduce the usual $O(N)$ models equations in the limiting case $J_\sigma \to 0$. On the other hand when we use LR-dimensions we have only two equations (since we do not have any anomalous dimension) and we may define a SR coupling $J_2 = Z_2/Z_\sigma$: when J_2 runs to zero we recover the equations obtained for the pure LR approximation.

We conclude then that the last truncation proposed includes the results obtained in previous ones and extends them in the whole σ range. SR-dimensions prove better to investigate the boundary $\sigma \simeq \sigma_*$, due to the fact that Z_σ is always constant during the flow, while Z_2 is diverging in the case of dominant SR interactions and must be absorbed in the field.

4.1.3 SR–Dimensions

We are going to investigate the region $\sigma > \sigma_*$, where we believe the p^2 term to be dominant, so we choose the SR-dimensions in order to be able to recover exactly the SR case. We define our anomalous dimension as

$$\eta_2 = -\frac{1}{Z_2}\partial_t Z_2\,, \tag{4.14}$$

(following the usual SR analysis [31]), but in addition one gets the renormalized LR coupling defined as

$$J_\sigma = \frac{Z_\sigma}{Z_2}\,. \tag{4.15}$$

The flow equations for the renormalized dimensionless couplings are

$$\partial_t \bar{J}_\sigma = (\sigma-2)\bar{J}_\sigma + \eta_2 \bar{J}_\sigma\,, \tag{4.16a}$$

$$\eta_2 = \frac{(2+\sigma\bar{J}_\sigma)^2\bar{\rho}_0\bar{U}_k''(\bar{\rho}_0)^2}{(1+\bar{J}_\sigma)^2(1+\bar{J}_\sigma+2\bar{\rho}_0\bar{U}_k''(\bar{\rho}_0))^2}\,, \tag{4.16b}$$

$$\begin{aligned}\partial_t \bar{U}_k(\bar{\rho}) &= -d\bar{U}_k(\bar{\rho}) + (d-2+\eta_2)\bar{\rho}\,\bar{U}_k'(\bar{\rho}) \\ &+(N-1)\frac{1-\frac{\eta_2}{d+2}+\frac{\sigma}{2}\bar{J}_\sigma}{1+\bar{J}_\sigma+\bar{U}_k'(\bar{\rho})} + \frac{1-\frac{\eta_2}{d+2}+\frac{\sigma}{2}\bar{J}_\sigma}{1+\bar{J}_\sigma+\bar{U}_k'(\bar{\rho})+2\bar{\rho}\,\bar{U}_k''(\bar{\rho})}\,.\end{aligned} \tag{4.16c}$$

Looking at equation (4.16a) we see that there are only two possibilities for the r.h.s. to vanish and for $\bar{J}_\sigma$ to attain some fixed point value $\bar{J}^*_\sigma$.

The first possibility is $\bar{J}^*_\sigma = 0$ and we are in the SR case, the second is $\eta_2 = 2-\sigma$ which is a characteristic of the LR fixed point, a least at this approximation level. This shows that we have no necessity to change the field dimension to study the case of a dominant LR term, since the p^2 term is still present in the LR fixed point.
In order to check these properties we turn to the approximation where we expand the potential around its minimum:

$$\bar{U}_k(\bar{\rho}) = \frac{1}{2}\lambda_k(\bar{\rho}-\kappa_k)^2\,. \tag{4.17}$$

Projecting the flow equation for the potential we can get the beta functions of these two couplings which, together with the flow equation for $\bar{J}_\sigma$, form a closed set:

$$\partial_t \bar{J}_\sigma = (\sigma-2)\bar{J}_\sigma + \eta_2 \bar{J}_\sigma\,, \tag{4.18a}$$

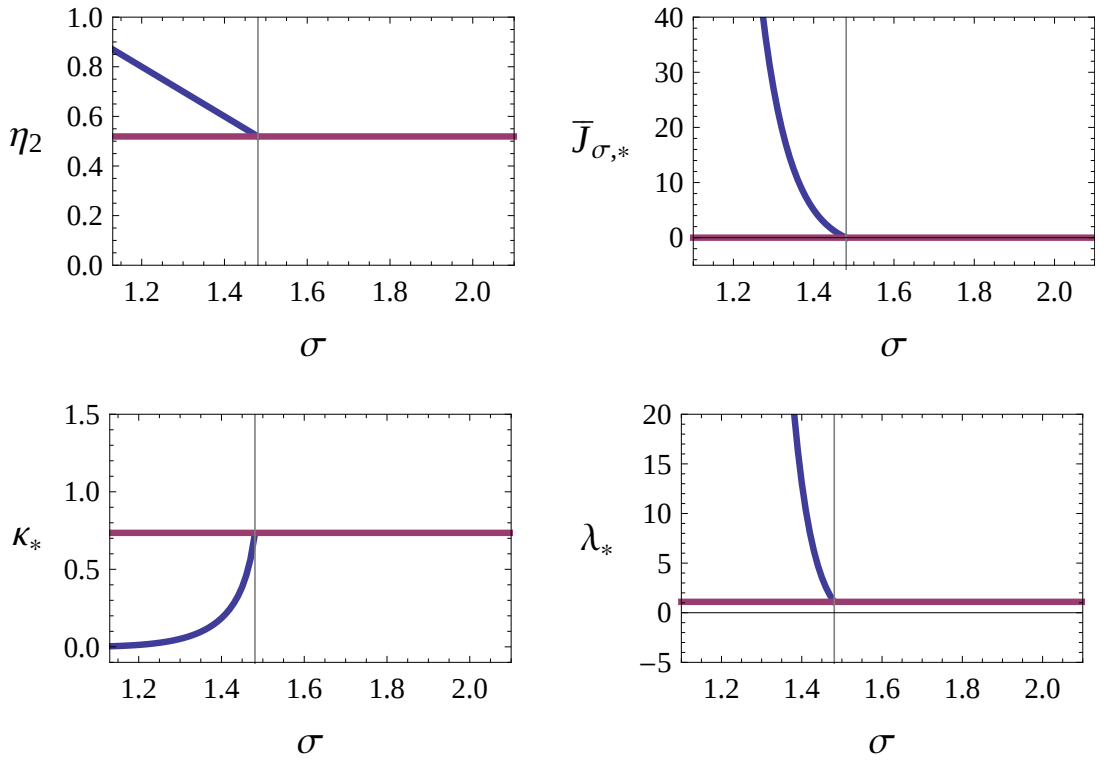

Fig. 4.4 Anomalous dimension η_2 and fixed point values $J_{\sigma,*}$,κ_*,λ_* in the truncation considered in the text for the Ising model in $d = 2$. For $\sigma > \sigma_* \equiv 2 - \eta_{SR}$ only the fixed point (red line) is present characterized by $\eta_2 = \eta_{SR}$ and $J_{\sigma,*} = 0$. At $\sigma = \sigma_*$ the LR fixed point (blue lines) branches from the SR fixed point and then controls the critical behavior for every $\sigma < \sigma_*$. Thus even in the case of both SR and LR terms in the propagator the anomalous dimension as a function of σ is thus LR ($\eta_2 = 2 - \sigma$) for $\sigma < \sigma_*$ and SR for $\sigma > \sigma_*$.

$$\eta_2 = \frac{(2+\sigma\bar{J}_\sigma)^2\kappa_k\lambda_k^2}{(1+\bar{J}_\sigma)^2(1+\bar{J}_\sigma+2\kappa_k\lambda_k)^2}\,, \tag{4.18b}$$

$$\begin{aligned}\partial_t\kappa_k = &-(d-2+\eta_2)\kappa_k + 3\frac{1-\frac{\eta_2}{d+2}+\frac{\sigma}{2}\bar{J}_\sigma}{(1+\bar{J}_\sigma+2\kappa_k\lambda_k)^2}+\\ &(N-1)\frac{1-\frac{\eta_2}{d+2}+\frac{\sigma}{2}\bar{J}_\sigma}{(1+\bar{J}_\sigma)^2}\,,\end{aligned} \tag{4.18c}$$

$$\begin{aligned}\partial_t\lambda_k =&(d-4+2\eta_2)\lambda_k + 18\lambda_k\frac{1-\frac{\eta_2}{d+2}+\frac{\sigma}{2}\bar{J}_\sigma}{(1+\bar{J}_\sigma+2\kappa_k\lambda_k)^3}+\\ &2\lambda_k(N-1)\frac{1-\frac{\eta_2}{d+2}+\frac{\sigma}{2}\bar{J}_\sigma}{(1+\bar{J}_\sigma)^3}\,.\end{aligned} \tag{4.18d}$$

As discussed SR-dimensions are well suited to study the case $\sigma < \sigma_*$, since Z_2 is well defined in this case and is not brought to zero by the presence of a dominant LR term. The results for the couplings and the anomalous dimension at the fixed point is shown in Fig. 4.4. We see that the anomalous dimension η_2 follows naturally the Sak's behavior with no possible LR fixed point solution for $\sigma > \sigma_*$, however at $\sigma = \sigma_*$ the LR fixed point (blue lines) appears and the value of the coupling in that point is shown. It is possible to see that the $\bar{J}_{\sigma,*}$ grows very fast when we approach $\sigma = d/2$ (which is 1 in this case since we are plotting 2 dimensional results). This coupling is actually diverging at $\sigma = 1$ since at that point the LR fixed point merges with the Gaussian LR fixed point, which can be suitably described only in LR-dimensions, since it has no SR term in its propagator. This has been verified for different values of $\sigma > \sigma_*$, at different (also non-integer) dimensions and for various $O(N)$ models. It is also possible to show that the truncation of the potentials despite changing the value of any quantity at the fixed point does not modify the qualitative behavior of the system nor the existence of the threshold σ_*.

In Fig. 4.5 we show the critical exponents of both SR and LR fixed points obtained from RG equations (4.18). The SR fixed point has just one repulsive direction for $\sigma > \sigma_*$ (the standard Wilson–Fisher one) and the LR fixed point does not exist at all. At $\sigma = \sigma_*$ the smallest attractive eigenvalue hits zero and the LR fixed point emerges from the SR fixed point. For $\sigma < \sigma_*$, the SR fixed points has two repulsive directions while the LR one has just one repulsive direction. Finally at $\sigma = \frac{d}{2}$ the LR fixed point becomes Gaussian and for all $\sigma < \frac{d}{2}$ the behavior is mean field.

From the analysis of Fig. 4.5 one clearly understands that the LR fixed point is attractive along the direction which connects it to the SR (Wilson–Fisher) fixed point, thus for $\sigma < \sigma_*$ the SR fixed point becomes repulsive in the $\bar{J}_{\sigma,k}$ direction and the LR fixed point controls the critical properties of the system. In the $\sigma \to \sigma_*$ limit the LR fixed point moves towards the SR one and finally merges with it at $\sigma = \sigma_*$. This structure for the phase diagram implies that the anomalous dimension is given (as show in the left inset of Fig. 4.5) by the LR value $\eta_2 = 2 - \sigma$ for $\sigma < 2 - \eta_{SR}$ and by the SR value $\eta_2 = \eta_{SR}$ for $\sigma > 2 - \eta_{SR}$, thus confirming Sak's scenario. It is important to stress that we are not imposing this picture by hand as one does by considering only the p^σ in the propagator. It is also important to underline that the threshold $\sigma_* = 2 - \eta_{SR}$ is also generated dynamically, with the SR anomalous dimension appearing in it being the one pertinent to the approximation level considered. Retaining other terms in the expansion of the effective potential would not modify the qualitative picture described above, but will change the numerical values reported.

In the right inset of Fig. 4.5 we also show the difference between the value of ν computed by using ansatz (4.9) and the one obtained by using the effective dimension (4.7): this result confirms that the effective dimension relation is not exact and it gives the error done by using it, even though the error is found to be rather small and actually less than 1% also close to σ_*.

4.1.4 LR–Dimensions

Here for the sake of completeness we also report the results obtained using LR dimensionless variables. In this case we renormalize the field using the wave function Z_σ and we define the SR coupling $\bar{J}_2 = \bar{Z}_2/Z_\sigma$

$$\partial_t Z_\sigma = 0\,, \tag{4.19a}$$

$$\partial_t \bar{J}_2 = (2-\sigma)\bar{J}_2 - \frac{\bar{\rho}_0 \bar{U}_k''(\bar{\rho}_0)^2(\sigma + 2\bar{J}_2)^2}{(1+\bar{J}_2)^2(1+\bar{J}_2+2\kappa_k \bar{U}_k''(\bar{\rho}_0))^2}\,, \tag{4.19b}$$

$$\begin{aligned}\partial_t U_k(\rho) = &-d\bar{U}_k(\bar{\rho}) + (d-\sigma)\bar{\rho}\,\bar{U}_k'(\bar{\rho}) + \\ &\frac{\bar{J}_2 - \frac{(2-\sigma)\bar{J}_2 + \partial_t \bar{J}_2}{d+2} + \frac{\sigma}{2}}{1+\bar{J}_2+\bar{U}_k'(\bar{\rho}) + 2\bar{\rho}\,\bar{U}_k''(\bar{\rho})} \\ &+ (N-1)\frac{\bar{J}_2 - \frac{(2-\sigma)\bar{J}_2 + \partial_t \bar{J}_2}{d+2} + \frac{\sigma}{2}}{1+\bar{J}_2+\bar{U}_k'(\bar{\rho})}\,.\end{aligned} \tag{4.19c}$$

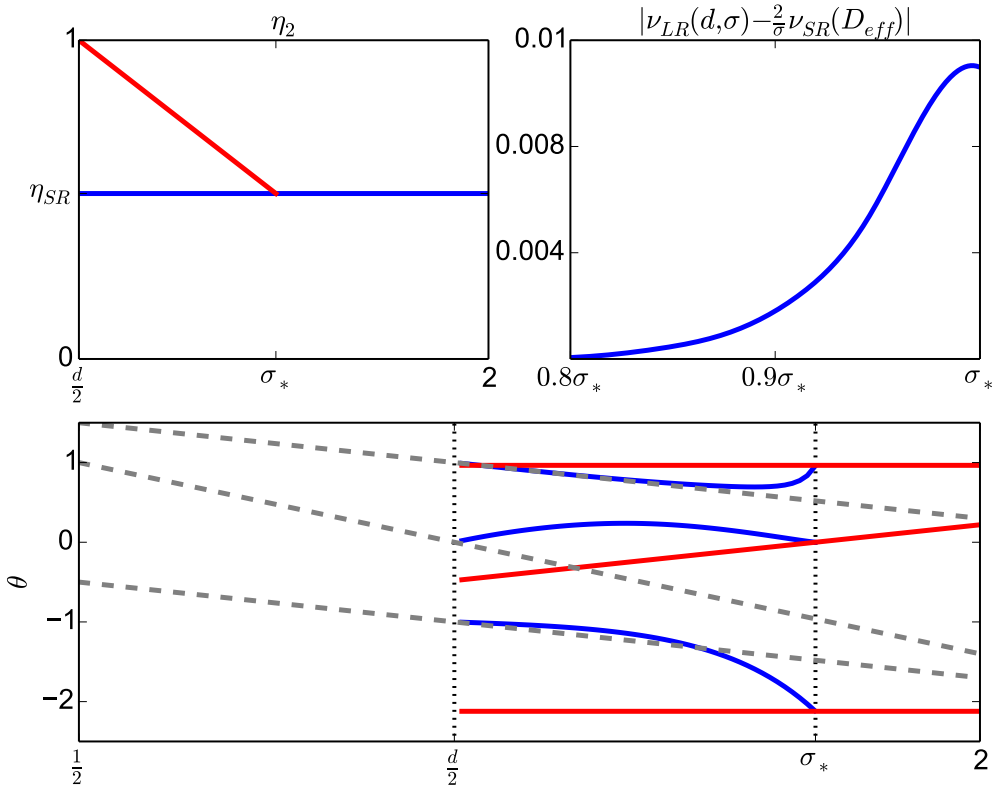

Fig. 4.5 The main figure shows the eigenvalues θ of the RG stability matrix in $d = 2$ and $N = 1$ as a function of σ for the SR (red lines) and LR (blue lines) fixed points. For $\sigma > \sigma_*$ only the SR solution exists and two of the three exponents are independent of σ, the third exponent describes the flow in the direction of the $\bar{J}_\sigma$ coupling and it is positive, showing that the SR fixed point is attractive in this direction. For $\sigma < \sigma_*$ the situation changes and the SR fixed point has two repulsive directions (two negative exponents), while a new LR fixed point emerges. This LR fixed point is repulsive in one single direction and has non-trivial σ-dependent exponents (blue lines). Finally for $\sigma < d/2$ the SR and LR interacting fixed points disappear, leaving only a LR Gaussian fixed point solution, whose exponents can be obtained using mean field approximation on the original LR Ising model (gray dashed lines). In the left panel we show the anomalous dimension vs σ. In the right panel we show the difference between the ν exponent found using ansatz (4.9) and the same exponent calculated using the effective dimension relation (4.50).

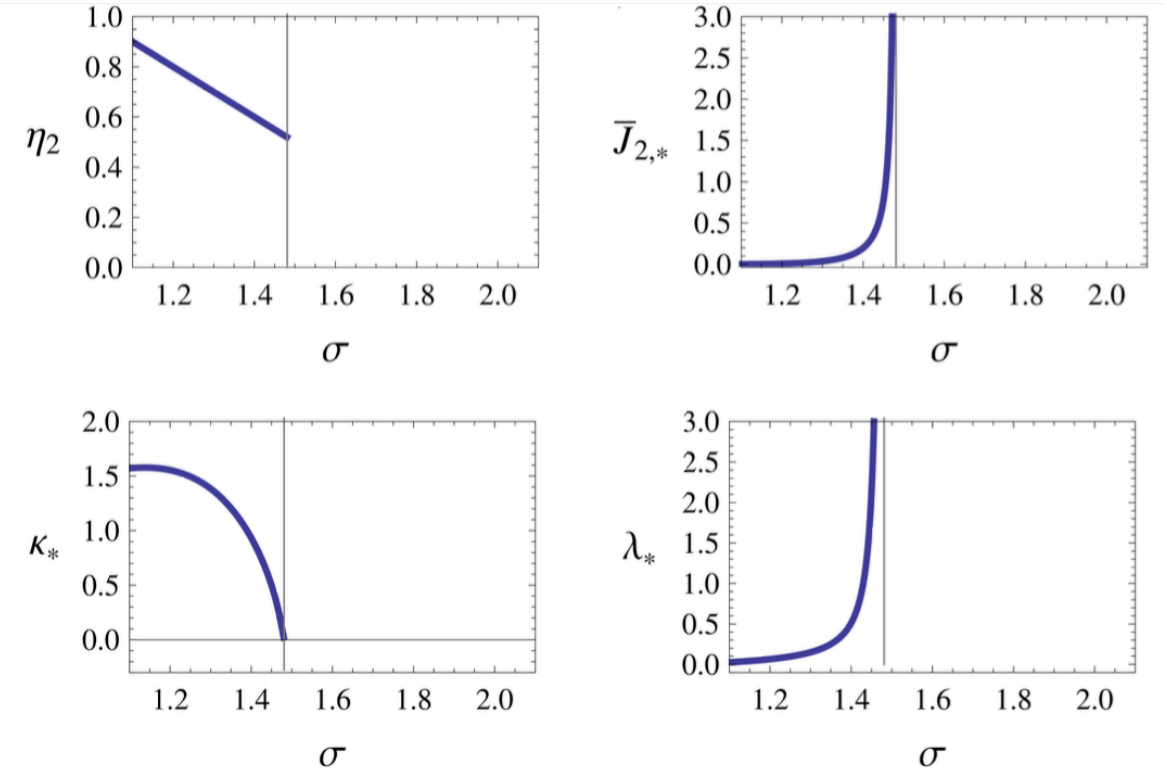

Fig. 4.6 Anomalous dimension η_2 and fixed point values $\bar{J}_{\sigma,*}, \kappa_*, \lambda_*$ in the truncation (4.9) with LR–dimensions for the Ising model in $d = 2$. With this dimensional choice we are able to describe only the $\sigma < \sigma_*$ region, since in the other region the coupling $\bar{J}_{2,k}$ is divergent, as can be understood from the $\bar{J}_{2,k}$ plot. Also in this case, the anomalous dimension as a function of σ is LR ($\eta_2 = 2 - \sigma$) for $\sigma < \sigma_*$.

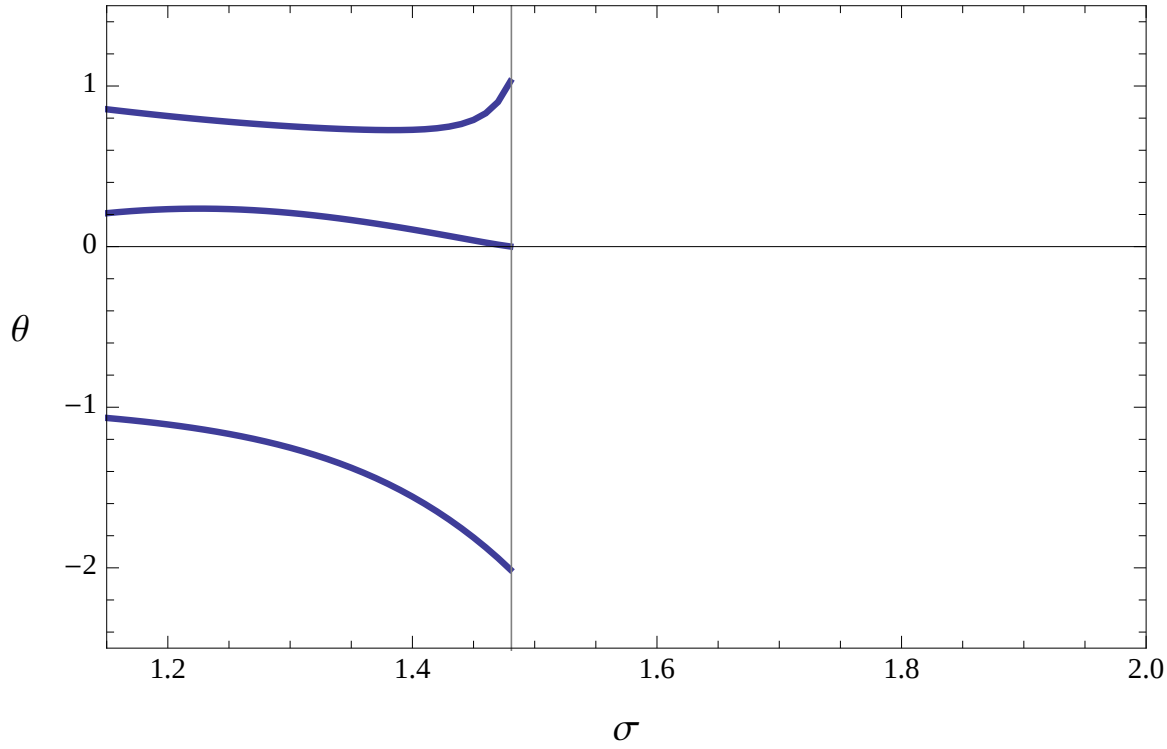

Fig. 4.7 Eigenvalues (θ) of the RG stability matrix as a function of σ for the LR (blue lines) fixed points in the case of LR-dimensions for the Ising model in $d = 2$. In this case we are not able to describe only the LR fixed point present when $\sigma < \sigma_*$ and,since RG eigenvalues are universal quantities, they agree with SR-dimensions ones.

These equations in the $\bar{J}_2 \to 0$ limit reproduce the results obtained for the previous approximations. Thus this approximation reproduces, as expected, all the previous results in the range $\sigma < \sigma_*$, but also gives information on their validity. Comparing latter equation with (4.16c) we see that they are equal up to a term of order $\bar{J}_2$. In fact if we use LR-dimensions we find coherently that $\bar{J}_2^* \neq 0$ is very small for all $\sigma < \sigma_*$ but in the region $\sigma \simeq \sigma_*$, when as we expected the effective dimension relations are spoiled (this is shown in Fig.4.6).

We can then repeat the previous analysis. We have in this case one, very important, difference: we are renormalizing the field with the Z_σ wave function. This is consistent in the range $\sigma < \sigma_*$ where LR interactions are irrelevant, while in the case of a dominant p^2 interaction ($\sigma > \sigma_*$) we expect the Z_2 wave function to be diverging. Such divergence is not absorbed in the field as an anomalous dimension and cannot be balanced by Z_σ which we know to be constant at this approximation level. Thus this divergence will still be present in our flow and this choice for the dimensionless coupling is not suited in the case $\sigma > \sigma_*$ (Fig. 4.6).

We then investigate the case $\sigma < \sigma_*$ where our variable are well defined. As usual we refer to the very simple truncation shown in equation (4.17) and we use the renormalization time $t = \log(k/k_0)$. The flow equations are:

$$\partial_t \bar{J}_2 = (2-\sigma)\bar{J}_2 + \frac{\kappa_k \lambda_k^2 (\sigma + 2\bar{J}_2)^2}{(1+\bar{J}_2)^2(1+\bar{J}_2+2\kappa_k\lambda_k)^2}\,, \tag{4.20a}$$

$$\begin{aligned}\partial_t \kappa_k = & -(d-\sigma)\kappa_k + 3\frac{\bar{J}_2 - \frac{(2-\sigma)\bar{J}_2 + \partial_t \bar{J}_2}{d+2} + \frac{\sigma}{2}}{(1+\bar{J}_2+2\kappa_k\lambda_k)^2} \\ & + (N-1)\frac{\bar{J}_2 - \frac{(2-\sigma)\bar{J}_2 + \partial_t \bar{J}_2}{d+2} + \frac{\sigma}{2}}{(1+\bar{J}_2)^2}\,,\end{aligned} \tag{4.20b}$$

$$\begin{aligned}\partial_t \lambda_k = & (d-2\sigma)\lambda_k + 18\lambda_k \frac{\bar{J}_2 - \frac{(2-\sigma)\bar{J}_2 + \partial_t \bar{J}_2}{d+2} + \frac{\sigma}{2}}{(1+\bar{J}_2+2\kappa_k\lambda_k)^3} \\ & + 2\lambda_k(N-1)\frac{\bar{J}_2 - \frac{(2-\sigma)\bar{J}_2 + \partial_t \bar{J}_2}{d+2} + \frac{\sigma}{2}}{(1+\bar{J}_2)^3}\,.\end{aligned} \tag{4.20c}$$

The fixed points solutions of the couplings are reported in Fig. 4.6, where we see that only the LR fixed points solution are present and then only the region $\sigma < \sigma_*$ is investigated. In fact, as well as previous couplings showed a diverging $\bar{J}_{\sigma,*}$ for $\sigma \to 1$, these couplings show a divergence in the limit $\sigma \to \sigma_*$ where the LR term in the propagator is vanishing. However the results for the critical exponents, in the region where both the couplings sets are defined, are in perfect agreement between themselves, as it should be and as it is shown in Fig.4.7. Then using these RG equations we are able to describe in detail the structure of the phase diagram. The anomalous dimension of LR $O(N)$ models is still $\eta_2 = 2-\sigma$, then for $\sigma > \sigma_* = 2 - \eta_{SR}$ the dimensionless coupling $\bar{J}_{\sigma,k}$ is always renormalized to zero, whatever initial conditions we choose and the system behaves as if only SR interactions were present. On the other hand when $\sigma < \sigma_*$ a new interacting LR fixed point branches from the SR one and is characterized by a finite value of $\bar{J}_{\sigma,*}$.

In Fig. 4.7 we show the critical exponents of both SR and LR fixed points obtained from RG equations. The SR fixed point has just one repulsive direction for $\sigma > \sigma_*$ (the standard Wilson–Fisher one) and the LR fixed point does not exist at all. At $\sigma = \sigma_*$ the smallest attractive eigenvalue hits zero and the LR fixed point emerges from the SR fixed point. For $\sigma < \sigma_*$, the SR fixed points has two repulsive directions while the LR one has just one

repulsive direction. Finally at $\sigma = \frac{d}{2}$ the LR fixed point becomes Gaussian and for all $\sigma < \frac{d}{2}$ the behavior is mean field.

From the analysis of Fig. 4.7 one clearly understands that the LR fixed point is attractive along the direction which connects it to the SR (Wilson–Fisher) fixed point, thus for $\sigma < \sigma_*$ the SR fixed point becomes repulsive in the $\bar{J}_{\sigma,k}$ direction and the LR fixed point controls the critical properties of the system. In the $\sigma \to \sigma_*$ limit the LR fixed point moves towards the SR one and finally merges with it at $\sigma = \sigma_*$. This structure for the phase diagram implies that the anomalous dimension is given (as show in the left inset of Fig. 4.7) by the LR value $\eta_2 = 2 - \sigma$ for $\sigma < 2 - \eta_{SR}$ and by the SR value $\eta_2 = \eta_{SR}$ for $\sigma > 2 - \eta_{SR}$, thus confirming Sak's scenario. It is important to stress that we are not imposing this picture by hand as one does by considering only the p^σ in the propagator. It is also important to underline that the threshold $\sigma_* = 2 - \eta_{SR}$ is also generated dynamically, with the SR anomalous dimension appearing in it being the one pertinent to the approximation level considered. Retaining other terms in the expansion of the effective potential would not modify the qualitative picture described above, but will change the numerical values reported.

In the right inset of Fig. 4.7 we also show the difference between the value of ν computed by using ansatz (4.9) and the one obtained by using the effective dimension (4.7): this result confirms that the effective dimension relation is not exact and it gives the error done by using it, even though the error is found to be rather small and actually less than 1% also close to σ_*.

4.2 Spatial anisotropy

Anisotropic interactions are present in a variety of physical systems. They are characterized by the property that the interaction energy V among two constituents of the system located in $\vec{r}_1$ and $\vec{r}_2$ depends on the relative distance $\vec{r}_{12} = \vec{r}_1 - \vec{r}_2$ so that $V(\vec{r}_{12})$ assumes different values (possibly a different functional form) for $\vec{r}_{12}$ in different directions. A typical instance is provided by dipolar interactions [120]. For example, with a fixed direction of the dipoles, say $\hat{z}$, as it happens for ultracold dipolar gases [121], there is repulsion if the two dipoles have $\vec{r}_{12}$ in the $x-y$ plane and attraction if $\vec{r}_{12}$ is parallel to $\hat{z}$, with $V(\vec{r}_{12}) \propto 1 - 3\cos^2\theta$ and θ being the angle between $\vec{r}_{12}$ and $\hat{z}$.

Anisotropy is one of the fundamental features of molecular interactions and it is responsible for phase transitions between tilted hexatic phases in liquid-crystal films [122]. Liquid crystals can be described using low energy theories [123], where the order parameter represents the bond angle between molecules. At particular points of the phase diagram liquid crystals are efficiently described by the so-called Lifshitz point effective action [124, 125].

Another major example of anisotropic systems is provided by layered supercondutors. The layered structure can be described by the Lawrence-Doniach model which has different masses in different directions [126] (typically $m_{\|}$ in the $x-y$ plane and $m_{\perp}$ in the $\hat{z}$ direction). Layered systems can occur naturally or be artificially created. Examples of artificial structures are alternating layers of graphite and alkali metals [127] or samples with layers of different metals [128]. On the other hand naturally occurring layered supercondutors range from compounds of transition-metal dichalcogenides layers intercalated with organic, insulating molecules [129] to cuprates [126]. Vortex dynamics in magnetically coupled layered superconductors were studied [95] by a multi-layer sine-Gordon type model [130]. Layered ultracold superfluids can be induced by using a deep optical lattice in one spatial direction for fermions [131] or bosons [132].

A simple way of studying the effect of layering (and anisotropy in general) is to consider statistical mechanics models with different couplings in different directions. A typical case is provided by the study of the XY model in 3 dimensions with a coupling between nearest neighbours sites i and j equal to $J_{\|}$ if i, j belong to the same $x-y$ plane and to $J_{\perp}$ if i, j belong to nearest neighbour planes in the $\hat{z}$ direction [133]. This model has been studied also in relation with layered superconductors and cuprates [134]. Depending on the value of the ratio $J_{\perp}/J_{\|}$ the behaviour of the system can pass from being $3D$ to effectively $2D$ [133].

The main point of these and similar studies of anisotropic spin systems with SR couplings is that far from the critical point anisotropy induces a series of very interesting effects, but for general reasons at the critical point isotropy is restored and strictly speaking an isotropic critical point is found for any finite value of the $J_{\perp}/J_{\|}$ ratio (different is the case of a finite number of $2D$ systems). This is a consequence of the divergence of the correlation length, so that the system does not see the anisotropy any longer at criticality. As another example, for fermions in the BCS-BEC crossover [135] in presence of layering the anisotropy is strongly depressed at the unitary limit [131] even though there is no phase transition, but the system is scale invariant due to the divergence of the scattering length.

Therefore a general interesting question is to study the conditions under which one can have genuinely anisotropic critical points. A main observation of this section is that, in presence of anisotropic LR interactions, the interplay between the divergence of the correlations and the LR nature of the couplings may induce such anisotropic critical behaviour.

The interest in the statistical physics of systems with LR interactions is in general motivated by a large number of possible applications, ranging from plasma physics to astrophysics and cosmology [100, 101]. The shape of LR interactions is typically considered as decaying as a power law of the distance $r^{-d-\sigma}$, where r is the distance between two elementary components of the system, d is the dimensionality and σ is a real parameter

determining the range of the interactions. Simple considerations show that for $\sigma < 0$ the mean-field interaction energy diverges and the system is ill defined. It is still possible to study this case using the so-called Kac rescaling [136], leading to many interesting results such as ensembles inequivalence and inhomogeneous ground-states [100, 137].

For $\sigma > 0$ the thermodynamics is well defined and spin systems may present in general a phase transition at a certain critical temperature T_c. In the isotropic case, as a function of the parameter σ, three regions are found [103]. For $\sigma \leq \frac{d}{2}$ the universal behavior is the one obtained at mean-field level, for σ larger than a critical value σ^* the system behaves as a SR one at criticality and for $d/2 < \sigma < \sigma^*$ the system has peculiar non mean-field critical exponents. The precise determination of σ^* has been the subject of perduring interest [80, 116]. Moreover, recent results on conformal invariance in LR systems are also available [138]. The theoretical interest for these systems is also supported by the recent exciting progress in the experimental realization of quantum systems with tunable LR interactions [139–144].

The goal of present section is to introduce and study anisotropic spin models with LR interactions having different decay exponents in different directions: σ_1 in d_1 dimensions and σ_2 in the remaining $d_2 \equiv d - d_1$ ones. The SR limit is provided by such decay exponents going to infinite. Clearly, when both σ_1 and σ_2 go to infinity the isotropic SR limit is retrieved, while when only one of the two – say σ_2 – is diverging the model is SR in the corresponding d_2 directions. It is expected that when one of the two exponents, σ_1 or σ_2, is larger than some threshold value, say σ_1^* or σ_2^*, the corresponding directions behave as if SR interactions only were present at criticality.

Apart from the already mentioned interest in investigating anisotropic fixed points, three other motivations underly our work. From one side we think it is interesting to study a problem in which rotational invariance is broken at criticality due to the division of the system in two subspaces, which is somehow the simplest global form in which such rotational invariance can be broken. From the other side in a natural way quantum systems with LR couplings are an example of the systems under study: indeed, if one considers a quantum model in D dimensions with LR interactions or couplings, then at criticality one can map it on a classical system in dimension $d > D$, with the interactions along the $d - d_1$ remaining directions being of SR type [145]. This is of course the generalization of what happens for SR quantum systems: as an example in which the mapping can be worked out explicitly [7, 146] we mention the mapping of the SR Ising chain in a transverse field on the classical SR Ising model, with the second dimension corresponding to the imaginary time. Therefore generically a D-dimensional quantum spin system with LR interactions can be seen as an example of an anisotropic classical system where the interaction is LR in D dimensions

and SR in the remaining ones. A similar situation would occur for LR quantum systems in the models in which two extra-time dimensions are added and the time can be regarded as a complex variable [147]. Finally, experiments of quantum systems with tunable LR interactions provide an experimental counterpart to implement and test the results we present in the following.

To study anisotropic LR spin systems we introduce a model, whose low energy behavior is well described by an anisotropic Lifshitz point effective action with non analytic momentum terms in the propagator. At variance with the usual Lifshitz point case in our system a standard second order phase transition is found, and there is no additional external field to tune in order to reach criticality.

Using functional renormalization group (RG) methods we study in the following the critical behavior of anisotropic LR spin systems determining the independent critical exponents and depicting the phase diagram in the parameter space of σ_1 and σ_2, mostly focusing on the case $\sigma_1, \sigma_2 \leq 2$.

4.2.1 The model

The model we consider is a lattice spin system in dimension d, with an arbitrary number of spin components N. The spins are classical but comments on quantum spin systems with LR interactions will be also presented.

The interactions among the spins is LR with different exponents depending on the spatial directions. The system is divided into two subspaces of dimension d_1 and d_2 with $d_1 + d_2 = d$. In the first subspace the interaction between the spins decays with the distance as a power law with exponent $d_1 + \sigma_1$, while in the other subspace it decays with exponent $d_2 + \sigma_2$.

This formally amounts to write the position of a spin, $\vec{r} = (r_1, \cdots, r_d)$, as $\vec{r} \equiv \vec{r}_\parallel + \vec{r}_\perp$ with $\vec{r}_\parallel = (r_1, \cdots, r_{d_1}, 0, \cdots, 0)$ and $\vec{r}_\perp = (0, \cdots, 0, r_{d_1+1}, \cdots, r_d)$. The i-th spin is located in $\vec{r}_i = (r_{1,i}, \cdots, r_{d,i})$, so that $\vec{r}_{\parallel,i} = (r_{1,i}, \cdots, r_{d_1,i}, 0, \cdots, 0)$ and $\vec{r}_{\perp,i} = (0, \cdots, 0, r_{d_1+1,i}, \cdots, r_{d,i})$ with $d = d_1 + d_2$.

Given the two spins in $\vec{r}_i$ and $\vec{r}_j$ we define $\vec{r}_{ij}$ as $\vec{r}_{ij} = \vec{r}_i - \vec{r}_j$ and similarly we put $\vec{r}_{\parallel,ij} = \vec{r}_{\parallel,i} - \vec{r}_{\parallel,j}$ and $\vec{r}_{\perp,ij} = \vec{r}_{\perp,i} - \vec{r}_{\perp,j}$. The couplings between two spins in $\vec{r}_i$ and $\vec{r}_j$ decay with power law exponent $d_1 + \sigma_1$ if $\vec{r}_{ij}$ is parallel to $\vec{r}_{\parallel,ij}$ and with power law exponent $d_2 + \sigma_2$ if $\vec{r}_{ij}$ is parallel to the $\vec{r}_{\perp,ij}$ direction.

The model we consider then reads

$$H = -\sum_{i \neq j} \frac{J_\parallel}{2} \frac{\vec{S}_i \cdot \vec{S}_j}{r_{\parallel,ij}^{d_1+\sigma_1}} \delta(\vec{r}_{\perp,ij}) - \sum_{i \neq j} \frac{J_\perp}{2} \frac{\vec{S}_i \cdot \vec{S}_j}{r_{\perp,ij}^{d_2+\sigma_2}} \delta(\vec{r}_{\parallel,ij}), \tag{4.21}$$

where the $\vec{S}_i$ are classical N component vectors (normalized to 1). The distance $r_{\parallel,ij}$ is calculated on a d_1–dimensional volume, to which both spins $\vec{S}_i$ and $\vec{S}_j$ belong, as ensured by the presence of the $\delta(\vec{r}_{\perp,ij})$. On the same ground $r_{\perp,ij}$ measures the distance between two spins i, j belonging to the same d_2–dimensional volume. Thus any spin of the model belongs to two different subspaces, one of dimension d_1 and the other of dimension d_2, and interacts only with the spins sitting on the same subspace. For example, given an Ising model in two dimensions for variables $S_i = \pm 1$, setting $i \equiv (i_1, i_2)$ we are considering couplings nonvanishing only if $i_1 = j_1$ (and interactions decaying as $|i_2 - j_2|^{-d_2-\sigma_2}$, with $d_2 = 1$, in the same column) and if $i_2 = j_2$ (and interactions decaying as $|i_1 - j_1|^{-d_1-\sigma_1}$, with $d_1 = 1$, in the same row).

When one of the two exponent goes is infinite the interaction becomes SR in the correspondent subspace. However, in analogy with the isotropic LR case, two threshold values σ_1^* and σ_2^* exist such that for $\sigma_1 > \sigma_1^*$ or $\sigma_2 > \sigma_2^*$ the systems behaves as if only SR interactions were present in respectively the d_1 or d_2 dimensional subspace.

In (4.21) we disregard for simplicity interactions between spins if their relative distance $\vec{r}_{ij}$ is not perpendicular or parallel to $\vec{r}_{\perp,ij}$ (or $\vec{r}_{\parallel,ij}$). Notice that, although it is chosen as a simplifying assumption, this is the case for a d_1 dimensional quantum spin system with LR interactions, e.g. of transverse Ising type, when mapped to a classical system (couplings along the imaginary time are among same column discretized points). Additional finite-range interactions for spins of different columns or rows does not qualitatively affect our results.

To discuss a specific example, we consider the ferromagnetic quantum Ising model in dimension D in presence of LR interactions

$$H = -\frac{J}{2}\sum_{i\neq j}\frac{\sigma_i^{(z)}\sigma_j^{(z)}}{|i-j|^{d_1+\sigma_1}} - h\sum_i \sigma_i^{(x)}\,, \tag{4.22}$$

where $\sigma^{(z),(x)}$ are the z,x component of the quantum spin $\vec{\sigma}$ and J is the positive magnetic coupling. In the thermodynamic limit a quantum spin system can be mapped onto a classical analogue [145, 148, 149]. Thus the quantum phase transition at zero temperature of a quantum spin system in dimension D lies in the same universality class of a classical system in dimension $d > D$. Then we can map a quantum Ising model on a classical analogue in $d = D+1$. A similar result is generally also valid with LR interactions and the mapping is between the quantum Ising model described in (4.22) and the anisotropic classical model (4.21) with $d_1 = D$, $d_2 = 1$ and $\sigma_2 > \sigma_2^*$. For larger N we expect in general that a quantum spin system in a dimension D with LR interactions decaying with exponent σ_1 has a phase transition which lies in the same universality class of the one found in the classical system

(4.21) with $d_1 + d_2 > D$ and $\sigma_2 > 2$. To this respect we point out that in our treatment d_1 and d_2 may be considered continuous variables.

4.2.2 Effective field theory

In order to study the critical behavior of anisotropic LR $O(N)$ models, we introduce the following low energy effective field theory:

$$S[\phi] = -\int d^d x \Big(Z_{\sigma_1} \phi_i(x) \Delta_{\|}^{\frac{\sigma_1}{2}} \phi_i(x) + Z_{\sigma_2} \phi_i(x) \Delta_{\perp}^{\frac{\sigma_2}{2}} \phi_i(x) - U(\rho) \Big), \tag{4.23}$$

where $\rho = \phi_i \phi_i / 2$ and the summation over the index $i \in [1, 2, \cdots, N]$ is implicit. The effective field theory in equation (4.40) is obtained by the low momentum expansion of the bare propagator of Hamiltonian (4.21). The higher order analytic terms $\Delta_{\|}$ and $\Delta_{\perp}$ were neglected and this expansion is valid only as long as $\sigma_1 \leq 2$ and $\sigma_2 \leq 2$.

In the following we choose the convention that $\sigma_1 < \sigma_2$. To make the presentation of the results more compact we will also adopt the symbol $\vee$ standing for "or" or, according to the context, "or respectively" .

It is worth noting that along different spatial directions physical properties essentially differ and this difference cannot be removed by a simple rescaling of the theory. Accordingly, the d-dimensional coordinate space is split into two subspaces $\mathbb{R}^{d_1}$ and $\mathbb{R}^{d_2}$. Each position vector $x \equiv (x_1, x_2) \in \mathbb{R}^{d_1} \times \mathbb{R}^{d_2}$ has a d_1-dimensional "parallel" component x_1 and a d_2-dimensional "perpendicular" one, x_2.

The laplacian operators $\Delta_{\|}$ and $\Delta_{\perp}$ act respectively in $\mathbb{R}^{d_1}$ and $\mathbb{R}^{d_2}$. When the dimension of one of the subspaces, say $d_1 \vee d_2$ [i.e., d_1 or respectively d_2] shrinks to zero we retrieve an isotropic LR $O(N)$ model in dimension $d_2 \vee d_1$ [i.e., d_2 or respectively d_1] with the upper critical dimension $d^*_{2,1} = 2\sigma_{2,1}$ [i.e., $d^*_2 = 2\sigma_2$ or respectively $d^*_1 = 2\sigma_1$] and the critical behavior described in [80, 116].

In the following we derive general results which are valid for every value of d_1, d_2, σ_1 and σ_2, but more attention will be paid on the special cases $d_2 = 1$ and $\sigma_2 > \sigma^*_2$ which is the interesting case for quantum spin chains with LR interactions.

Using the notation $\vee$, in the special case $\sigma_1 \vee \sigma_2 = 2$ and $\sigma_2 \vee \sigma_1 = 4$, expression (4.23) reduces to the fixed point effective action of a $d_1 \vee d_2$ axial anisotropic Lifshitz point. However, in the standard Lifshitz point case, the SR analytic terms cannot be neglected, outside the fixed point, as in effective action (4.23) since they are relevant with respect to the $\sigma_2 \vee \sigma_1 = 4$ kinetic term. Thus the usual Lifshitz point behavior is only found in multi-critical

universality classes, where diverse fields are at their critical value. On the other hand the critical behavior described by the low energy action (4.23) is a standard second order one and it is found in anisotropic LR systems for some critical value of the temperature.

4.2.3 Dimensional analysis

The scaling hypothesis for the Green function in the asymptotic long wavelength limit are

$$G(q_1,q_1) = q_1^{-\sigma_1+\eta_{\sigma_1}} G(1, q_2 q_1^{-\theta}) = q_2^{-\sigma_2+\eta_{\sigma_2}} G(q_1 q_2^{-\frac{1}{\theta}}, 1) \tag{4.24}$$

where η_{σ_1} and η_{σ_2} are the two anomalous dimensions and the anisotropy index

$$\theta = \frac{\sigma_1 - \eta_{\sigma_1}}{\sigma_2 - \eta_{\sigma_2}}$$

has been defined. The system possesses two different correlation lengths ξ_1 and ξ_2, both diverging at the same critical temperature T_c, but following two different scaling laws:

$$\xi_1 \propto (T - T_c)^{-\nu_1}, \tag{4.25}$$

$$\xi_2 \propto (T - T_c)^{-\nu_2}. \tag{4.26}$$

The latter equations also define the correlation length exponents ν_1 and ν_2.

One could expect to have four independent critical exponents $(\eta_{\sigma_1}, \eta_{\sigma_2}, \nu_1, \nu_2)$. However in analogy with the standard anisotropic Lifshitz point treatment [150], we can derive the following scaling relation

$$\frac{\sigma_1 - \eta_{\sigma_1}}{\sigma_2 - \eta_{\sigma_2}} = \frac{\nu_2}{\nu_1} = \theta \tag{4.27}$$

which leaves us with only three independent exponents. Relation (4.27) was obtained by generalizing the usual scaling relation for the susceptibility exponent γ. Due to spatial anisotropy, we define two momentum scales in our renormalization procedure [151, 152]

$$[x_1] = k_1^{-1} \tag{4.28}$$

$$[x_2] = k_2^{-1}, \tag{4.29}$$

and both these scales must vanish in order to reach the thermodynamic limit.

As it will become clear in the following in order to enforce scale invariance at the critical point we must require both kinetic terms in effective action (4.40) to have the same scaling

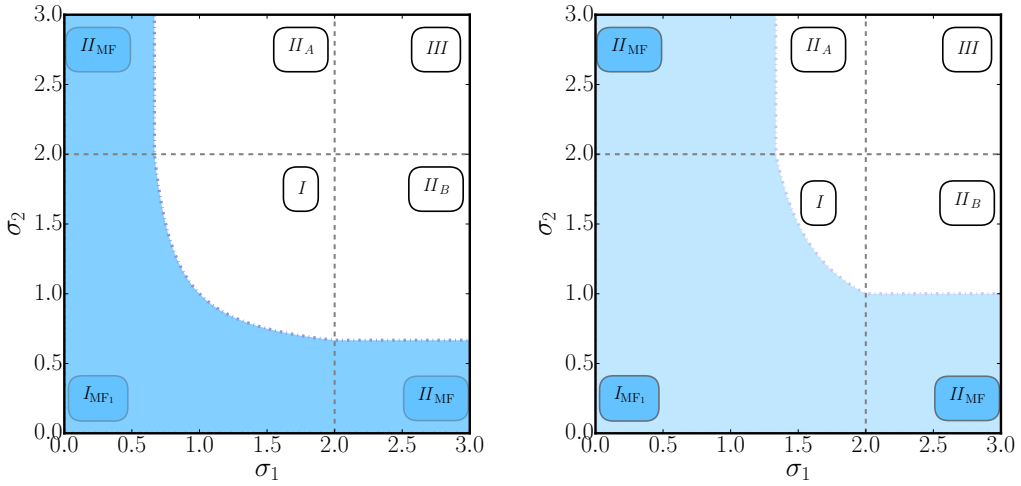

(a) N=1 (b) N=2

Fig. 4.8 The parameter space of a LR anisotropic spin system with dimensions $d_1 = d_2 = 1$, panel (a), and $d_1 = 2$ and $d_2 = 1$, panel (b).

dimension. Consequently the following relation between the two momentum scales emerges

$$k_2 = k_1^{\theta} = k^{\theta}, \tag{4.30}$$

where $k \equiv k_1$. The choice $k \equiv k_1$ is arbitrary but consistent with the former choice of θ. All the physical results in this model are evidently invariant under the simultaneous exchange of dimensions and exponents $d_1 \to d_2$ and $\sigma_1 \to \sigma_2$. The last operation is equivalent to exchanging the definitions of θ and k ($k = k_2$ and $\theta \to \theta^{-1}$).

It is possible to develop the local potential as

$$U(\rho) = \sum_i \lambda_i \rho^i. \tag{4.31}$$

where latter equations defines the couplings λ_i. The scaling dimensions of the field and the couplings are expressed in terms of the general scale k,

$$\phi = k^{D_\phi} \tilde{\phi} \tag{4.32}$$

$$\lambda_i = k^{D_{\lambda_i}} \tilde{\lambda}_i, \tag{4.33}$$

with the scaling dimensions

$$D_\phi = \frac{d_1 + \theta d_2 - \sigma_1 + \eta_{\sigma_1}}{2}, \tag{4.34}$$

$$D_{\lambda_i} = d_1 + \theta d_2 - i(d_1 + \theta d_2 - \sigma_1), \tag{4.35}$$

In order to draw the phase diagram of the system we can rely on canonical dimension arguments, studying the relevance of the coupling at bare level. This is equivalent to using the Ginzburg criterion to predict the range of validity of the mean-field approximation [153]. We then impose $\eta_{\sigma_1} = \eta_{\sigma_2} = 0$ and the system develops a non trivial ith-order critical point when the coupling λ_i is relevant (i.e. diverges) in the infrared limit ($k \to 0$). From the condition $D_{\lambda_i} < 0$ we obtain

$$\frac{d_1}{\sigma_1} + \frac{d_2}{\sigma_2} < \frac{i}{i-1}. \tag{4.36}$$

When this condition is fulfilled the system presents $i-1$ universality classes, with the ith-order universality class describing an i phases coexistence critical point [22, 25, 61]. Since each new fixed point branches from the Gaussian one, the assumption of vanishing anomalous dimension is consistent and the existence of multi-critical anisotropic LR $O(N)$ universality classes can be extrapolated to be valid in the full theory.

In the following we will focus only on the Wilson-Fisher (WF) universality class which appears in ϕ^4 theories. We then consider the case $i = 2$,

$$\frac{d_1}{\sigma_1} + \frac{d_2}{\sigma_2} < 2, \tag{4.37}$$

which is the condition for having a non mean-field second order phase transition.

When $\sigma_1 = \sigma_2 = 2$ we recover the usual lower critical dimension of the Ising model in dimension d, i.e. 4. While the case $d_2 = 0$ reproduces the result for a d_1 dimensional LR $O(N)$ model, i.e. $d_1 < 2\sigma_1$. It is worth noting that while the numerical results we report in the following are calculated in the specific $i = 2$ case, most of the analytic results are valid even in the general i case.

4.2.4 Mean-field results

At mean-field level we have the following results for the critical exponents of the system

$$\begin{aligned} \eta_{\sigma_1} &= 0, & \eta_{\sigma_2} &= 0, \\ \nu_1 &= \frac{1}{\sigma_1}, & \nu_2 &= \frac{1}{\sigma_2}. \end{aligned} \tag{4.38}$$

We remind that, for any value of $\sigma_1 \vee \sigma_2$ larger than 2, the results are reduced to the case of only SR interactions in the subspace $\mathbb{R}^{d_1} \vee \mathbb{R}^{d_2}$. Thus the (σ_1, σ_2) parameter space can be divided into four areas, as shown in figure 4.8. At the mean-field level one has two thresholds (dashed lines) at $\sigma_1 = 2$ and $\sigma_2 = 2$, dividing the parameter space into four regions. The region I ($\sigma_1 < 2$, $\sigma_2 < 2$) is the pure anisotropic LR region, where the saddle point of effective action (4.23) is valid. In regions $IIa \vee b$ the exponent $\sigma_1 \vee \sigma_2$ is larger than two and the correct effective field theory is given by expression (4.40) with $\sigma_1 = 2 \vee \sigma_2 = 2$. In region III both kinetic terms are irrelevant compared to the SR kinetic terms and the model becomes equivalent to a $d = d_1 + d_2$ dimensional isotropic SR system. The shaded areas correspond to the region where inequality (4.37) is fulfilled only for $i = 1$ and then mean-field is valid. Here the region names the mean field subscript MF. In region $I(\sigma_1, \sigma_2 < 2)$ the system is LR in both subspaces. The cyan shaded area in figure 4.8a is the gaussian region in $d_1 = d_2 = 1$ and light cyan in figure 4.8b is for $d_1 = 1$ and $d_2 = 2$. In region $II_{A \vee B}$ the system is SR in the subspace of dimension $d_1 \vee d_2$ and LR in the other. It should be noted that for the $d_1 = d_2 = 1$ case, shown in figure 4.8a, region $II_{A \vee B}$ are completely equivalent since the system is invariant under the exchange of the two exponents. This is not true in the case $d_1 \neq d_2$, figure 4.8b where $d_1 = 1$ and $d_2 = 2$. Finally in region III $(\sigma_1, \sigma_2 > 2)$ the system is in the same universality class of an isotropic SR system.

The previous analysis is valid at mean-field level, but, when fluctuations are relevant, we shall take into account the competition between analytic and non analytic momentum terms close to the boundaries $\sigma_1 \vee \sigma_2 \approx 2$. Indeed, while non analytic terms do not develop anomalous dimensions, the SR analytic terms normally do and at the renormalized level the boundaries of the non analytic regions σ_1^* and σ_2^* could be different from the canonical dimension result $\sigma_1^* = \sigma_2^* = 2$, as it happens in usual LR systems [80, 103, 116, 154].

Regarding the case of the quantum spin Hamiltonians it is possible to use mean-field arguments to dig out the non trivial phase transition region. Denoting the dimension of the quantum system by D and the exponent of the decay of the coupling by $D + \sigma_1$, we should then substitute $d_1 = D$, and $\sigma_2 = 2$ into relation (4.37) to obtain

$$d_2 < 4 - \frac{2D}{\sigma_1}. \tag{4.39}$$

Then, a quantum spin system in dimension D with dynamic exponent with LR interactions decaying with exponent σ_1 develops a non trivial phase transition when equation (4.39) is satisfied. This region is reported with the WF label in figure 4.9 for the $d_1 = 1$ case.

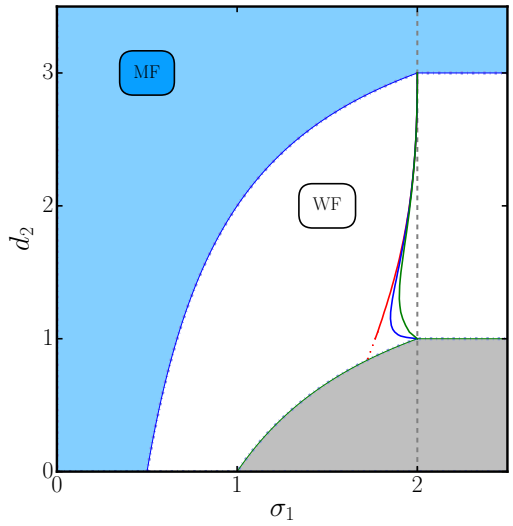

Fig. 4.9 The phase space of a LR anisotropic spin system with dimensions $d_1 = 1$ as a function of d_2 with $\sigma_2 > \sigma_2^*$ for general σ_1. The cyan shaded region represents the mean-field validity region while in the white region WF type universality is found. The gray dashed line is the mean-field threshold above which SR behavior is recovered. The solid colored lines represent the dressed threshold values for the $N = 1,2,3$ cases in red, blue and green respectively. The gray area is the region where we expect the critical behavior to disappear and only a single phase i found.

4.2.5 Effective action and RG approach

To further proceed with the analysis of the critical behavior of LR anisotropic $O(N)$ models we use the functional RG approach [19, 31]. We should choose a reasonable ansatz for our effective action in such a way that we can project the exact Wetterich equation [17, 18]. We then consider the same functional form of action (4.23) including also highest order analytic kinetic terms in order to efficiently describe the boundary regions.

$$\Gamma_k[\phi] = -\int d^d x \Big(Z_{\sigma_1} \phi_i(x) \Delta_{\parallel}^{\frac{\sigma_1}{2}} \phi_i(x) + \phi_i(x) \Delta_{\parallel} \phi_i(x) + Z_{\sigma_2} \phi_i(x) \Delta_{\perp}^{\frac{\sigma_2}{2}} \phi_i(x) + \phi_i(x) \Delta_{\perp} \phi_i(x) - U_k(\rho) \Big), \tag{4.40}$$

where the summation over repeated indices is assumed. The two wave-function renormalization terms Z_{σ_1,σ_2} are running and we are considering anomalous dimension effects for the analytic momentum powers, including them directly into the field scaling dimension, as in [18].

As already discussed in [80], the two wave-function renormalization flows vanish, since the RG evolution of the propagator does not contain any non analytic term

$$k\partial_k Z_{\sigma_1} = 0, \tag{4.41}$$

$$k\partial_k Z_{\sigma_2} = 0, \tag{4.42}$$

where k is the isotropic scale already introduced in equation (4.32).

In order to extract the critical behavior of the system, we study the FRG equations in terms of the scaled variables. We then define the scaled wave-functions $\tilde{Z}_{\sigma_1}$ and $\tilde{Z}_{\sigma_2}$, as it was done for the field and the couplings in equations (4.32) and (4.34).

Transforming equations (4.41) and (4.42) to scaled variables, the flow of the scaled wave-functions is an eigen-direction of the RG evolution

$$k\partial_k \tilde{Z}_{\sigma_1,\sigma_2} = D_{\sigma_1,\sigma_2}\tilde{Z}_{\sigma_1,\sigma_2}. \tag{4.43}$$

In order to explicitly calculate the scaling dimension of the two wave-functions it is necessary to define the dimension of the field. In the case of expression (4.40) we choose the analytic kinetic terms as reference for the field dimension rather than the non analytic terms we considered in the bare action (4.23). The dimension of the field becomes

$$D_\phi = \frac{d_1 + \theta d_2 - 2 + \eta_1}{2} \tag{4.44}$$

where $\theta = \frac{2-\eta_1}{2-\eta_2}$ and η_1, η_2 are respectively the anomalous dimensions of the analytic terms in the $\mathbb{R}^{d_1}$ and $\mathbb{R}^{d_2}$ subspaces. The assumption of two different anomalous dimensions is the obvious consequence of anisotropy.

At the fixed point all the β functions of the scaled couplings vanish. We thus impose

$$D_{\sigma_1} = (2 - \sigma_1 - \eta_1) = 0 \quad or \quad \tilde{Z}_{\sigma_1} = 0, \tag{4.45}$$

$$D_{\sigma_2} = (2 - \sigma_2 - \eta_2) = 0 \quad or \quad \tilde{Z}_{\sigma_2} = 0, \tag{4.46}$$

where one of the conditions (4.45) shall be true to enforce the vanishing of $k\partial_k\tilde{Z}_{\sigma_1}$, while the same shall occur in conditions (4.46) to ensure $k\partial_k\tilde{Z}_{\sigma_2} = 0$.

From the two equations (4.45) and (4.46) we derive the existence of two thresholds values σ_1^* and σ_2^*. For $\sigma_1 < \sigma_1^* \vee \sigma_2 < \sigma_2^*$ we have $\eta_1 = 2 - \sigma_1 \vee \eta_2 = 2 - \sigma_2$ and the left condition in (4.45) $\vee$ (4.46) is fulfilled, conversely for $\sigma_1 > \sigma_1^* \vee \sigma_2 > \sigma_2^*$ we have to impose $\tilde{Z}_{\sigma_1} = 0 \vee \tilde{Z}_{\sigma_2} = 0$. The two conditions are independent, then four regimes exist in the system,

obtained by the four possible combinations of σ_1 smaller or larger than σ_1^* and σ_2 smaller or larger than σ_2^*.

These regions have the same structure, obtained in Section 4.2.3 with naive scaling arguments, see figure 4.8. However when we are focusing on non trivial fixed points the competition between the renormalized couplings of different kinetic terms is ruled by the dressed value of the scaling dimension. It is then necessary to consider renormalized values also for the boundary lines. These lines will not be at $\sigma_1 = \sigma_2 = 2$, as in figure 4.8, but they are now one dimensional curves with non trivial shape $\sigma_1^*(\sigma_2) = 2 - \eta_1(\sigma_2)$ and $\sigma_2^*(\sigma_1) = 2 - \eta_2(\sigma_1)$.

4.2.6 The pure non analytic region

The values of σ_1^* and σ_2^* and their actual location could be different from the mean-field values $\sigma_1^* = \sigma_2^* = 2$, as it happens for isotropic LR systems [103]. For the discussions in this Section the precise values of σ_1^* and σ_2^* are not essential and we defer the study of σ_1^* and σ_2^* to Section 4.2.7. Let us focus on the case $\sigma_1 < \sigma_1^*$ and $\sigma_2 < \sigma_2^*$ where the dominant

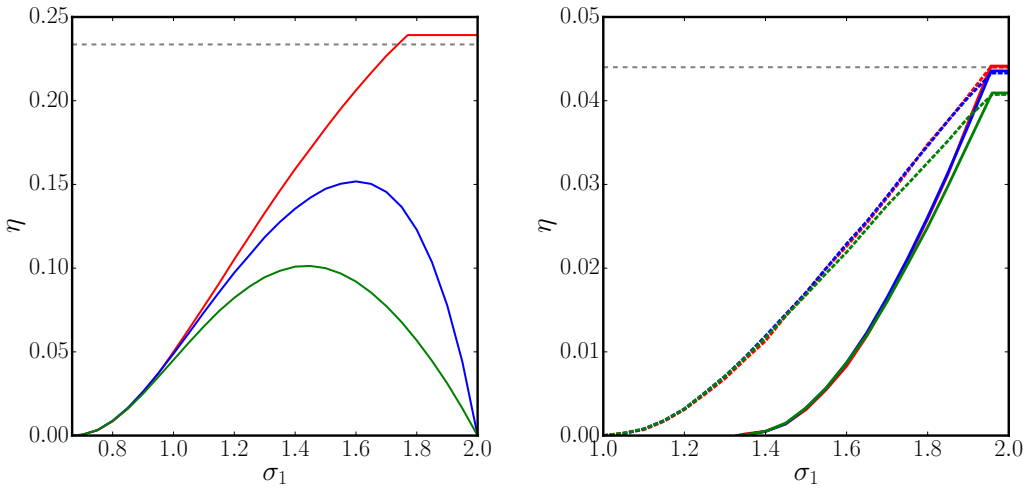

(a) $d_1 = d_2 = 1$ (b) $d_1 = 1 \vee 2$ and $d_2 = 2 \vee 1$

Fig. 4.10 In the left panel we plot the anomalous dimension in $d_1 = d_2 = 1$ for field component numbers $N = 1,2,3$ respectively in red, blue, green from the top. In the right panel the anomalous dimension in $d_1 = 1 \vee 2, d_2 = 2 \vee 1$ in the case $\sigma_2 > \sigma_2^*$ for the field component numbers $N = 1,2,3$ respectively in red, blue, green is shown (the solid $\vee$ dashed lines are for $d_1 = 2 \vee 1$ and $d_2 = 1 \vee 2$). In this case the lack of analytic term in the $\mathbb{R}^{d_1}$ subspace produces two different results for the isotropic limit $\sigma_1 \to \sigma_1^*$ between the two cases $d_2 = 2,1$ solid and dashed lines respectively.

kinetic terms are non analytic. The two conditions (4.45) and (4.46) are both satisfied in their left side. We thus have $\eta_1 = 2-\sigma_1$ and $\eta_2 = 2-\sigma_2$.

At renormalized level the two analytic kinetic terms become equal to the non analytic ones, as it happens in the usual isotropic LR case [80]. Eventually analytic terms give only small contributions to the numerical value of the universal quantities and will be discarded in this Section.

We focus on the pure non analytic effective action:

$$\Gamma_k[\phi] = -\int d^dx \Big(Z_{\sigma_1}\phi_i(x)\Delta_{\parallel}^{\frac{\sigma_1}{2}}\phi_i(x) + \phi_i(x) + Z_{\sigma_2}\phi_i(x)\Delta_{\perp}^{\frac{\sigma_2}{2}}\phi_i(x) - U_k(\rho)\Big). \tag{4.47}$$

To proceed with the functional RG calculation we introduce an infrared cutoff function $R_k(q_1,q_2)$, which plays the role of a momentum dependent mass of the excitations [17, 18]. This artificial mass should be vanishing for excitations with momentum $q_1 \vee q_2 >> k$, while it should prevent the propagation of low momentum $q \vee q_2 << k$ ones. We then introduce the function

$$R_k(q_1,q_2) = \left(Z_{\sigma_1}(k_1^{\sigma_1}-q^{\sigma_1}) + Z_{\sigma_2}(k_1^{\sigma_2}-q^{\sigma_2})\right) \theta\left(Z_{\sigma_1}(k_1^{\sigma_1}-q^{\sigma_1}) + Z_{\sigma_2}(k_1^{\sigma_2}-q^{\sigma_2})\right), \tag{4.48}$$

obtained by generalizing the so-called optimized cutoff [31].

With this explicit choice for the cutoff we can explicitly evaluate the form of the potential flow equation

$$\partial_t \bar{U}_k = (d_1+\theta d_2)\bar{U}_k(\bar{\rho}) - (d_1+\theta d_2-\sigma_1)\bar{\rho}\,\bar{U}_k'(\bar{\rho}) - \frac{\sigma_1}{2}(N-1)\frac{1}{1+\bar{U}_k'(\bar{\rho})} - \frac{\sigma_1}{2}\frac{1}{1+\bar{U}_k'(\bar{\rho})+2\bar{\rho}\,\bar{U}_k''(\bar{\rho})}, \tag{4.49}$$

where $t = -\log(k/k_0)$ is the RG time and k_0 is some ultraviolet scale. For convenience sake we removed a geometric coefficient using scaling invariance of the field [18]. The wave-functions still obey equations (4.41) and (4.42), but, in absence of SR terms, they are dimensionless and therefore they do not have any flow.

Effective dimension

Comparing expression (4.49) with the one reported in [80] we have an equivalence between the ν_1 exponent of this model and the one of an isotropic LR model in dimension

$$d_{\text{eff}} = d_1 + \theta d_2. \tag{4.50}$$

From ν_1 we can calculate ν_2 using scaling relation (4.27), with the anisotropic index which is stuck to its bare value $\theta = \frac{\sigma_1}{\sigma_2}$.

Similar effective dimension results already appeared in different treatments of the isotropic LR O(N) models [41, 80, 116] and can be recovered using standard scaling arguments. Using functional RG approach such effective dimension relations appear naturally without further assumptions, but they are valid only within our approximations [80]. Anyway effective dimension arguments proved able to provide reasonable quantitative agreement with numerical simulations [80, 116]. We can thus rely on them to calculate the correlations length exponents ν_1 and ν_2 as a function of the two parameters σ_1 and σ_2.

Since the wave-function renormalization terms are not running we have $\eta_{\sigma_1} = \eta_{\sigma_2} = 0$ and the momentum dependence of the propagator is the same at the bare and at the renormalized level. This result is evident at this approximation level, but it is conjectured to be valid also in the full theory as it happens for the usual LR case. In the latter case this result was verified at higher approximation levels both in the perturbative and non perturbative RG approaches [102, 111].

We are thus able to derive all the critical exponents in the pure LR region (region I in figure 4.8), but since we do not know exactly the threshold values σ_1^* and σ_2^* we have to extend our analysis to the mixed analytic non analytic kinetic terms ranges (regions $II_{A\vee B}$).

The $N = \infty$ limit

For isotropic interactions the spherical model is obtained in the large components limit $N \to \infty$ of the $O(N)$ spin systems. This model is exactly solvable [41] and in this limit the approximated flow equation (4.49) provides exact universal quantities. The results for the critical exponents are

$$\nu_1 = \frac{\sigma_2}{\sigma_2 d_1 + \sigma_1 d_2 - \sigma_2 \sigma_1}, \tag{4.51}$$

$$\nu_2 = \frac{\sigma_1}{\sigma_2 d_1 + \sigma_1 d_2 - \sigma_2 \sigma_1}. \tag{4.52}$$

In the $d_2 \to 0 \vee d_1 \to 0$ limit the exponent $\nu_1 \vee \nu_2$ is reduced to the one of the spherical LR model in dimension d_1 [41], $\nu_1 = \frac{1}{d_1-\sigma_1} \vee \nu_2 = \frac{1}{d_2-\sigma_2}$, while $\nu_2 = \theta\nu_1 \vee \nu_2 = \frac{\nu_1}{\theta}$ looses any significance. Also in the $\sigma_1 = \sigma_2 = 2$ limit the expressions become equal to the exact SR case.

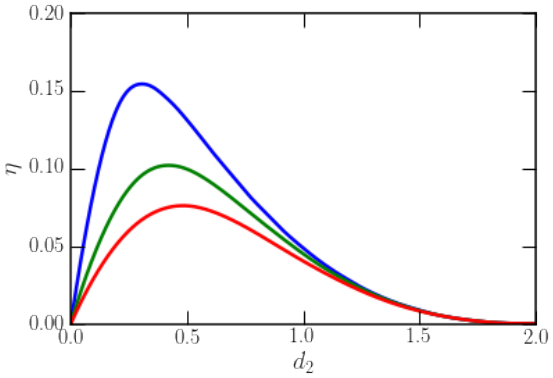

Fig. 4.11 Anomalous dimension for $d_1 = 1$ and $d_2 = z$ when $\sigma_1 = 1$ and $\sigma_2 > \sigma_2^*$ for field component numbers $N = 2,3,4$ respectively in blue, green, red from the top. To apply these results to quantum spin chains one should know the exponent z and obtain the corresponding value of η.

Due to vanishing anomalous dimension in the spherical model limit we can apply the results of this Section even to the case of higher analytic powers in the kinetic term of, say, the $\mathbb{R}^{d_2}$ subspace. This is the case $\sigma_2 = 2L$ with $L \in \mathbb{N}^+$, our results are in general not valid in this case $L \neq 1$, which is the case of the anisotropic next nearest neighbor Ising (ANNNI) model.

In the case of the ANNNI model the fixed point is the usual axial anisotropic Lifshitz point. It is different from the case depicted in this work, since it is a multi-critical fixed point. Indeed next nearest neighbors interaction is sub-leading with respect to the usual SR interaction and needs an additional external field to act on the system to become relevant.

However, we are interested only in the fixed point quantities of the ANNNI model in order to make a consistency check of our $N \to \infty$ results. It is then sufficient to assume to be at the Lifshitz point and make the substitutions $\sigma_1 \to 2$ and $\sigma_2 \to 2L$ ignoring the presence of further more relevant kinetic terms. We then immediately retrieve the ANNNI case [155]:

$$\nu_1 = \frac{L}{(d_1-2)L+d_2}, \tag{4.53}$$

$$\nu_2 = \frac{1}{(d_1-2)L+d_2}. \tag{4.54}$$

The ANNNI model is paradigmatic in the physics of spin systems and it would be interesting to have results also in the $N < \infty$ case. This is however beyond the scope of present analysis, since we would need to explicitly consider SR analytic terms in our ansatz (4.40). This will be the subject of future work.

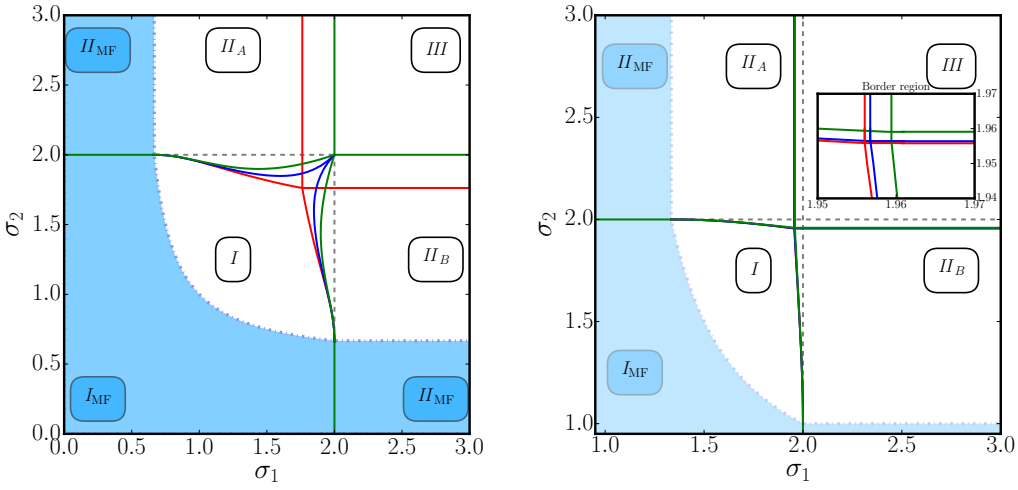

(a) $d_1 = d_2 = 1$ (b) $d_1 = 2$ and $d_2 = 1$

Fig. 4.12 In panel (a) we plot the parameter space of a anisotropic LR spin system for $d_1 = d_2 = 1$. In the cyan shaded area fluctuations are unimportant and the universal quantities are correctly reproduced by the mean-field approximation. The solid curves are the boundary regions σ_1^* and σ_2^* where the non analytic kinetic term becomes irrelevant. We show results for $N = 1, 2, 3$ respectively in red, blue, green. The dashed lines are the mean-field results for the boundary curves. In panel (b) we show the parameter space of the model in $d_1 = 2$ and $d_2 = 1$. In light cyan shaded area fluctuations are unimportant and the universal quantities are correctly reproduced by mean-field approximation. The solid curves are the boundary regions σ_1^* and σ_2^* where the non analytic kinetic term becomes irrelevant. We then show the boundaries in an enlarged scale, inset of panel (b).

4.2.7 The mixed regions

When one of the two exponents overcomes its threshold, say $\sigma_1 > \sigma_1^* \vee \sigma_2 > \sigma_2^*$ the correspondent analytic term in (4.40) becomes relevant and condition (4.45)$\vee$(4.46) shall be satisfied in its right side. We have then $Z_{\sigma_1} = 0 \vee Z_{\sigma_2} = 0$ and the system is purely analytic in one of the two subspaces. In this case it is necessary to use ansatz (4.49) without the non analytic term in the $\mathbb{R}^{d_1} \vee \mathbb{R}^{d_2}$ subspace, since it has become irrelevant with respect to the corresponding analytic term.

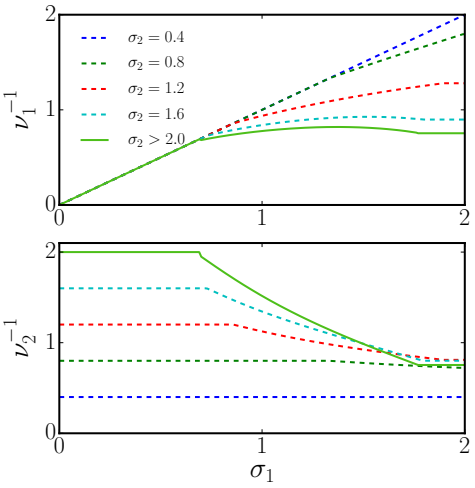

(a) $N = 1, d_1 = d_2 = 1$

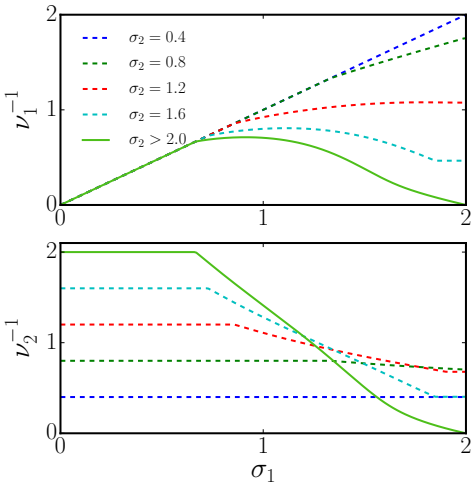

(b) $N = 2, d_1 = d_2 = 1$

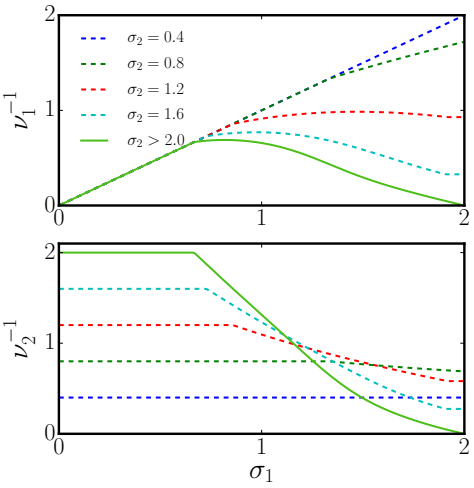

(c) $N = 3, d_1 = d_2 = 1$

Fig. 4.13 In panel (a) the correlation length exponents for the critical point of an anisotropic spin system for dimensions $d_1 = d_2 = 1$ are reported. The two exponents are shown for three values of the number of components $N = 1, 2, 3$ in panels (a), (b) and (c) respectively. For different values of σ_2 we report the behavior of the inverse exponents as a function of σ_1.

Due to the SR dominant term we have now finite anomalous dimension effects. Let us focus on the $\sigma_1 = 2$ case, since the $\sigma_2 = 2$ case can be obtained trivially exchanging the

subspaces dimensions $d_1 \leftrightarrow d_2$. The flow equation for the potential becomes,

$$\begin{aligned}\partial_t \bar{U}_k =&(d_1+\theta d_2)\bar{U}_k(\bar{\rho}) - (d_1+\theta d_2 - 2 + \eta)\bar{\rho}\,\bar{U}_k'(\bar{\rho}) \\ &- (N-1)\frac{1-\frac{\eta}{d_1+2}-\frac{2\eta d_2}{d_1\sigma_2+2(d_2+\sigma_2)}}{1+\bar{U}_k'(\bar{\rho})} \\ &- \frac{1-\frac{\eta}{d_1+2}-\frac{2\eta d_2}{d_1\sigma_2+2(d_2+\sigma_2)}}{1+\bar{U}_k'(\bar{\rho})+2\bar{\rho}\,\bar{U}_k''(\bar{\rho})},\end{aligned} \tag{4.55}$$

where obviously $\eta_1 = \eta$. The anisotropy index is now given by $\theta = \frac{2-\eta}{\sigma_2}$. The anomalous dimension is then given by

$$\eta = \frac{f(\tilde{\rho}_0, \tilde{U}^{(2)}(\tilde{\rho}_0))(\sigma_2 d_1 + 2d_2 + 2\sigma_2)}{2d_2 f(\tilde{\rho}_0, \tilde{U}^{(2)}(\tilde{\rho}_0) + \sigma_2 d_1 + 2d_2 + 2\sigma_2}, \tag{4.56}$$

where the function $f(\tilde{\rho}_0, \tilde{U}^{(2)}(\tilde{\rho}_0))$ is the expression for the anomalous dimension of the correspondent SR range $O(N)$ model

$$f(\tilde{\rho}_0, \tilde{U}^{(2)}(\tilde{\rho}_0)) = \frac{4\tilde{\rho}_0 \tilde{U}^{(2)}(\tilde{\rho}_0)^2}{(1+2\tilde{\rho}_0\tilde{U}^{(2)}(\tilde{\rho}_0))^2} \tag{4.57}$$

as is found in [22] after rescaling an unimportant geometric coefficient. Another possible definition of equation (4.57) is given in [24]. The two definitions are found depending on wether we calculate this quantity respectively from the Goldstone or the Higgs excitation propagator. In the following we always use result (4.57) in the numerical computation of the critical exponents.

One could be tempted to conclude that in region $II_{A\vee B}$ the system is equivalent to a SR system in dimension $d_1 + \theta d_2$ but this is not actually the case, since the value of the anomalous dimension η is different from the one in the isotropic case.

The results for the anomalous dimension in regions $II_{A\vee B}$ as a function of σ_2 for the $d_2 = 1, 2$ cases are reported in figures 4.10a and 4.10b respectively. In $d = 2$ the system is exactly solvable and $\eta = \frac{1}{4}$, however at the lowest order in derivative expansion the isotropic SR Ising approximated result is $\eta \approx 0.2336$, which is shown as a gray dashed line in figures 4.10a and 4.10b. Our approximation level however is not able to recover this result, since we are not including any SR term in the $\mathbb{R}^{d_1}$ subspace. This is not a crucial issue of the method, indeed our result differs from the usual SR result by only 0.0058 which is smaller than the isotropic SR approximation error $|\eta_{LPA} - \eta_{exact}| \simeq 0.0164$. Thus the threshold value $\sigma_2^* = 2 - \eta_{SR}$ does not directly appear in our treatment, since we do not include any SR correction to the non analytic term in the $\mathbb{R}^{d_2}$ subspace. However, for $\sigma_2 > \sigma_2^*$ isotropy is

restored and then the anomalous dimensions in both subspaces should coincide $\eta_1 = \eta_2$. The threshold σ_2^* is readily evaluated as $\sigma_2^* = 2 - \eta(\sigma_2^*)$. Using the latter procedure we do not exactly reproduce the expected boundary value in the mixed regions $\sigma_2^* = 2 - \eta_{SR}$, with η_{SR} the anomalous dimension of the SR isotropic case in $d = d_1 + d_2$ dimensions. However, as explained in the caption of figure 4.10, the difference between the two results is small and the approximation of neglecting the analytic term in the $\mathbb{R}^{d_2}$ subspace appears to be very well justified.

The results depicted in figure 4.10 can be used for a quantum spin system in the $N = 1$ case. In the general case $N \neq 1$ case the mapping with a anisotropic LR model in region II_A in dimension $d_1 \equiv D$ and $d_2 = 1$ can be no longer valid and we have to turn to the general d_2 case (that of course depends on the quantum LR model). We report the result as a function of d_2 in figure 4.9 for a one dimensional chain $d_1 = 1$ with $\sigma_1 = 1$.

The threshold values σ_1^* and σ_2^*

We have now all the information necessary to identify the correct values for the boundaries. Considering the results obtained both in the case of $\sigma_1 < \sigma_1^*$ and $\sigma_1 > \sigma_1^*$ we can deduce the existence of two fixed points in the full theory described by ansatz (4.40). One of these fixed points occurs at $Z_{\sigma_1} \neq 0$, while the other at $Z_{\sigma_1} = 0$. However, this second fixed point is unstable in region I since any infinitesimal perturbation of the Z_{σ_1} value around zero generates a non vanishing flow which increases Z_{σ_1} itself.

Looking at condition (4.45) it is evident that this happens when $\sigma_1 < 2 - \eta_1$. However when $\sigma_1 > 2 - \eta_1$ the non analytic term vanishes and, then, the value of η_1 is actually independent of σ_1. The value of η_1 is thus equal to its value in region II_b i.e. $\eta_1 = \eta$. From previous arguments we also deduce the threshold value $\sigma_1^* = 2 - \eta$.

As shown in equation (4.56) the value of η is actually a function of σ_2 and the boundary between region I and II_A is a curve in the (σ_1, σ_2) parameter space. Applying the same argument to the boundary between region I and II_b we can deduce that $\sigma_2^* = 2 - \eta(\sigma_1)$. The final picture for the phase space of our theory is depicted in figure 4.12. For $d_1 = d_2 = 1$ and $N \geq 2$ the curves all terminate at the point $\sigma_1 = \sigma_2 = 2$, due to the presence of the Mermin-Wagner theorem, which prevents symmetry breaking for SR interactions and which is correctly described by FRG truncations[80], as is shown in figure . For $N = 1$ the system shows discrete symmetry and the anisotropic region terminates at the point $\sigma_2^* = \sigma_1^* = 2 - \eta_{SR}$. In figure 4.12b we show results for $N = 1, 2, 3$ with $d_1 = 2$ and $d_2 = 1$ respectively in red blue and green. In this case the boundaries are different from 2 even at the intersection where the system behaves as an isotropic classical SR system in dimension $d = d_1 + d_2$. The difference between the anomalous dimensions in the cases $N = 1, 2, 3$ is so small that the

different boundaries cannot be distinguished. We are now able compute the correlation length

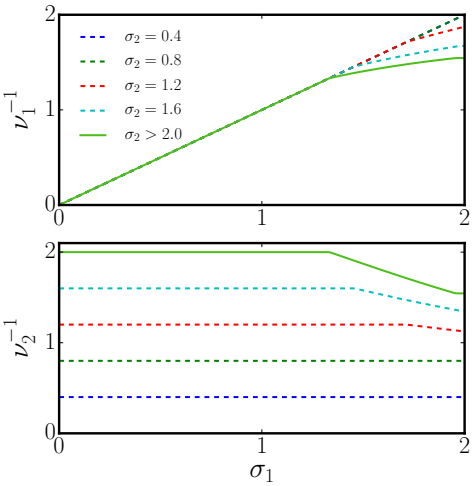

(a) $N = 1$, $d_1 = 2$ and $d_2 = 1$

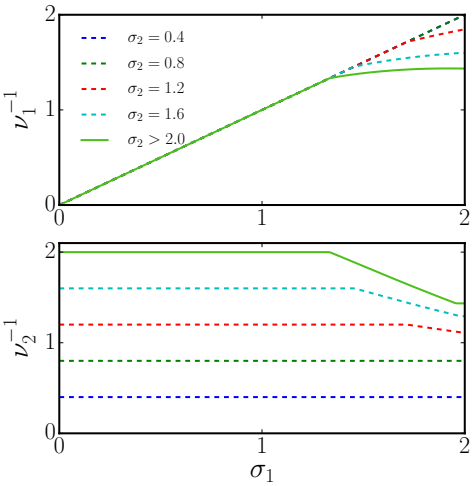

(b) $N = 2$, $d_1 = 2$ and $d_2 = 1$

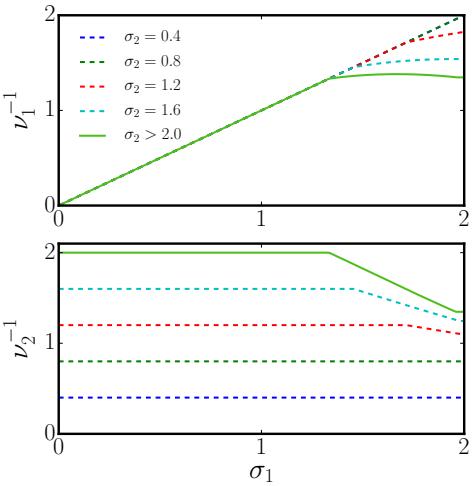

(c) $N = 3$, $d_1 = 2$ and $d_2 = 1$

Fig. 4.14 In figure 4.14a we plot the correlation length exponents for the critical point of an anisotropic spin system with dimensions $d_1 = 1$ and $d_2 = 2$. The two exponents are shown for three values of the components number $N = 1, 2, 3$ in panels (a), (b) and (c) respectively. For different values of σ_2 we report the behavior of the inverse exponents as a function of σ_1.

exponents of the system for different values of σ_1 and σ_2. In region I we can rely on the effective dimension relation (4.50) to compute them. Indeed, the correlation length exponent ν_1 is the same of an isotropic LR system of exponent σ_1 in dimension (4.50). The correlation length exponent ν_2 is determined from ν_1 using the scaling relation (4.27) with $\theta = \frac{\sigma_1}{\sigma_2}$.

In the regions $II_{A\vee B}$ the effective dimension is strictly not valid and one should in principle compute the correlation length exponent ν_1 by studying the stability equation around the fixed points, as described in [25]. It is still possible to reintroduce the effective dimension (4.50) neglecting the anomalous dimension terms in equation (4.49).

The procedure of neglecting the anomalous dimension in the potential flow is commonly employed to solve FRG equations [19]. Indeed the dependence of the potential equation of anomalous dimension is only due to small cutoff dependent coefficients, which have little effect on the universal quantities, at least at this approximation level.

Once these coefficients are neglected, we can impose the fixed point condition $\partial_t \tilde{U}_k = 0$ and divide equation (4.49) by θ obtaining

$$\begin{aligned}&(d_2+\theta' d_1)\bar{U}_k(\bar{\rho}) - (d_2+\theta' d_1-\sigma_2)\bar{\rho}\,\bar{U}_k'(\bar{\rho}) \\ &-(N-1)\frac{\sigma_2}{2+2\bar{U}_k'(\bar{\rho})} - \frac{\sigma_2}{2+2\bar{U}_k'(\bar{\rho})+4\bar{\rho}\,\bar{U}_k''(\bar{\rho})} = 0,\end{aligned} \tag{4.58}$$

where $\theta' = \theta^{-1} = \frac{\sigma_2}{2-\eta}$ in the regions $II_{A\vee B}$.

It is worth noting that for $d_2 = z$ and $\sigma_2 > \sigma_2^*$ the model represents the low energy field theory of a LR quantum spin system in dimension $d_1 = D$. The regions $\mathrm{II}_{A\vee B}$ are then the most interesting regions. In this case the propagator is analytic in the $d_2 = z$ directions (with $z = 1$ for the quantum Ising case), while the other $d_1 = D$ directions are the spatial dimensions of the quantum system.

In figures 4.13 and 4.14 we show the results for the correlation length exponents for various values of σ_1 as a function of the exponent σ_2 in dimensions $d_2 = 1$ (figure 4.13) and $d_2 = 2$ (figure 4.14) with $d_1 = 1$ in both cases in the trivial region, equation (4.37), the relevant exponents in each subspace are independent of the presence of the other subspace and it is $\nu_1 = \sigma_1^{-1}$ and $\nu_2 = \sigma_2^{-1}$. Then in the pure LR region the exponents become non trivial curves as a function of σ_1. For some value of σ_1 we will cross the boundary region $\sigma_1^*(\sigma_2)$ which is a function σ_2. For $\sigma_1 > \sigma_1^*$ the exponents become both constant. When $\sigma_2 > 2$ we are in the region where SR interactions are dominant in the subspace $\mathbb{R}^{d_1}$ (this is the relevant case for the quantum spin Ising system) and the exponents are shown by a solid line. In this case the exponents are non trivial functions of σ_1 for $\sigma_1 < \sigma_1^* = 2 - \eta_{SR}$, where η_{SR} is the anomalous dimension of the isotropic SR system in dimension $d_1 + d_2$, while they become constant for $\sigma_1 > \sigma_1^*$ and both equal to the correlation length exponent of the isotropic SR systems $\nu_1 = \nu_2 = \nu_{\mathrm{SR}}$. These results, together with the anomalous dimensions in the regions $\mathrm{II}_{A\vee B}$, complete the characterization of the phase diagram of LR anisotropic spin system, showing also how a LR quantum spin system is not in general equivalent to its SR counterpart, when $\sigma_1 < \sigma_1^*$.

4.3 Conclusions

We studied $O(N)$ long range (LR) models in dimension $d \geq 2$. Using the flow equation for the effective potential alone we found that universality classes of $O(N)$ LR models are in correspondence with those of $O(N)$ short range (SR) models in effective dimension $D_{\text{eff}} = 2d/\sigma$. We also found new multicritical potentials which are present, at fixed d, above certain critical values of the parameter σ.

We then considered anomalous dimension effects considering also the flow of a field independent wave function renormalization. We found $\delta\eta = 0$, i.e. the Sak's result [103] in which there are no correction to the mean–field value of the anomalous dimension. The relation between the LR model and the SR model is now valid at the effective dimension D'_{eff} defined by equation (4.7), while the correlation length exponent is given according to equation (4.8). Quantitative predictions for the exponent ν_{LR} for various values of N were as well presented in $d = 2$ and $d = 3$.

Finally we introduced an effective action where both the SR and LR terms are present in the propagator. This approach does not impose *a priori* which is the dominant coupling in the RG flow. We showed how Sak's result is again justified by the fixed point structure of the model, where a LR interacting fixed point appears only if $\sigma < \sigma_*$ and it controls the critical behavior of the system. An important result is that the effective dimension D'_{eff} can be shown to be not exact at this improved approximation level: it is possible to estimate the error present using the effective dimension D'_{eff}, and, also close to σ_*, this error is found to be rather small. Given the fact that often models with an effective dimension are used to take into account effects of long ranginess, competing interactions and disorder, we hope that our analysis based on the action (4.9) and the estimate of the error done for the critical exponents may call for similar analyses in a variety of other physical systems where the effective dimension is introduced.

The final picture emerging from our analysis is the following: starting at $\sigma = 0$ and increasing σ towards 2, we have found that for $\sigma < d/2$ only the LR Gaussian fixed point exists and no SR terms in the fixed point propagator are present. At $\sigma = d/2$ a new interacting fixed point emerges from the LR Gaussian one and the same happens at the values $\sigma_{c,i}$ where new LR universality classes appear (in the same way as the multicritical SR fixed points are generated below the upper critical dimensions). Finally, when σ approaches σ_* the LR Wilson–Fisher fixed point merges with its SR equivalent and the LR term in the propagator disappears for $\sigma > \sigma_*$: this has to be contrasted with the case $\sigma < \sigma_*$ where at the interacting LR fixed points the propagator contains also a SR term. The same scenario is valid for all multicritical fixed points, provided that the σ_* values are computed with the corresponding SR anomalous dimensions.

Anisotropic LR spin systems have a rich phase diagram as a function of the two exponents σ_1 and σ_2 and of the two dimensions d_1, d_2. In the $\sigma_1 - \sigma_2$ plane two boundary curves exist, namely $\sigma_1^* = \sigma_1^*(\sigma_2)$ and $\sigma_2^* = \sigma_2^*(\sigma_1)$, where the LR interactions in the subspaces $\mathbb{R}^{d_2}$ and $\mathbb{R}^{d_1}$ become irrelevant. At mean-field level the two boundaries are straight lines, $\sigma_1^* = \sigma_2^* = 2$, as shown in figure 4.8. Beyond mean-field these boundaries become non trivial curves, see figure 4.12. At the intersection between the boundaries the system recovers both SR and isotropic behaviors and then the intersection point is simply given by $\sigma_1 = \sigma_2 = 2 - \eta_{SR}$, with η_{SR} the anomalous dimension of an isotropic SR system in dimension $d_1 + d_2$, as it is found for isotropic LR systems [80, 103, 116, 116].

In the pure LR region, denoted by I in figures 4.8 and 4.12, the low energy behavior can be described by the effective action (4.40). The field dynamics is characterized by two non analytic powers of the momentum excitations with respectively real exponents σ_1 and σ_2 in the two subspaces $\mathbb{R}^{d_1}$ and $\mathbb{R}^{d_2}$. In this case the system universality class is equivalent to an isotropic LR system in an effective dimension $d_{\text{eff}} = d_1 + \theta d_2$, defined in equation (4.50).

When one of the two exponents $\sigma_1 \vee \sigma_2$ become larger than its threshold value $\sigma_1^* \vee \sigma_2^*$ the corresponding non analytic kinetic term in the effective action (4.40) becomes sub-leading with respect to the analytic term, and LR interactions lie in the same universality of SR ones. The system enters then in the mixed regions $II_{A \vee B}$ where the subspace $\mathbb{R}^{d_1 \vee d_2}$ effectively behaves as if only SR interactions were present.

In regions $II_{A \vee B}$ the system is described by the effective action (4.40) with $\sigma_1 \vee \sigma_2 = 2$. In this case we can study the model with equation (4.55) and the anomalous dimension defined by (4.56). The result for the anomalous dimension in regions $II_{A \vee B}$ is given in figure 4.10. Once the anomalous dimension of the analytic term in presence of non analytic anisotropic terms is known we can calculate the threshold curves, which are $\sigma_2^*(\sigma_1) = 2 - \eta(\sigma_1)$ and $\sigma_1^*(\sigma_2) = 2 - \eta(\sigma_2)$, as depicted in figure 4.12.

Regions $II_{A \vee B}$ are relevant for our purposes, since the quantum critical points at zero temperature of a quantum spin system with LR couplings lie in these regions. In particular the effective action (4.40) describes the universality of a quantum spin system in dimension $d_1 = D$, when one of the two subspaces has dimension d_1 with real exponent σ_1 and the other subspace, with dimension $d_2 = z$ contains only SR interactions.

Anisotropic LR systems have two different correlation length exponents which are connected by scaling relation (4.27). The exponent ν_1 can be obtained by studying the stability around the fixed points of equation (4.49) in region I or of equation (4.55) in regions $II_{A \vee B}$. On the other hand ν_1 is also equal to the correlation length exponent of an isotropic LR system in dimension d_{eff}, equation (4.50). In regions $II_{A \vee B}$ the effective dimension relation

(4.50) is not strictly valid, but we can reintroduce it, neglecting small anomalous dimension terms in equation (4.55).

Using the effective dimension relations (4.50), it is possible to compute the critical exponents for the anisotropic LR $O(N)$ models for general values of the dimensions d_1 and d_2 and for different values of the field components N. An interesting case is the one with a one dimensionsal subspace ($d_1 \vee d_2 = 1$). The results are reported in Figs. 4.13 and 4.14.

The analysis of ansatz (4.40) also leads to exact results in the $N \to \infty$ limit, where only the correlation length exponents are different from zero in all the regions, see equations (4.51) and (4.54). The validity of ansatz (4.40) in the $N \to \infty$ limit also resulted in the reproduction of the correct result for the ANNNI models, equations (4.53) and (4.54).

This work provides a step forward in the comprehension of LR interaction effects in the critical behavior of spin systems. Since anisotropic interactions are widely present in condensed matter systems, it would be interesting to investigate whether anisotropic LR critical behavior could be responsible for various phase transitions occurring in presence of multi-axial anisotropy. Our results can also be useful for the study of quantum LR systems via the quantum-to-classical equivalence, once the dynamic critical exponent z is known.

Our work [27] also calls for further investigations of the critical behavior of anisotropic LR systems both in the numerical simulations and in experiments, in order to confirm the reliability of field theory description used in the last section of this chapter.

Finally it is worth noting that we focused on the description of the second order phase transition occurring in these models, mostly studying the case $\sigma_1, \sigma_2 \leq 2$ and therefore not considering the standard Lifshitz point critical behavior. For σ_1 or $\sigma_2 > 2$ higher order critical behavior can be found as in the standard Lifshitz point case. This very interesting study is left for future work. It would be also interesting to study LR interactions depending on the angle of the relative distance as for dipolar gases.

Chapter 5

Conclusions

The main focus of this thesis was on exploiting the more powerful aspects of FRG approach and on their use to investigate non trivial aspects of spin systems and long range (LR) models which are still not fully understood. Here we briefly remind the main findings of the thesis and we rather comment more in detail on possible future work motivated by the presented results.

Starting with the lowest order derivative expansion, the so-called Local Potential Approximation (LPA), and performing a series approximation around zero field a spurious spontaneous symmetry breaking (SSB) is found for $O(N)$ models in $d \leq 2$, while the series expansion centered in the field minimum fails in $d \lesssim 2.5$ for $N = 1$, as discussed in Section 2.2 or [80], leading to difficulties in overcoming standard perturbative results at this approximation level [156]. However, when the full functional form of the potential is considered we found no SSB in $d \leq 2$ for every N, see Section 2.2. This result is in agreement with the Mermin-Wagner theorem [33], but still do not reproduce the exact result of the $N = 1$ case which, being a discrete $\mathbb{Z}_2$ symmetry, *may* undergo SSB for $d \leq 2$ [157]. A step forward may be solved introducing anomalous dimension effects, see the LPA$'$ scheme Section 2.3. It is found that the number of solutions of equation (2.76) is controlled by the field dimension $\Delta_\varphi = d - 2 + \eta$ with the values of the anomalous dimension η given by equation (2.75a). The SSB disappears for $\Delta_\varphi \leq 0$. The anomalous dimension obtained from equation (2.75a) vanishes in $d = 2$ for all $N \geq 2$ while it stays finite in the $N < 2$ case and thus the lower critical dimension for the SSB is given by $d = 2$ for $N \geq 2$.

The latter discussion leaves open the fate of the SSB for $N < 2$ and $d < 2$. Indeed, for discrete symmetries, the expression (2.75a) remains finite and $\Delta_\varphi > 0$ in $d = 2$, so that one could wonder about the existence of a lower critical dimension $d_{l,c}$ at which the SSB may disappear also for discrete symmetries. Obviously for $N = 1$ it has to be $1 \leq d_{l,c} < 2$ since the Ising model is solvable for $d = 1, 2$ (and of course no SSB occurring for $d = 1$). The approach

of Section 2.3 can be easily extended in the $d < 2$ case and indeed it may apparently exist a value $d_{l,c}$ at which $\eta < d-2$ and SSB disappears, in agreement with [158]. Nevertheless this result should be more carefully investigated, since for the Ising model on graphs the transition is considered to be not universal [38, 39, 159, 160] in the sense that the existence of a finite temperature phase transition on a self similar fractal lattice is not regulated by a single parameter, like the fractal dimension, but rather by the geometrical lattice properties such as ramification, connectivity, lacunarity and others.

Several Monte Carlo and RG investigations exist for the SR Ising model on self-similar fractal lattices [161–167], still the universality of the phase transition remains elusive. While the case of fractal lattices with finite and infinite connectivity has been studied [163, 164]. Connectivity alone does not seem to be sufficient to characterize the phase transition [166], and the role played by the spectral dimension has still to be clarified [167]. The investigation of SSB in $d < 2$ for discrete symmetries and the identification (or refutation of the existence) of a lower (spectral) dimension $d_{l,c}$ will be the subject of future work. The identification of the continuous dimension d of the field theory with some quantity defined on the graph such as fractal dimension or spectral dimension will be investigated by means of numerical simulation on fractals or on diluted graphs and by comparison with conformal bootstrap results [70].

The conjecture on the possible existence of a lower critical dimension $d_{l,c} > 1$ opens some interesting scenario. Indeed when $\Delta_\varphi = 0$ a Berezinskii-Kosterlitz-Thouless (BKT)-type transition may appear. Let us consider only continuous symmetries: the Mermin-Wagner theorem manifests itself by the vanishing of the anomalous dimension in $d = 2$, see Fig. 2.11b, and then $\Delta_\varphi = 0$ exactly at $d = 2$. It is commonly believed that for $N = 2$, in the radial parametrization $\varphi = \rho e^{i\theta}$, the amplitude fluctuations are frozen and the physics of the $O(2)$ model is given by the sine-Gordon (SG) model described in detail in Chapter 3. Thus the $O(2)$ model in $d = 2$ behaves effectively as a scalar model with periodic symmetry in addition to $\mathbb{Z}_2$ symmetry. However the $O(2)$ model in $d = 2$ is not the only one showing BKT behavior, this also happens in the $\sigma = d = 1$ LR Ising model introduced in Chapter 4. Our approach is not able to recover effective BKT behavior when explicit periodic symmetry is not present, nevertheless it is evident that even in this case $\Delta_\varphi = d - \sigma = 0$. One possible conjecture/work hypothesis is that *BKT behavior is found in all the cases where* $\Delta_\varphi = 0$ *for discrete symmetries*. The latter statement is in agreement with results existing in 1 dimensional models [104, 107, 109, 168], where LR Ising chains with interactions $\propto \frac{1}{r^2}$, having in fact $\Delta_\varphi = 0$, are shown to undergo BKT behavior. According to this conjecture the short range Ising model at $d = d_{l,c}$ could show BKT behavior. The detection of such behavior would not only strongly confirm the validity of our conjecture but would be also numerically

checkable on diluted graphs [169, 170]. Since, as we previuosly stated, the behaviour of Ising systems for $d < 2$ call for a conclusive explaination, an intriguing aspect may be study as future work whether the BKT transition for short range Ising models in $d < 2$ is possible.

The above described conjecture leaves the case of continuous symmetries aside, even if the $N = 2$ vector model is commonly believed to undergo BKT behavior, it is a rather special case, since the finite mass of amplitude excitations freeze that degree of freedom and the $O(2)$ model can be related to the 2 dimensional SG model. This mapping is however not exact, moreover there have been recent results pointing to the possibility that the BKT behavior in two component field theories is the result of a crossover phenomenon rather than a true phase transition [82, 171]. The BKT behavior was confirmed by numerous numerical evidences both numerically [172, 173] and experimentally [174–176]. Even if numerical and experimental evidences can still be justified with sharp crossover behavior, it is again necessary to reconcile such findings with analytical results. Indeed the results of [171] question the existence of actual BKT phase transition in the $O(2)$ model when the joined renormalization of transverse and amplitude excitations is considered. This result will also affect the XY spin model, which is exactly mapped into the $O(2)$ model, appendix B.1, and should have the same universal properties. However the XY model is believed to undergo BKT behavior, but on this point we have to notice that formal demonstrations are carried out for the Coulomb gas [108] which is related to the XY model only in approximate way [177, 178].

In order to reconcile the above picture it would be determinant to extend the approach of [82, 171] to the radial parametrization $\varphi = \sqrt{\rho}e^{i\theta}$ in such a way that one can employ the approach described in Chapter 2 but including also amplitude fluctuations. The latter procedure will have the advantage to explicitly retain periodic symmetry in the field phase [49, 57] allowing to actual non perturbative treatment of both angular and amplitude degrees of freedom. Since FRG approach has proven particularly suitable for the study of SG models and their generalization, as discussed in Chapter 2, we expect that the treatment of the resulting SG model may substantially modify of confirm the findings of [82, 171], possibly recovering actual BKT behavior.

Whatever would be the outcome of the proposed investigation on the $O(2)$ model, it will probably result in a deeper understanding of BKT behavior and of the interplay between vortex degrees of freedom and density modulations in finite systems. A natural step forward in this direction will be to generalize the above proposed formalism to the case of 2 dimensional interacting fermions in the continuum.

Evidences of the BKT transition have been recently found in fermionic cold atom systems [176], where the decay of the correlation in the low temperature is in good agreement with

the expected power law behavior. Nevertheless the value of the exponent η_{BKT} obtained from the data at the temperature $T = T_{BKT}$ is $\eta_{exp} \simeq 1.4$ to be compared with the exactly known result $\eta_{BKT} = \frac{1}{4}$. The huge mismatch between these two results has been attributed to the non homogeneous density profile of the system due to the presence of the optical trap [179, 180], but many points are still to be clarified since it is not clear the reason why such effect have not been observed in trapped Bosonic systems [174]. SG-inspired approaches could help the understanding of these complex experimental realizations while retaining the crucial features of BKT physics.

While the above proposed approach substantially rely on Yukawa description of fermionic interaction, a non perturbative treatment of direct fermionic interactions seems still out of reach. Indeed most of the approaches rely on partial bosonization [181] or in perturbative approximation of the Wetterich equation [32, 81]. However both approaches lead to serious drawbacks. Partial bosonization is obtained by means of Hubbard–Stratonovich transformation which in many body systems is known not to yield reliable results due to the ambiguity in the choice of the bosonic channel [182]. On the other hand perturbative approximations of the Wetterich equation, even if substantially more stable and easily convergent, due to the presence of the regulator function, rather than standard perturbation approaches or dimensional regularization technique, still yield plausible results only in the small interacting limit.

The need to improve and extend non perturbative approaches to interacting fermion system is quite widespread into the FRG community and various possible alternative approaches to fermionic systems have been developed. One possibility is to merge the FRG technique with other successful technique adopted on many body systems, typical examples are Dynamical Mean Field Theory (DMFT)+FRG approach [183] or Density Functional Theory (DFT)+FRG approach [184–188]. The latter may be particularly important since it is formulated in two particle formalism and it seems more suitable to construct non perturbative approximation schemes for fermionic systems. In this perspective an interesting application would be to combine the two particle FRG formalism in the density channel [188, 189] with the theory of adiabatic connection [190, 191]. The obtained RG flow will not only reproduce the known results of adiabatic connection [185], but possibly produce, due to the regulator presence, a generalized form of adiabatic connection which will be possibly not spoiled by the presence of phase transition.

A step further in this direction would be to rewrite in FRG language not only the usual adiabatic connection between non interacting and interacting fermion systems [185], but rather to use FRG approach to investigate the connection between an interacting system with its infinitely interacting correspondent where quantum fluctuation are frozen. This strategy

has already been exploited using DFT techniques [192], suggesting that RG flow starting at infinite value of the coupling could yield useful results for the study of strongly interacting fermionic systems in the lattice.

The last chapter of this thesis, Chapter 4, was dedicated to the study of LR interacting systems using a non analytic ansatz for the effective action. In the standard isotropic case we recovered the expected results on the critical exponents of LR $O(N)$ spin system, helping to clarify some existing controversies over the correct value of the anomalous dimension of these systems. Subsequentely we introduced spatial anisotropy; these results are *per se* interesting in the physics of anisotropic classical phase transition and they show how in a correlated systems the presence of strong anisotropy in the propagator can radically modify the phase diagram. These results should be compared to the case of weak anisotropy, which has been shown to be irrelevant for the universal quantities [193, 194], and to the case of anisotropic finite range interactions, which lead to multi-critical transition phenomena [195–197]. Indeed while our formalism can be easily generalized to latter case, which will be subject of future work, the investigation reported in Section 4.2 shows a standard second order phase transition which is the leading critical behavior in anisotropic LR systems.

The latter picture can be employed to uncover the universal quantities of the Quantum LR rotor model [198, 199]. Later these results will be applied to the case of critical engines [200, 201], where fine tuning of the long range power law σ the dimension d and the number of rotor components N could be used to increase the efficiency at finite power of the engine.

Apart from possible applications of the LR model discussed in this thesis to quantum thermodynamics, the investigations of Chapter 4 pave the way to the application of FRG techniques to strong LR interactions where the decay exponent is lower than the system dimension $\sigma < 0$. In that case universal properties are not an issue, since Strong LR (SLR) models are known to be well inside the Mean Field (MF) region [101].

SLR interacting systems have crucial importance in physics, since they describe the physics of Newtonian and Coulomb interaction, the thermodynamics is in this case not well defined but it can be recovered by the so called Kac's rescaling [136]. The regularized theory has finite interaction energies but, as the not regularized one, it is not additive, thus the study of SLR models can be resumed into the study of non additive systems. These systems show rather spectacular properties when the out of equilibrium is considered, such as quasi-stationary states having lifetime diverging with the size of the system [202].

In order to deal with non equilibrium properties in SLR systems it will be necessary to introduce the Martin-Siggia-Rose formalism [203], the so-called boundary FRG [156]. Once this formalism will be set for the LR interactions defined in Chapter 4 it will be necessary to extend it to the negative σ range where non additive effects appear.

This preliminary investigation over the dynamics of SLR classical systems will be the basis to develop and benchmark the FRG formalism in SLR dynamical systems, in such a way to later extend the FRG framework to the dynamics of quantum systems into optical cavities [204–206]. There the LR interactions are mediated by long lived photons trapped in the cavity and the system shows the peculiar dynamics expected by a SLR fully interacting classical systems. However quantum effects and the presence of dissipation are important in those systems and they have to be explicitly included into the computation to compare the theoretical results with numerical simulations and experiments.

FRG is a very flexible approach, which includes the theoretical insight of the RG concept in an in principle exact scheme which helps in developing approximation schemes. However the possibility to achieve very precise numerical results is still hindered by the complexity of high order derivative expansion. Nevertheless the lowest order derivative expansion already allows to catch all the qualitative features of the $O(N)$ phase diagram. FRG technique can be also employed to compute non universal quantities and lattice computation are available both in the classical and in the quantum case [28, 207].

The FRG method has demonstrated crucial in the understanding of out-of equilibrium phase transitions [208, 209] and in the investigation of frustrated spin systems [210]. Many issues of this technique still need to be clarified and the necessity to develop more quantitative approximation schemes has been still not be fully satisfied. Moreover the lack for a systematic non perturbative approximation scheme for fermionic systems makes the field open to methodological investigations on the foundations of field theory and RG concepts. This thesis was in the stream of this line of research, and it aimed at clarifyng some of the numerical and methodological issues of basic FRG applications while enlightening the potentialities of non perturbative techniques.

List of figures

List of tables

References

[1] E. Ising, *Beitrag zur Theorie des Ferromagnetismus*, *Zeitschrift für Phys.* **31** (feb, 1925) 253–258.

[2] R. Peierls, M. Born, W. Heisenberg, W. L. Bragg, E. J. Williams and R. H. Fowler, *On Ising's model of ferromagnetism*, *Math. Proc. Cambridge Philos. Soc.* **32** (oct, 1936) 477.

[3] S. G. Brush, *History of the Lenz-Ising model*, *Rev. Mod. Phys.* **39** (oct, 1967) 883–893.

[4] L. Onsager, *Crystal Statistics. I. A Two-Dimensional Model with an Order-Disorder Transition*, *Phys. Rev.* **65** (feb, 1944) 117–149.

[5] S. El-Showk, M. F. Paulos, D. Poland, S. Rychkov, D. Simmons-Duffin and A. Vichi, *Solving the 3D Ising model with the conformal bootstrap*, *Phys. Rev. D* **86** (jul, 2012) 025022.

[6] A. M. Ferrenberg and D. P. Landau, *Critical behavior of the three-dimensional Ising model: A high-resolution Monte Carlo study*, *Phys. Rev. B* **44** (sep, 1991) 5081–5091.

[7] G. Mussardo, *Statistical field theory : an introduction to exactly solved models in statistical physics*. Oxford University Press, 2010.

[8] H. Kleinert and V. Schulte-Frohlinde, *Critical Properties of Phi 4 -Theories*. WORLD SCIENTIFIC, jul, 2001, 10.1142/4733.

[9] K. G. Wilson, *Renormalization Group and Critical Phenomena. I. Renormalization Group and the Kadanoff Scaling Picture*, *Phys. Rev. B* **4** (nov, 1971) 3174–3183.

[10] J. Zinn-Justin, *Critical Phenomena: field theoretical approach*, *Scholarpedia* **5** (2010) 8346.

[11] K. G. Wilson, *Feynman-Graph Expansion for Critical Exponents*, *Phys. Rev. Lett.* **28** (feb, 1972) 548–551.

[12] K. G. Wilson and M. E. Fisher, *Critical Exponents in 3.99 Dimensions*, *Phys. Rev. Lett.* **28** (jan, 1972) 240–243.

[13] K. G. Wilson, *The renormalization group: Critical phenomena and the Kondo problem*, *Rev. Mod. Phys.* **47** (oct, 1975) 773–840.

[14] K. G. Wilson, *The renormalization group and critical phenomena*, *Rev. Mod. Phys.* **55** (jul, 1983) 583–600.

[15] F. J. Wegner and A. Houghton, *Renormalization Group Equation for Critical Phenomena*, *Phys. Rev. A* **8** (jul, 1973) 401–412.

[16] S. R. White, *Density matrix formulation for quantum renormalization groups*, *Phys. Rev. Lett.* **69** (nov, 1992) 2863–2866.

[17] C. Wetterich, *Exact evolution equation for the effective potential*, *Phys. Lett. B* **301** (feb, 1993) 90–94.

[18] T. R. MORRIS, *THE EXACT RENORMALIZATION GROUP AND APPROXIMATE SOLUTIONS*, *Int. J. Mod. Phys. A* **09** (jun, 1994) 2411–2449.

[19] J. Berges, N. Tetradis and C. Wetterich, *Non-perturbative renormalization flow in quantum field theory and statistical physics*, *Phys. Rep.* **363** (jun, 2002) 223–386.

[20] K. Huang, *Statistical mechanics*. Wiley, 1987.

[21] N. Defenu, P. Mati, I. G. Márián, I. Nándori and A. Trombettoni, *Truncation effects in the functional renormalization group study of spontaneous symmetry breaking*, *J. High Energy Phys.* **2015** (may, 2015) 141.

[22] A. Codello and G. D'Odorico, *O (N) -Universality Classes and the Mermin-Wagner Theorem*, *Phys. Rev. Lett.* **110** (apr, 2013) 141601.

[23] A. Codello, N. Defenu and G. D'Odorico, *Critical exponents of O (N) models in fractional dimensions*, *Phys. Rev. D* **91** (may, 2015) 105003.

[24] A. Codello, *Scaling solutions in a continuous dimension*, *J. Phys. A Math. Theor.* **45** (nov, 2012) 465006.

[25] A. Codello, G. D'Odorico and C. Pagani, *A functional RG equation for the c-function*, *J. High Energy Phys.* **2014** (jul, 2014) 40.

[26] V. Bacsó, N. Defenu, A. Trombettoni and I. Nándori, *c-function and central charge of the sine-Gordon model from the non-perturbative renormalization group flow*, *Nucl. Phys. B* **901** (2015) 444–460.

[27] N. Defenu, A. Trombettoni and S. Ruffo, *Anisotropic Long-Range Spin Systems*, `1606.07756`.

[28] T. Machado and N. Dupuis, *From local to critical fluctuations in lattice models: A nonperturbative renormalization-group approach*, *Phys. Rev. E* **82** (oct, 2010) 041128.

[29] A. Rançon, *Nonperturbative renormalization group approach to quantum X Y spin models*, *Phys. Rev. B* **89** (jun, 2014) 214418.

[30] G. Parisi, *Statistical field theory*. Perseus Books, 1998.

[31] B. Delamotte, *An Introduction to the Nonperturbative Renormalization Group*, pp. 49–132. 2012. DOI.

[32] P. Kopietz, L. Bartosch and F. Schütz, *Introduction to the Functional Renormalization Group*, vol. 798 of *Lecture Notes in Physics*. Springer Berlin Heidelberg, Berlin, Heidelberg, 2010, 10.1007/978-3-642-05094-7.

[33] N. D. Mermin and H. Wagner, *Absence of Ferromagnetism or Antiferromagnetism in One- or Two-Dimensional Isotropic Heisenberg Models*, *Phys. Rev. Lett.* **17** (nov, 1966) 1133–1136.

[34] P. C. Hohenberg, *Existence of Long-Range Order in One and Two Dimensions*, *Phys. Rev.* **158** (jun, 1967) 383–386.

[35] S. Coleman, *There are no Goldstone bosons in two dimensions*, *Commun. Math. Phys.* **31** (dec, 1973) 259–264.

[36] L. P. Kadanoff, *Statistical Physics*. WORLD SCIENTIFIC, may, 2000, 10.1142/4016.

[37] D. Cassi, *Phase transitions and random walks on graphs: A generalization of the Mermin-Wagner theorem to disordered lattices, fractals, and other discrete structures*, *Phys. Rev. Lett.* **68** (jun, 1992) 3631–3634.

[38] R. Burioni and D. Cassi, *Universal Properties of Spectral Dimension*, *Phys. Rev. Lett.* **76** (feb, 1996) 1091–1093.

[39] R. Burioni, D. Cassi and A. Vezzani, *Inverse Mermin-Wagner theorem for classical spin models on graphs*, *Phys. Rev. E* **60** (aug, 1999) 1500–1502.

[40] H. E. Stanley, *Dependence of Critical Properties on Dimensionality of Spins*, *Phys. Rev. Lett.* **20** (mar, 1968) 589–592.

[41] G. S. Joyce, *Spherical Model with Long-Range Ferromagnetic Interactions*, *Phys. Rev.* **146** (jun, 1966) 349–358.

[42] C. Bagnuls and C. Bervillier, *Exact renormalization group equations: an introductory review*, *Phys. Rep.* **348** (jul, 2001) 91–157.

[43] J. Polonyi, *Lectures on the functional renormalization group method*, *Cent. Eur. J. Phys.* **1** (jan, 2003) 1, [0110026].

[44] H. Gies, *Introduction to the Functional RG and Applications to Gauge Theories*, pp. 287–348. 2012. DOI.

[45] O. J. Rosten, *Fundamentals of the exact renormalization group*, *Phys. Rep.* **511** (feb, 2012) 177–272.

[46] N. Tetradis and C. Wetterich, *Critical exponents from the effective average action*, *Nucl. Phys. B* **422** (jul, 1994) 541–592.

[47] M. D'Attanasio and T. R. Morris, *Large N and the renormalization group*, *Phys. Lett. B* **409** (sep, 1997) 363–370.

[48] N. Tetradis and C. Wetterich, *Scale dependence of the average potential around the maximum in $\phi 4$ theories*, *Nucl. Phys. B* **383** (sep, 1992) 197–217.

[49] S. Nagy, I. Nándori, J. Polonyi and K. Sailer, *Functional Renormalization Group Approach to the Sine-Gordon Model*, *Phys. Rev. Lett.* **102** (jun, 2009) 241603.

[50] J. Braun, H. Gies and D. D. Scherer, *Asymptotic safety: A simple example*, *Phys. Rev. D* **83** (apr, 2011) 085012.

[51] S. Nagy, *Lectures on renormalization and asymptotic safety*, *Ann. Phys. (N. Y).* **350** (nov, 2014) 310–346.

[52] S. Nagy, J. Krizsan and K. Sailer, *Infrared fixed point in quantum Einstein gravity*, *J. High Energy Phys.* **2012** (jul, 2012) 102.

[53] P. Mati, *Vanishing beta function curves from the functional renormalization group*, *Phys. Rev. D* **91** (jun, 2015) 125038.

[54] J. Zinn-Justin, *Quantum Field Theory and Critical Phenomena*, .

[55] T. R. Morris, *Properties of Derivative Expansion Approximations to the Renormalization Group*, *Int. J. Mod. Phys. B* **12** (may, 1998) 1343–1354.

[56] I. Nándori, I. Márián and V. Bacsó, *Spontaneous symmetry breaking and optimization of functional renormalization group*, *Phys. Rev. D* **89** (feb, 2014) 047701.

[57] I. Nándori, J. Polonyi and K. Sailer, *Renormalization of periodic potentials*, *Phys. Rev. D* **63** (jan, 2001) 045022.

[58] I. G. Márián, U. D. Jentschura and I. Nándori, *The numerically optimized regulator and the functional renormalization group*, *J. Phys. G Nucl. Part. Phys.* **41** (may, 2014) 055001.

[59] T. R. Morris, *The renormalization group and two dimensional multicritical effective scalar field theory*, *Phys. Lett. B* **345** (feb, 1995) 139–148.

[60] T. Hellwig, A. Wipf and O. Zanusso, *Scaling and superscaling solutions from the functional renormalization group*, *Phys. Rev. D* **92** (oct, 2015) 085027.

[61] C. Domb and J. L. Lebowitz, *Phase transitions and critical phenomena. 9.* Academic Press, 1984.

[62] R. Percacci and G. P. Vacca, *Are there scaling solutions in the O (N) -models for large N in d > 4 ?*, *Phys. Rev. D* **90** (nov, 2014) 107702.

[63] L. Fei, S. Giombi and I. R. Klebanov, *Critical O(N) models in 6 {$$} dimensions*, *Phys. Rev. D* **90** (jul, 2014) 25018, [arXiv:1404.1094v1].

[64] T. R. Morris, *Three-dimensional massive scalar field theory and the derivative expansion of the renormalization group*, *Nucl. Phys. B* **495** (jun, 1997) 477–504.

[65] J. M. Kosterlitz and D. J. Thouless, *Ordering, metastability and phase transitions in two-dimensional systems*, *J. Phys. C Solid State Phys.* **6** (apr, 1973) 1181–1203.

[66] C. Domb, J. L. Lebowitz and M. S. Green, *Phase transitions and critical phenomena*. Acad. Press, 2001.

[67] P. de Gennes, *Exponents for the excluded volume problem as derived by the Wilson method*, *Phys. Lett. A* **38** (feb, 1972) 339–340.

[68] M. E. Fisher, *Classical, n -Component Spin Systems or Fields with Negative Even Integral n*, *Phys. Rev. Lett.* **30** (apr, 1973) 679–681.

[69] S. El-Showk, M. F. Paulos, D. Poland, S. Rychkov, D. Simmons-Duffin and A. Vichi, *Solving the 3d ising model with the conformal bootstrap II. c-Minimization and precise critical exponents*, *J. Stat. Phys.* **157** (dec, 2014) 869–914, [1403.4545].

[70] S. El-Showk, M. Paulos, D. Poland, S. Rychkov, D. Simmons-Duffin and A. Vichi, *Conformal Field Theories in Fractional Dimensions*, *Phys. Rev. Lett.* **112** (apr, 2014) 141601.

[71] F. Kos, D. Poland and D. Simmons-Duffin, *Bootstrapping the O(N) vector models*, *J. High Energy Phys.* **2014** (jun, 2014) 91.

[72] S. Ma, *Statistical Mechanics*. WORLD SCIENTIFIC, may, 1985, 10.1142/0073.

[73] C. N. Yang, *The Spontaneous Magnetization of a Two-Dimensional Ising Model*, *Phys. Rev.* **85** (mar, 1952) 808–816.

[74] L. Canet, B. Delamotte, D. Mouhanna and J. Vidal, *Nonperturbative renormalization group approach to the Ising model: A derivative expansion at order 4*, *Phys. Rev. B* **68** (aug, 2003) 064421.

[75] L. Canet, B. Delamotte, D. Mouhanna and J. Vidal, *Optimization of the derivative expansion in the nonperturbative renormalization group*, *Phys. Rev. D* **67** (mar, 2003) 065004.

[76] A. L. Lewis and F. W. Adams, *Tricritical behavior in two dimensions. II. Universal quantities from the ε expansion*, *Phys. Rev. B* **18** (nov, 1978) 5099–5111.

[77] B. Nienhuis, *Exact Critical Point and Critical Exponents of O (n) Models in Two Dimensions*, *Phys. Rev. Lett.* **49** (oct, 1982) 1062–1065.

[78] A. Pelissetto and E. Vicari, *Critical phenomena and renormalization-group theory*, *Phys. Rep.* **368** (oct, 2002) 549–727.

[79] T. R. Morris, *On truncations of the exact renormalization group*, *Phys. Lett. B* **334** (aug, 1994) 355–362.

[80] N. Defenu, A. Trombettoni and A. Codello, *Fixed-point structure and effective fractional dimensionality for O(N) models with long-range interactions*, *Phys. Rev. E* **92** (nov, 2015) 052113.

[81] W. Metzner, M. Salmhofer, C. Honerkamp, V. Meden and K. Schönhammer, *Functional renormalization group approach to correlated fermion systems*, *Rev. Mod. Phys.* **84** (mar, 2012) 299–352.

[82] G. v. Gersdorff and C. Wetterich, *Nonperturbative renormalization flow and essential scaling for the Kosterlitz-Thouless transition*, *Phys. Rev. B* **64** (jul, 2001) 054513.

[83] P. Jakubczyk, N. Dupuis and B. Delamotte, *Reexamination of the nonperturbative renormalization-group approach to the Kosterlitz-Thouless transition*, *Phys. Rev. E* **90** (dec, 2014) 062105.

[84] A. Zamolodchikov, *Irreversibility of the Flux of the Renormalization Group in a 2D Field Theory*, *JETP Lett.* **43** (1986) 565–567.

[85] A. Fring, G. Mussardo and P. Simonetti, *Form factors for integrable lagrangian field theories, the sinh-Gordon model*, *Nucl. Phys. B* **393** (mar, 1993) 413–441.

[86] J. L. Cardy, *Central Charge and Universal Combinations of Amplitudes in Two-Dimensional Theories Away from Criticality*, *Phys. Rev. Lett.* **60** (jun, 1988) 2709–2711.

[87] P. Dorey, G. Siviour and G. Takács, *Form factor relocalisation and interpolating renormalisation group flows from the staircase model*, *J. High Energy Phys.* **2015** (mar, 2015) 54.

[88] P. Minnhagen, *The two-dimensional Coulomb gas, vortex unbinding, and superfluid-superconducting films*, *Rev. Mod. Phys.* **59** (oct, 1987) 1001–1066.

[89] V. E. Korepin, N. M. Bogoliubov and A. G. Izergin, *Quantum Inverse Scattering Method and Correlation Functions*. Cambridge University Press, Cambridge, 1993, 10.1017/CBO9780511628832.

[90] A. Gogolin, A. Nersesyan and A. Tsvelik, *Bosonization and strongly correlated systems*, .

[91] S. Coleman, *Quantum sine-Gordon equation as the massive thirring model*, *Phys. Rev. D* **11** (apr, 1975) 2088–2097.

[92] G. v. Gersdorff and C. Wetterich, *Nonperturbative renormalization flow and essential scaling for the Kosterlitz-Thouless transition*, *Phys. Rev. B* **64** (jul, 2001) 054513.

[93] M. Gräter and C. Wetterich, *Kosterlitz-Thouless Phase Transition in the Two Dimensional Linear σ Model*, *Phys. Rev. Lett.* **75** (jul, 1995) 378–381.

[94] I. Nándori, *Lecture Notes on the Functional Renormalization Group Study of Sine-Gordon Models*, *Lecture Notes* (sep, 2016) .

[95] I. Nándori, S. Nagy, K. Sailer and A. Trombettoni, *Comparison of renormalization group schemes for sine-Gordon-type models*, *Phys. Rev. D* **80** (jul, 2009) 025008.

[96] I. Nándori, *Bosonization and functional renormalization group approach in the framework of QED 2*, *Phys. Rev. D* **84** (sep, 2011) 065024.

[97] S. Nagy, *Degeneracy induced scaling of the correlation length for periodic models*, *Nucl. Phys. B* **864** (nov, 2012) 226–240.

[98] S. NAGY and K. SAILER, *INTERPLAY OF FIXED POINTS IN SCALAR MODELS*, *Int. J. Mod. Phys. A* **28** (oct, 2013) 1350130.

[99] P. Dorey, *Exact S-matrices*, *Conform. F. Theor. Integr. Model.* (1998) 85–125, [9810026].

[100] T. Dauxois, P. de Buyl, L. Lori, S. Ruffo, D. T. Campa A, R. S et al., *Models with short- and long-range interactions: the phase diagram and the reentrant phase*, *J. Stat. Mech. Theory Exp.* **2010** (jun, 2010) P06015.

[101] A. Campa, T. Dauxois and S. Ruffo, *Statistical mechanics and dynamics of solvable models with long-range interactions*, *Phys. Rep.* **480** (sep, 2009) 57–159.

[102] M. E. Fisher, S.-k. Ma and B. G. Nickel, *Critical Exponents for Long-Range Interactions*, *Phys. Rev. Lett.* **29** (oct, 1972) 917–920.

[103] J. Sak, *Recursion Relations and Fixed Points for Ferromagnets with Long-Range Interactions*, *Phys. Rev. B* **8** (jul, 1973) 281–285.

[104] F. J. Dyson, *Existence of a phase-transition in a one-dimensional Ising ferromagnet*, *Commun. Math. Phys.* **12** (jun, 1969) 91–107.

[105] D. J. Thouless, *Long-Range Order in One-Dimensional Ising Systems*, *Phys. Rev.* **187** (nov, 1969) 732–733.

[106] P. W. Anderson, G. Yuval and D. R. Hamann, *Exact Results in the Kondo Problem. II. Scaling Theory, Qualitatively Correct Solution, and Some New Results on One-Dimensional Classical Statistical Models*, *Phys. Rev. B* **1** (jun, 1970) 4464–4473.

[107] J. L. Cardy, *One-dimensional models with 1/r ² interactions*, *J. Phys. A. Math. Gen.* **14** (jun, 1981) 1407–1415.

[108] J. Fröhlich and T. Spencer, *The phase transition in the one-dimensional Ising Model with 1/r 2 interaction energy*, *Commun. Math. Phys.* **84** (mar, 1982) 87–101.

[109] E. Luijten and H. Meßingfeld, *Criticality in One Dimension with Inverse Square-Law Potentials*, *Phys. Rev. Lett.* **86** (jun, 2001) 5305–5308.

[110] E. Luijten and H. W. J. Blöte, *Classical critical behavior of spin models with long-range interactions*, *Phys. Rev. B* **56** (oct, 1997) 8945–8958.

[111] I. Balog, G. Tarjus, M. Tissier, I. Y. K, M. S, N. T et al., *Critical behaviour of the random-field Ising model with long-range interactions in one dimension*, *J. Stat. Mech. Theory Exp.* **2014** (oct, 2014) P10017.

[112] E. LUIJTEN and H. W. BLÖTE, *MONTE CARLO METHOD FOR SPIN MODELS WITH LONG-RANGE INTERACTIONS*, *Int. J. Mod. Phys. C* **06** (jun, 1995) 359–370.

[113] E. Luijten and H. W. J. Blöte, *Boundary between Long-Range and Short-Range Critical Behavior in Systems with Algebraic Interactions*, *Phys. Rev. Lett.* **89** (jun, 2002) 025703.

[114] T. Blanchard, M. Picco and M. A. Rajabpour, *Influence of long-range interactions on the critical behavior of the Ising model*, *EPL (Europhysics Lett.* **101** (mar, 2013) 56003.

[115] P. Grassberger, *Two-Dimensional SIR Epidemics with Long Range Infection*, *J. Stat. Phys.* **153** (oct, 2013) 289–311.

[116] M. C. Angelini, G. Parisi and F. Ricci-Tersenghi, *Relations between short-range and long-range Ising models*, *Phys. Rev. E* **89** (jun, 2014) 062120.

[117] R. A. Baños, L. A. Fernandez, V. Martin-Mayor and A. P. Young, *Correspondence between long-range and short-range spin glasses*, *Phys. Rev. B* **86** (oct, 2012) 134416.

[118] S. L. Katz, M. Droz and J. D. Gunton, *Approximate renormalization-group calculations of critical exponents in continuous dimensions*, *Phys. Rev. B* **15** (feb, 1977) 1597–1599.

[119] Y. HOLOVATCH, *PHASE TRANSITION IN CONTINUOUS SYMMETRY MODEL IN GENERAL DIMENSIONS — FIXED DIMENSION RENORMALIZATION GROUP APPROACH*, *Int. J. Mod. Phys. A* **08** (dec, 1993) 5329–5351.

[120] S. T. Bramwell, S. R. Giblin, S. Calder, R. Aldus, D. Prabhakaran and T. Fennell, *Measurement of the charge and current of magnetic monopoles in spin ice*, *Nature* **461** (oct, 2009) 956–959.

[121] T. Lahaye, C. Menotti, L. Santos, M. Lewenstein and T. Pfau, *The physics of dipolar bosonic quantum gases*, *Reports Prog. Phys.* **72** (dec, 2009) 126401.

[122] M. J. P. Gingras, P. C. W. Holdsworth, B. Bergersen, S. K. J, M. N. D, N. D. R. I et al., *Monte Carlo Study of Bond and Molecular Orientational Ordering in Two-Dimensional Nematic Liquid-Crystal Systems*, *Europhys. Lett.* **9** (jul, 1989) 539–544.

[123] J. V. Selinger and D. R. Nelson, *Theory of transitions among tilted hexatic phases in liquid crystals*, *Phys. Rev. A* **39** (mar, 1989) 3135–3147.

[124] A. Michelson, *Physical Realization of a Lifshitz Point in Liquid Crystals*, *Phys. Rev. Lett.* **39** (aug, 1977) 464–467.

[125] S. B. Rananavare, V. G. K. M. Pisipati and E. W. Wong, *Smectic- A –smectic- C –smectic- C * multicritical point in ferroelectric liquid crystals*, *Phys. Rev. Lett.* **72** (may, 1994) 3558–3561.

[126] M. Tinkham, *Introduction to superconductivity*, .

[127] N. B. Hannay, T. H. Geballe, B. T. Matthias, K. Andres, P. Schmidt and D. MacNair, *Superconductivity in Graphitic Compounds*, *Phys. Rev. Lett.* **14** (feb, 1965) 225–226.

[128] S. T. Ruggiero, T. W. Barbee and M. R. Beasley, *Superconductivity in Quasi-Two-Dimensional Layered Composites*, *Phys. Rev. Lett.* **45** (oct, 1980) 1299–1302.

[129] F. R. Gamble, F. J. DiSalvo, R. A. Klemm and T. H. Geballe, *Superconductivity in Layered Structure Organometallic Crystals*, *Science (80-.).* **168** (may, 1970) 568–570.

[130] U. Jentschura, I. Nándori and J. Zinn-Justin, *Effective action and phase structure of multi-layer sine-Gordon type models*, *Ann. Phys. (N. Y).* **321** (nov, 2006) 2647–2659.

[131] M. Iazzi, S. Fantoni and A. Trombettoni, *Anisotropic Ginzburg-Landau and Lawrence-Doniach models for layered ultracold Fermi gases*, *EPL (Europhysics Lett.* **100** (nov, 2012) 36007.

[132] M. A. Cazalilla, A. Iucci and T. Giamarchi, *Competition between vortex unbinding and tunneling in an optical lattice*, *Phys. Rev. A* **75** (may, 2007) 051603.

[133] B. Chattopadhyay and S. R. Shenoy, *Kosterlitz-Thouless signatures from 3D vortex loops in layered superconductors*, *Phys. Rev. Lett.* **72** (jan, 1994) 400–403.

[134] J. Singer, T. Schneider and M. Pedersen, *On the phase diagram of the attractive Hubbard model: Crossover and quantum critical phenomena*, *Eur. Phys. J. B* **2** (apr, 1998) 17–30.

[135] M. Randeria, W. Zwerger and M. Zwierlein, *The BCS–BEC Crossover and the Unitary Fermi Gas*, in *BCS-BEC Crossover Unitary Fermi Gas, Lect. Notes Physics, Vol. 836. ISBN 978-3-642-21977-1. Springer-Verlag Berlin Heidelberg, 2012, p. 1*, vol. 836, pp. 1–32. 2012. DOI.

[136] T. H. Berlin and M. Kac, *The Spherical Model of a Ferromagnet*, *Phys. Rev.* **86** (jun, 1952) 821–835.

[137] T. Mori, *Instability of the mean-field states and generalization of phase separation in long-range interacting systems*, *Phys. Rev. E* **84** (sep, 2011) 031128.

[138] M. F. Paulos, S. Rychkov, B. C. van Rees and B. Zan, *Conformal invariance in the long-range Ising model*, *Nucl. Phys. B* **902** (jan, 2016) 246–291.

[139] J. W. Britton, B. C. Sawyer, A. C. Keith, C.-C. J. Wang, J. K. Freericks, H. Uys et al., *Engineered two-dimensional Ising interactions in a trapped-ion quantum simulator with hundreds of spins*, *Nature* **484** (apr, 2012) 489–492.

[140] P. Schauß, M. Cheneau, M. Endres, T. Fukuhara, S. Hild, A. Omran et al., *Observation of spatially ordered structures in a two-dimensional Rydberg gas*, *Nature* **491** (oct, 2012) 87–91.

[141] B. Yan, S. A. Moses, B. Gadway, J. P. Covey, K. R. A. Hazzard, A. M. Rey et al., *Observation of dipolar spin-exchange interactions with lattice-confined polar molecules*, *Nature* **501** (sep, 2013) 521–525.

[142] O. Firstenberg, T. Peyronel, Q.-Y. Liang, A. V. Gorshkov, M. D. Lukin and V. Vuletić, *Attractive photons in a quantum nonlinear medium*, *Nature* **502** (sep, 2013) 71–75.

[143] R. Islam, C. Senko, W. C. Campbell, S. Korenblit, J. Smith, A. Lee et al., *Emergence and Frustration of Magnetism with Variable-Range Interactions in a Quantum Simulator*, *Science (80-.).* **340** (may, 2013) 583–587.

[144] H. Schempp, G. Günter, S. Wüster, M. Weidemüller and S. Whitlock, *Correlated Exciton Transport in Rydberg-Dressed-Atom Spin Chains*, *Phys. Rev. Lett.* **115** (aug, 2015) 093002, [arXiv:1504.01892v1].

[145] S. Sachdev, *Quantum Phase Transitions*. Cambridge University Press, Cambridge, 2011, 10.1017/CBO9780511973765.

[146] T. D. SCHULTZ, D. C. MATTIS and E. H. LIEB, *Two-Dimensional Ising Model as a Soluble Problem of Many Fermions*, *Rev. Mod. Phys.* **36** (jul, 1964) 856–871.

[147] I. Bars, C. Deliduman and O. Andreev, *Gauged duality, conformal symmetry, and spacetime with two times*, *Phys. Rev. D* **58** (aug, 1998) 066004.

[148] E. H. Lieb, *The classical limit of quantum spin systems*, *Commun. Math. Phys.* **31** (dec, 1973) 327–340.

[149] D. Podolsky, E. Shimshoni, P. Silvi, S. Montangero, T. Calarco, G. Morigi et al., *From classical to quantum criticality*, *Phys. Rev. B* **89** (jun, 2014) 214408.

[150] R. M. Hornreich, M. Luban and S. Shtrikman, *Critical behavior at the onset of {$k0$}-space instability on the {$$} line*, *Phys. Rev. Lett.* **35** (dec, 1975) 1678–1681.

[151] C. Mergulhão and C. E. I. Carneiro, *Field-theoretic approach to the Lifshitz point*, *Phys. Rev. B* **58** (sep, 1998) 6047–6056.

[152] H. W. Diehl and M. Shpot, *Critical behavior at m -axial Lifshitz points: Field-theory analysis and ε-expansion results*, *Phys. Rev. B* **62** (nov, 2000) 12338–12349.

[153] J. Als-Nielsen, *Mean field theory, the Ginzburg criterion, and marginal dimensionality of phase transitions*, *Am. J. Phys.* **45** (1977) 554.

[154] E. Brezin, G. Parisi and F. Ricci-Tersenghi, *The Crossover Region Between Long-Range and Short-Range Interactions for the Critical Exponents*, *J. Stat. Phys.* **157** (dec, 2014) 855–868.

[155] L. Frachebourg and M. Henkel, *Exact correlation function at the Lifshitz points of the spherical model*, *Phys. A Stat. Mech. its Appl.* **195** (may, 1993) 577–602.

[156] A. Chiocchetta, A. Gambassi, S. Diehl and J. Marino, *Universal short-time dynamics: boundary functional renormalization group for a temperature quench*, 1606.06272.

[157] A. Vezzani, *Spontaneous magnetization of the Ising model on the Sierpinski carpet fractal, a rigorous result*, *J. Phys. A. Math. Gen.* **36** (feb, 2003) 1593–1604, [0212497v2].

[158] H. Ballhausen, J. Berges and C. Wetterich, *Critical phenomena in continuous dimension*, *Phys. Lett. B* **582** (feb, 2004) 144–150.

[159] E. Agliari, R. Burioni, D. Cassi and A. Vezzani, *Fractal geometry of Ising magnetic patterns: signatures of criticality and diffusive dynamics*, *Eur. Phys. J. B* **49** (jan, 2006) 119–125.

[160] E. Agliari, R. Burioni and P. Sgrignoli, *A Two-populations Ising model on diluted Random Graphs*, 1009.0251.

[161] P. Monceau and M. Perreau, *Critical behavior of the Ising model on fractal structures in dimensions between one and two: Finite-size scaling effects*, *Phys. Rev. B* **63** (apr, 2001) 1–10.

[162] M. Perreau and J. C. S. Levy, *Randomness in fractals, connectivity dimensions, and percolation*, *Phys. Rev. A* **40** (oct, 1989) 4690–4699.

[163] Y. Gefen, A. Aharony and B. B. Mandelbrot, *Phase transitions on fractals. III. Infinitely ramified lattices*, *J. Phys. A. Math. Gen.* **17** (apr, 1984) 1277–1289.

[164] Y. Gefen, A. Aharony, Y. Shapirs and B. Benoit, *Phase transitions on fractals : II . Sierpinski gaskets*, *J. Phys.* **435** (feb, 1984) 435–444.

[165] P. Monceau, M. Perreau and F. Hébert, *Magnetic critical behavior of the Ising model on fractal structures*, *Phys. Rev. B* **58** (sep, 1998) 6386–6393.

[166] Y. Gefen, B. B. Mandelbrot and A. Aharony, *Critical phenomena on fractal lattices*, *Phys. Rev. Lett.* **45** (sep, 1980) 855–858.

[167] J. Carmona, U. Marconi, J. Ruiz-Lorenzo and A. Tarancón, *Critical properties of the Ising model on Sierpinski fractals: A finite-size scaling-analysis approach*, dec, 1998. 10.1103/PhysRevB.58.14387.

[168] Z. Glumac and K. Uzelac, *Critical behaviour of the 1D q-state Potts model with long-range interactions*, *J. Phys. A. Math. Gen.* **26** (oct, 1993) 5267–5278.

[169] L. Leuzzi, G. Parisi, F. Ricci-Tersenghi and J. J. Ruiz-Lorenzo, *Dilute One-Dimensional Spin Glasses with Power Law Decaying Interactions*, *Phys. Rev. Lett.* **101** (sep, 2008) 107203.

[170] M. I. Berganza and L. Leuzzi, *Critical behavior of the X Y model in complex topologies*, *Phys. Rev. B* **88** (oct, 2013) 144104.

[171] P. Jakubczyk and W. Metzner, *Amplitude fluctuations in the Berezinskii-Kosterlitz-Thouless phase*, `1606.04547`.

[172] N. Prokof'ev, O. Ruebenacker and B. Svistunov, *Critical Point of a Weakly Interacting Two-Dimensional Bose Gas*, *Phys. Rev. Lett.* **87** (dec, 2001) 270402.

[173] M. Holzmann and W. Krauth, *Kosterlitz-Thouless transition of the quasi-two-dimensional trapped bose gas*, *Phys. Rev. Lett.* **100** (may, 2008) 190402, [`arXiv:0710.5060v1`].

[174] Z. Hadzibabic, P. Krüger, M. Cheneau, B. Battelier and J. Dalibard, *Berezinskii–Kosterlitz–Thouless crossover in a trapped atomic gas*, *Nature* **441** (jun, 2006) 1118–1121.

[175] D. Bishop and J. Reppy, *Study of the Superfluid Transition in Two-Dimensional ^{4}He Films*, *Phys. Rev. Lett.* **40** (jun, 1978) 1727–1730.

[176] P. A. Murthy, I. Boettcher, L. Bayha, M. Holzmann, D. Kedar, M. Neidig et al., *Observation of the Berezinskii-Kosterlitz-Thouless Phase Transition in an Ultracold Fermi Gas*, *Phys. Rev. Lett.* **115** (jun, 2015) 010401.

[177] H. Kleinert, *Gauge fields in condensed matter*. World Scientific, 1989.

[178] L. Benfatto, C. Castellani and T. Giamarchi, *Beresinskii-Kosterlitz-Thouless transition within the sine-Gordon approach: the role of the vortex-core energy*, *arXiv Prepr. arXiv1201.2307* (jan, 2012) 1–21, [1201.2307].

[179] C.-T. Wu, B. M. Anderson, R. Boyack and K. Levin, *Quasicondensation in Two-Dimensional Fermi Gases*, *Phys. Rev. Lett.* **115** (dec, 2015) 240401.

[180] I. Boettcher and M. Holzmann, *Quasi-long-range order in trapped two-dimensional Bose gases*, *Phys. Rev. A* **94** (jul, 2016) 011602.

[181] I. Boettcher, J. M. Pawlowski and S. Diehl, *Ultracold atoms and the Functional Renormalization Group*, *Nucl. Phys. B - Proc. Suppl.* **228** (2012) 63–135.

[182] H. Kleinert, *Hubbard-Stratonovich Transformation: Successes, Failure, and Cure*, 1104.5161.

[183] C. Taranto, S. Andergassen, J. Bauer, K. Held, A. Katanin, W. Metzner et al., *From Infinite to Two Dimensions through the Functional Renormalization Group*, *Phys. Rev. Lett.* **112** (may, 2014) 196402.

[184] S. Kemler, J. Braun, H. P. W, Kohn, K. W. L, Sham et al., *Towards a renormalization group approach to density functional theory—general formalism and case studies*, *J. Phys. G Nucl. Part. Phys.* **40** (aug, 2013) 085105.

[185] J. Polonyi and K. Sailer, *Effective action and density-functional theory*, *Phys. Rev. B* **66** (oct, 2002) 155113.

[186] A. Schwenk and J. Polonyi, *Towards Density Functional Calculations from Nuclear Forces*, 0403011.

[187] S. Puglia, A. Bhattacharyya and R. Furnstahl, *Density functional theory for a confined Fermi system with short-range interaction*, *Nucl. Phys. A* **723** (2003) 145–180.

[188] J. F. Rentrop, S. G. Jakobs, V. Meden, M. V. Metzner W, Salmhofer M, Honerkamp C, S. K, B. L. Kopietz P et al., *Two-particle irreducible functional renormalization group schemes—a comparative study*, *J. Phys. A Math. Theor.* **48** (apr, 2015) 145002.

[189] N. Dupuis, *Nonperturbative renormalization-group approach to fermion systems in the two-particle-irreducible effective action formalism*, *Phys. Rev. B* **89** (jan, 2014) 035113.

[190] J. Harris, *Adiabatic-connection approach to Kohn-Sham theory*, *Phys. Rev. A* **29** (apr, 1984) 1648–1659.

[191] A. Savin, F. Colonna and R. Pollet, *Adiabatic connection approach to density functional theory of electronic systems*, *Int. J. Quantum Chem.* **93** (2003) 166–190.

[192] F. Malet and P. Gori-Giorgi, *Strong Correlation in Kohn-Sham Density Functional Theory*, *Phys. Rev. Lett.* **109** (dec, 2012) 246402.

[193] S. R. Shenoy and B. Chattopadhyay, *Anisotropic three-dimensional XY model and vortex-loop scaling*, *Phys. Rev. B* **51** (apr, 1995) 9129–9147.

[194] B. Chattopadhyay and S. R. Shenoy, *Kosterlitz-Thouless signatures from 3D vortex loops in layered superconductors*, *Phys. Rev. Lett.* **72** (jan, 1994) 400–403.

[195] R. J. Elliott, *Phenomenological Discussion of Magnetic Ordering in the Heavy Rare-Earth Metals*, *Phys. Rev.* **124** (oct, 1961) 346–353.

[196] M. E. Fisher and W. Selke, *Infinitely Many Commensurate Phases in a Simple Ising Model*, *Phys. Rev. Lett.* **44** (jun, 1980) 1502–1505.

[197] W. Selke, *The ANNNI model — Theoretical analysis and experimental application*, *Phys. Rep.* **170** (1988) 213–264.

[198] A. Dutta and J. K. Bhattacharjee, *Phase transitions in the quantum Ising and rotor models with a long-range interaction*, *Phys. Rev. B* **64** (oct, 2001) 184106.

[199] M. F. Maghrebi, Z.-X. Gong and A. V. Gorshkov, *Continuous symmetry breaking and a new universality class in 1D long-range interacting quantum systems*, 1510.01325.

[200] M. Campisi and R. Fazio, *Dissipation, Correlation and Lags in Heat Engines*, 1603.05029.

[201] M. Campisi and R. Fazio, *The power of a critical heat engine*, *Nat. Commun.* **7** (jun, 2016) 11895.

[202] A. Campa, T. Dauxois, D. Fanelli and S. Ruffo, *Physics of long-range interacting systems*, .

[203] P. C. Martin, E. D. Siggia and H. A. Rose, *Statistical Dynamics of Classical Systems*, *Phys. Rev. A* **8** (jul, 1973) 423–437.

[204] S. Schütz, H. Habibian and G. Morigi, *Cooling of atomic ensembles in optical cavities: Semiclassical limit*, *Phys. Rev. A* **88** (sep, 2013) 033427.

[205] S. Schütz and G. Morigi, *Prethermalization of Atoms Due to Photon-Mediated Long-Range Interactions*, *Phys. Rev. Lett.* **113** (nov, 2014) 203002.

[206] S. Schütz, S. B. Jäger and G. Morigi, *Thermodynamics and dynamics of atomic self-organization in an optical cavity*, *Phys. Rev. A* **92** (dec, 2015) 063808.

[207] A. Rançon and N. Dupuis, *Nonperturbative renormalization group approach to the Bose-Hubbard model*, *Phys. Rev. B* **83** (may, 2011) 172501.

[208] L. M. Sieberer, M. Buchhold and S. Diehl, *Keldysh Field Theory for Driven Open Quantum Systems*, 1512.00637.

[209] J. Berges, S. Borsányi, U. Reinosa and J. Serreau, *Nonperturbative renormalization for 2PI effective action techniques*, *Ann. Phys. (N. Y).* **320** (2005) 344–398.

[210] Y. Iqbal, R. Thomale, F. P. Toldin, S. Rachel and J. Reuther, *Functional Renormalization Group for three-dimensional Quantum Magnetism*, 1604.03438.

[211] I. Nándori, *Functional renormalization group with a compactly supported smooth regulator function*, *J. High Energy Phys.* **2013** (apr, 2013) 150.

[212] D. F. Litim, *Critical exponents from optimised renormalisation group flows*, *Nucl. Phys. B* **631** (jun, 2002) 128–158.

Appendix A

Derivations of Chapter 1

A.1 Two point connected correlation

Let us show that this is the right generator for the two point connected correlation function,

$$\begin{aligned}
&\frac{\partial^2 W[J]}{\partial J_i \partial J_j}\Big|_{\{J_i\}=0} = \frac{\partial}{\partial J_j}\frac{Z'[J]}{Z[J]}\Big|_{\{J_i\}=0} \\
&= \frac{1}{Z[j]}\frac{\partial^2 Z[J]}{\partial J_i \partial J_j}\Big|_{\{J_i\}=0} - \frac{1}{Z[J]^2}\frac{\partial Z[J]}{\partial J_j}\frac{\partial Z[J]}{\partial J_i}\Big|_{\{J_i\}=0} \\
&= \langle \phi_i \phi_j \rangle - \langle \phi_i \rangle \langle \phi_j \rangle \\
&= \langle \phi_i \phi_j \rangle - \varphi_i \varphi_j,
\end{aligned} \tag{A.1}$$

where we used the three equations

$$\begin{aligned}
Z[0] &= 1, \\
Z'[J] &= \frac{\partial Z[J]}{\partial J_i}, \\
Z'[0] &= W'[0] = \langle \phi_i \rangle = \varphi_i,
\end{aligned}$$

together with equation (1.2).

A.2 Connected correlation functions from effective action

Let us consider the second derivatives of the free energy and of the effective action

$$\frac{\partial^2 W[J]}{\partial J_i \partial J_k}\Big|_{J=0} = \frac{\partial \varphi_i[J]}{\partial J_k}\Big|_{J=0} = \langle \phi_i \phi_j \rangle - \varphi_i \varphi_j = G_{ik}, \tag{A.2}$$

$$\frac{\partial^2 \Gamma[\varphi]}{\partial \varphi_i \partial \varphi_k}\Big|_{\varphi=\varphi^*} = \frac{\partial J_i[\varphi]}{\partial \varphi_k}\Big|_{\varphi=\varphi^*} = \Gamma_{ik}, \tag{A.3}$$

thus if we perform the row by column product between the matrix G_{ik} and the Hessian of the effective action Γ_{ik} we immediately obtain

$$\sum_k G_{ik}\Gamma_{kl} = \frac{\partial \varphi_i}{\partial J_k}\frac{\partial J_k}{\partial \varphi_l} = \delta_{il} \to \Gamma^{-1}_{ik} = G_{ik}. \tag{A.4}$$

while for the three points connected correlations we have

$$\begin{aligned}
\langle \varphi_i \varphi_j \varphi_k \rangle_c &= -\sum_{lmn} G_{il} G_{jm} G_{kn} \Gamma_{lmn} \\
&= -\sum_{lmn} \Big(\frac{\partial^2 W[J]}{\partial J_i \partial J_l}\Big)\Big(\frac{\partial^2 W[J]}{\partial J_j \partial J_m}\Big)\Big(\frac{\partial^2 W[J]}{\partial J_k \partial J_n}\Big)\frac{\partial^3 \Gamma}{\partial \varphi_l \partial \varphi_m \partial \varphi_n} \\
&= -\sum_{lmn} \Big(\frac{\partial \varphi_l}{\partial J_i}\Big)\Big(\frac{\partial \varphi_m}{\partial J_j}\Big)\Big(\frac{\partial \varphi_n}{\partial J_k}\Big)\frac{\partial^3 \Gamma}{\partial \varphi_l \partial \varphi_m \partial \varphi_n} \\
&= -\frac{\partial^3 \Gamma[\varphi[J]]}{\partial J_i \partial J_j \partial J_k}\Big|_{J=0} = \frac{\partial^3 W[J]}{\partial J_i \partial J_j \partial J_k}\Big|_{J=0},
\end{aligned}$$

where we used the fact that

$$\sum_i \frac{\partial \varphi_i}{\partial J}\frac{\partial}{\partial \varphi_i} = \frac{\partial}{\partial J}.$$

Appendix B

Derivations of Chapter 2

B.1 Spin systems as $O(N)$ field theories

In the following we will demonstrate the equivalence between the partition function of spin systems and $O(N)$ field theories, we will demonstrate this equivalence for the $N = 2$ case, the so called XY model, but the demonstration is easily generalized to generic N components spin vectors, also we will only focus on the case of first neighbor interaction and we will only comment on the case of general interaction form. We thus start from the XY Hamiltonian

$$H_{XY} = -\frac{J}{2}\sum_{\langle ij\rangle}\cos\left(\theta_i - \theta_j\right), \tag{B.1}$$

we will now show that this model is equivalent to a $O(2)$ scalar field theory. First of all we shall transform it to standard spin Hamiltonian

$$H_{XY} = -\frac{J}{2}\sum_{\langle ij\rangle}\cos\left(\theta_i - \theta_j\right) = -\frac{J}{2}\sum_{\langle ij\rangle}\cos\left(\theta_i\right)\cos\left(\theta_j\right) + \sin\left(\theta_i\right)\sin\left(\theta_j\right), \tag{B.2}$$

using the trqansformation

$$s_x = s\cos\theta \tag{B.3}$$

$$s_y = s\sin\theta \tag{B.4}$$

we obtain

$$H_{XY} = -\frac{J}{2}\sum_{\langle ij\rangle}\left(s_{x,i}s_{x,j} + s_{y,i}s_{y,j}\right), \tag{B.5}$$

and obviously $s^2 = 1$. The partition function for such Hamiltonian can be written as

$$Z(\beta) = \int \mathscr{D}s \Pi_j \delta\left(s_j^2 - 1\right) e^{-\beta H_{XY}} \tag{B.6}$$

where $Ds = \Pi_i ds_{x,j} ds_{y,j}$. Latter expression can be rewritten as in the following

$$Z(\beta) = \int \mathscr{D}s\, e^{\frac{\beta J}{2}\Sigma_{\langle ij\rangle}\left(s_{x,i}s_{x,j}+s_{y,i}s_{y,j}\right)} \Pi_j \delta\left(s_j^2 - 1\right). \tag{B.7}$$

A more compact notation is

$$Z(\beta) = \int e^{-s\cdot\frac{K'}{2}\cdot s} \Pi_j \delta\left(s_j^2 - 1\right) \mathscr{D}s \tag{B.8}$$

where $s = (s_{x,1}, s_{y,1}, \cdots, s_{x,N}, s_{y,N})$ is a $2N \times 2N$ vector and N is the number of lattice sites in our system. The matrix K' has elements βJ on the upper and lower diagonals. We shall now use the identity coming from the Gaussian integral,

$$e^{-s\cdot\frac{K'}{2}\cdot s} = \left[(2\pi)^N \sqrt{\det K'}\right]^{-1} \int \mathscr{D}\phi e^{-\phi\cdot\frac{K'^{-1}}{2}\cdot\phi - s\cdot\phi} \tag{B.9}$$

Latter formula is valid for positively defined matrix, which is not the case of K'. One sufficient condition for a matrix to be positively defined is to have only positive eigenvalues. In our case we can simply redefine the matrix as follows

$$K = K' + \mu\, \mathbb{1} \tag{B.10}$$

where μ is an appropriately chosen constant to be determined. Latter transformation amounts to rescale the partition function of a constant which does not affects the physical results. We have then rewritten the partition function as

$$\begin{aligned} Z(\beta) &= \left[(2\pi)^N \sqrt{\det K'}\right]^{-1} \int \mathscr{D}\phi \int \mathscr{D}s e^{-\phi\cdot\frac{K^{-1}}{2}\cdot\phi - s\cdot\phi} \Pi_j \delta\left(s_j^2 - 1\right) \\ &= \left[(2\pi)^N \sqrt{\det K'}\right]^{-1} \int \mathscr{D}\phi\, e^{-\phi\cdot\frac{K^{-1}}{2}\cdot\phi + \Sigma_j U(\phi_j)} \end{aligned} \tag{B.11}$$

where ϕ_j are two compnents vectot and ϕ is a $2N$ vector obtained by the external product of the N two components vectors. $U(\phi) \equiv U(\rho)$ is a function of the quadratic invariant

$\rho = \phi_x^2 + \phi_y^2$. Latter statement can be demonstrated as follows

$$e^{U(\phi)} = \int ds\, e^{-s\phi}\, \delta\left(s^2-1\right) = \int \frac{dq}{2\pi} \int ds\, e^{-iq(s^2-1)} \left(\sum_j \frac{(-1)^j}{j!} (\phi \cdot s)^j \right)$$
$$= \int \frac{dq}{2\pi} e^{iq} \sum_j \frac{(-1)^j}{j!} \left\langle (\phi \cdot s)^j \right\rangle_q \tag{B.12}$$

where both s and ϕ are two components vector. $\left\langle (\phi \cdot s)^j \right\rangle_q$ is the average of s over a gaussian distribution of variance q. Such averages depend only on the square modulus of ϕ due to the properties of the Gaussian distribution. Indeed

$$\left\langle (\phi \cdot s)^j \right\rangle_q = \int d^2 s e^{-iqs^2} (s \cdot \phi)^j = \int_{-\pi}^{\pi} d\theta \int_0^{\infty} ds\, s e^{-iqs^2} (s\sqrt{\rho}\cos\theta)^j$$
$$= \sqrt{\rho}^{\,j} \int_{-\pi}^{\pi} \cos^j\theta \int_0^{\infty} ds\, e^{-iqs^2} s^{j+1}, \tag{B.13}$$

where $\rho = \phi \cdot \phi$ is the square modulus of ϕ and θ is the angle between the vector s and the vector ϕ. The integral over the angle θ immediately shows that all the odd powers of $\sqrt{\rho}$ vanish

$$\int_{-\pi}^{\pi} \cos^j\theta = \frac{\pi^2 (-1)^j 2^{j+1}}{\Gamma\left(\frac{1}{2} - \frac{j}{2}\right)^2 \Gamma(j+1)} \tag{B.14}$$

which vanishes for all the positive odd integers j. We are then left to conider only the case of $j \equiv 2n$. Each term in the series then reduce to

$$\int_0^{\infty} ds\, e^{-iqs^2} s^{2n+1} = (-1)^{n+1} \frac{i^{n+1}}{2} \frac{\Gamma(n+1)}{q^{n+1}} \tag{B.15}$$

We are left with the integral

$$-\frac{2^{2(n-1)} \pi\, i^{n+1} \Gamma(n)}{\Gamma\left(\frac{1}{2} - n\right)^2 \Gamma(2n)} \int dq \frac{e^{iq}}{q^{n+1}} \tag{B.16}$$

Finally the last integral is

$$\int_{-\infty}^{\infty} dq \frac{e^{iq}}{q^{n+1}} = 2ie^{-\frac{1}{2}i\pi n} \sin(\pi n)\Gamma(-n) = (-1)^{\frac{n}{2}} \frac{2i\pi}{n!} \tag{B.17}$$

and the potential is obtained as

$$e^{U(\rho)} = \sum_n \frac{2^{2n-1}\pi^2}{\Gamma\left(\frac{1-2n}{2}\right)^2 (2n)!}\rho^n \tag{B.18}$$

Latter result justifies expression B.11. Let us now return to the matrix K^{-1}

$$K^{-1} = \frac{\mu^{-1}}{\mathbb{1} + \frac{K'}{\mu}} = \sum_l \mu^{-l-1}(-1)^l K'^l \tag{B.19}$$

Rewriting everything in terms of the N two components vector ϕ and in the large μ limit we get

$$Z(\beta) = \left[(2\pi)^N \sqrt{\det K'}\right]^{-1} \int \mathscr{D}\phi\, e^{-\beta \frac{J}{\mu^2}\sum_{\langle ij\rangle}\phi_i\phi_j + \frac{1}{\mu}\sum_j \phi_j^2 + \sum_j U(\phi_j)} \tag{B.20}$$

which is an $O(2)$ field theory.

B.2 Regulator functions

Regulator functions have already been discussed in the literature by introducing their dimensionless form

$$R_k(p) = p^2 r(y), \quad y = p^2/k^2, \tag{B.21}$$

where $r(y)$ is dimensionless. Various types of regulator functions can be chosen, but a more general choice is the so called CSS regulator [211] which recovers all major types of regulators in its appropriate limits. By using a particular normalization [56, 58] it has the following form

$$r_{\text{css}}^{\text{norm}}(y) = \frac{\exp[\ln(2)c] - 1}{\exp\left[\frac{\ln(2)cy^b}{1-hy^b}\right] - 1}\theta(1-hy^b), \tag{B.22}$$

with the Heaviside step function $\theta(y)$ where the limits are

$$\lim_{c\to 0, h\to 1} r_{\text{css}}^{\text{norm}} = \left(\frac{1}{y^b} - 1\right)\theta(1-y^b), \tag{B.23a}$$

$$\lim_{c\to 0, h\to 0} r_{\text{css}}^{\text{norm}} = \frac{1}{y^b}, \tag{B.23b}$$

$$\lim_{c\to 1, h\to 0} r_{\text{css}}^{\text{norm}} = \frac{1}{\exp[\ln(2)y^b] - 1}. \tag{B.23c}$$

Thus, the CSS regulator has indeed the property to recover all major types of regulators: the Litim [212], the power-law [18] and the exponential [17] ones.

B.3 Flow equations at LPA'

In this appendix it is reported the derivation of the flow equations for the effective potential and the wavefunction renormalization of $O(N)$ field theory at LPA$'$ level. The ansatz for the effective action is

$$\Gamma[\phi] = \int d^d x \left\{ Z_k \partial_\mu \phi_i(x) \partial_\mu \phi_i(x) + U_t(\rho) \right\} \tag{B.24}$$

where as usual $\mu = x, y, z$, $\rho = \frac{\phi_i(x)\phi_i(x)}{2}$, and the sum over repeated indexes are implicit. The derivative of the effective action with respect to the field reads

$$\Gamma_t^{(2)}(-p, p) = Z_k p^2 + \mu_{g,m} \tag{B.25}$$

where $p^2 = p_x^2 + p_y^2 + p_z^2$ and

$$\begin{aligned} \mu_m &= U^{(1)}(\rho) + 2\rho U^{(2)}(\rho), \\ \mu_g &= U^{(1)}(\rho). \end{aligned} \tag{B.26}$$

The index (g, m) depends if the derivation is taken in the component on the field which have zero or non zero average.

The scale derivative of the two point function is

$$\partial_t \Gamma_{ii}^{(2)}(-p, p) = \partial_t Z_k p^2 + \partial_t \mu \tag{B.27}$$

where the value of the μ depends on whether the index i indicates finite average field component $i = 1$ or zero average field components $i \neq 1$. The second derivative of the Wetterich equation with respect to the field yields

$$\partial_t \Gamma_{ii}^{(2)}(-p, p) = \sum_{jl} \int \frac{d^d q}{(2\pi)^d} \partial_t R_t(q) G_l(q)^2 \Gamma_{ijl}^{(3)}(\rho)^2 G_j(p+q), \tag{B.28}$$

for the flow of the wavefunction renormalization we can then use two definitions,

$$Z_k = \frac{1}{2}\lim_{p\to 0}\frac{d^2}{dp}\partial_t\Gamma^{(2)}_{11}(-p,p). \tag{B.29}$$

$$Z_k = \frac{1}{2}\lim_{p\to 0}\frac{d^2}{dp^2}\partial_t\Gamma^{(2)}_{ii}(-p,p). \tag{B.30}$$

depending if we define the wavefunction from the massive, $i = 1$, or Goldstone $i \neq 1$ propagator. When we apply the derivatives on the right end side of equation (B.29) or (B.30), they go under the integral sign and act in the only part of the integrand which depends on p,i.e. $G(p+q)$, thus we get,

$$\partial_t Z_k = \int \frac{d^d q}{(2\pi)^d}\partial_t R_t(q) G_g(q)^2 \Gamma^{(3)}(\rho)^2 \frac{d}{dp_z^2} G_m(p+q)\Big|_{p=0} \tag{B.31}$$

$$\partial_t Z_k = \int \frac{d^d q}{(2\pi)^d}\partial_t R_t(q) G_m(q)^2 \Gamma^{(3)}(\rho)^2 \frac{d^2}{dp^2} G_m(p+q)\Big|_{p=0} \tag{B.32}$$

The green functions are

$$G(p+q) = \frac{1}{Z_k|p+q|^2 + \mu + R_t(p+q)}, \tag{B.33}$$

It is convenient to introduce the definitions

$$x = (p^2 + q^2 + 2pq\cos\theta), \tag{B.34}$$

where θ is the angle between p and q. We use the equivalence

$$\frac{1}{2}\frac{d^2}{dp^2} = \frac{1}{2}\left(\frac{d^2x}{dp^2}\frac{d}{dx} + \left(\frac{dx}{dp}\right)^2\frac{d^2}{dx^2}\right) \tag{B.35}$$

The derivatives are

$$\begin{aligned}\frac{dx}{dp}\Big|_0 &= 2q\cos\theta.\\ \frac{d^2x}{dp^2}\Big|_0 &= 2.\end{aligned} \tag{B.36}$$

We introduce the Litim regulator

$$R_t(q) = Z_k(k^2 - q^2)\theta(k^2 - q^2), \tag{B.37}$$

or rewriting it in the x variable,

$$R_t(x) = Z_k(k^2 - x)\theta(k^2 - x). \tag{B.38}$$

We also need to compute its time derivative

$$\partial_t R_t(q) = \partial_t Z_k(k^2 - q^2)\theta(k^2 - q^2) - 2Z_k k^2 \theta(k^2 - q^2) \tag{B.39}$$

Now we list the derivatives of the cutoff,

$$R_{t,x}(x)\Big|_{p=0} = -Z_k\theta(k^2 - q^2) - Z_k(k^\sigma - q^2)\delta(k^\sigma - q^2 - \gamma q_z^2). \tag{B.40}$$

$$R_{t,xx}(x)\Big|_{p=0} = Z_k\delta(k^2 - q^2), \tag{B.41}$$

using above expressions into (B.35) we obtain that only one terms of the derivatives survive,

$$\begin{aligned} \frac{d}{dx}G(q+p) &= G_x = 0 \\ \frac{d^2}{dx^2}G(q+p) &= G_{xx} = -G(x)^2 R_{t,xx}(x). \end{aligned} \tag{B.42}$$

The derivation now proceeds taking into account only definition (B.31) which is the one mostly used in FRG application to $O(N)$ models. The result for definition (B.10) is given at last.

$$\begin{aligned} \partial_t Z_k &= -\Gamma^{(3)}(\rho)^2 \int \frac{d^d q}{(2\pi)^d} G_g(q)^2 G_m(q)^2 \partial_t R_t(q) \left(\frac{dx}{dp}\right)^2 R_{t,xx}(x) = \\ &= -\Gamma^{(3)}(\rho)^2 \int \frac{d^d q}{(2\pi)^d} G_g(q)^2 G_m(q)^2 \partial_t R_t(q) 4q^2 \cos\theta^2 Z_k \delta(k^2 - q^2). \end{aligned} \tag{B.43}$$

The expression for the Green function is,

$$G(q) = \frac{1}{Z_k k^2 + \mu}, \tag{B.44}$$

which do not actually depend on the momentum. Expression (B.42) becomes,

$$\partial_t Z_k = -\Gamma^{(3)}(\rho)^2 G_m(\rho)^2 G_g(\rho)^2 \int \frac{d^d q}{(2\pi)^d} \partial_t R_t(q) 4q^2 \cos\theta^2 Z_k \delta(k^2 - q^2). \tag{B.45}$$

Thus the calculation reduces to the integration,

$$-\int \frac{d^d q}{(2\pi)^d} Z_k 4q^2 \cos\theta^2 2 Z_k k^2 \theta(k^2-q^2)\delta(k^2-q^2), \tag{B.46}$$

in order to explicitly pursue the integration we should pass to cilindical coordinates, for simplicity we restrict ourselves to three dimensions $d^3q \to qdqd\theta dq_z$ and remember that $\delta(x)\theta(x) = \delta(x)/2$,

$$-\int_0^{+\infty} \frac{q^{d-1}dq}{2\pi} \int_0^{2\pi} \frac{d\theta}{2\pi} 4Z_k^2 q^2 \cos\theta^2 k^2 \delta(k^2-q^2), \tag{B.47}$$

Next steps are to integrate over the angle varibles which are not present into the eqution but in the $\cos\theta^2$ term in (B.47), the results are $\int_0^{2\pi} d\theta \cos\theta^2 = \pi$ and $\int_0^{2\pi} d\theta = 2\pi$. Also we have to modify the integration tems in such a way to take the δ-function into account. The δ-function can be trasformed according to

$$\delta(f(q)) = \frac{\delta(q-q_0)}{|f'(q)|} \tag{B.48}$$

where q_0 is the solution of $f(q_0) = 0$. In our case we have

$$\begin{aligned} f(q) &= k^2 - q^2 \\ f'(q) &= -2q \\ q_0 &= k \end{aligned} \tag{B.49}$$

After pursuing the integration and writing explicitly the value of $\Gamma^{(3)}(\rho)$ we obtain the result for the flow of the Z_k,

$$\partial_t Z_k = \frac{4c_d Z_k^2 k^5 \rho_0 U^{(2)}(\rho)^2}{(Z_k k^2 + \mu_m)^2 (Z_k k^2 + \mu_g)^2} \tag{B.50a}$$

$$\partial_t Z_k = \frac{4\rho\, c_d Z_k^2 k^5 \left(2\rho U^{(3)}(\rho) + 3U^{(2)}(\rho)\right)^2}{(Z_k k^2 + \mu_m)^4} \tag{B.50b}$$

where the first result has been obtained using definition (B.31) and the second using the alternative definition (B.32). The equation for the potential can be obtained directly from the wetterich equation when evaluated at constant fields,

$$\partial_t U_t(\rho) = \frac{1}{2}\int \frac{d^3 q}{(2\pi)^3} \partial_t R_t(q)(G_m(q) + (N-1)G_g(q)) \tag{B.51}$$

again using expressions (B.43) and (B.42) we obtain,

$$\partial_t U_t(\rho) = (G_m(\rho) + (N-1)G_g(\rho))\frac{1}{2}\int \frac{d^3q}{(2\pi)^3}(\partial_t Z_k(k^2-q^2) - 2Z_k k^2)\theta(k^2-q^2). \quad \text{(B.52)}$$

Everything reduce to the simple integration,

$$\int \frac{d^3q}{(2\pi)^3}(\partial_t Z_k(k^2-q^2-\gamma q_z^2) - 2Z_k k^2 - Z_k \partial_t \gamma q_z^2)\theta(k^2-q^2-\gamma q_z^2). \quad \text{(B.53)}$$

which yields the result

$$\partial_t U_t(\rho) = -Z_k k^5 c_d \left(\frac{1-\frac{\eta}{d+2}}{Z_k+\mu_m} + (N-1)\frac{1-\frac{\eta}{d+2}}{Z_k+\mu_g} \right) \quad \text{(B.54)}$$

B.4 Derivation of $\partial_t V_k$ and $\partial_t Z_k$

The effective average action to the second order in the derivative expansion is given by:

$$\Gamma_k = \int_x \left(\frac{1}{2} Z(\varphi)\partial_\mu \varphi \partial^\mu \varphi + V(\varphi) \right), \quad \text{(B.55)}$$

where $V(\varphi)$ is the effective potential and $Z(\varphi)$ is the generalized wave function renormalization.

First of all we need to calculate the functional derivatives of this action. The the second functional derivative is

$$\Gamma^{(2)}_{x_1 x_2} = \int d^d x \left\{ \frac{1}{2} Z^{(2)} \delta(x-x_2)\delta(x-x_1)\partial_\mu \varphi\, \partial^\mu \varphi + Z^{(1)}\delta(x-x_2)\partial_\mu \varphi\, \partial^\mu \delta(x-x_1) + \right.$$
$$\left. + Z^{(1)}\delta(x-x_1)\partial_\mu \varphi\, \partial^\mu \delta(x-x_2) + Z\,\partial_\mu \delta(x-x_2)\partial^\mu \delta(x-x_1) + V^{(2)}\delta(x-x_1)\delta(x-x_2) \right\}, \quad \text{(B.56)}$$

The third functional derivative is

$$\Gamma^{(3)}_{x_1 x_2 x_3} = \int d^d x \left\{ \frac{1}{2} Z^{(3)} \delta(x-x_3)\delta(x-x_2)\delta(x-x_1)\partial_\mu \varphi\, \partial^\mu \varphi + Z^{(2)}\delta(x-x_2)\delta(x-x_1)\partial_\mu \varphi\, \partial^\mu \delta(x-x_3) + \right.$$
$$+ Z^{(2)}\delta(x-x_3)\delta(x-x_2)\partial_\mu \varphi\, \partial^\mu \delta(x-x_1) + Z^{(2)}\delta(x-x_3)\delta(x-x_1)\partial_\mu \varphi\, \partial^\mu \delta(x-x_2) +$$
$$+ Z^{(1)}\delta(x-x_2)\partial_\mu \delta(x-x_3)\,\partial^\mu \delta(x-x_1) + Z^{(1)}\delta(x-x_1)\partial_\mu \delta(x-x_3)\,\partial^\mu \delta(x-x_2) +$$
$$\left. + Z^{(1)}\delta(x-x_3)\,\partial_\mu \delta(x-x_2)\partial^\mu \delta(x-x_1) + V^{(3)}\delta(x-x_1)\delta(x-x_2)\delta(x-x_3) \right). \quad \text{(B.57)}$$

For the fourth we give it directly for constant field

$$\begin{aligned}\Gamma^{(4)}_{x_1x_2x_3x_4} = \int d^dx \Big\{ &\frac{1}{2}Z^{(4)}\delta(x-x_4)\delta(x-x_3)\delta(x-x_2)\delta(x-x_1)\partial_\mu\varphi\,\partial^\mu\varphi + \\ &Z^{(3)}\delta(x-x_3)\delta(x-x_2)\delta(x-x_1)\partial_\mu\varphi\,\partial^\mu\delta(x-x_4) + \\ &Z^{(3)}\delta(x-x_4)\delta(x-x_2)\delta(x-x_1)\partial_\mu\varphi\,\partial^\mu\delta(x-x_3) + \\ &Z^{(3)}\delta(x-x_3)\delta(x-x_4)\delta(x-x_1)\partial_\mu\varphi\,\partial^\mu\delta(x-x_2) + \\ &Z^{(3)}\delta(x-x_4)\delta(x-x_2)\delta(x-x_3)\partial_\mu\varphi\,\partial^\mu\delta(x-x_1) + \\ &Z^{(2)}\delta(x-x_2)\delta(x-x_1)\partial_\mu\delta(x-x_3)\,\partial^\mu\delta(x-x_4) + \\ &Z^{(2)}\delta(x-x_2)\delta(x-x_1)\partial_\mu\delta(x-x_4)\,\partial^\mu\delta(x-x_3) + \\ &Z^{(2)}\delta(x-x_3)\delta(x-x_1)\partial_\mu\delta(x-x_4)\,\partial^\mu\delta(x-x_2) + \\ &Z^{(2)}\delta(x-x_2)\delta(x-x_3)\partial_\mu\delta(x-x_4)\,\partial^\mu\delta(x-x_1) + \\ &V^{(4)}\delta(x-x_1)\delta(x-x_2)\delta(x-x_3)\delta(x-x_4)\Big\}\,. \end{aligned} \tag{B.58}$$

Higher functional derivatives are easely written.

Since we are interested in equilibrium constant field configuration we evaluate latter expressions in constant field $\varphi(x) = \varphi$,

$$\Gamma^{(2)}_{x_1x_2} = Z\int d^dx \Big\{ \partial_\mu\delta(x-x_2)\partial^\mu\delta(x-x_1) + V^{(2)}\delta(x-x_1)\delta(x-x_2)\Big\}\,, \tag{B.59}$$

$$\begin{aligned}\Gamma^{(3)}_{x_1x_2x_3} = Z^{(1)}\int_x \big\{ &\delta(x-x_2)\partial_\mu\delta(x-x_3)\,\partial^\mu\delta(x-x_1) + \delta(x-x_1)\partial_\mu\delta(x-x_3)\,\partial^\mu\delta(x-x_2) + \\ &+\delta(x-x_3)\,\partial_\mu\delta(x-x_2)\partial^\mu\delta(x-x_1)\big\} + V^{(3)}\delta(x_1-x_2)\delta(x_1-x_3)\,. \end{aligned} \tag{B.60}$$

$$\begin{aligned}\Gamma^{(4)}_{x_1x_2x_3x_4} = \int d^dx \Big\{ &Z^{(2)}\delta(x-x_2)\delta(x-x_1)\partial_\mu\delta(x-x_3)\,\partial^\mu\delta(x-x_4) + \\ &Z^{(2)}\delta(x-x_2)\delta(x-x_1)\partial_\mu\delta(x-x_4)\,\partial^\mu\delta(x-x_3) + \\ &Z^{(2)}\delta(x-x_3)\delta(x-x_1)\partial_\mu\delta(x-x_4)\,\partial^\mu\delta(x-x_2) + \\ &Z^{(2)}\delta(x-x_2)\delta(x-x_3)\partial_\mu\delta(x-x_4)\,\partial^\mu\delta(x-x_1) + \\ &V^{(4)}\delta(x-x_1)\delta(x-x_2)\delta(x-x_3)\delta(x-x_4)\Big\} \end{aligned} \tag{B.61}$$

It is now convenient to rewrite everything in momentum space

$$\begin{aligned}\varphi_x &= \frac{1}{(2\pi)^d}\int d^d q\, \varphi_q\, e^{-ixq} \\ \varphi_q &= \int d^d x\, \varphi_x\, e^{ixq}\end{aligned} \tag{B.62}$$

The relation for the dirac δ-function becomes

$$\delta(x) = \frac{1}{(2\pi)^d}\int d^d q\, e^{-ixq}\,. \tag{B.63}$$

We can know calculate

$$\begin{aligned}\Gamma^{(2)}_{q_1 q_2} &= \int d^d x_1 d^d x_2\, \Gamma^{(2)}_{x_1 x_2}\, e^{i(x_1 q_1 + x_2 q_2)} \\ &= \int d^d x_1 d^d x_2 \left(\partial_\mu \delta(x-x_2)\partial^\mu \delta(x-x_1) + V^{(2)}\delta(x-x_1)\delta(x-x_2)\right) e^{i(x_1 q_1 + x_2 q_2)} \\ &= (2\pi)^{-2d}\int d^d x_1 d^d x_2 d^d p_1 d^d p_2 d^d x \left(-Z\, p_1\cdot p_2 + V^{(2)}\right) e^{ip_1(x-x_1)}\, e^{ip_2(x-x_2)}\, e^{i(x_1 q_1 + x_2 q_2)} \\ &= (2\pi)^d \int_{p_1 p_2} \left(-Z\, p_1\cdot p_2 + V^{(2)}\right)\delta(p_1 - q_1)\delta(p_2 - q_2)\delta(p_1 + p_2) \\ &= (2\pi)^d \left(-Z\, q_1\cdot q_2 + V^{(2)}\right)\delta(q_1 + q_2)\,.\end{aligned} \tag{B.64}$$

On the same lines we get

$$\Gamma^{(3)}_{q_1 q_2 q_3} = (2\pi)^d \left[-Z^{(1)}\left(q_1\cdot q_2 + q_1\cdot q_3 + q_2\cdot q_3\right) + V^{(3)}\right]\delta(q_1 + q_2 + q_3) \tag{B.65}$$

and

$$\begin{aligned}\Gamma^{(4)}_{q_1 q_2 q_3 q_4} = (2\pi)^d \Big[&-Z^{(2)}\left(q_1\cdot q_2 + q_1\cdot q_3 + q_1\cdot q_4 + \right. \\ &\left. + q_2\cdot q_3 + q_2\cdot q_4 + q_3\cdot q_4\right) + V^{(4)}\Big]\delta(q_1 + q_2 + q_3 + q_4)\,.\end{aligned} \tag{B.66}$$

The flow equations for the potential is

$$\partial_t V_t = \int \frac{d^d q}{(2\pi)^d} G(q) R_k(q), \tag{B.67}$$

and for the two point function in the standard form is

$$\begin{aligned}\partial_t \Gamma^{(2)}_{t,p,-p} = &\int d^d q\, G(q)\Gamma^{(3)}_{q,p,-q-p} G(q+p)\Gamma^{(3)}_{q+p,-p,-q} G(q)\partial_t R_k(q) \\ &-\frac{1}{2}\int d^d q\, G(q)\Gamma^{(4)}_{q,p,-p,-q} G(q)\partial_t R_k(q)\,,\end{aligned} \tag{B.68}$$

where the short hands are obvious. We have

$$\begin{aligned}\Gamma^{(4)}_{q,p,-p,-q} &= Z^{(2)}\left(q^2+p^2\right)+V^{(4)} \\ \Gamma^{(3)}_{q,p,-q-p} &= Z^{(1)}\left(q^2+q\cdot p+p^2\right)+V^{(3)} \\ \Gamma^{(3)}_{q+p,-p,-q} &= Z^{(1)}\left(q^2+q\cdot p+p^2\right)+V^{(3)}.\end{aligned} \tag{B.69}$$

In order to evaluate the flow of the field dependent wave-function we use the definition

$$\partial_t Z(\varphi) = \frac{1}{2}\lim_{p\to 0}\frac{d^2}{dp^2}\partial_t \Gamma^{(2)}_t(-p,p). \tag{B.70}$$

When we apply the derivatives on the right end side of equation (B.68), they go under the integral sign and act in the only part of the integrand which depends on p,i.e. $G(p+q)$, thus we get,

$$\partial_t Z(\varphi) = \frac{1}{2}\int \frac{d^d q}{(2\pi)^d}\partial_t R_t(q) G(q)^2 \Gamma^{(3)}_{q,p,-p-q}\frac{d^2}{dp^2} G(p+q)\Gamma^{(3)}_{-q,-p,p+q}\Big|_{p=0} \tag{B.71}$$

$$+\int \frac{d^d q}{(2\pi)^d}\partial_t R_t(q) G(q)^2 \Gamma^{(3)}_{q,p,-p-q} G(p+q)\frac{d^2}{dp^2}\Gamma^{(3)}_{-q,-p,p+q}\Big|_{p=0} \tag{B.72}$$

$$+4\int \frac{d^d q}{(2\pi)^d}\partial_t R_t(q) G(q)^2 \Gamma^{(3)}_{q,p,-p-q}\frac{d}{dp} G(p+q)\frac{d}{dp}\Gamma^{(3)}_{-q,-p,p+q}\Big|_{p=0} \tag{B.73}$$

$$+\int \frac{d^d q}{(2\pi)^d}\partial_t R_t(q) G(q)^2 G(p+q)\left(\frac{d}{dp}\Gamma^{(3)}_{-q,-p,p+q}\right)^2\Big|_{p=0} \tag{B.74}$$

$$-\frac{1}{4}\int d^d q\, G(q)\frac{d^2}{dp^2}\Gamma^{(4)}_{q,p,-p,-q} G(q)\partial_t R_k(q)\Big|_{p=0}. \tag{B.75}$$

The calculation is straightforward but complex, we shall then carry it out term by term. We then define the first term T_1 as the right hand side of (B.71)

$$T_1 = \int \frac{d^d q}{(2\pi)^d}\partial_t R_t(q) G(q)^2 \Gamma^{(3)}_{q,p,-p-q}\frac{1}{2}\frac{d^2}{dp^2} G(p+q)\Gamma^{(3)}_{-q,-p,p+q}\Big|_{p=0} \tag{B.76}$$

with the other terms defined as in lines (B.72), (B.73), (B.74) and (B.75)

$$T_2 = 2\int \frac{d^d q}{(2\pi)^d}\partial_t R_t(q)G(q)^2\Gamma^{(3)}_{q,p,-p-q}G(p+q)\frac{1}{2}\frac{d^2}{dp^2}\Gamma^{(3)}_{-q,-p,p+q}\Big|_{p=0} \tag{B.77}$$

and

$$T_3 = 2\int \frac{d^d q}{(2\pi)^d}\partial_t R_t(q)G(q)^2\Gamma^{(3)}_{q,p,-p-q}\frac{d}{dp}G(p+q)\frac{d}{dp}\Gamma^{(3)}_{-q,-p,p+q}\Big|_{p=0} \tag{B.78}$$

and

$$T_4 = \int \frac{d^d q}{(2\pi)^d}\partial_t R_t(q)G(q)^2 G(p+q)\left(\frac{d}{dp}\Gamma^{(3)}_{-q,-p,p+q}\right)^2\Big|_{p=0} \tag{B.79}$$

and

$$T_5 = -\frac{1}{2}\int \frac{d^d q}{(2\pi)^d}\,G(q)\frac{1}{2}\frac{d^2}{dp^2}\Gamma^{(4)}_{q,p,-p,-q}G(q)\partial_t R_k(q)\,. \tag{B.80}$$

The most complex term to evaluate is T_1 we will then left it aside for the moment. We the pursue the evaluation of these terms in reverse order. After deriving the vertex term in (B.80) we obtain

$$T_5 = -\frac{Z^{(2)}}{2}\int \frac{d^d q}{(2\pi)^d}\,G(q)^2\partial_t R_k(q)\,. \tag{B.81}$$

we should then pass to spherical coordinates, integrate over the angular variables and finally transform the integration variable accordingly to $q^2 = x$,

$$T_5 = -Z^{(2)}\frac{s_d}{4}\int x^{\frac{d}{2}-1}\,G(x)^2\partial_t R_k(x)dx = -Z^{(2)}\frac{s_d}{4}Q_{\frac{d}{2}}[G^2\dot{R}]. \tag{B.82}$$

where we introduced the Mellin transformation,

$$Q_m[f] = \int x^{m-1}f(x)dx \tag{B.83}$$

and the short hand notation $\dot{A} = \partial_t A$. Applying the same notation to (B.79) we obtain,

$$T_4 = (Z^{(1)})^2\frac{s_d}{2d}\int x^{\frac{d}{2}}\partial_t R_t(x)G(x)^3dx = (Z^{(1)})^2\frac{s_d}{2d}Q_{\frac{d}{2}+1}[G^3\dot{R}] \tag{B.84}$$

while for (B.78)

$$\begin{aligned} T_3 &= (Z^{(1)})^2\frac{2s_d}{d}\int x^{\frac{d}{2}+1}\partial_t R_t(x)G(x)^2G_x(x)dx + Z^{(1)}V^{(3)}\frac{2s_d}{d}\int x^{\frac{d}{2}}\partial_t R_t(x)G(x)^2G_x(x)dx \\ &= (Z^{(1)})^2\frac{2s_d}{d}Q_{\frac{d}{2}+2}[G^2G_x\dot{R}] + Z^{(1)}V^{(3)}\frac{2s_d}{d}Q_{\frac{d}{2}+1}[G^2G_x\dot{R}] \end{aligned} \tag{B.85}$$

and for (B.77)

$$\begin{aligned} T_2 &= (Z^{(1)})^2 s_d \int x^{\frac{d}{2}} \partial_t R_t(x) G(x)^3 dx + Z^{(1)} V^{(3)} s_d \int x^{\frac{d}{2}-1} \partial_t R_t(x) G(x)^3 dx \\ &= (Z^{(1)})^2 s_d Q_{\frac{d}{2}+1}[G^3 \dot{R}] + Z^{(1)} V^{(3)} s_d Q_{\frac{d}{2}}[G^3 \dot{R}] \end{aligned} \tag{B.86}$$

The computation of T_1 needs some more efforts, we should firstly write the Green function form explicitly

$$G(p+q) = \frac{1}{Z(\varphi)|p+q|^2 + U_k^{(2)}(\varphi) + R_t(p+q)}, \tag{B.87}$$

We can transform the derivative using the definitions

$$x = (p^2 + q^2 + 2pq\cos\theta), \tag{B.88}$$

We use the equivalence

$$\frac{1}{2}\frac{d^2}{dp^2} = \frac{1}{2}\left(\frac{d^2x}{dp^2}\frac{d}{dx} + \left(\frac{dx}{dp}\right)^2 \frac{d^2}{dx^2}\right) \tag{B.89}$$

The derivatives are

$$\begin{aligned} \frac{dx}{dp}\Big|_0 &= 2q\cos\theta. \\ \frac{d^2x}{dp^2}\Big|_0 &= 2. \end{aligned} \tag{B.90}$$

We can also explicitly compute the derivatives of the propagator with respect to x,

$$\begin{aligned} &\frac{d}{dx}G(q+p) = G_x = -G(x)^2(Z(\varphi) + R_{t,x}(x)), \\ &\frac{d^2}{dx^2}G(q+p) = G_{xx} = 2G(x)^3(Z(\varphi) + R_{t,x}(x))^2 - G(x)^2 R_{t,xx}(x). \end{aligned} \tag{B.91}$$

The same must be done for the vertexes,

$$\begin{aligned} \frac{1}{2}\frac{d^2}{dp^2}\Gamma^{(3)}_{-q,-p,p+q}\Big|_{p=0} &= Z^{(1)}(\varphi), \\ \frac{1}{2}\frac{d^2}{dp^2}\Gamma^{(4)}_{-q,-p,p+q}\Big|_{p=0} &= Z^{(2)}(\varphi). \end{aligned} \tag{B.92}$$

We can then rewrite the T_1 coefficient in the following way,

$$T_1 = \int \frac{d^d q}{(2\pi)^d} \partial_t R_t(q) G(q)^2 \left(Z^{(1)} x + V^{(3)} \right)^2 \left(G_x + 2q^2 \cos^2\theta G_{xx} \right) \Big|_{p=0}. \tag{B.93}$$

When evaluated in $p = 0$ we obtain $x = q^2$, we then use latter relation and we rewrite the integrals using only the x variable, we also integrate over the angular variables obtaining

$$\begin{aligned} T_1 &= \frac{s_d}{2} \int x^{\frac{d}{2}-1} dx\, \partial_t R_t(x) G(x)^2 \left(Z^{(1)} x + V^{(3)} \right)^2 \left(G_x(x) + \frac{2}{d} x G_{xx}(x) \right) \\ &= (Z^{(1)})^2 \frac{s_d}{2} Q_{\frac{d}{2}+2}[G^2 G_x \dot{R}] + (Z^{(1)})^2 \frac{s_d}{d} Q_{\frac{d}{2}+3}[G^2 G_{xx} \dot{R}] + Z^{(1)} V^{(3)} s_d Q_{\frac{d}{2}+1}[G^2 G_x \dot{R}] \\ &+ Z^{(1)} V^{(3)} \frac{2 s_d}{d} Q_{\frac{d}{2}+2}[G^2 G_{xx} \dot{R}] + (V^{(3)})^2 \frac{s_d}{2} Q_{\frac{d}{2}}[G^2 G_x \dot{R}] + (V^{(3)})^2 \frac{s_d}{d} Q_{\frac{d}{2}+1}[G^2 G_{xx} \dot{R}]. \end{aligned}$$

It should be noted that the universal quantities of the model under study are invariant under transformations of the field and the actions, which leave the mass of the model invariant,

$$\begin{aligned} \varphi &\to \Omega \varphi, \\ \Gamma[\varphi] &\to \Omega \Gamma[\varphi]. \end{aligned} \tag{B.94}$$

We can choice $\Omega = \frac{s_d}{2d}$ and scale out this coefficient from our flow equation. We finally obtain for the flow equations,

$$\begin{aligned} \partial_t V_k(\varphi) &= Q_{\frac{d}{2}}[G\dot{R}] \\ \partial_t Z_k(\varphi) &= -\frac{d}{2} Z^{(2)}(\varphi) Q_{\frac{d}{2}}[G^2 \dot{R}] + Z^{(1)}(\varphi)^2 (2d+1) Q_{\frac{d}{2}+1}[G^3 \dot{R}] + Z^{(1)}(\varphi)^2 (d+4) Q_{\frac{d}{2}+2}[G^2 G_x \dot{R}] \\ &+ Z^{(1)}(\varphi)^2 2 Q_{\frac{d}{2}+3}[G^2 G_{xx} \dot{R}] + Z^{(1)}(\varphi) V^{(3)}(\varphi) 2d Q_{\frac{d}{2}}[G^3 \dot{R}] \\ &+ Z^{(1)}(\varphi) V^{(3)}(\varphi) 2(d+2) Q_{\frac{d}{2}+1}[G^2 G_x \dot{R}] + Z^{(1)}(\varphi) V^{(3)}(\varphi) 4 Q_{\frac{d}{2}+2}[G^2 G_{xx} \dot{R}] \\ &+ V^{(3)}(\varphi)^2 d Q_{\frac{d}{2}}[G^2 G_x \dot{R}] + V^{(3)}(\varphi)^2 2 Q_{\frac{d}{2}+1}[G^2 G_{xx} \dot{R}]. \end{aligned} \tag{B.95}$$

To further proceed it is necessary to specify the cutoff functions. We will focus on two particular forms. The Litim or optimized cutoff case is

$$\begin{aligned} R_k(x) &= Z_k (k^2 - x) \theta(k^2 - x) \\ R_{k,x}(x) &= -Z_k \theta(k^2 - x) \\ R_{k,xx}(x) &= Z_k \delta(k^2 - x) \\ \dot{R}_k(x) &= 2 Z_k k^2 \theta(k^2 - x) - \dot{Z}_k (k^2 - x) \theta(k^2 - x). \end{aligned} \tag{B.96}$$

while the Morris or power law regulator is written as

$$\begin{aligned} R_k(x) &= Z_k \frac{k^4}{x} \\ R_{k,x}(x) &= -Z_k \frac{k^4}{x^2} \\ R_{k,xx}(x) &= Z_k \frac{2k^4}{x^3} \\ \dot{R}_k(x) &= \dot{Z}_k \frac{k^4}{x} + Z_k \frac{4k^4}{x}. \end{aligned} \tag{B.97}$$

Let us start with the Litim cutoff, to give an explicit expression for equations (**??**) and (B.95) it is necessary to calculate the following quantities,

$$\begin{aligned} Q_m[G^n \dot{R}] &= \int_0^{k^2} x^{m-1} dx \frac{2Z_k k^2 + \dot{Z}_k (k^2 - x)}{((Z_k(\varphi) - Z_k)x + Z_k k^2 + V_k^{(2)}(\varphi))^n}, \\ Q_m[G^n G_x \dot{R}] &= -\int_0^{k^2} x^{m-1} dx \frac{(2Z_k k^2 + \dot{Z}_k (k^2 - x))(Z_k(\varphi) - Z_k)}{((Z_k(\varphi) - Z_k)x + Z_k k^2 + V_k^{(2)}(\varphi))^{n+2}}, \\ Q_m[G^n G_{xx} \dot{R}] &= \int_0^{k^2} x^{m-1} dx \frac{2(2Z_k k^2 + \dot{Z}_k (k^2 - x))(Z_k(\varphi) - Z_k)^2}{((Z_k(\varphi) - Z_k)x + Z_k k^2 + V_k^{(2)}(\varphi))^{n+3}} - \frac{2Z_k^2 \delta(k^2 - x)}{((Z_k(\varphi) - Z_k)x + Z_k k^2 + V_k^{(2)}(\varphi))^{n+2}}. \end{aligned} \tag{B.98}$$

While in the Morris case,

$$\begin{aligned} Q_m[G^n \dot{R}] &= \int_0^{\infty} x^{m+n-2} dx \frac{4Z_k k^4 + \dot{Z}_k k^4}{(Z_k(\varphi)x^2 + Z_k k^4 + U^{(2)}(\varphi)x)^n}, \\ Q_m[G^n G_x \dot{R}] &= -\int_0^{\infty} x^{m+n-2} dx \frac{(4Z_k k^4 + \dot{Z}_k k^4)(Z_k(\varphi)x^2 - Z_k k^4)}{(Z_k(\varphi)x^2 + Z_k k^4 + U^{(2)}(\varphi)x)^{n+2}}, \\ Q_m[G^n G_{xx} \dot{R}] &= 2\int_0^{\infty} x^{m+n-3} dx \frac{(4Z_k k^4 + \dot{Z}_k k^4)(Z_k(\varphi)x - Z_k k^4)^2}{(Z_k(\varphi)x^2 + Z_k k^4 + U^{(2)}(\varphi)x)^{n+3}} \\ &\quad - 2\int_0^{k^2} x^{m+n-3} dx \frac{Z_k k^4 (4Z_k k^4 + \dot{Z}_k k^4)}{(Z_k(\varphi)x^2 + Z_k k^4 + U^{(2)}(\varphi)x)^{n+2}}. \end{aligned} \tag{B.99}$$

B.4.1 Dimensionless variables

In order to obtain a consistent RG procedure we must consider dimensionless (or scaled) variables, which have finite fixed point values. These are defined as

$$\begin{aligned}
x =& k^2 \bar{x}. \\
\varphi =& Z_k^{-\frac{1}{2}} k^{\frac{d-2}{2}} \tilde{\varphi}, \\
Z_k(\varphi) =& Z_k \bar{Z}_k(\tilde{\varphi}), \\
R_k(x) =& Z_k k^2 \tilde{x} r(\tilde{x}), \\
V_k(\varphi) =& k^d \tilde{V}_k(\tilde{\varphi}), \\
Q_m[G^n \dot{R}] =& k^{2(m-n)} \tilde{Q}_{m+1}[\tilde{G}^n \left(2r'(\tilde{x}) - \eta\, r(\tilde{x})\right)], \\
Q_m[G^n G_x \dot{R}] =& k^{2(m-n-1)} \tilde{Q}_{m+1}[\tilde{G}^n \tilde{G}_x \left(2r'(\tilde{x}) - \eta\, r(\tilde{x})\right)], \\
Q_m[G^n G_{xx} \dot{R}] =& k^{2(m-n)-3} \tilde{Q}_{m+1}[\tilde{G}^n \tilde{G}_{xx} \left(2r'(\tilde{x}) - \eta\, r(\tilde{x})\right)],
\end{aligned} \tag{B.100}$$

where we used the definition $\eta = -\partial_t Z_k / Z_k$.

Litim cutoff

In the Litim cutoff case we obtain for the $\tilde{Q}$-functionals in terms of a single threshold function

$$q_{m,n}(z,v) = \int_0^1 \frac{\bar{x}^{m-1} d\bar{x}}{((z-1)x+1+v)^n}, \tag{B.101}$$

the three Q-functionals then read

$$\begin{aligned}
k^{2(n-m)} Q_m[G^n \dot{R}] &= (2-\eta) q_{m,n}(\tilde{Z}, \tilde{V}^{(2)}) + \eta\, q_{m+1,n}(\tilde{Z}, \tilde{V}^{(2)}), \\
k^{2(n-m+1)} Q_m[G^n G_x \dot{R}] &= \left[(2-\eta) q_{m,n+2}(\tilde{Z}, \tilde{V}^{(2)}) + \eta\, q_{m+1,n+2}(\tilde{Z}, \tilde{V}^{(2)})\right] (\tilde{Z}-1), \\
k^{2(n-m)+3} Q_m[G^n G_{xx} \dot{R}] &= 2\left[(2-\eta) q_{m,n+3}(\tilde{Z}, \tilde{V}^{(2)}) + \eta\, q_{m+1,n+3}(\tilde{Z}, \tilde{V}^{(2)})\right] (\tilde{Z}-1)^2 \\
&\quad - \frac{1}{\tilde{Z} + \tilde{V}^{(2)}}
\end{aligned} \tag{B.102}$$

All the complexity of flow equations has been reduced to a single q-functional. We define dimensionless quantities as

$$\tilde{\varphi} = \sqrt{Z_0}\, k^{-\left(\frac{d}{2}-1\right)} \varphi, \qquad V(\varphi) = k^d\, \tilde{V}(\tilde{\varphi}), \qquad Z(\varphi) = Z_0\, \tilde{Z}(\tilde{\varphi}) \tag{B.103}$$

from which the t-derivatives follow

$$\partial_t \tilde{\varphi} = \left(-\frac{d-2}{2}\sqrt{Z_0} + \frac{\dot{Z}_0}{2\sqrt{Z_0}} \right) k^{-\left(\frac{d}{2}-1\right)} \varphi = -\frac{d-2+\eta}{2}\,\tilde{\varphi} \tag{B.104}$$

$$\begin{aligned} \partial_t V &= d\,k^d \tilde{V} + k^d \partial_t \tilde{V} + k^d \tilde{V}' \partial_t \tilde{\varphi} \\ &= k^d \left(d\tilde{V} + \partial_t \tilde{V} - \frac{d-2+\eta}{2}\,\tilde{\varphi}\tilde{V}' \right) \end{aligned} \tag{B.105}$$

$$\begin{aligned} \partial_t Z &= (\partial_t Z_0)\tilde{Z} + Z_0 \left(\partial_t \tilde{Z} + \tilde{Z}' \partial_t \tilde{\varphi} \right) \\ &= Z_0 \left(\partial_t \tilde{Z} - \frac{d-2+\eta}{2}\,\tilde{\varphi}\tilde{Z}' - \eta \tilde{Z} \right) \end{aligned} \tag{B.106}$$

In the following we work with the tilde quantities $\tilde{V}(\tilde{\varphi})$ and $\tilde{Z}(\tilde{\varphi})$ and remove the tildes from now on.

B.4.2 $d = 2$

In $d = 2$ and for the Litim cutoff the flow equations become

$$\partial_t V + 2V - \frac{\eta}{2}\,\varphi V' = \frac{\eta}{(Z-1)} + \frac{2(Z-1) - \eta(Z+V'')}{(Z-1)^2} \log\left(\frac{Z+V''}{1+V''} \right) \tag{B.107}$$

and

$$\begin{aligned}
\partial_t Z - \frac{\eta}{2}\varphi Z' - \eta Z = &-Z''\left[\frac{2(Z-1)-\eta(V''+Z)}{(1+V'')(Z+V'')(Z-1)} + \frac{\eta}{(Z-1)^2}\log\left(\frac{Z+V''}{1+V''}\right)\right] \\
&+ (V''')^2\left[\frac{2-\eta}{3}\left(\frac{1}{(Z+V'')^3} - \frac{1}{(1+V'')^3}\right) - \frac{6Z}{(Z+V'')^4}\right] \\
&+ Z'V'''\left[\frac{2(V'')^3(4-\eta)}{(1+V'')^2(V''+Z)^4} + \frac{2(V'')^2(Z(18-7\eta)+2(6-\eta))}{3(1+V'')^2(Z+V'')^4}\right. \\
&\left.+ \frac{V''(2Z^2(8-3\eta)+2Z(2-\eta)+4-\eta)}{3(1+V'')^2(Z+V'')^4} + \frac{2Z^3(2-\eta)+4Z^2-Z(2+\eta)}{3(1+V'')^2(Z+V'')^4}\right] \\
&+ (Z')^2\left[-\frac{(V'')^4 3\eta}{(1+V'')(Z-1)^2(Z+V'')^4} - \frac{(V'')^3 3\eta(7Z+1)}{2(1+V'')(Z-1)^2(Z+V'')^4}\right. \\
&+ \frac{(V'')^2((30-83\eta)Z^2-(23\eta+60)Z+(30-2\eta))}{6(1+V'')(Z-1)^2(Z+V'')^4} \\
&+ \frac{V''((36-47\eta)Z^3-(25\eta+60)Z^2+2(6+\eta)Z+2(6-\eta))}{6(1+V'')(Z-1)^2(Z+V'')^4} \\
&+ \frac{9(2-\eta)Z^4-(11\eta+36)Z^3+(18+4\eta)Z^2-2\eta Z}{6(1+V'')(Z-1)^2(Z+V'')^4} \\
&\left.+ \frac{3\eta}{(Z-1)^3}\log\left(\frac{Z+V''}{1+V''}\right)\right] \qquad \text{(B.108)}
\end{aligned}$$

For Morris cutoff instead the flow equations are

$$\partial_t V + 2V - \frac{\eta}{2}\varphi V' = 2\frac{(4-\eta)\operatorname{arctanh}\left(\frac{\sqrt{(V'')^2-4Z}}{V''}\right)}{\sqrt{(V'')^2-4Z}} \qquad \text{(B.109)}$$

and

$$
\begin{aligned}
&\partial_t Z - \frac{\eta}{2}\varphi Z' - \eta Z \\
&= -2(4-\eta)Z'' \left(\frac{V'' \operatorname{arctanh}\left(\frac{\sqrt{(V'')^2-4Z}}{V''}\right)}{((V'')^2-4Z)^{\frac{3}{2}}} - \frac{1}{(V'')^2-4Z} \right) \\
&-4(4-\eta)(V''')^2 \left(\frac{ZV''(6Z+(V'')^2)\operatorname{arctanh}\left(\frac{\sqrt{(V'')^2-4Z}}{V''}\right)}{((V'')^2-4Z)^{\frac{7}{2}}} - \frac{Z(16Z+11(V'')^2)}{6((V'')^2-4Z)^3} \right) \\
&+8(4-\eta)Z'V''' \left(\frac{((V'')^4+2Z(V'')^2-4Z^2)\operatorname{arctanh}\left(\frac{\sqrt{(V'')^2-4Z}}{V''}\right)}{((V'')^2-4Z)^{\frac{7}{2}}} - \frac{5V''((V'')^2-Z)}{3((V'')^2-4Z)^3} \right) \\
&+2(4-\eta)(Z')^2 \left(\frac{(32ZV''-13(V'')^3)\operatorname{arctanh}\left(\frac{\sqrt{(V'')^2-4Z}}{V''}\right)}{((V'')^2-4Z)^{\frac{7}{2}}} + \frac{11(V'')^4+88Z(V'')^2-288Z^2}{12Z((V'')^2-4Z)^3} \right)
\end{aligned}
\tag{B.110}
$$

B.4.3 $d = 3$

In $d = 3$ and for Litim cutoff we get

$$
\begin{aligned}
\partial_t \tilde{V} + 3\tilde{V} - \frac{1+\eta}{2}\tilde{\varphi}\tilde{V}' &= \frac{-3\eta V'' + 2Z(3-\eta) - \eta - 6}{2(Z-1)^2} \\
&\quad - \frac{3\sqrt{V''+1}\,(-\eta V'' + Z(2-\eta) - 2)}{2(Z-1)^{5/2}} \arctan\sqrt{\frac{Z-1}{V''+1}}
\end{aligned}
\tag{B.111}
$$

and

$$
\begin{aligned}
&\partial_t \tilde{Z} - \frac{1+\eta}{2}\,\tilde{\varphi}\tilde{Z}' - \eta\tilde{Z} = \\
&3Z''\left[\frac{Z(2-3\eta)-2-3\eta V''}{4(Z-1)^2\,(V''+Z)} - \frac{Z(2-\eta)-2\eta-2-3\eta V''}{4(Z-1)^{5/2}\sqrt{V''+1}}\,\arctan\sqrt{\frac{Z-1}{V''+1}}\right] \\
&+(V''')^2\left[\frac{(V''-3Z+4)\,(3V''+Z+2)}{8\,(V''+1)^2\,(V''+Z)^3} + \frac{\eta\left(2(Z+2)V''+3\,(V'')^2+Z(3Z-4)+4\right)}{16(Z-1)\,(V''+1)^2\,(V''+Z)^2}\right. \\
&-\frac{(Z-1)^2\left(Z\left((3\eta-8)V''+\eta-4\right)+V''\left(2(\eta-6)V''+\eta-16\right)+Z^2(\eta-2)-6\right)}{6\,(V''+1)^3\,(V''+Z)^4} \\
&\left.-\frac{1}{(V''+Z)^4} + \frac{2-2\eta+(\eta-2)Z-\eta V''}{4(Z-1)^{3/2}\,(V''+1)^{5/2}}\,\arctan\sqrt{\frac{Z-1}{V''+1}}\right] \\
&+Z'V'''\left[\frac{3(7\eta+2)V''-8Z(\eta-2)+29\eta-10}{24(Z-1)^2\,(V''+1)^2} - \frac{(\eta-6)V''+Z\eta}{3\,(V''+Z)^4}\right. \\
&+\frac{\eta-7}{6(Z(\varphi)-1)\,(V''(\varphi)+Z(\varphi))^2} - \frac{1}{4(Z-1)^2\,(V''+Z)} \\
&\left.+\frac{-7\eta V''-Z(\eta-2)-6\eta-2}{8(Z-1)^{5/2}\,(V''+1)^{3/2}}\,\arctan\sqrt{\frac{Z-1}{V''+1}}\right] \\
&+(Z')^2\left[\frac{245\eta}{32(Z-1)^3} - \frac{(\eta-7)V''+Z(\eta-1)}{6\,(V''+Z)^4} - \frac{49}{24(Z-1)\,(V''+Z)^2}\right. \\
&\left.-\frac{49(\eta+3)}{48(Z-1)^2\,(V''+Z)} - \frac{49\,(5\eta V''+Z(\eta-2)+4\eta+2)}{32(Z-1)^{7/2}\sqrt{V''+1}}\,\arctan\sqrt{\frac{Z-1}{V''+1}}\right]
\end{aligned}
\tag{B.112}
$$

while for Morris cutoff we get

$$
\partial_t \tilde{V} + 3\tilde{V} - \frac{1+\eta}{2}\,\tilde{\varphi}\tilde{V}' = \frac{4-\eta}{8\pi\sqrt{Z\left(V''+2\sqrt{Z}\right)}} \tag{B.113}
$$

and

$$\begin{aligned}\partial_t \tilde{Z} - \frac{1+\eta}{2}\,\tilde{\varphi}\tilde{Z}' - \eta\tilde{Z} = &\frac{4-\eta}{16\pi\sqrt{Z}\left(V''+2\sqrt{Z}\right)^{3/2}}Z'' - \frac{(4-\eta)\left(V''-18\sqrt{Z}\right)}{384\pi\left(V''+2\sqrt{Z}\right)^{7/2}}\left(V'''\right)^2 \\ &- \frac{(4-\eta)\left(29V''+38\sqrt{Z}\right)}{192\pi\sqrt{Z}\left(V''+2\sqrt{Z}\right)^{7/2}}Z'V''' \\ &- \frac{(4-\eta)\left(133\sqrt{Z}V''+19\left(V''\right)^2+170Z\right)}{384\pi Z^{3/2}\left(V''+2\sqrt{Z}\right)^{7/2}}\left(Z'\right)^2 \end{aligned} \tag{B.114}$$